Wisconsin Highway Research Program

Determination of Typical Resilient Modulus Values for Selected Soils in Wisconsin

SPR# 0092-03-11

Hani H. Titi, Mohammed B. Elias, and Sam Helwany
Department of Civil Engineering and Mechanics
UW-Milwaukee

May 2006

WHRP 06-06

Wisconsin Highway Research Program Project ID 0092-03-11

Determination of Typical Resilient Modulus Values for Selected Soils in Wisconsin

Final Report

Hani H. Titi, Ph.D., P.E.
Associate Professor

Mohammed B. Elias, M.S.
Graduate Research Fellow

and

Sam Helwany, Ph.D., P.E.
Associate Professor

Department of Civil Engineering and Mechanics
University of Wisconsin – Milwaukee
3200 N. Cramer St.
Milwaukee, WI 53211

Submitted to
The Wisconsin Department of Transportation

May 2006

1. Report No.	2. Government Accession No	3. Recipient's Catalog No
4. Title and Subtitle **Determination of Typical Resilient Modulus Values for Selected Soils in Wisconsin**		5. Report Date **May 2006** 6. Performing Organization Code
7. Authors **Hani H. Titi, Mohammed B. Elias, and Sam Helwany**		Performing Organization Report No.
8. Performing Organization Name and Address **University of Wisconsin-Milwaukee** **Office of Research Services and Administration** **Mitchell Hall, Room 273Milwaukee, WI 53201**		10. Work Unit No. (TRAIS) 11. Contract or Grant No. **WHRP 0092-03-11**
12. Sponsoring Agency Name and Address **Wisconsin Department of Transportation** **Division of Transportation Infrastructure Development** **Research Coordination Section** **4802 Sheboygan Avenue** **Madison, WI 53707**		13. Type of Report and Period Covered 14. Sponsoring Agency Code

15. Supplementary Notes

16. Abstract

The objective of this research is to develop correlations for estimating the resilient modulus of various Wisconsin subgrade soils from basic soil properties. Laboratory testing program was conducted on common subgrade soils to evaluate their physical and compaction properties. The resilient modulus of the investigated soils was determined from the repeated load triaxial test following the AASHTO T 307 procedure. The laboratory testing program produced a high quality and consistent test results database. The high quality test results were assured through a repeatability study and also by performing two tests on each soil specimen at the specified physical conditions.

The resilient modulus constitutive equation adopted by NCHRP Project 1-37A was selected for this study. Comprehensive statistical analysis was performed to develop correlations between basic soil properties and the resilient modulus model parameters k_i. The analysis did not yield good results when the whole test database was used. However, good results were obtained when fine-grained and coarse-grained soils were analyzed separately. The correlations developed in this study were able to estimate the resilient modulus of the compacted subgrade soils with reasonable accuracy. In order to inspect the performance of the models developed in this study, comparison with the models developed based on LTPP database was made. The LTPP models did not yield good results compared to the models proposed by this study. This is due to differences in the test procedures, test equipment, sample preparation, and other conditions involved with development of both LTPP and the models of this study.

17. Key Words	18. Distribution Statement
Resilient modulus, repeated load triaxial test, Wisconsin soils, statistical analysis, mechanistic-empirical pavement design.	No restriction. This document is available to the public through the National Technical Information Service 5285 Port Royal Road Springfield, VA 22161

19. Security Classif.(of this report)	19. Security Classif. (of this page)	20. No. of Pages	21. Price
Unclassified	Unclassified	91	

Disclaimer

This research was funded through the Wisconsin Highway Research Program by the Wisconsin Department of Transportation and the Federal Highway Administration under Project # 0092-03-11. The contents of this report reflect the views of the authors who are responsible for the facts and the accuracy of the data presented herein. The contents do not necessarily reflect the official views of the Wisconsin Department of Transportation or the Federal Highway Administration at the time of publication.

Abstract

The objective of this research is to develop correlations for estimating the resilient modulus of various Wisconsin subgrade soils from basic soil properties. Laboratory testing program was conducted on common subgrade soils to evaluate their physical and compaction properties. The resilient modulus of the investigated soils was determined from the repeated load triaxial test following the AASHTO T 307 procedure. The laboratory testing program produced a high quality and consistent test results database. The high quality test results were assured through a repeatability study and also by performing two tests on each soil specimen at the specified physical conditions.

The resilient modulus constitutive equation adopted by NCHRP Project 1-37A was selected for this study. Comprehensive statistical analysis was performed to develop correlations between basic soil properties and the resilient modulus model parameters k_i. The analysis did not yield good results when the whole test database was used. However, good results were obtained when fine-grained and coarse-grained soils were analyzed separately. The correlations developed in this study were able to estimate the resilient modulus of the compacted subgrade soils with reasonable accuracy. In order to inspect the performance of the models developed in this study, comparison with the models developed based on LTPP database was made. The LTPP models did not yield good results compared to the models proposed by this study. This is due to differences in the test procedures, test equipment, sample preparation, and other conditions involved with development of both LTPP and the models of this study.

Acknowledgement

This research project is financially supported by the Wisconsin Department of Transportation (WisDOT) through the Wisconsin Highway Research Program (WHRP).

The authors would like to acknowledge the WisDOT Project Research Committee: Bruce Pfister, Steven Krebs, and Tom Brokaw, for their guidance and valuable input in this research project. The authors also would like to thank Robert Arndorfer, WHRP Geotechnical TOC Chair for his support and Dennis Althaus for his effort and help in collecting soil samples.

The research team would like to thank many people at UW-Milwaukee who helped in the accomplishment of the research project, namely: Joe Holbus who manufactured the special compaction molds, Jaskaran Singh who helped in performing experimental testing on different soils, Dan Mielke, who helped in soil properties testing, and Rahim Reshadi, who helped in various stages during the assembly of the dynamic materials test system.

The effort and help of Adam Titi during the preparation of the report is appreciated. The authors would like to thank Dr. Marjorie Piechowski for the valuable comments on the final report.

Table of Contents

List of Tables

List of Figures

Executive Summary

A major effort was undertaken by the National Cooperative Highway Research Program (NCHRP) to develop Mechanistic-Empirical pavement design procedures based on the existing technology in which state of the art models and databases are utilized. The NCHRP project 1-37A: "Development of the 2002 Guide for Design of New and Rehabilitated Pavement Structures" was completed and the final report and software was published on July 2004. The outcome of the NCHRP project 1-37A is the "Guide for Mechanistic-Empirical Design of New and Rehabilitated Pavement Structures," which is currently undergoing extensive evaluation and review by state highway agencies across the country.

Currently, the Wisconsin Department of Transportation uses the AASHTO 1972 Design Guide for flexible pavement design in which the SSV is used to characterize subgrade soils. There is a need to adopt the mechanistic-empirical methodology for pavement design and rehabilitation in Wisconsin, which uses the resilient modulus to characterize subgrade soils. The mechanistic-empirical approach takes into account several important variables such as repeated loading, environmental conditions, pavement materials, and subgrade materials. The mechanistic-empirical pavement design should significantly reduce variations in pavement performance as related to design life and produce significant savings from reductions in premature failures and lower maintenance over the life cycle of the pavements.

The Wisconsin Department of Transportation is currently reviewing and evaluating the new guide for adoption and implementation in the design of pavement structures. The new mechanistic-empirical pavement design guide requires design input parameters that were not previously evaluated by WisDOT for pavement design such as the resilient modulus of Wisconsin subgrade soils. However, conducting resilient modulus tests requires specialized and expensive equipment. In addition, the resilient modulus test is laborious and time consuming. These limitations signify the need for developing methodologies to reliably estimate the resilient modulus of Wisconsin subgrade soils based on correlations with fundamental soil properties.

This research project was initiated to develop correlations for estimating the resilient modulus of various Wisconsin subgrade soils from basic soil properties. A laboratory testing program was conducted on common subgrade soils to evaluate their physical and compaction properties. The resilient modulus of the investigated soils was determined from the repeated load triaxial test following the AASHTO T 307 procedure. The laboratory testing program produced a high quality and consistent test results database. The high quality test results were assured through a repeatability study and also by performing two tests on each soil specimen at the specified physical conditions.

The resilient modulus constitutive equation adopted by NCHRP Project 1-37A was selected for this study. Comprehensive statistical analysis was performed to develop correlations between basic soil properties and the resilient modulus model parameters k_i.

The analysis did not yield good results when the whole test database was used. However, good results were obtained when fine-grained and coarse-grained soils were analyzed separately. The correlations developed in this study were able to estimate the resilient modulus of the compacted subgrade soils with reasonable accuracy. In order to inspect the performance of the models developed in this study, comparison with the models developed based on LTPP database was made. The LTPP models did not yield good results compared to the models proposed by this study. This is due to differences in the test procedures, test equipment, sample preparation, and other conditions involved with development of both LTPP and the models of this study.

The results of the repeated load triaxial test on the investigated Wisconsin subgrade soils provide resilient modulus database that can be utilized to estimate values for mechanistic-empirical pavement design in the absence of basic soils testing (level 3 input parameters). The equations, developed herein, that correlate resilient modulus model parameters (k_1, k_2, and k_3) to basic soil properties for fine-grained and coarse-grained soils can be utilized to estimate level 2 resilient modulus input for the mechanistic-empirical pavement design. These equations (correlations) are based on statistical analysis of laboratory test results that were limited to the soil physical conditions specified. Estimation of resilient modulus of subgrade soils beyond these conditions was not validated.

Chapter 1

Introduction

1.1 Problem Statement

The design and evaluation of pavement structures on base and subgrade soils requires a significant amount of supporting data such as traffic loading characteristics, base, subbase and subgrade material properties, environmental conditions and construction procedures. Currently, empirical correlations developed between field and laboratory material properties are used to obtain highway performance characteristics (Barksdale et al., 1990). These correlations do not satisfy the design and analysis requirements since they neglect all possible failure mechanisms in the field. Also, most of these methods, which use California Bearing Ratio (CBR) and Soil Support Value (SSV), do not represent the conditions of a pavement subjected to repeated traffic loading. Recognizing this deficiency, the 1986 and the subsequent 1993 American Association of State Highway and Transportation Officials (AASHTO) design guides recommended the use of resilient modulus (M_r) for characterizing base and subgrade soils and for designing flexible pavements. The resilient modulus accounts for soil deformation under repeated traffic loading with consideration of seasonal variations of moisture conditions.

A major effort was recently undertaken by the National Cooperative Highway Research Program (NCHRP) to develop Mechanistic-Empirical pavement design procedures based on the existing technology in which state of the art models and databases are utilized. The NCHRP project 1-37A: "Development of the 2002 Guide for Design of New and Rehabilitated Pavement Structures" was recently completed and the final report and software was published on July 2004. The outcome of the NCHRP project 1-37A is the "Guide for Mechanistic-Empirical Design of New and Rehabilitated Pavement Structures," which is currently undergoing extensive evaluation and review by state highway agencies across the country.

Currently, the Wisconsin Department of Transportation (WisDOT) uses the AASHTO 1972 Design Guide for flexible pavement design in which the SSV is used to characterize subgrade soils. There is a need to adopt the mechanistic-empirical methodology for pavement design and rehabilitation in Wisconsin, which uses the resilient modulus to characterize subgrade soils. The mechanistic-empirical approach takes into account several important variables such as repeated loading, environmental conditions, pavement materials, and subgrade materials. The mechanistic-empirical pavement design should significantly reduce variations in pavement performance as related to design life and produce significant savings from reductions in premature failures and lower maintenance over the life cycle of the pavements (NCHRP Project 1-37A Summary, 2000 and 2001).

Therefore, WisDOT is currently reviewing and evaluating the new guide for adoption and implementation in the design of pavement structures. The new mechanistic-empirical pavement design guide requires design input parameters that were not previously

evaluated by WisDOT for pavement design such as the resilient modulus of Wisconsin subgrade soils. However, conducting resilient modulus tests requires specialized and expensive equipment. In addition, the resilient modulus test is laborious and time consuming. These limitations signify the need for developing methodologies to reliably estimate the resilient modulus of Wisconsin subgrade soils based on correlations with fundamental soil properties.

1.2 Research Objectives

The primary objective of this research project is to develop a methodology for estimating the resilient modulus of various Wisconsin subgrade soils from basic soil properties. The following specific objectives are identified for successful accomplishment of this research:

1. To conduct repeated load triaxial tests to determine resilient modulus of representative Wisconsin subgrade soils. WisDOT engineers and the research team will select these "typical" subgrade soils. The focus is on investigating the effect of soil type, soil physical properties, stress level, and environmental conditions on the resilient modulus of the selected soils. This work establishes a test result database that is used to develop correlations between various soil properties and the resilient modulus model parameters.

2. To develop and validate correlations (models) between soil properties and the resilient modulus model parameters. Applicability of theoretical and statistical methods for developing these correlations is investigated.

1.3 Scope

The laboratory-testing program is conducted on selected soils that are considered representative of the soil distributions in Wisconsin. The repeated load triaxial test is conducted to determine the resilient modulus of the selected soils according to the standard procedure: AASHTO T 307. Other laboratory tests are conducted following standard test procedures that are used by WisDOT. The resilient modulus correlations with soil properties, that are developed and validated, are based on the results of the experimental testing program.

1.4 Research Report

This report summarizes the research effort conducted at the University of Wisconsin-Milwaukee (UWM) to evaluate resilient modulus of common Wisconsin subgrade soils. A laboratory testing program was conducted on soils representative of the soil distributions of Wisconsin. Laboratory testing was conducted to evaluate basic properties and to determine the resilient modulus of the investigated soils. Comprehensive statistical analysis was performed to develop correlations between basic soil properties and the resilient modulus model input parameters. The resilient modulus model is the constitutive equation developed by NCHRP project 1-28A and adopted by the NCHRP project 1-37A

for the “Guide for Mechanistic-Empirical Design of New and Rehabilitated Pavement Structures.”

This report is organized in five chapters. Chapter One presents the problem statement, objectives and scope of the study. Background information on resilient modulus of subgrade soils is summarized in Chapter Two. Chapter Three describes the research methodology and laboratory-testing program conducted on Wisconsin subgrade soils. Chapter Four presents the test results, statistical analysis, and the models developed to estimate the resilient modulus of Wisconsin subgrade soils from basic soil properties. Finally, Chapter Five presents the conclusions and recommendations of the study.

Chapter 2

Background

This chapter presents background information on the resilient modulus of subgrade soils. The information includes a description of the repeated load triaxial test, factors affecting resilient modulus, and models used to estimate the resilient modulus for pavement design and rehabilitation. In addition, background information on Wisconsin soils is also presented.

2.1 Determination of Resilient Modulus of Soils

Several laboratory and field nondestructive test methods have been used to determine resilient modulus of subgrade soils. Laboratory test methods include the repeated load triaxial test, which is the most commonly used method for the determination of resilient modulus of soils. Field nondestructive test methods using Dynaflect and Falling Weight Deflectometer (FWD) have been used to estimate the resilient modulus of subgrade soils under existing pavements. Deflection measurements of pavement layers are used through backcalculation subroutines to estimate the resilient properties. Both laboratory and field methods are improving with new developments in hardware technologies, particularly in data acquisition systems and computer technology.

The repeated load triaxial test is specified for determining the resilient modulus by AASHTO T 294: "*Resilient Modulus of Unbound Granular Base/Subbase Materials and Subgrade Soils*-SHRP Protocol P 46," and by AASHTO T 307: "*Determining the Resilient Modulus of Soils and Aggregate Materials*." The repeated load triaxial test consists of applying a cyclic load on a cylindrical specimen under constant confining pressure (σ_3 or σ_c) and measuring the axial recoverable strain (ε_r). The repeated load triaxial test setup is shown in Figure 2.1.

The system consists of a loading frame with a crosshead mounted hydraulic actuator. A load cell is attached to the actuator to measure the applied load. The soil sample is housed in a triaxial cell where confining pressure is applied. As the actuator applies the repeated load, sample deformation is measured by a set of Linear Variable Differential Transducers (LVDT's). A data acquisitions system records all data during testing.

The resilient modulus determined from the repeated load triaxial test is defined as the ratio of the repeated axial deviator stress to the recoverable or resilient axial strain:

$$M_r \quad \frac{\sigma_d}{\varepsilon_r} \tag{2.1}$$

where M_r is the resilient modulus, σ_d is the deviator stress (cyclic stress in excess of confining pressure), and ε_r is the resilient (recoverable) strain in the vertical direction.

Figure 2.2 depicts a graphical representation of the definition of resilient modulus from a repeated load triaxial test.

AASHTO provided standard test procedures for determination of resilient modulus using the repeated load triaxial test, which include AASHTO T 292, AASHTO T 294 and AASHTO T 307. There were some problems and issues associated with some procedures, which were improved with time. The AASHTO T 307 is the current protocol for determination of resilient modulus of soils and aggregate materials. It evolved from the Long Term Pavement Performance (LTPP) protocol P46. Detailed background and discussion on AASHTO T 307 is presented by Groeger et al. (2003).

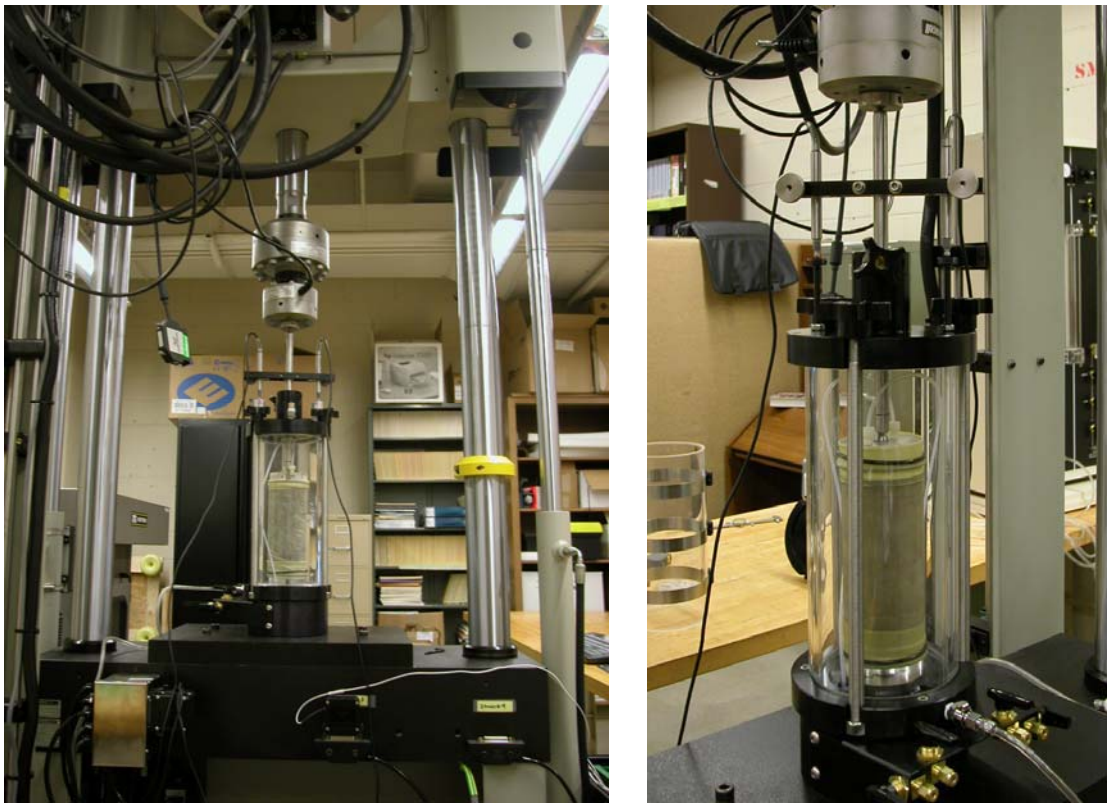

Figure 2.1: Repeated load triaxial test setup (Instron 8802 dynamic materials test system)

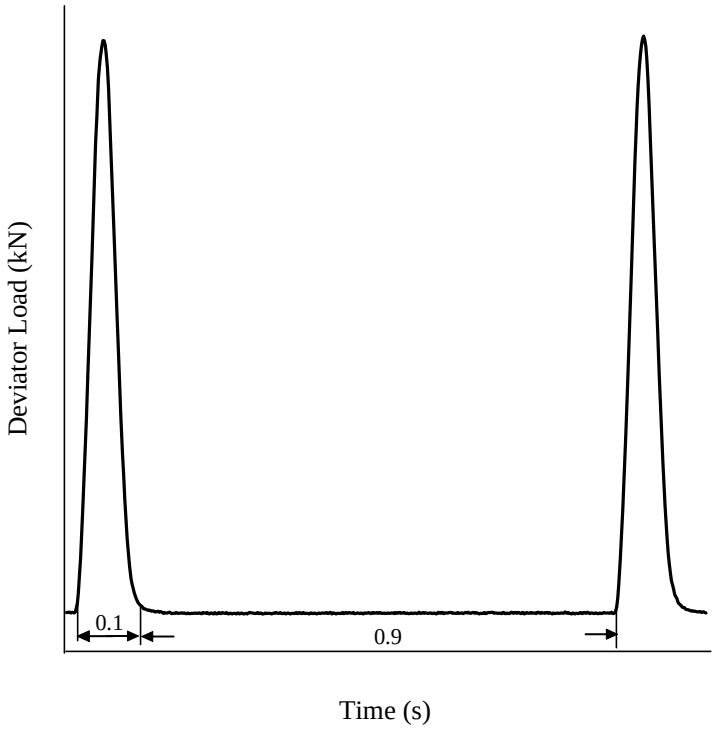

(a) Shape and duration of repeated load

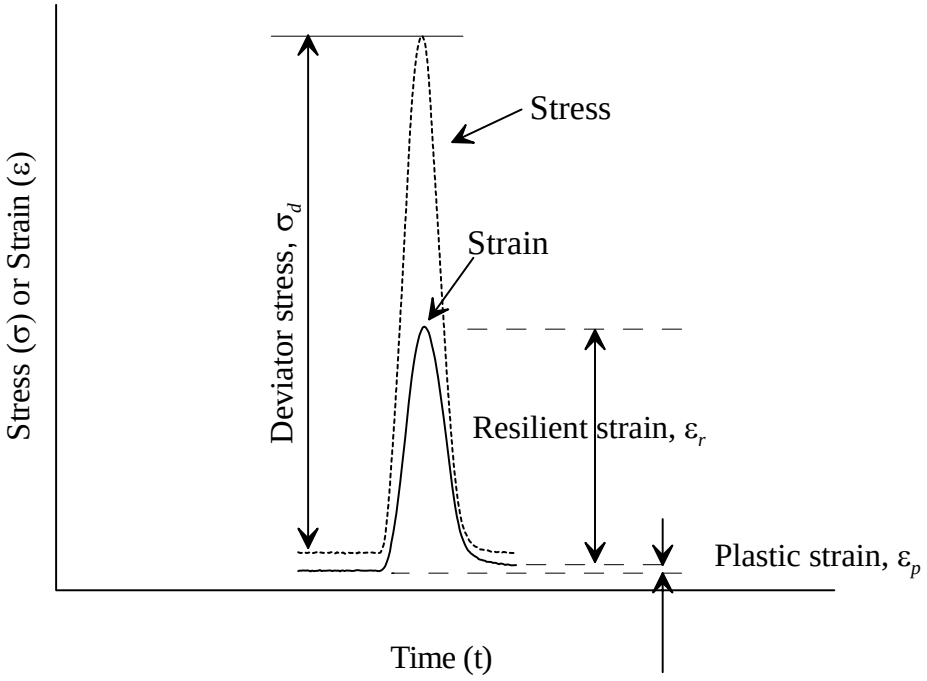

(b) Stresses and strains of one load cycle

Figure 2.2: Definition of the resilient modulus in a repeated load triaxial test

AASHTO T 307 requires a haversine-shaped loading waveform as shown in Figure 2.2a. The load cycle duration, when using a hydraulic loading device, is 1 second that includes a 0.1 second load duration and a 0.9 second rest period. The repeated axial load is applied on top of a cylindrical specimen under confining pressure. The total recoverable axial deformation response of the specimen is measured and used to calculate the resilient modulus. AASHTO T 307 requires the use of a load cell and deformation devices mounted outside the triaxial chamber. Air is specified as the confining fluid, and the specimen size is required to have a minimum diameter to length ratio of 1:2. Figure 2.3 shows a schematic of soil specimen in a triaxial chamber according to AASHTO T 307 requirements.

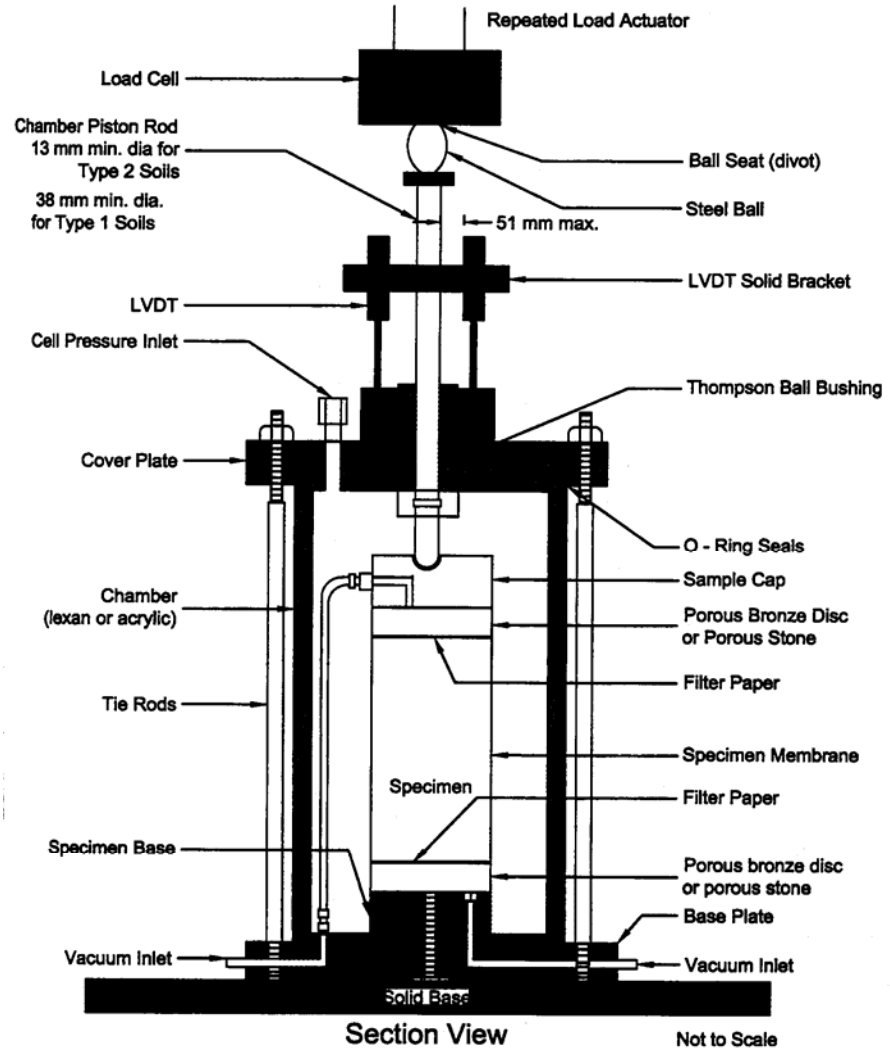

Figure 2.3: Schematic of soil specimen in a triaxial chamber according to AASHTO T 307

2.2 Factors Affecting Resilient Modulus of Subgrade Soils

Factors that influence the resilient modulus of subgrade soils include physical condition of the soil (moisture content and unit weight), stress level and soil type. Many studies have been conducted to investigate these effects on the resilient modulus. For example, Zaman (1994) reported that the results of the repeated load triaxial test depend on soil gradation, compaction method, specimen size and testing procedure. The effect of some of these factors on the resilient modulus of subgrade soils is significant. Li and Selig (1994) reported that a resilient modulus range between 14 and 140 MPa can be obtained for the same fine-grained subgrade soil by changing parameters such as stress state or moisture content. Therefore, it is essential to understand the factors affecting the resilient modulus of subgrade soils.

2.2.1 Soil Physical Conditions

Research studies showed that the moisture content and unit weight (or density) have a significant effect on the resilient modulus of subgrade soils. The resilient modulus of subgrade soil decreases with the increase of the moisture content or the degree of saturation (Barksdale 1972, Fredlund 1977, Drumm et al. 1997, Huang 2001, Butalia 2003, and Heydinger 2003). Butalia et al. (2003) investigated the effects of moisture content and pore pressures buildup on the resilient modulus of Ohio soils. Tests on unsaturated cohesive soils showed that the resilient modulus decreases with the increase in moisture content.

Drumm et al. (1997) studied the variation of resilient modulus with a post-compaction increase in moisture content. Soil samples were compacted at maximum dry unit weight and optimum moisture content; then the moisture content was increased. Investigated soils exhibited a decrease in resilient modulus with the increase in saturation. Heydinger (2003) stated that moisture content is the primary variable for predicting seasonal variation of resilient modulus of subgrade soils.

The effect of unit weight on the resilient modulus of subgrade soils also has been largely investigated (e.g., Smith and Nair 1973, Chou 1976, Allen 1996, Drumm 1997). Test results indicated that the resilient modulus increases with the increase of the dry unit weight (density) of the soil. However, this effect is small compared to the effect of moisture content and stress level on resilient modulus (Rada and Witczak 1981). At any dry unit weight (density) level, the resilient modulus has two values: one when the soil is tested under dry of optimum moisture content and another value when the soil is tested under wet of optimum moisture content. The resilient modulus of the soil compacted on the dry side of optimum is larger than that when the soil is compacted at the wet of optimum.

2.2.2 Effect of Loading Conditions

The resilient modulus is a stress-dependent soil property as it is a measure of soil stiffness. According to Rada and Witczak (1981), the most significant loading condition

factor that affects resilient modulus response is the stress level. In general, the increase in the deviator stress results in decreasing the resilient modulus of cohesive soils due to the softening effect. The increase of the confinement results in an increase in the resilient modulus of granular soils. Lekarp et al. (2000) reported that the confining pressure has more effect on material stiffness than deviator or shear stress.

Rada and Witczak (1981) reported that for loading characteristics, factors such as stress duration, stress frequency, sequence of load and number of stress repetitions necessary to reach an equilibrium-resilient strain response have little effect on resilient modulus response.

Laboratory investigations of the effect of stress history on the resilient modulus results showed that the resilient modulus increases with the increase of the repeated number of loads. This increase was mainly attributed to the reduction in moisture content of the soil. AASHTO T 307 requires the specimen to undergo 500-1000 conditioning cycles before testing to provide a uniform contact between the soil specimen and the top and bottom platens. However, Pezo et al. (1992) and Nazarian and Feliberti (1993) reported that specimen conditioning affected the resilient modulus of the specimen and indicated that stress history plays an important role in the modulus of soils.

Effect of Confining Stress

Most laboratory studies on subgrade soils and unbound materials show that the resilient modulus increases with the increase of the confining stress (Seed et al. 1962, Thomson and Robnett 1976, Rada and Witczak 1981, and Pezo and Hudson 1994). Thompson and Robnett (1979) concluded that the resilient modulus of fine-grained soils does not depend on the confining pressure and that confining pressures in the upper soil layers under pavements are normally less than 35 kPa (5 psi). In general, the effect of confining stress is more significant in granular soils than in fine-grained soils. For granular materials, the increase in confining pressure can significantly increase the resilient modulus (Rada and Witczak 1981). Resilient modulus of coarse-grained materials is usually described as a function of bulk stress.

Effect of Deviator Stress

The resilient modulus of cohesive soils is significantly influenced by the deviator stress. The resilient modulus of fine-grained soils decreases with the increase of the deviator stress. For granular materials, the resilient modulus increases with increasing deviator stress, which typically indicates strain hardening due to reorientation of the grains into a denser state (Maher et al. 2000). Resilient modulus of cohesive soils is usually described as a function of deviator stress.

2.2.3 Other Factors Affecting Resilient Modulus of Subgrade Soils

There are other factors that affect the resilient modulus of subgrade soils. These factors include soil type and properties such as amount of fines and plasticity characteristics. In

addition, the sample preparation method and the sample size have influence on the test results. Material stiffness is affected by particle size and particle size distribution. Thompson and Robnett (1979) reported that low clay content and high silt content results in lower resilient modulus values. Thompson and Robnett (1979) also showed that low plasticity index and liquid limit, low specific gravity, and high organic content result in lower resilient modulus. Other research results indicated that the amount of fines has no general trend on the resilient modulus of granular materials (Chou 1976). Lekarp et al. (2000) reported that the resilient modulus generally decreases when the amount of fines increases. Janoo and Bayer II (2001) noticed an increase in the resilient modulus with the increase in maximum particle size.

Seed et al. (1962) reported that the compaction method used to prepare soil samples affected the resilient modulus response. In general, samples that were compacted statically showed higher resilient modulus compared to those prepared by kneading compaction.

Cycles of freezing and thawing may have a significant influence on the resilient modulus of the pavement system. Scrivner et al. (1989) reported that freezing results in a sharp reduction in surface deflections while thawing produces an immediate deflection increase. Chamberlain (1969) reported that the decrease in resilient modulus accompanying freezing and thawing was caused by the increase in moisture content and decrease in unit weight.

In addition to the above mentioned factors, other factors of minor effects on the resilient modulus of subgrade soils were also investigated. Pezo and Hudson (1994) correlated the resilient modulus to the soil specimen age and plasticity index. They showed that the older the specimen is at the time of testing, the less the resilient strain, which indicates higher resilient modulus.

2.3 Resilient Modulus Models

Mathematical models are generally used to express the resilient modulus of subgrade soils such as the bulk stress model and the deviatoric stress model. These models were utilized to correlate resilient modulus with stresses and fundamental soil properties. A valid resilient modulus model should represent and address most factors that affect the resilient modulus of subgrade soils.

Bulk Stress Model

The bulk stress (θ or σ_b) is the sum of the principal stresses σ_1, σ_2, and σ_3. The bulk stress is considered a major factor for estimating the resilient modulus of granular soils. The resilient modulus can be estimated using the bulk stress from the following equation:

$$M_r \quad k_1\theta^{k_2} \qquad \textbf{(2.2)}$$

where M_r is the resilient modulus, θ is the bulk stress = $\sigma_1 + \sigma_2 + \sigma_3$, and k_1 and k_2 are material constants.
Although this model was used to characterize the resilient modulus of granular soils, it does not account for shear stress/strain and volumetric strain. Uzan (1985) demonstrated that the bulk stress model does not sufficiently describe the behavior of granular materials.

May and Witczak (1981) modified the bulk stress model by adding a new factor as follows:

$$M_r \quad K_1 k_1 \theta^{k_2} \qquad \textbf{(2.3)}$$

where K_1 is a function of pavement structure, test load and developed shear strain.

Deviatoric Stress "Semi- log" Model

The deviator stress is the cyclic stress in excess of confining pressure. The resilient modulus of cohesive soils is a function of the deviatoric stress, as it decreases with increasing the deviatoric stress. The deviatoric stress model was recommended by AASHTO to estimate resilient modulus of cohesive soils. In the deviatoric stress model, the resilient modulus is expressed by the following equation:

$$M_r \quad k_3 \sigma_d^{k_4} \qquad \textbf{(2.4)}$$

where σ_d is the deviator stress and k_3 and k_4 are material constants.

The disadvantage of the deviatoric stress model is that it does not account for the effect of confining pressure. Li and Selig (1994) reported that for fine-grained soils the effect of confining pressure is much less significant than the effect of deviatoric stress. However, cohesive soils that are subjected to traffic loading are affected by confining stresses.

Uzan Model

Uzan (1985) studied and discussed different existing models for estimating resilient modulus. He developed a model to overcome the bulk stress model limitations by including the deviatoric stress to account for the actual field stress state. The model defined the resilient modulus as follows:

$$M_r \quad k_1 \theta^{k_2} \sigma_d^{k_3} \qquad \textbf{(2.5)}$$

where k_1, k_2, and k_3 are material constants and θ and σ_d are the bulk and deviatoric stresses, respectively.

By normalizing the resilient modulus and stresses in the above model, it can be written as follows:

$$M_r \quad k_1 P_a \left[\frac{\theta}{P_a}\right]^{k_2} \left[\frac{\sigma_d}{P_a}\right]^{k_3} \qquad \textbf{(2.6)}$$

where P_a is the atmospheric pressure, expressed in the same unit as M_r, σ_d and θ.

Uzan also suggested that the above model can be used for all types of soils. By setting k_3 to zero the bulk model is obtained, and the semi-log model can be obtained by setting k_2 to zero.

Octahedral Shear Stress Model

The Uzan model was modified by Witzak and Uzan (1988) by replacing the deviatoric stress with octahedral shear stress as follows:

$$M_r \quad k_1 P_a \left[\frac{\theta}{P_a}\right]^{k_2} \left[\frac{\tau_{oct}}{P_a}\right]^{k_3} \qquad \textbf{(2.7)}$$

where τ_{oct} is the octahedral shear stress, P_a is the atmospheric pressure, and k_1, k_2, and k_3 are material constants.

AASHTO Mechanistic-Empirical Pavement Design Models

The general constitutive equation (resilient modulus model) that was developed through NCHRP project 1-28A was selected for implementation in the upcoming mechanistic-empirical AASHTO *Guide for the Design of New and Rehabilitated Pavement Structures*. The resilient modulus model can be used for all types of subgrade materials. The resilient modulus model is defined by (NCHRP 1-28A):

$$M_r \quad k_1 P_a \left(\frac{\sigma_b}{P_a}\right)^{k_2} \left(\frac{\tau_{oct}}{P_a} + 1\right)^{k_3} \qquad \textbf{(2.8)}$$

where:

M_r = resilient modulus
P_a = atmospheric pressure (101.325 kPa)
σ_b = bulk stress = $\sigma_1 + \sigma_2 + \sigma_3$
σ_1 = major principal stress
σ_2 = intermediate principal stress = σ_3 for axisymmetric condition (triaxial test)
σ_3 = minor principal stress or confining pressure in the repeated load triaxial test
τ_{oct} = octahedral shear stress
k_1, k_2 and k_3 = model parameters (material constatnts)

2.4 Mechanistic-Empirical Pavement Design

The NCHRP project 1-37A: "Development of the 2002 Guide for Design of New and Rehabilitated Pavement Structures" was recently completed and the final report and software was published on July 2004. The outcome of the NCHRP 1-37A is the "Guide for Mechanistic-Empirical Design of New and Rehabilitated Pavement Structures," which is currently undergoing extensive evaluation and review by state highway agencies across the country.

The Wisconsin Department of Transportation is currently reviewing and evaluating the new guide for adoption and implementation in design of pavement structures. The new Mechanistic-Empirical guide requires numerous design input parameters that were not previously evaluated by WisDOT for pavement design. For flexible pavements, this includes the determination of the resilient modulus of subgrade soils as input parameter. This parameter can be determined by carrying out a laboratory testing program following the AASHTO T 307 procedure.

Design procedures for the new Mechanistic-Empirical guide are based on the existing technology in which state of the art models and databases are utilized. Design input parameters are required generally in three major categories: (1) traffic; (2) material properties; and (3) environmental conditions.

The new Mechanistic-Empirical design guide also identifies three levels of design input parameters in a hierarchical way. This provides the pavement designer with flexibility in achieving pavement design with available resources based on the significance of the project. The three levels of input parameters apply to traffic characterization, material properties, and environmental conditions. The following is a description of these input levels:

1. Level 1: These design input parameters are the most accurate, with highest reliability and lowest level of uncertainty. They require the designer to conduct laboratory/field testing program for the project considered in the design. This requires extensive effort and would increase cost.

2. Level 2: When resources are not available to obtain the high accuracy level 1 input parameters, then level 2 inputs provide an intermediate level of accuracy for pavement design. Level 2 inputs can be obtained by developing correlations among different variables such as estimating the resilient modulus of subgrade soils from the results of basic soil tests.

3. Level 3: Input parameters that provide the highest level of uncertainty and the lowest level of accuracy. They are usually typical average values for the region. Level 3 inputs might be used in projects associated with minimal consequences of early failure such as low volume roads.

2.5 Soil Distributions in Wisconsin

Hole (1980) divided Wisconsin soils into ten major pedological groups. These groups are summarized along with their general characteristics in Table 2.1. Figure 2.4 depicts the distribution of the different pedological groups in a Wisconsin map. The ten soil regions are considered as refinements of five Wisconsin geographic provinces. Within the same group, soils may vary from coarse-grained to fine-grained or organic.

Table 2.1: Wisconsin pedological soil groups (After Hole 1980)

Group No.	Soil Region	General Characteristics of the soils and landscapes	% Area of State
A	Southwest Ridges and Valleys	Silty soils overlying dolomite bedrock on undulating to rolling uplands and valley flats, with steep stony slopes between.	11
B	Southeast Upland	Silty to loamy soils on rolling to level uplands and associated wetlands on gray brown calcareous, dolomite glacial drift.	13
C	Central Sandy Uplands and Plains	Very sandy soils on plains, rolling upland, and occasional buttes of sandstone.	7
D	Western Sand Stone Uplands, Valley Slopes, and Plains	Silty to sandy loam soils on hilly uplands, valley slopes and associated plains.	9
E	Northern and Eastern Sandy and Loamy Drift Uplands and Plains	Sandy loams and loams of northeastern rolling uplands and plains on calcareous pink glacial drift.	5
F	Northern Silty Uplands and Plains	Silty soils on undulating uplands on acid, compact glacial drift	16
G	Northern Loamy Uplands and Plains	Sandy loams and loams on hilly uplands and plains over acid gravelly and stony reddish brown glacial drift.	17
H	Northern Sandy Uplands and Plains	Very sandy soils on hilly uplands and plains on sandy glacial drift.	7
I	Northern and Eastern Clayey and Reddish Drift Uplands and Plains	Silty and clayey soils on nearly level to rolling upland on calcareous reddish brown clayey glacial drift.	7
J	Major Wetlands	Wet soils, including some silts and loams on alluvium; more silts and loams, peats and mucks in wetlands.	8

Figure 2.4: Wisconsin pedological soil groups (Hole, 1980)

Madison and Gundlach (1993) presented a geological map that divides Wisconsin soils into five regions as follows: (1) soils of northern and eastern Wisconsin, (2) soils of central Wisconsin, (3) soils of southern and western Wisconsin, (4) soils of southern Wisconsin and (5) statewide soils. The five soil regions were subdivided into smaller regions. Figure 2.5 shows a map of Wisconsin soil regions presented by Madison and Gundlach (1993). The following is a description of these regions:

(1) Soils of northern and eastern Wisconsin

Region E: forested, sandy loamy soils with uplands covered by loamy soils underlain by calcareous silt.
Region Er: forested, loamy or clayey soils underlain by dolomite bedrock with calcareous materials in some parts.
Region F: forested, silty soils. Uplands covered by silt over very dense acid loam till, also Antigo and Brill soils occur.
Region G: forested, loamy soils. Uplands covered by silty materials over acid. Antigo silt loam is found in some areas in which silt overlay sand and gravel.
Region H: forested, sandy soils. There are also some places where loamy materials over acid sand and gravel exist.
Region I: forested, clayey or loamy soils. There are thin silty materials that overlie calcareous red clay till exist near Lake Michigan and some other places.

(2) Soils of central Wisconsin

Region C: forested, sandy soils. Also sandy materials overlie limy till in uplands.
Region Cm: prairie, sandy soils. The region is dominated by dark sandy soils.
Region Fr: forested, silty soils over igneous and metamorphic rock

(3) Soils of Southwestern and Western Wisconsin

Region A: forested, silty soils or deep silty and clayey soils that sometimes overlie limestone bedrock.
Region Am: prairie, silty soils. Silty soils overlying limestone on broad ridge tops.
Region Dr: forested soils over sandstone bedrock.

(4) Soils of Southeastern Wisconsin

Region B: forested, silty soils. Organic soils have formed where plant materials accumulated.
Region Bm: prairie, silty soils. Uplands are covered by silty loamy soils overlaying limy till. Clayey soils over limy till occur near Milwaukee and Racine-Kenosha.

(5) Statewide Soils

Region J: wetland soils, occurs in depression and drainage ways across the state. Soils are varied between silty clayey loamy sandy as well as organic soils.

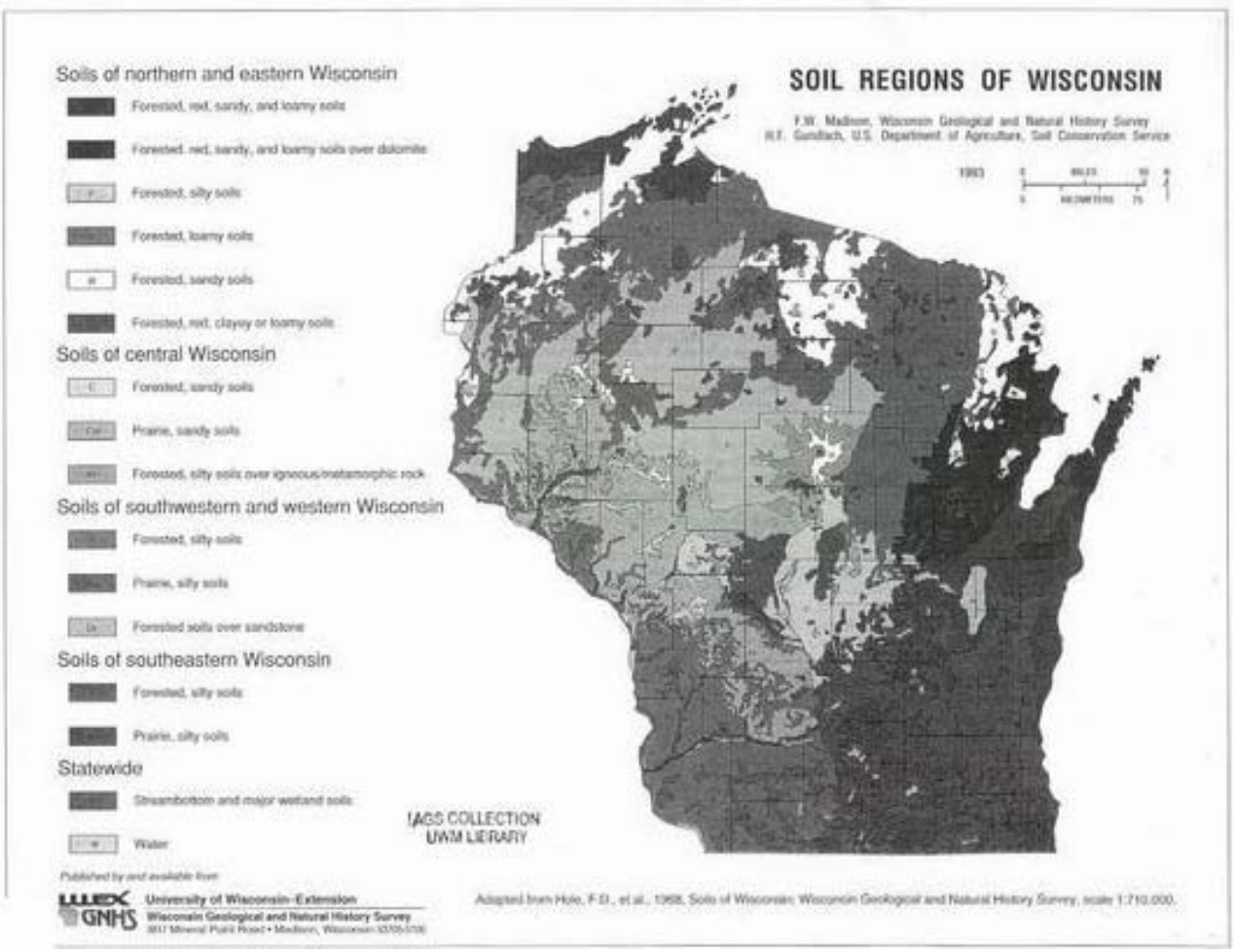

Figure 2.5: Wisconsin Soil Regions, Madison and Gundlach (1993)

Chapter 3

Research Methodology

A laboratory testing program was conducted on nineteen soils, which comprise common subgrade soils in Wisconsin. The testing program was conducted at the Geotechnical and Pavement Research Laboratory at the University of Wisconsin-Milwaukee. Soil samples were subjected to different tests to determine their physical properties, compaction characteristics, and resilient modulus. In this chapter, a description of the soils collected and laboratory tests and equipment used is presented.

3.1 Investigated Soils

The investigated soils were selected by the WisDOT project oversight committee to represent common soil distributions in Wisconsin. Disturbed soil samples were collected by Wisconsin DOT personnel and then delivered to UWM. The locations of these soils are shown on a map of Wisconsin in Figure 3.1.

The investigated soils were selected so that test results can be utilized to establish and validate correlations to estimate resilient modulus of Wisconsin soils from basic soil properties. The soils cover a wide range of types and were obtained from various places across Wisconsin as shown in Figure 3.1. Pictures of some soil samples are presented in Figure 3.2.

3.2 Laboratory Testing Program

3.2.1 Physical Properties and Compaction Characteristics

Collected soils were subjected to standard laboratory tests to determine their physical properties and compaction characteristics. Soil testing consisted of the following: grain size distribution (sieve and hydrometer analyses), Atterberg limits (liquid limit, *LL* and plastic limit, *PL*), and specific gravity (G_s). Soils were also subjected to Standard Proctor test to determine the optimum moisture content ($w_{opt.}$) and maximum dry unit weight (γ_{dmax}).

Laboratory tests were conducted following the standard test procedures used by WisDOT. Therefore, most laboratory tests were conducted according to the standard procedures of the American Society for Testing and Materials (ASTM). Only the Standard Procter test was conducted following the AASHTO T 99: *Standard Method of Test for Moisture – Density Relations of Soils Using a 2.5-kg (5.5 lb) Rammer and a 305-mm (12-in) Drop*. Table 3.1 presents a summary of the standard tests used in this study.

In order to obtain quality test results, most tests were conducted twice. The results of the two tests were compared. A third test was performed when the results of the two conducted tests were not consistent.

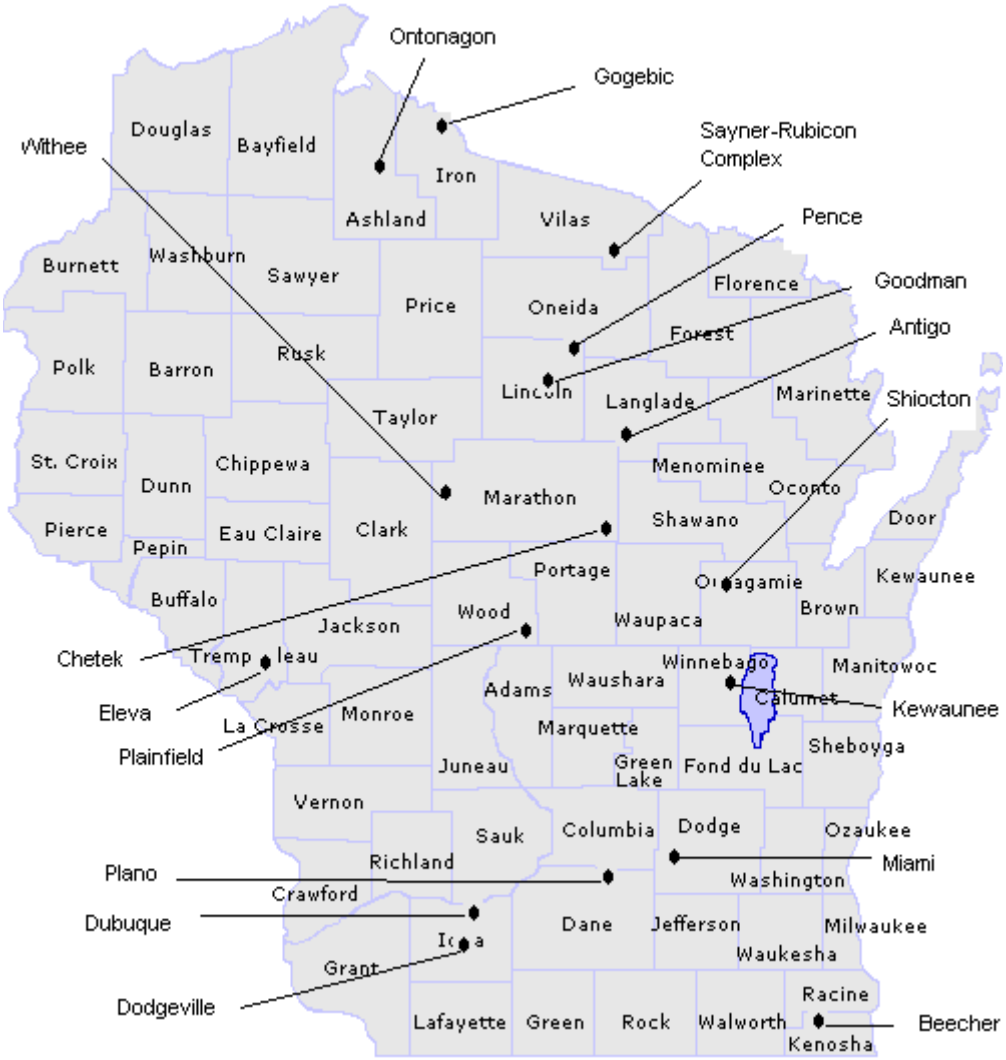

Figure 3.1: Locations of the investigated Wisconsin soils

(a) Dodgeville soil

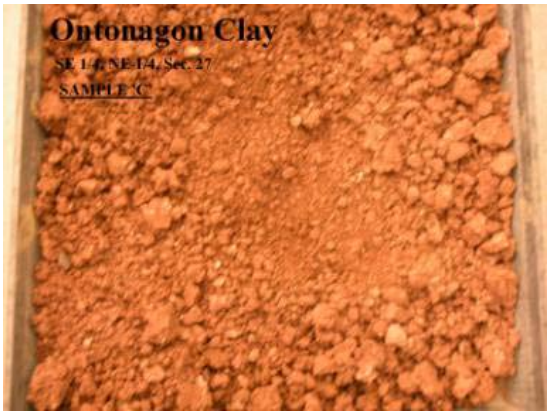

(b) Ontonagon soil

(c) Miami soil

(d) Plainfield sand

Figure 3.2: Pictures of some of the investigated Wisconsin soils

Table 3.1: Standard tests used in this investigation

Soil Property	Standard Test Designation
Particle Size Analysis	ASTM D 422: Standard Test Method for Particle –Size Analysis of Soils
Atterberg Limits	ASTM D 4318: Standard Test Methods for Liquid Limit, Plastic Limit, and Plasticity Index of Soils
Specific Gravity	ASTM D 854: Standard Test Method for Specific Gravity of Soils
Standard Proctor Test	AASHTO T 99: Standard Method of Test for Moisture – Density Relations of Soils Using a 2.5-kg (5.5 lb) Rammer and a 305-mm (12-in) Drop
ASTM Soil Classification	ASTM D 2487: Standard Classification of Soils for Engineering Purposes (Unified Soil Classification System)
AASHTO Soil Classification	AASHTO M 145: Classification of Soils and Soil-Aggregate Mixtures for Highway Construction Purposes

3.2.2 Repeated Load Triaxial Test

A repeated loading triaxial test was conducted, to determine the resilient modulus of the investigated soils, following AASHTO T 307*: Standard Method of Test for Determining the Resilient Modulus of Soils and Aggregate Materials*. The test was conducted on compacted soil specimens that were prepared in accordance with the procedure described by AASHTO T 307.

Dynamic Test System for Materials

The repeated load triaxial test was conducted using a state of the art Instron FastTrack 8802 closed loop servo-hydraulic dynamic materials test system at UWM. The system utilizes 8800 Controller with four control channels of 19-bit resolution and data acquisition. A computer with FastTrack Console is the main user interface. This is a fully digital controlled system with adaptive control that allows continuous update of PID terms at 1 kHz, which automatically compensates for the specimen stiffness during repeated load testing. The loading frame capacity of the system is 250 kN (56 kip) with a series 3690 actuator that has a stroke of 150 mm (6 in.) and with a load capacity of 250 kN (56 kip). The system has two dynamic load cells 5 and 1 kN (1.1 and 0.22 kip) for measurement of the repeated applied load. The load cells include integral accelerometer to remove the effect of dynamic loading on the moving load cell. Figure 3.3 shows pictures of the dynamic materials test system used in this study.

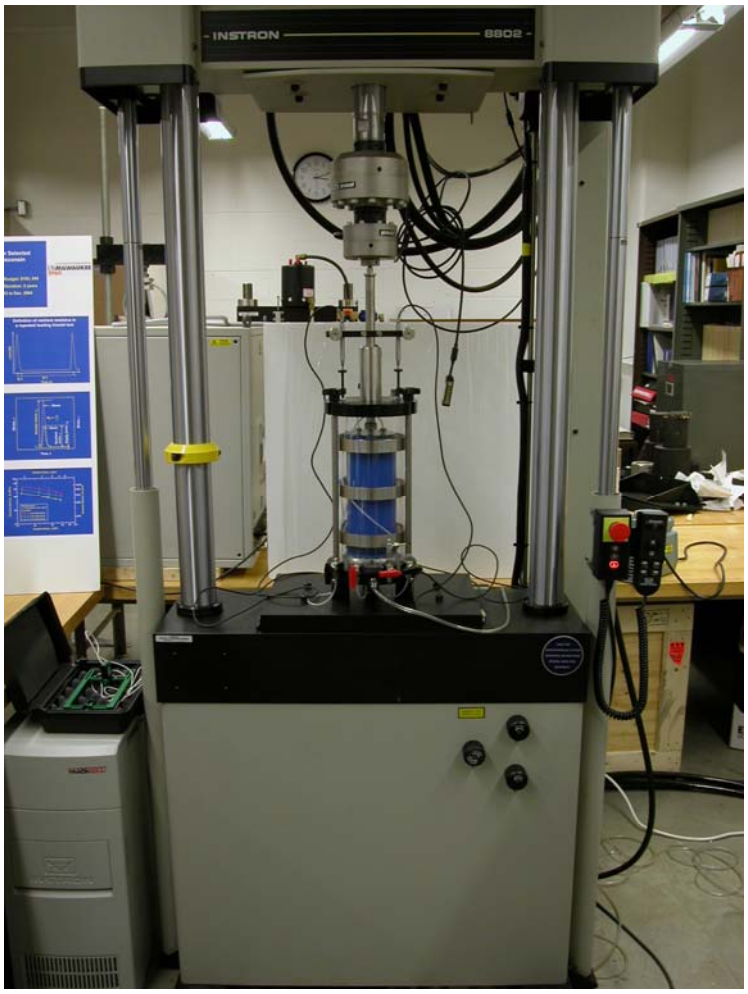

(a) Loading frame

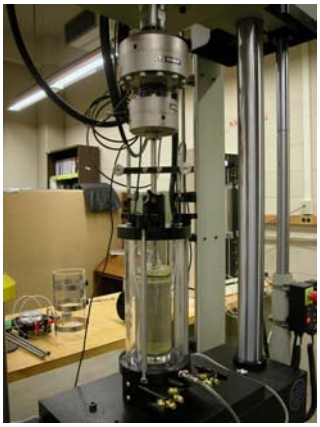

(b) Triaxial cell

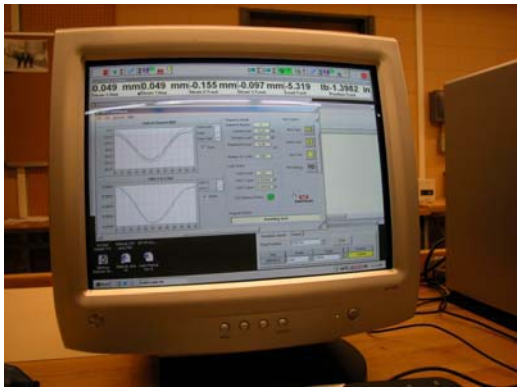

(c) Control software

Figure 3.3: The UWM servo-hydraulic closed-loop dynamic materials test system used in this study

Specimen Preparation

Compacted soil specimens were prepared according to the procedure described by AASHTO T 307, which requires five-lift static compaction. Therefore, special molds were designed and used to prepare soil specimens by static compaction of five equal layers. This compaction method provided uniform compacted lifts while using the same weight of soil for each lift. Figure 3.4 depicts pictures of the molds used to prepare soil specimens and pictures of specimen preparation procedure. The molds were made in three different diameters: 101.6, 71.1, and 35.6 mm (4.0, 2.8, and 1.4 in.).

For each soil type, compacted soil specimens were prepared at three different unit weight-moisture content combinations, namely: maximum dry unit weight and optimum moisture content, 95% of the maximum dry unit weight and the corresponding moisture content on the dry side, and 95% of the maximum dry unit weight and the corresponding moisture content on the wet side, as depicted in Figure 3.5. In order to ensure the repeatability of test results, a special study was conducted on soil specimens prepared under identical conditions of moisture content and unit weight. Statistical analysis was performed on the test results to evaluate the test repeatability. Thereafter, a repeated load triaxial test was performed on two specimens of each soil at the specified unit weight and moisture content.

After a soil specimen was prepared under a specified unit weight and moisture content, it was placed in a membrane and mounted on the base of the triaxial cell. Porous stones were placed at the top and bottom of the specimen. The triaxial cell was sealed and mounted on the base of the dynamic materials test system frame. All connections were tightened and checked. Cell pressure, LVTD's, load cell, and all other required setup were connected and checked. Figure 3.6 shows pictures of specimen preparation for the repeated load triaxial test.

Specimen Testing

The software that controls the materials dynamic test system was programmed to apply repeated loads according to the test sequences specified by AASHTO T 307 based on the material type. Once the triaxial cell is mounted on the system, the air pressure panel is connected to the cell. The required confining pressure (σ_c) is then applied. Figure 3.7 shows pictures of the software used to control and run the repeated load triaxial test.

The soil specimen was conditioned by applying 1,000 repetitions of a specified deviator stress (σ_d) at a certain confining pressure. Conditioning eliminates the effects of specimen disturbance from compaction and specimen preparation procedures and minimizes the imperfect contacts between end platens and the specimen. The specimen is then subjected to different deviator stress sequences according to AASHTO T 307. The

(a) Molds of different sizes

(b) Lubricating the mold

(c) Filling mold with one soil layer

(d) Placing compaction piston

(e) Applying static force

(f) Extracting compacted specimen

Figure 3.4: Special mold designed to prepare soil specimens according to AASHTO T 307 requirements

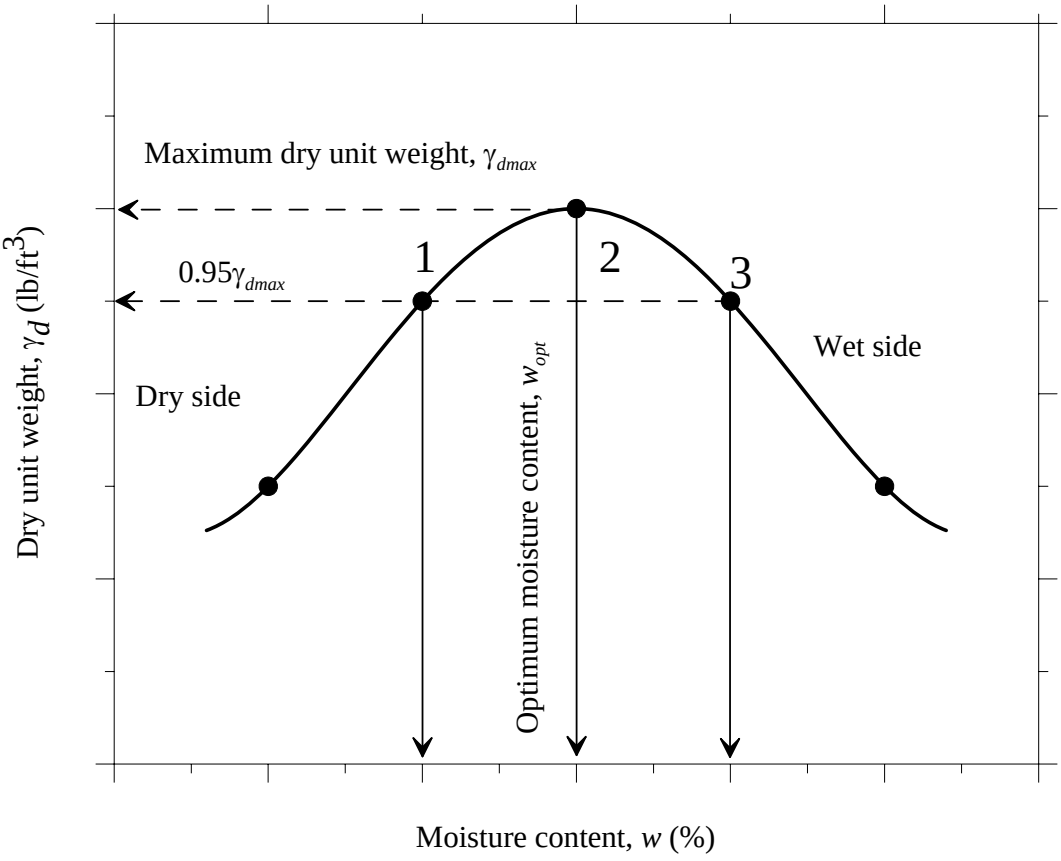

Figure 3.5: Conditions of unit weight and moisture content under which soil specimens were subjected to repeated load triaxial test

stress sequence is selected to cover the expected in-service range that a pavement or subgrade material experiences because of traffic loading.

It is very difficult to apply the exact specified loading on a soil specimen in a repeated load configuration. This is in part due to the controls of the equipment and soil specimen stiffness. However, the closed-loop servo hydraulic system is one of the most accurate systems used to apply repeated loads. In this system, the applied loads and measured displacements are continuously monitored. This is to make sure that the applied loads are within an acceptable tolerance. If there are out of range applied loads or measured displacements, then the system will display warning messages and can be programmed to terminate the test.

(a) Compacted specimen

(b) Housing a specimen in the membrane

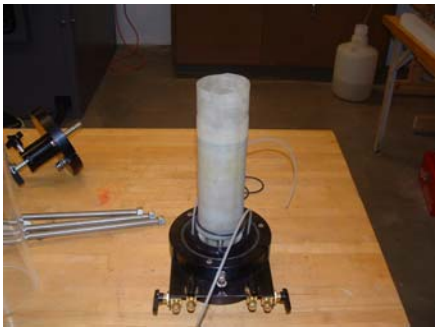

(c) Seating a specimen on the cell base

(d) Placing the top cap

(e) Assembling the triaxial cell

(f) Mounting the cell on the loading frame

Figure 3.6: Preparation of soil specimen for repeated load triaxial test

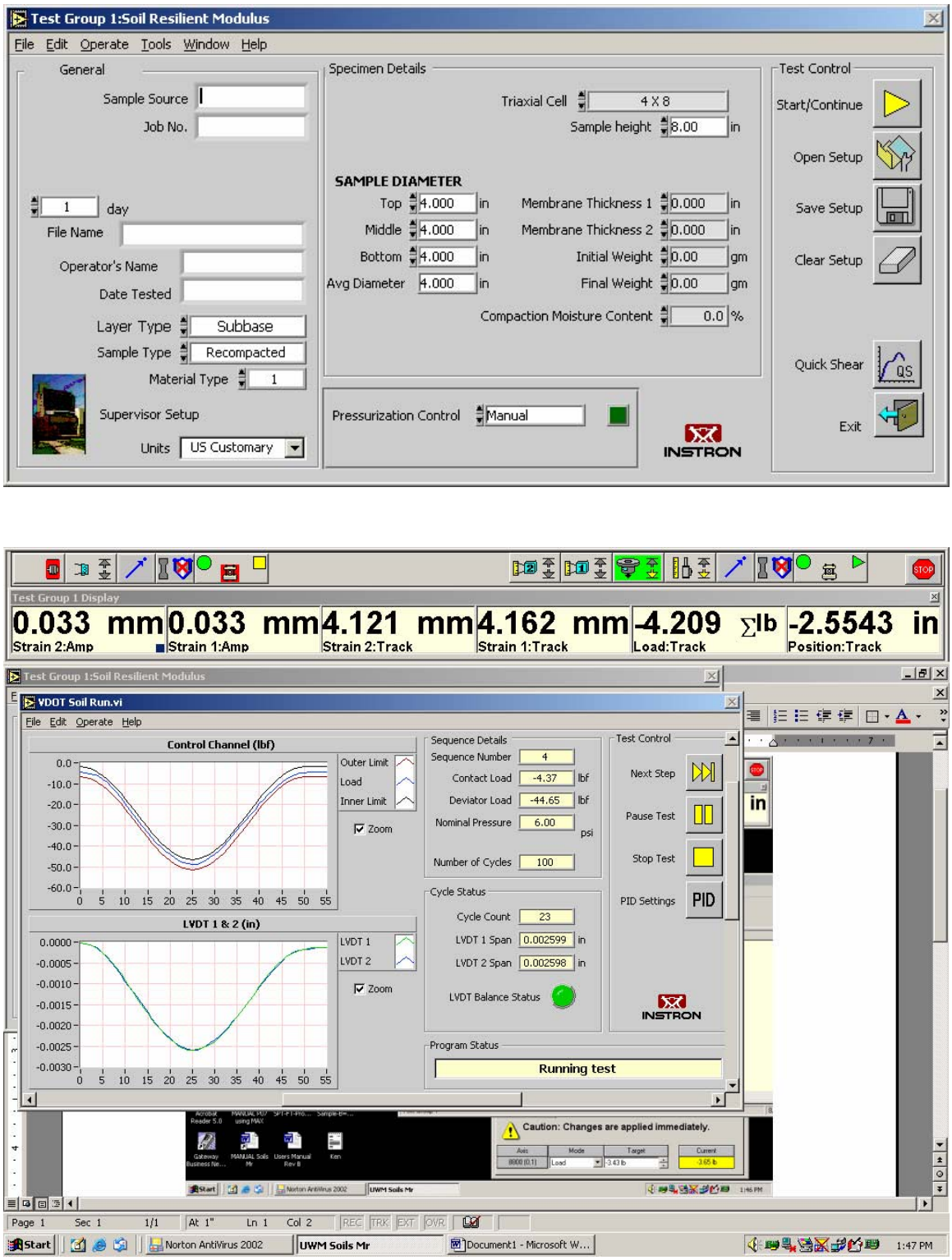

Figure 3.7: Computer program used to control and run the repeated load triaxial test for determination of resilient modulus

Chapter 4

Test Results and Analysis

This chapter presents the results of the laboratory testing program, analyses and evaluation of test results, and statistical analysis to develop resilient modulus prediction models. Physical and compaction properties of the investigated soils are presented and evaluated. In addition, the results of the repeated load triaxial test to evaluate the resilient modulus of the investigated soils are discussed. Statistical analyses are conducted to develop correlations for predicting the resilient modulus model parameters from basic soil properties. A critical evaluation and validation of the proposed correlations and discussion of the results are also presented.

4.1 Properties of the Investigated Soils

Evaluation of soil properties and identification and classification of the investigated soils are important steps to accomplish the research objective since the resilient modulus is highly influenced by soil properties. The investigated soils comprise common types that occur in Wisconsin. The results of laboratory tests conducted to evaluate soil properties are presented in Table 4.1. Soil names in Table 1 are described according to the Soil Conservation Services (SCS). The soil horizon designation is for the depth at which the soil sample was obtained. The data on soil properties consists of particle size analysis (sieve and hydrometer); consistency limits (*LL*, *PL*, and *PI*); specific gravity; maximum dry unit weight and optimum moisture content; soil classification using the Unified Soil Classification System (USCS); and soil classification using the AASHTO method including group index (*GI*). The following is a brief description of selected soils.

Dodgeville Soil (B)

Test results indicated that the soil consists of 97% of fine materials (passing sieve #200) with a plasticity index *PI* = 12, which was classified as lean clay (CL) according to the USCS and clayey soil (A-6) according to the AASHTO soil classification with a group index *GI* = 13. Figure 4.1 shows the particle size distribution curve of Dodgeville soil. The results of the Standard Proctor test on Dodgeville soil are depicted in Figure 4.2. Results of test #1 showed that the maximum dry unit weight γ_{dmax} =15.9 kN/m^3 and the optimum moisture content $w_{opt.}$ = 19.6%, while results of test #2 indicated that γ_{dmax} = 16.25 kN/m^3 and $w_{opt.}$ = 18.0 %. The results of the compaction tests are considered consistent.

Antigo Soil (B)

Figure 4.3 depicts the particle size distribution curve of Antigo soil. This soil consists of 91% passing sieve #200 with plasticity index *PI* = 11, which was classified as lean clay (CL) according to USCS and clayey soil (A-6) according to the AASHTO soil classification with *GI*=9. Standard Proctor test results showed that the average maximum dry unit weight γ_{dmax} = 17.5 kN/m^3 and the corresponding average optimum moisture content $w_{opt.}$ = 14.5%, as shown in Figure 4.4.

Table 4.1: Properties of the investigated soils

Soil name, horizon and location	Passing Sieve #200 (%)	Liquid Limit LL (%)	Plastic Limit PL (%)	Plasticity Index PI (%)	Specific Gravity G_s	Optimum Moisture Content $w_{opt.}$ (%)	Maximum Dry Unit Weight		Unified Soil Classification System (USCS)	Group Index (GI)	AASHTO Soil Classification
							γ_{dmax} (kN/m^3)	γ_{dmax} (pcf)			
Beecher, B, Kenosha County	48	29	17	12	2.67	13.9	18.3	116.5	SC (Clayey sand)	3	A-6 (Clayey soil)
Chetek, B, Marathon County	29	NP	NP	NP	2.67	8.5	20.1	128.0	SM (Silty sand)	0	A-2-4 (Silty or clayey gravel and sand)
Antigo, B, Langlade County	91	30	19	11	2.63	14.5	17.5	111.4	CL (Lean Clay)	9	A-6 (Clayey soil)
Goodman, B, Lincoln County	15	NP	NP	NP	2.62	10.5	19.1	121.6	SM (Silty sand with gravel)	0	A-2-4 (Silty or clayey gravel and sand)
Withee, B, Marathon County	35	35	16	19	2.59	15.7	17.4	110.8	SC (Clayey sand)	2	A-2-6 (Silty or clayey gravel and sand)
Shiocton, C, Outagmie County	41	NP	NP	NP	2.69	11.2	15.9	101.3	SM (Silty sand)	0	A-4 (Silty soil)
Pence, B, Lincoln County	22	NP	NP	NP	2.66	8.5	19.1	121.6	SM (Silty sand with gravel)	0	A-2-4 (Silty or clayey gravel and sand)
Gogebic, B, Iron County	32	NP	NP	NP	2.61	19.0	15.5	98.7	SM Silty sand	0	A-2-4 (Silty or clayey gravel and sand)

NP: Non Plastic

Table 4.1 (cont.): Properties of the investigated soils

Soil name, horizon and location	Passing Sieve #200 (%)	Liquid Limit LL (%)	Plastic Limit PL (%)	Plasticity Index PI (%)	Specific Gravity G_s	Optimum Moisture Content $w_{opt.}$ (%)	Maximum Dry Unit Weight		Unified Soil Classification System (USCS)	Group Index (GI)	AASHTO Soil Classification
							γ_{dmax} (kN/m^3)	γ_{dmax} (pcf)			
Dodgeville, B, Iowa County	97	37	25	12	2.55	18.8	16.1	102.5	CL (Lean clay)	13	A-6 (Clayey soil)
Miami, B, Dodge County	96	39	22	17	2.57	18.1	16.6	105.7	CL (Lean clay)	18	A-6 (Clayey soil)
Ontonagon - 1, C Ashland County	31	42	20	22	2.63	17.5	17.5	111.4	SC (Clayey sand)	2	A-2-7 (Silty or clayey sand and gravel)
Ontonagon - 2, C Ashland County	26	47	22	25	2.64	22.0	16.0	101.9	SC (Clayey sand)	2	A-2-7 (Silty or clayey sand and gravel)
Plainfield, C, Wood County	2	NP	NP	NP	2.65	-	-	-	SP (Poorly graded sand)	0	A-3 (Fine sand)
Plano, C Dane County	27	NP	NP	NP	2.66	7.8	20.5	130.5	SM (Silty sand)	0	A-2-4 (Silty or clayey sand and gravel)
Kewaunee - 1, C Winnebago County	30	NP	NP	NP	2.64	12.7	18.2	115.9	SM (Silty sand)	0	A-2-4 (Silty or clayey sand and gravel)
Kewaunee - 2, C Winnebago County	48	28	14	14	2.69	13.5	19.0	121.0	SC (Clayey sand)	3	A-6 (Clayey soil)

NP: Non plastic

Table 4.1 (cont.): Properties of the investigated soils

Soil name, horizon and location	Passing Sieve #200 (%)	Liquid Limit LL (%)	Plastic Limit PL (%)	Plasticity Index PI (%)	Specific Gravity G_s	Optimum Moisture Content $w_{opt.}$ (%)	Maximum Dry Unit Weight		Unified Soil Classification System (USCS)	Group Index (GI)	AASHTO Soil Classification
							γ_{dmax} (kN/m^3)	γ_{dmax} (pcf)			
Dubuque, C, Iowa County	72	35	23	12	2.55	18.0	16.6	105.7	CL (Lean clay)	8	A-6 (Clayey soil)
Eleva, B, Trempealeau County	20	NP	NP	NP	2.64	7.3	20.4	129.9	SM (Silty sand)	0	A-2-4 (Silty or clayey gravel and sand)
Sayner-Rubicon, C, Vilas County	1	NP	NP	NP	2.65	-	-	-	SP (Poorly graded sand with gravel)	0	A-1 (Stone fragments, gravel and sand)

NP: Non plastic

Soil name, horizon and location	e_{max}	min
Plainfield, C, Wood County	0.73 **e** 0.68	0.45 0.44
Sayner-Rubicon, C, Vilas County	0.71	0.45

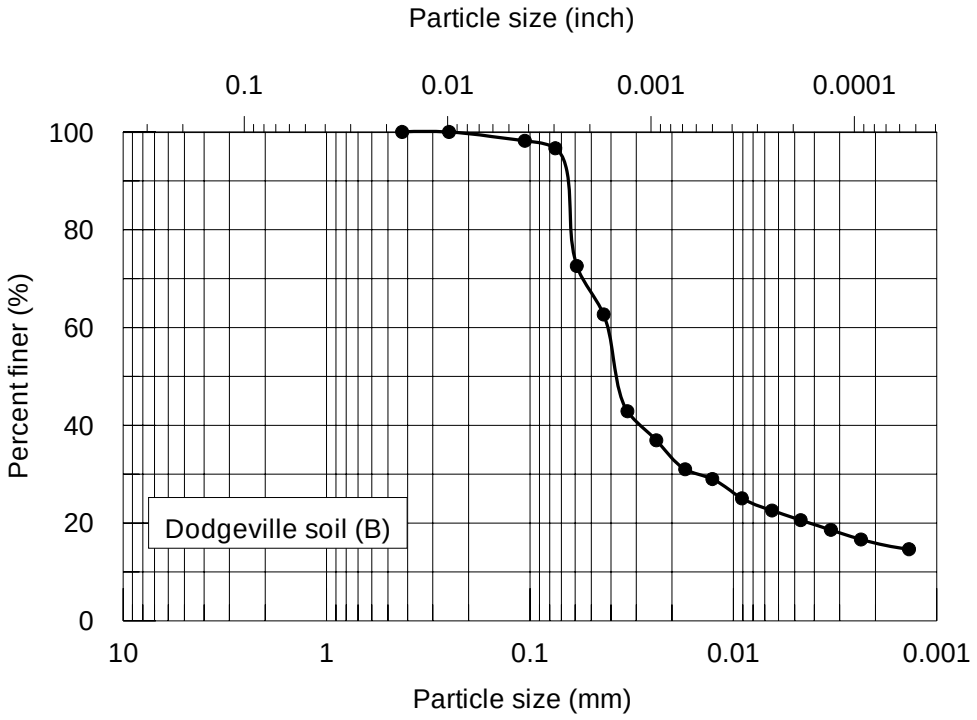

Figure 4.1: Particle size distribution curve of Dodgeville soil (B)

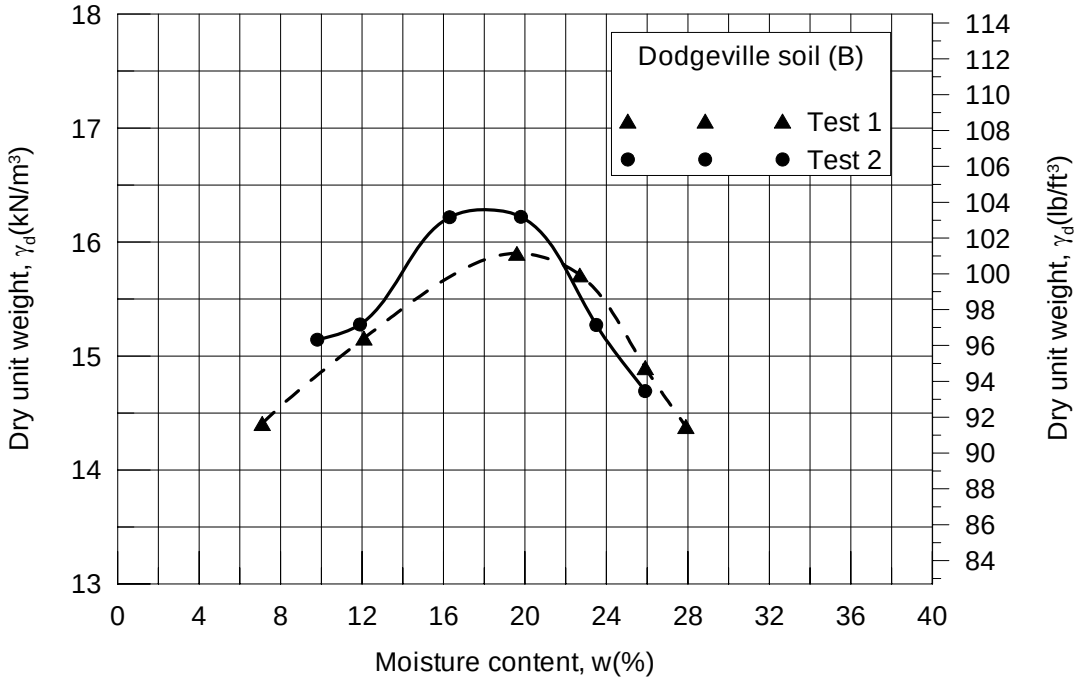

Figure 4.2: Results of Standard Proctor test for Dodgeville soil (B)

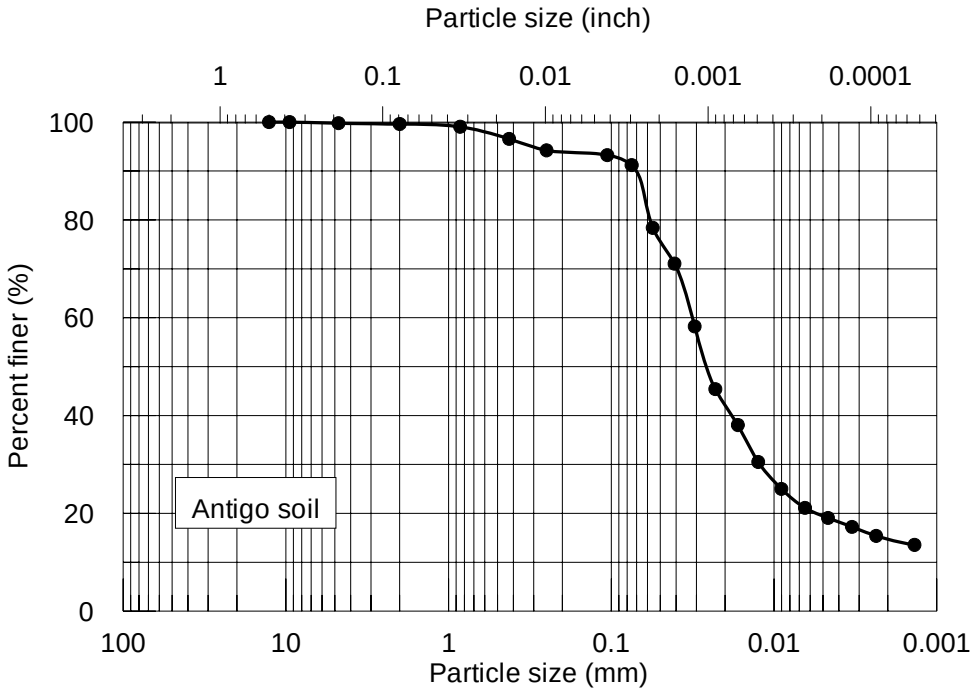

Figure 4.3: Particle size distribution curve of Antigo soil

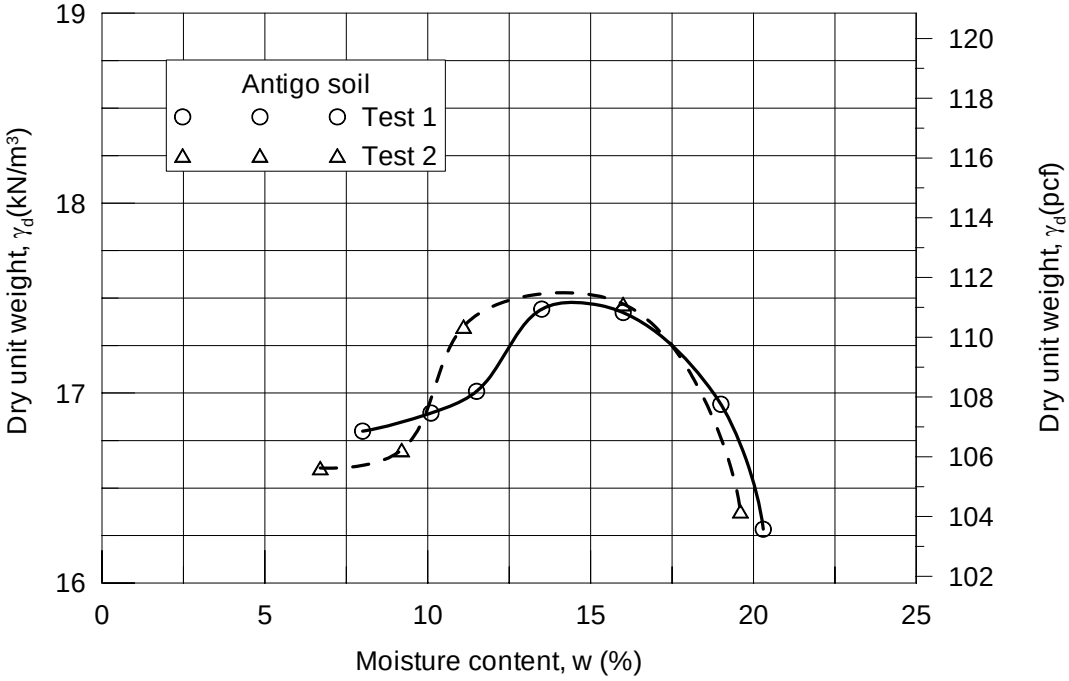

Figure 4.4: Results of Standard Proctor test for Antigo soil

Plano Soil (C)

This soil consists of 27% passing sieve #200. It was classified as silty sand (SM) according to the USCS and silty or clayey sand and gravel (A-2-4) according to the AASHTO soil classification with *GI* = 0. Figure 4.5 shows the particle size distribution curve of Plano soil. Standard Proctor test results (Figure 4.6) showed that the average maximum dry unit weight γ_{dmax} = 20.5 kN/m^3 and the average optimum moisture content $w_{opt.}$ = 7.8%.

Kewaunee Soil - 1 (C)

Test results showed that the soil consisted of 30% passing sieve #200 and was classified as silty sand (SM) according to USCS and silty or clayey sand and gravel (A-2-4) according to the AASHTO soil classification with GI = 0. Figure 4.7 shows the particle size distribution curve of Kewaunee soil - 1. Figure 4.8 depicts the results of the Standard Proctor test in which the average maximum dry unit weight γ_{dmax} = 18.2 kN/m^3 and the corresponding average optimum moisture content $w_{opt.}$ = 12.7%.

The results of particle size analysis and the Standard Proctor test for the investigated soils are presented in Appendix A. A summary of the Standard Proctor test results on the investigated soils is presented in Table 4.2.

4.2 Resilient Modulus of the Investigated Soils

Typical results of the repeated load triaxial test conducted on the investigated soils are shown in Table 4.3. The test was conducted on Antigo soil specimens 1 and 2 compacted at 0.95γ_{dmax} and moisture content $w > w_{opt.}$ (wet side). Table 4.3 presents the mean resilient modulus values, standard deviation, and coefficient of variation for the 15 test sequences conducted according to AASHTO T 307. The mean resilient modulus values, standard deviation and coefficient of variation summarized in Table 4.3 are obtained from the last five load cycles of each test sequence. The coefficient of variation for the test results presented in Table 4.3 ranges between 0.14 and 1.04% for specimen #1 and from 0.11 to 0.51% for specimen #2. This indicates that each soil specimen showed consistent behavior during each test sequence.

Figure 4.9 shows a graphical representation of the results presented in Table 4.3. Inspection of Figure 4.9 indicates that the resilient modulus (M_r) of Antigo clay decreases with the increase of the deviator stress (σ_d) under constant confining pressure (σ_c). Under constant σ_c = 41.4 kPa, the resilient modulus decreased from M_r = 49.65 MPa at σ_d = 12.45 kPa to M_r = 28.33 MPa at σ_d = 59.36 kPa for Antigo soil specimen #1. Moreover, the resilient modulus increases with the increase of confining pressure under constant deviator stress, which reflects a typical behavior. The results presented herein are typical resilient modulus results that are consistent with what was discussed in Chapter 2 “Background” and are significantly affected by the stress level.

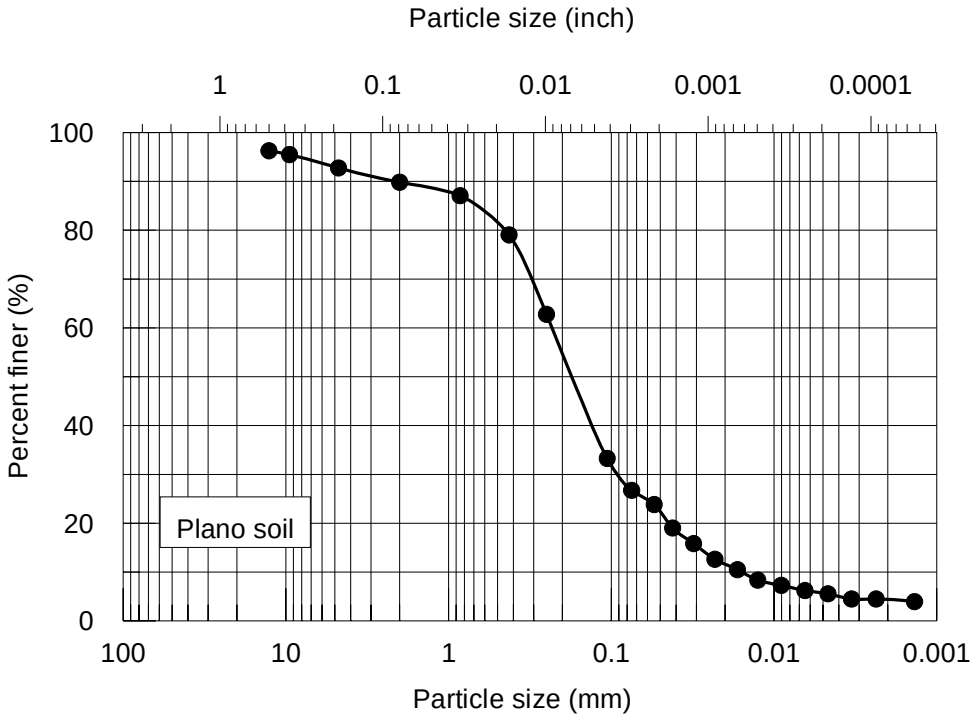

Figure 4.5: Particle size distribution curve of Plano soil

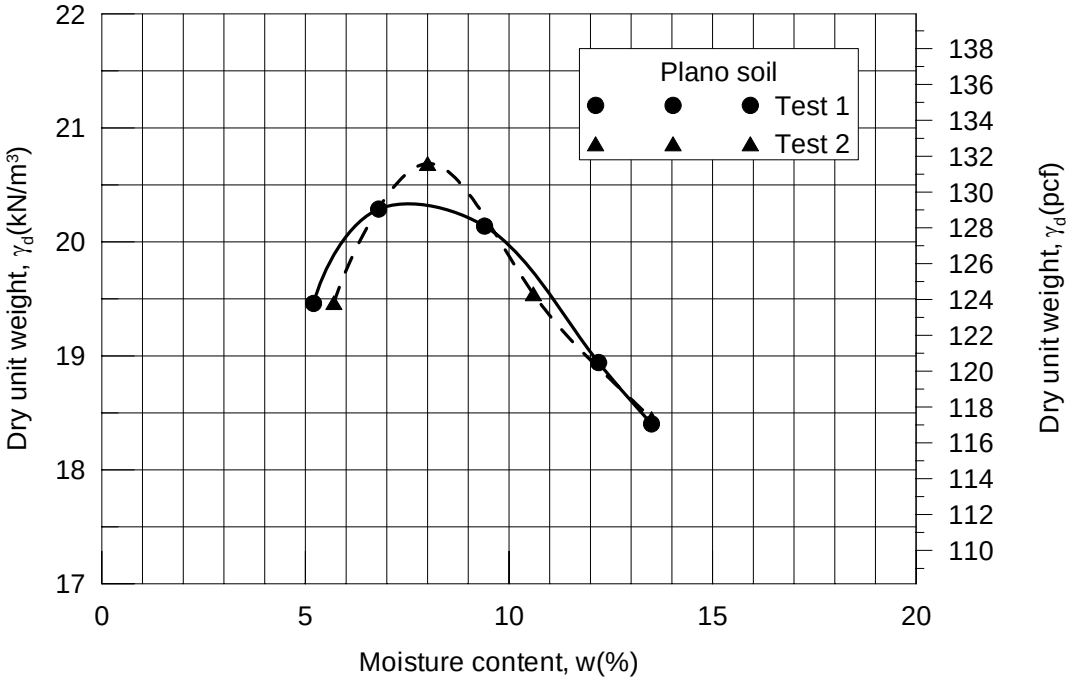

Figure 4.6: Results of Standard Proctor test for Plano soil

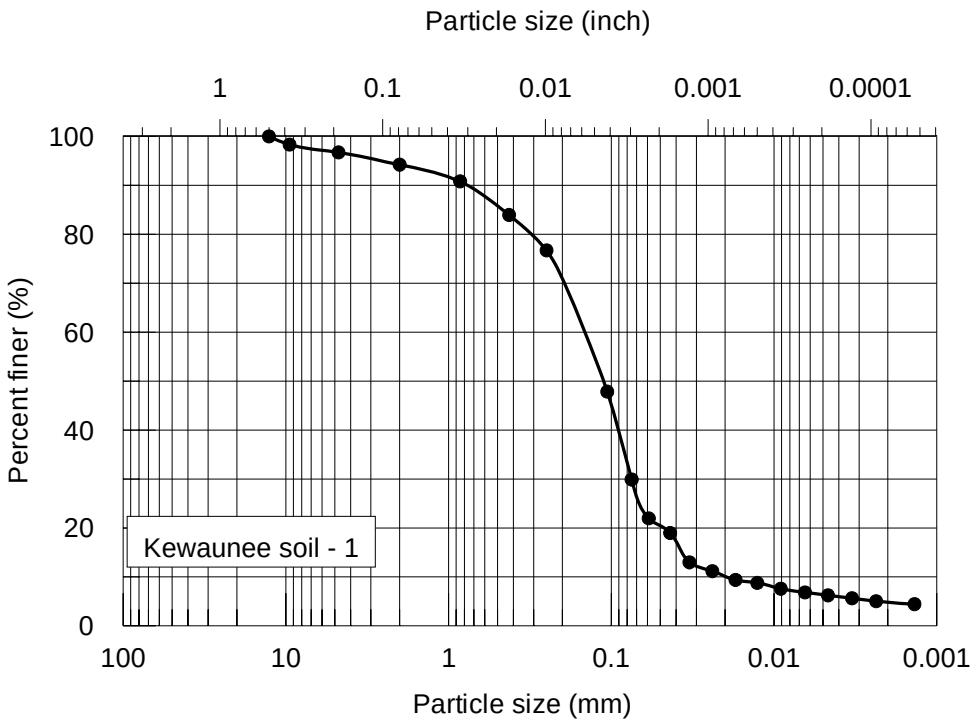

Figure 4.7: Particle size distribution curve of Kewaunee soil - 1

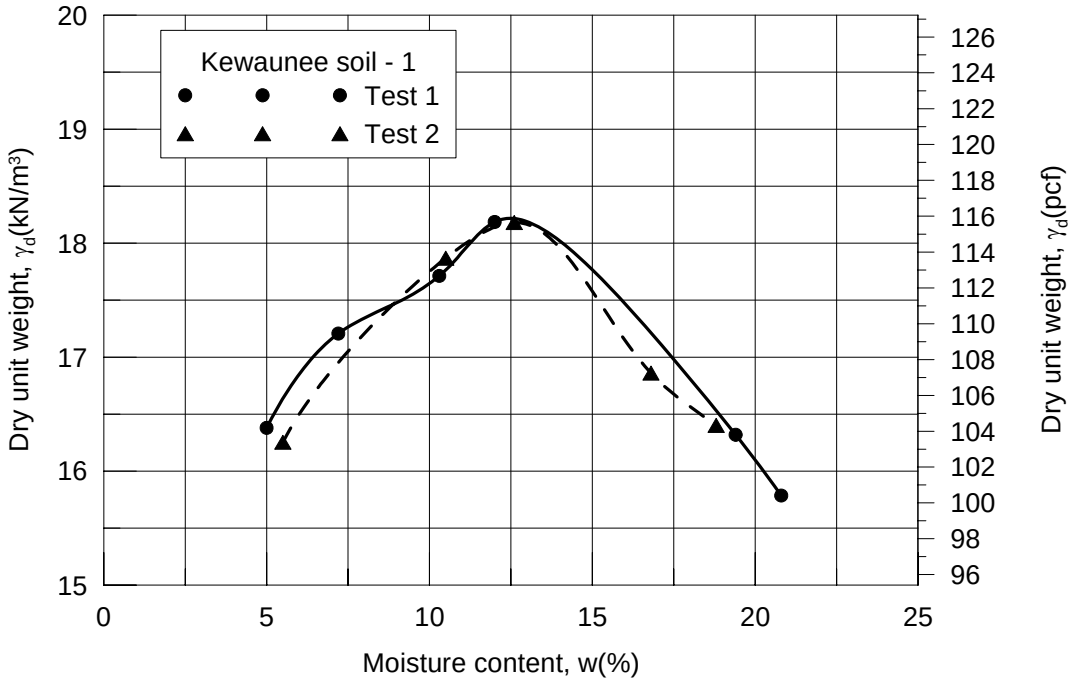

Figure 4.8: Results of Standard Proctor test for Kewaunee soil - 1

Table 4.2: Results of the standard compaction test on the investigated soils

Soil	Test 1		Test 2		Average	
	γ_{dmax} (kN/m^3)	$w_{opt.}$ (%)	γ_{dmax} (kN/m^3)	$w_{opt.}$ (%)	γ_{dmax} (kN/m^3)	$w_{opt.}$ (%)
Antigo	17.5	14.5	17.5	14.5	17.5	14.5
Beecher	18.3	14.1	18.3	13.7	18.3	13.9
Goodman	19.1	10.5	NA	NA	19.1	10.5
Plano	20.7	8.0	20.3	7.5	20.5	7.8
Dodgeville	15.9	19.6	16.2	18.0	16.1	18.8
Dubuque	16.5	18.0	16.7	18.0	16.6	18.0
Chetek	20.1	8.4	20.1	8.5	20.1	8.5
Eleva	20.2	7.5	20.7	7.1	20.4	7.3
Pence	19.1	8.5	NA	NA	19.1	8.5
Gogebic	16.0	17.5	15.0	20.5	15.5	19.0
Miami	16.5	18.4	16.7	17.8	16.6	18.1
Ontonagon -1	17.5	17.5	NA	NA	17.5	17.5
Ontonagon -2	16.0	22.0	NA	NA	16.0	22.0
Kewaunee - 1	18.2	12.8	18.2	12.5	18.2	12.7
Kewaunee - 2	19.0	13.0	18.9	14.0	19.0	13.5
Shiocton	16.0	11.0	15.7	11.3	15.9	11.2
Withee	17.6	15.5	17.2	15.8	17.4	15.7

Table 4.3: Typical results of the repeated load triaxial test conducted according to AASHTO T 307

Test Sequence No.	Confining Stress σ_c (kPa)	Deviator Stress σ_d (kPa)	Antigo wet #1 M_r (MPa)			Deviator Stress σ_d (kPa)	Antigo wet #2 M_r (MPa)		
			Mean	SD	CV (%)		Mean	SD	CV (%)
1	41.4	12.45	49.65	0.30	0.60	12.35	57.96	0.24	0.41
2	41.4	24.91	43.30	0.45	1.04	24.92	51.74	0.14	0.28
3	41.4	36.71	36.72	0.08	0.21	36.94	44.83	0.16	0.36
4	41.4	47.90	30.55	0.08	0.25	48.11	37.13	0.07	0.19
5	41.4	59.36	28.33	0.07	0.24	59.67	34.18	0.05	0.15
6	27.6	12.29	40.79	0.17	0.43	12.24	48.69	0.19	0.39
7	27.6	23.98	30.23	0.09	0.28	24.15	38.65	0.18	0.46
8	27.6	35.51	26.00	0.09	0.34	35.82	32.97	0.11	0.33
9	27.6	48.44	24.22	0.07	0.29	47.79	29.92	0.03	0.11
10	27.6	60.25	23.31	0.03	0.14	59.80	28.28	0.04	0.15
11	13.8	12.08	30.67	0.16	0.53	12.02	37.60	0.19	0.51
12	13.8	23.37	21.42	0.05	0.24	23.83	27.92	0.13	0.46
13	13.8	35.81	18.80	0.06	0.31	35.41	23.88	0.11	0.47
14	13.8	48.43	18.57	0.04	0.20	47.53	22.44	0.05	0.22
15	13.8	60.18	18.68	0.05	0.29	59.22	21.91	0.05	0.24

SD: Standard Deviation
CV: Coefficient of Variation

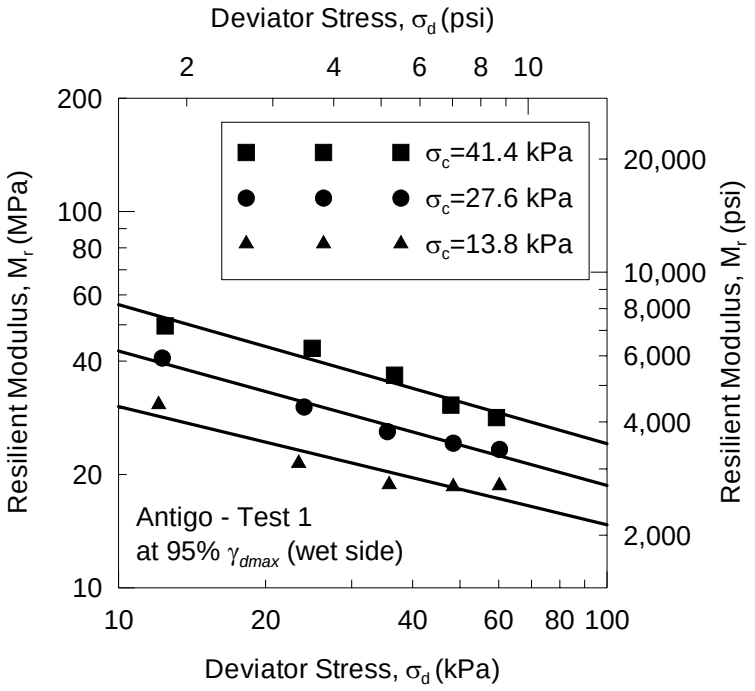

(a) Test on soil specimen #1

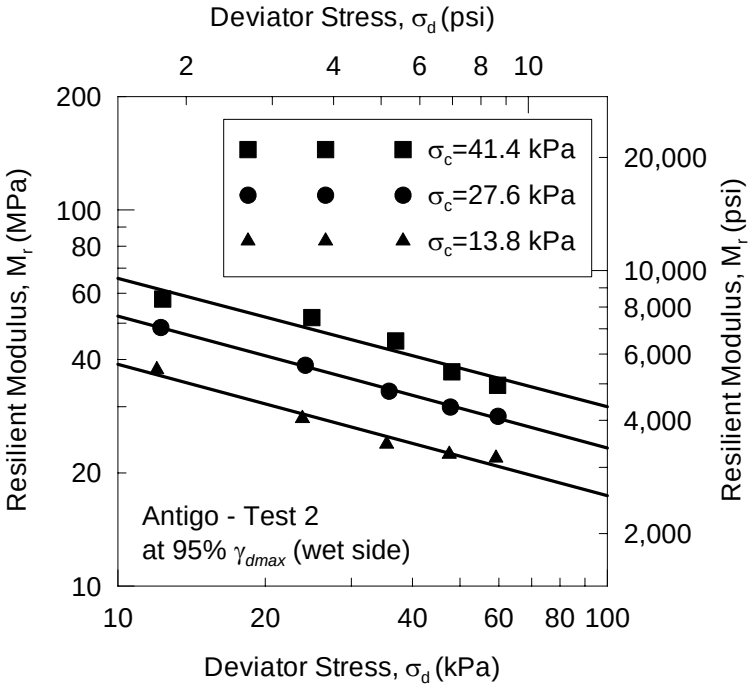

(b) Test on soil specimen #2

Figure 4.9: Results of repeated load triaxial test on Antigo soil compacted at 95% of maximum dry unit weight (γ_{dmax}) and moisture content more than $w_{opt.}$ (wet side)

A repeatability investigation was conducted to ensure that high quality test results can be obtained. This is essential since the data will be used to develop and validate resilient modulus correlations for use in the mechanistic-empirical pavement design. In addition, repeated load triaxial tests were conducted on two soil specimens of each investigated soil under identical moisture content and unit weight.

To investigate the repeatability of test results, Dodgeville soil was selected where seven soil specimens were prepared at maximum dry unit weight and optimum moisture content, four soil specimens were prepared at 95% of maximum dry unit weight and moisture content less than the optimum (dry side), and two soil specimens were prepared at 95% of maximum dry unit weight and moisture content greater than the optimum (wet side). Repeatability test results are shown in Figures 4.10, 4.11 and 4.12, respectively.

A statistical analysis was conducted on Dodgeville soil test results to evaluate test repeatability. Tables 4.4, 4.5, and 4.6 present the results of the analysis. Examination of Tables 4.4-4.6 indicates that the deviator stress applied by the system was accurate with coefficient of variation CV(σ_d) ranges from 0 to 4.4%. The coefficient of variation for the resilient modulus CV(M_r) varies from 0.2 to 2.9% for the maximum dry unit weight specimens, between 5.1 and 13.2% for the 95% of maximum dry unit weight specimens (dry side), and from 1.8 to 20.2% for the 95% of maximum dry unit weight specimens (wet side). The best repeatability results were obtained for the specimens compacted at the maximum dry unit weight and optimum moisture content. Based on this repeatability analysis, the test results are considered consistent and repeatable.

Figure 4.13 presents the results of the repeated load triaxial test on Antigo and Dodgeville soils compacted at maximum dry unit weight and optimum moisture content. Test results on Antigo soil (Figure 4.13a) showed that at confining pressure σ_c = 41.4 kPa, the resilient modulus decreased from M_r = 94 MPa at σ_d = 12.6 kPa to M_r = 81 MPa at σ_d = 61.5 kPa. For Dodgeville soil (Figure 4.13b) and under the same confining pressure, the resilient modulus decreased from M_r = 75 MPa at σ_d = 12.4 kPa to M_r = 59 MPa at σ_d = 60.6 kPa. Both soils showed that M_r is decreasing with the increase in the deviator stress; however, Antigo soil exhibited higher resilient modulus values compared to Dodgeville soil. This is attributed to the higher maximum dry unit weight and lower moisture content values of the Antigo specimen compared to the Dodgeville specimen. The Antigo soil specimen #1 (Figure 4.13a) was subjected to the repeated load triaxial test at γ_{dmax} = 17.4 kN/m^3 and $w_{opt.}$ = 14.6%, while the Dodgeville specimen #5 was tested at γ_{dmax} = 15.8 kN/m^3 and $w_{opt.}$ = 20.1%. The resilient modulus as a dynamic soil stiffness modulus is affected by moisture content and unit weight of the soil. Soils under higher unit weight and lower moisture content are expected to show higher stiffness modulus.

Figure 4.14 presents the results of the repeated load triaxial test on Beecher soil at 95% γ_{dmax} and $w < w_{opt}$, at γ_{dmax} and w_{opt}, and at 95% γ_{dmax} and $w > w_{opt}$. This is to demonstrate the effect of the moisture content on the resilient modulus of the investigated soils. Test results on the Beecher soil specimen tested at 95% γ_{dmax} and $w < w_{opt}$ (dry side) showed that

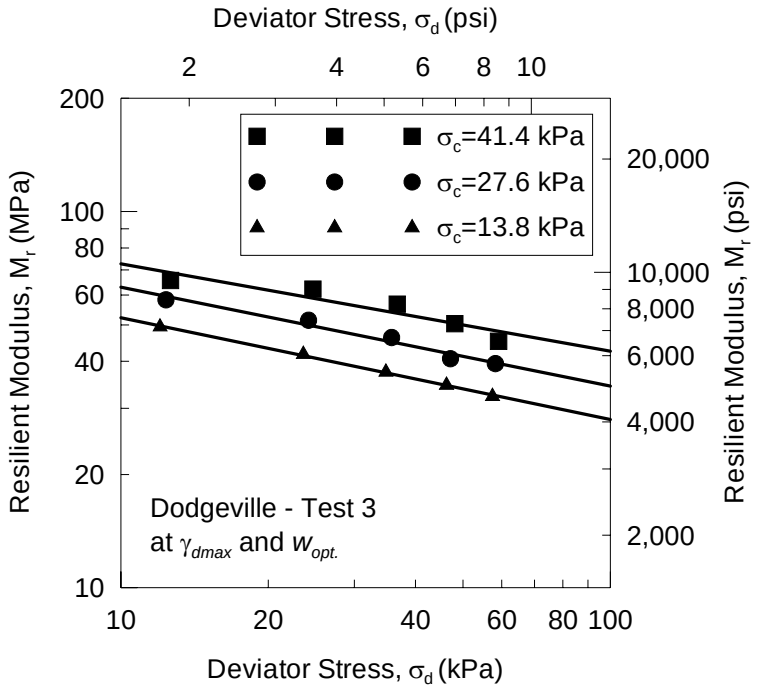

(a) Test on soil specimen #3

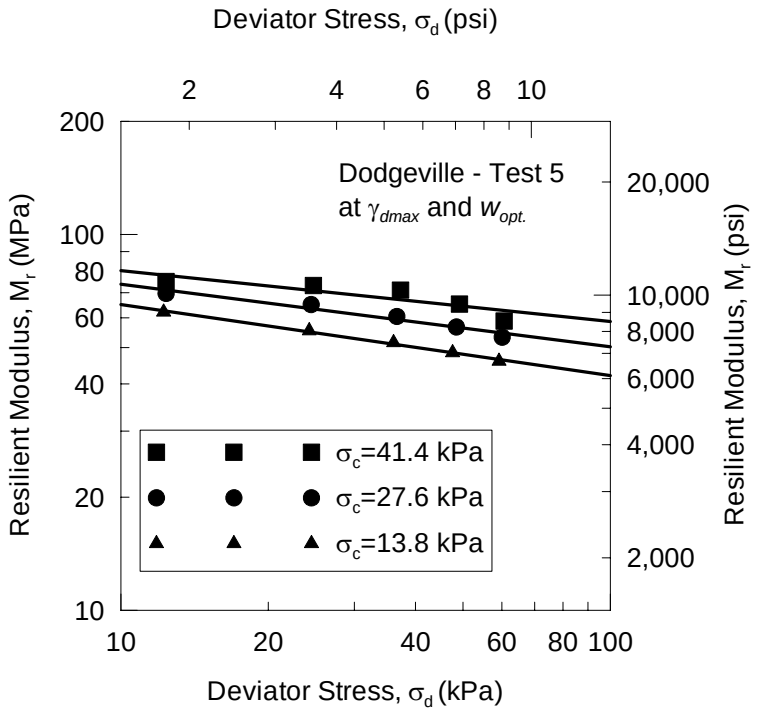

(b) Test on soil specimen #5

Figure 4.10: Results of repeated load triaxial test on Dodgeville soil compacted at maximum dry unit weight (γ_{dmax}) and optimum moisture content ($w_{opt.}$)

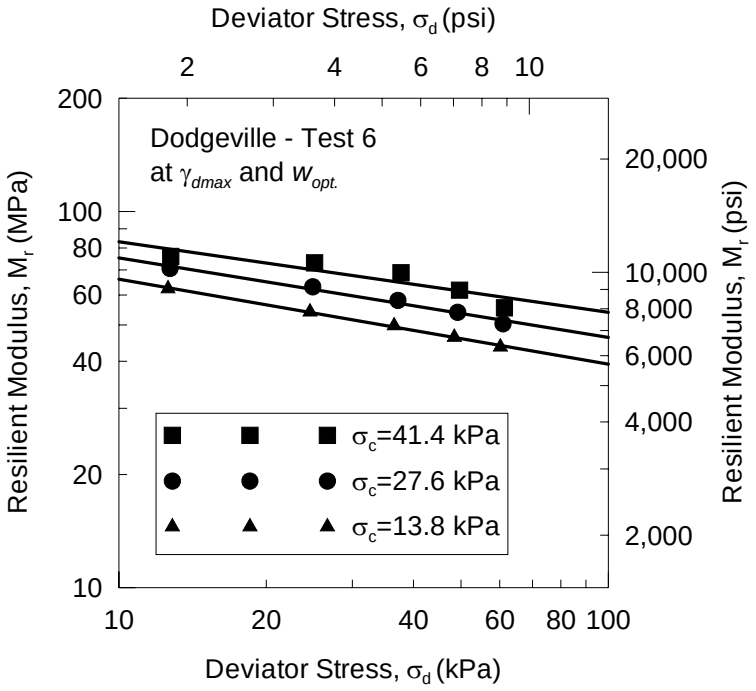

(c) Test on soil specimen #6

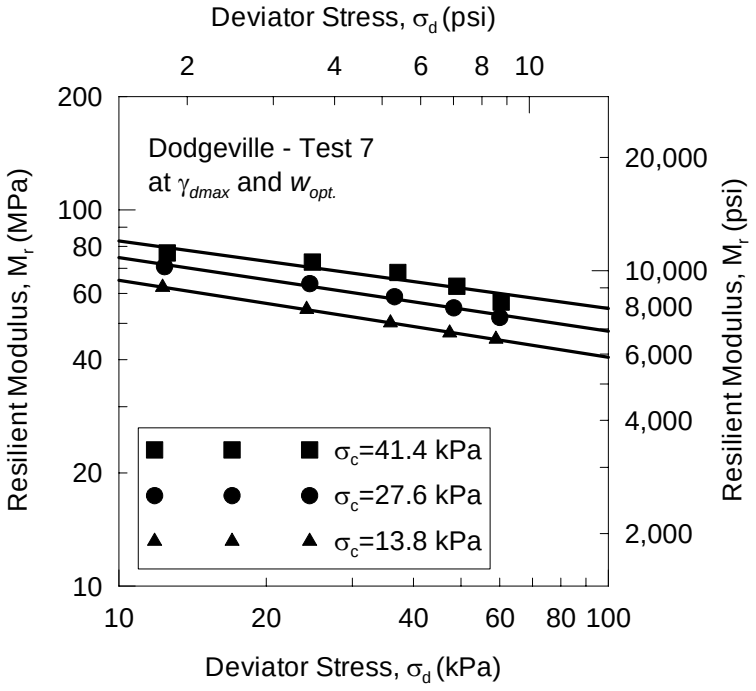

(d) Test on soil specimen #7

Figure 4.10 (cont.): Results of repeated load triaxial test on Dodgeville soil compacted at maximum dry unit weight (γ_{dmax}) and optimum moisture content ($w_{opt.}$)

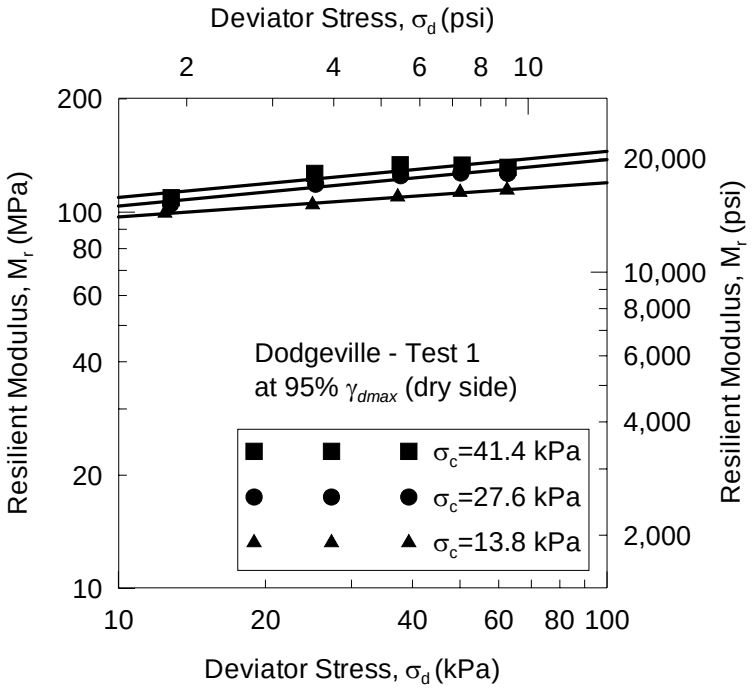

(a) Test on soil specimen #1

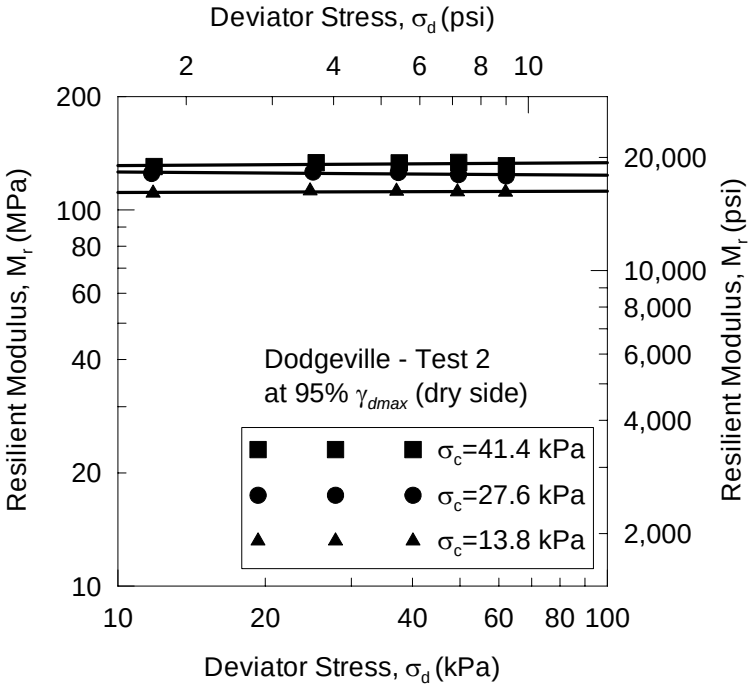

(b) Test on soil specimen #2

Figure 4.11: Results of repeated load triaxial test on Dodgeville soil compacted at 95% of maximum dry unit weight (γ_{dmax}) and moisture content less than $w_{opt.}$ (dry side)

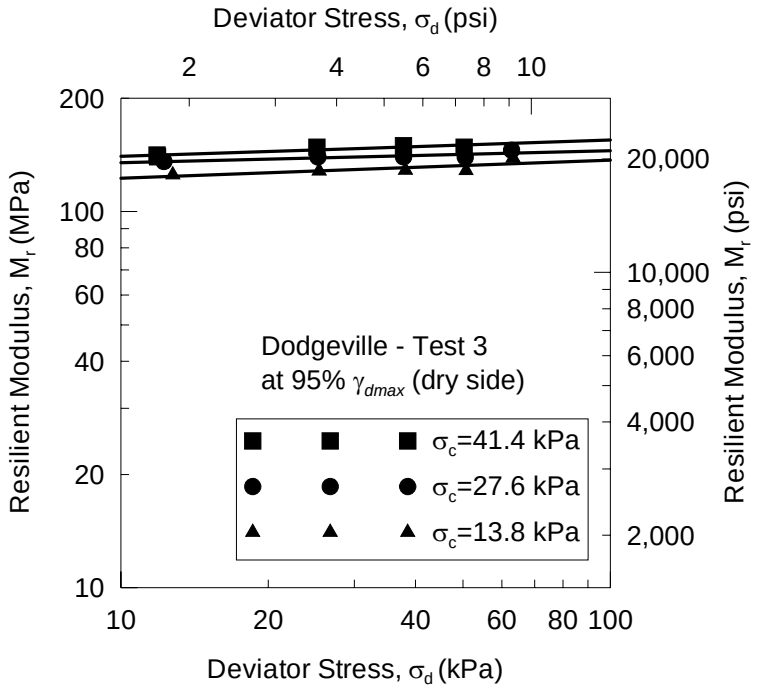

(c) Test on soil specimen #3

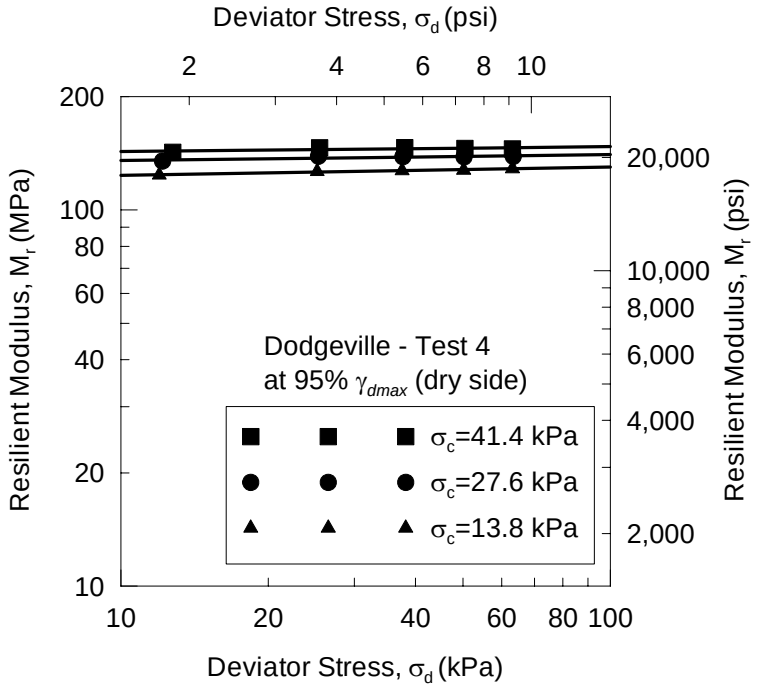

(d) Test on soil specimen #4

Figure 4.11 (cont.): Results of repeated load triaxial test on Dodgeville soil compacted at 95% of maximum dry unit weight (γ_{dmax}) and moisture content less than $w_{opt.}$ (dry side)

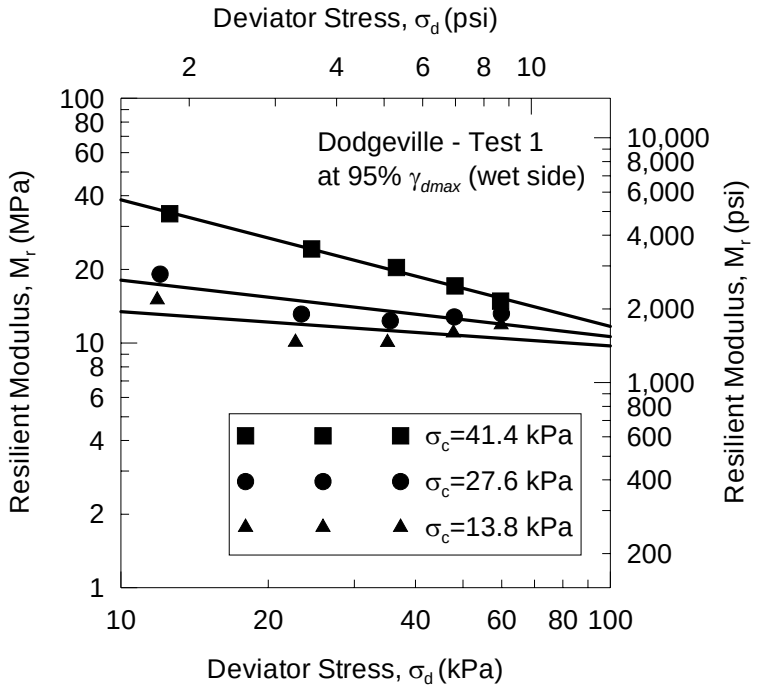

(a) Test on soil specimen #1

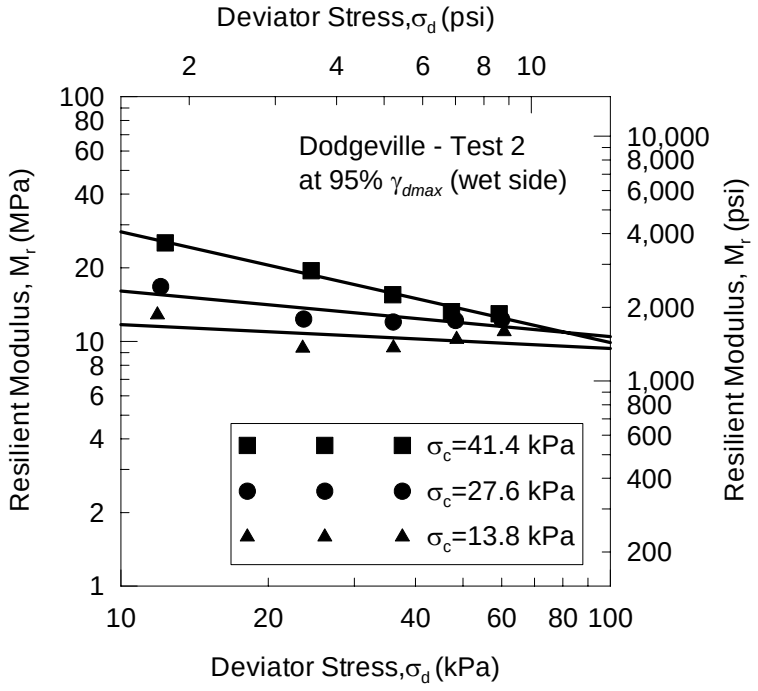

(b) Test on soil specimen #2

Figure 4.12: Results of repeated load triaxial test on Dodgeville soil compacted at 95% of maximum dry unit weight (γ_{dmax}) and moisture content more than $w_{opt.}$ (wet side)

Table 4.4: Analysis of repeatability tests on Dodgeville soil tested at maximum dry unit weight and optimum moisture content

Test Sequence	σ_c (kPa)	Test #5		Test #6		Test #7		Mean σ_d (kPa)	Mean M_r (MPa)	CV(σ_d)	CV(M_r)
		σ_d (kPa)	M_r (MPa)	σ_d (kPa)	M_r (MPa)	σ_d (kPa)	M_r (MPa)				
1	41.4	12.4	75.0	12.8	76.0	12.5	76.9	12.6	76.0	1.6	1.2
2		24.7	73.1	25.1	73.1	24.9	72.7	24.9	73.0	0.8	0.3
3		37.3	71.1	37.7	68.7	37.2	68.3	37.4	69.4	0.8	2.2
4		49.2	65.3	49.7	61.8	49.0	62.7	49.3	63.3	0.7	2.9
5		60.6	58.8	61.4	55.5	60.4	56.9	60.8	57.1	0.8	2.9
6	27.6	12.4	69.7	12.7	70.6	12.4	70.7	12.5	70.3	1.5	0.8
7		24.5	65.1	24.9	63.1	24.5	63.7	24.6	64.0	0.9	1.6
8		36.6	60.5	37.2	58.1	36.6	58.8	36.8	59.1	0.9	2.1
9		48.5	56.8	49.2	53.9	48.3	54.9	48.7	55.2	1.0	2.6
10		60.1	53.3	60.9	50.3	60.0	51.8	60.3	51.8	0.8	2.9
11	13.8	12.2	62.1	12.6	62.4	12.3	62.3	12.4	62.3	1.6	0.2
12		24.3	55.5	24.6	54.2	24.2	54.5	24.3	54.7	0.8	1.3
13		36.1	51.6	36.5	49.7	35.9	50.1	36.2	50.5	0.9	1.9
14		47.6	48.5	48.5	46.4	47.4	47.1	47.8	47.3	1.2	2.2
15		59.2	46.0	60.2	43.7	58.9	45.3	59.5	45.0	1.1	2.7

Table 4.5: Analysis of repeatability tests on Dodgeville soil tested at 95% of maximum dry unit weight and moisture content less than the optimum moisture content (dry side)

Test Sequence	σ_c (kPa)	Test #1		Test #2		Test #4		Mean σ_d (kPa)	Mean M_r (MPa)	CV(σ_d)	CV(M_r)
		σ_d (kPa)	M_r (MPa)	σ_d (kPa)	M_r (MPa)	σ_d (kPa)	M_r (MPa)				
1	41.4	12.8	109.2	11.9	130.3	12.8	142.3	12.5	127.3	4.4	13.2
2		25.2	126.8	25.4	133.5	25.5	146.4	25.4	135.6	0.5	7.3
3		37.7	133.6	37.6	133.3	38.0	146.5	37.8	137.8	0.6	5.5
4		50.5	133.5	49.7	133.7	50.5	145.7	50.2	137.6	0.9	5.1
5		62.7	131.6	62.2	131.0	63.1	145.3	62.7	136.0	0.7	6.0
6	27.6	12.8	105.0	11.7	125.1	12.2	134.9	12.2	121.7	4.4	12.5
7		25.3	118.7	25.0	126.1	25.3	138.9	25.2	127.9	0.7	8.0
8		37.8	125.1	37.4	125.7	37.7	138.5	37.6	129.8	0.5	5.8
9		50.2	127.1	49.6	124.2	50.3	138.4	50.0	129.9	0.7	5.8
10		62.6	126.8	62.1	123.2	63.3	138.8	62.7	129.6	1.0	6.3
11	13.8	12.4	99.5	11.8	110.8	12.0	123.8	12.1	111.4	2.8	10.9
12		25.0	104.6	24.7	112.4	25.2	126.7	25.0	114.6	1.0	9.8
13		37.3	109.8	37.1	112.2	37.5	127.3	37.3	116.4	0.6	8.2
14		50.0	113.0	49.4	111.7	50.2	127.7	49.9	117.5	0.8	7.5
15		62.4	114.5	61.9	111.5	63.1	128.8	62.5	118.3	1.0	7.8

Table 4.6: Analysis of repeatability tests on Dodgeville soil tested at 95% of maximum dry unit weight and moisture content greater than the optimum moisture content (wet side)

Test Sequence	σ_c (kPa)	Test #1		Test #2		Mean σ_d (kPa)	Mean M_r (MPa)	CV(σ_d)	CV(M_r)
		σ_d (kPa)	M_r (MPa)	σ_d (kPa)	M_r (MPa)				
1	41.4	12.6	33.7	12.3	25.3	12.5	29.5	1.4	20.2
2		24.5	24.3	24.5	19.5	24.5	21.9	0.2	15.5
3		36.6	20.4	35.9	15.5	36.2	17.9	1.2	19.1
4		48.2	17.1	47.3	13.2	47.8	15.2	1.2	18.1
5		59.7	14.9	59.2	13.0	59.5	13.9	0.5	9.5
6	27.6	12.0	19.1	12.1	16.7	12.0	17.9	0.2	9.4
7		23.4	13.1	23.6	12.3	23.5	12.7	0.8	4.4
8		35.5	12.3	36.0	12.0	35.8	12.2	1.0	1.8
9		48.0	12.8	48.3	12.2	48.1	12.5	0.4	3.5
10		59.9	13.2	60.0	12.3	59.9	12.7	0.1	4.9
11	13.8	11.9	15.0	11.9	12.8	11.9	13.9	0.0	11.1
12		22.7	10.1	23.5	9.4	23.1	9.7	2.4	5.0
13		35.1	10.1	36.0	9.4	35.6	9.7	1.9	4.7
14		47.8	11.0	48.5	10.2	48.2	10.6	1.1	5.3
15		59.8	11.9	60.7	11.0	60.3	11.4	1.0	5.6

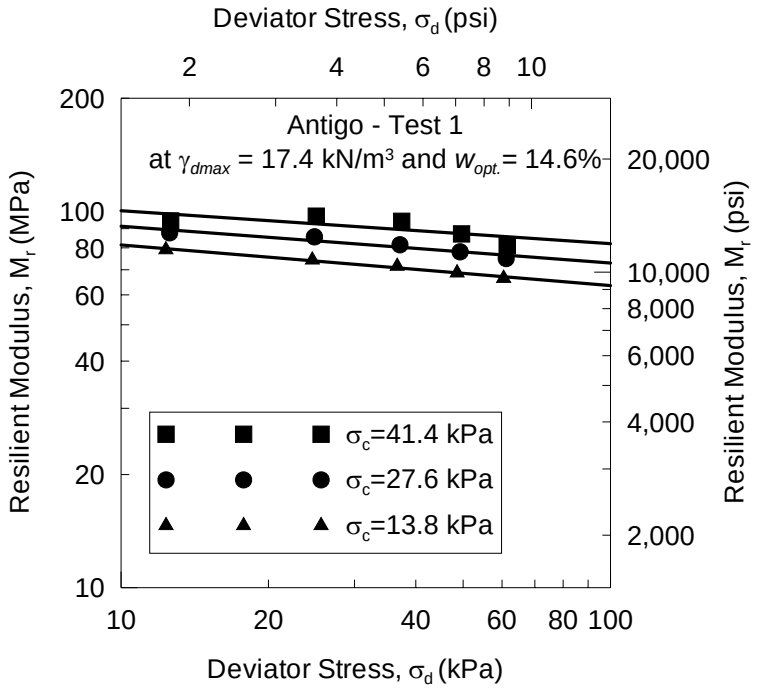

(a) Antigo

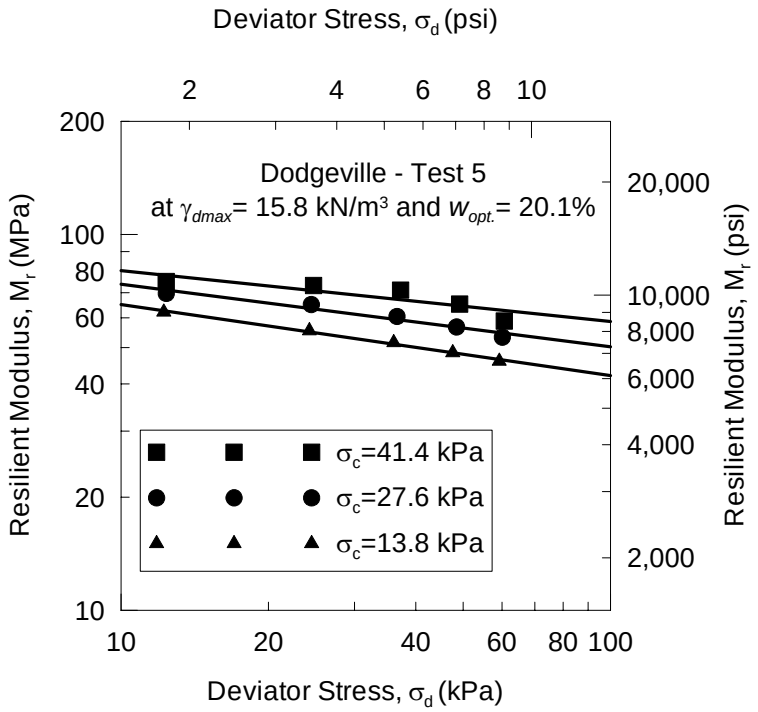

(b) Dodgeville

Figure 4.13: The effect of unit weight and moisture content on the resilient modulus of the investigated soils

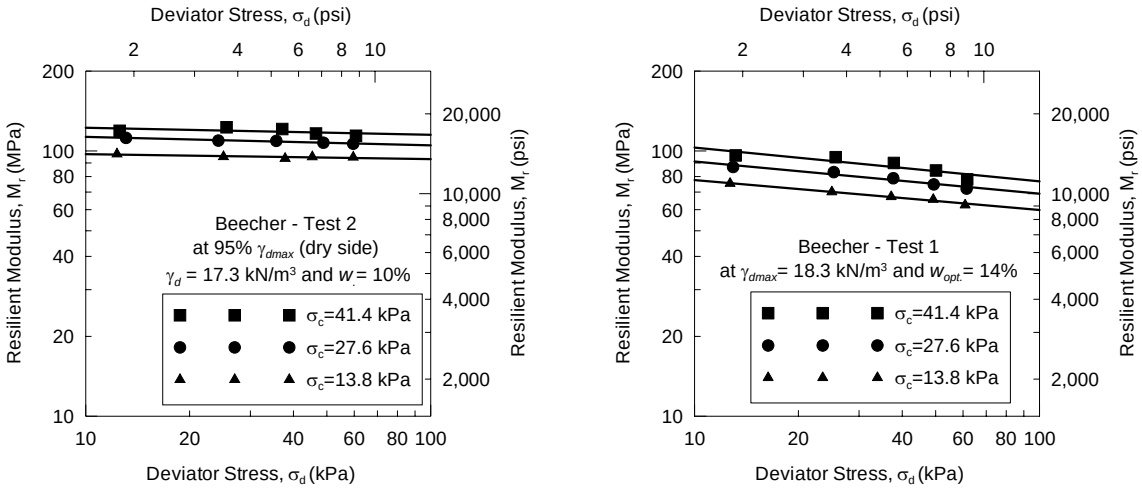

(a) Dry side **(b) Optimum**

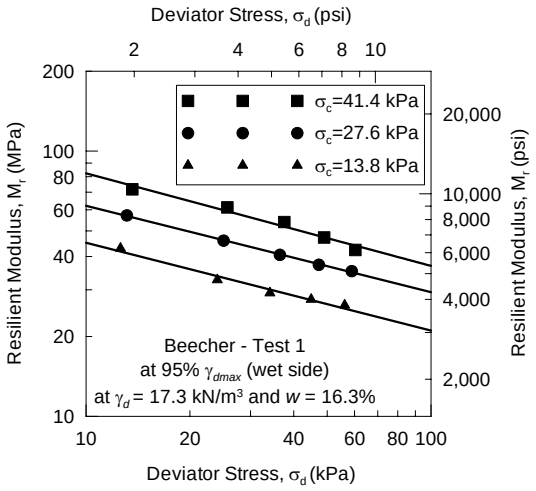

(c) Wet side

Figure 4.14: The effect of the moisture content on the resilient modulus of the investigated soils

at confining pressure σ_c = 41.4 kPa, the resilient modulus decreased from M_r = 119 MPa at σ_d = 12.5 kPa to M_r = 114 MPa at σ_d = 60.7 kPa. The Beecher specimen tested at 95% γ_{dmax} and $w > w_{opt}$ showed a decrease in the resilient modulus from M_r = 72 MPa at σ_d = 13.6 kPa to M_r = 42 MPa at σ_d = 60.3 kPa. Both specimens have similar unit weight values (γ_d = 17.3 kN/m^3) and different moisture content. The Beecher specimen with lower moisture content exhibited higher resilient modulus values compared to the other specimen with higher moisture content under the same unit weight. The effect of increased moisture content of the soil on reducing the resilient modulus is significant. The soil specimen tested at γ_{dmax} and w_{opt} exhibited resilient modulus values less than the specimen compacted at 95% γ_{dmax} and $w < w_{opt}$ (dry side). This is mainly attributed to the moisture content since the specimen compacted at optimum moisture content has 4% more moisture. Even though the specimen compacted at γ_{dmax} has higher unit weight, the influence of moisture content surpassed the effect of unit weight.

For many of the investigated soils, the resilient modulus values of the soil compacted at 95%γ_{dmax} on the dry side are higher than M_r values of the same soil compacted at γ_{dmax} and optimum moisture content. The soil compacted at moisture content less than the optimum and 95%γ_{dmax} exhibited hardening and showed higher values of resilient modulus with the increase of the deviator stress. The soil compacted at unit weight of 95% γ_{dmax} on the wet side exhibited low resilient modulus values compared to the same soil compacted at optimum moisture content.

The results of repeated load triaxial test on the investigated soils are presented in Appendix B.

4.3 Statistical Analysis

Results obtained from basic soil testing and repeated load triaxial test were used to develop correlations for predicting the resilient modulus model parameters using the resilient modulus constitutive equation selected by NCHRP Project 1-37A for the mechanistic-empirical pavement design. Repeated load triaxial tests were conducted, on average, six times on each soil type at three different moisture content levels and two dry unit weight levels (i.e. 95% γ_{dmax} and γ_{dmax}). It should be noted that Kewaunee soil was subjected to testing only once under each moisture content level due to unavailability of soil samples.

4.3.1 Evaluation of the Resilient Modulus Model Parameters

The resilient modulus model is a general constitutive equation that was developed through NCHRP project 1-28A and was selected for implementation in the upcoming AASHTO Guide for the Design of New and Rehabilitated Pavement Structures. The resilient modulus model can be used for all types of subgrade materials. The resilient modulus model is defined by (NCHRP 1-28A):

$$M_r \quad k_1 P_a \left(\frac{\sigma_b}{P_a} \right)^{k_2} \left(\frac{\tau_{oct}}{P_a} + 1 \right)^{k_3} \qquad \textbf{(4.1)}$$

where:

M_r = resilient modulus
P_a = atmospheric pressure (101.325 kPa)
σ_b = bulk stress = $\sigma_1 + \sigma_2 + \sigma_3$
σ_1 = major principal stress
σ_2 = intermediate principal stress = σ_3 in axisymmetric condition (triaxial test)
σ_3 = minor principal stress or confining pressure in the repeated load triaxial test
τ_{oct} = octahedral shear stress
k_1, k_2 and k_3 = material model parameters

The octahedral shear stress is defined in general as:

$$\tau_{oct} \quad \frac{1}{3}\sqrt{(\sigma_1 - \sigma_2)^2 + (\sigma_1 - \sigma_3)^2 + (\sigma_2 - \sigma_3)^2} \qquad \textbf{(4.2)}$$

For axisymmetric stress condition (triaxial), $\sigma_2 = \sigma_3$ and $\sigma_1 - \sigma_3 = \sigma_d$ (deviator stress), therefore the octahedral shear stress is reduced to:

$$\tau_{oct} \quad \frac{\sqrt{2}}{3}(\sigma_d) \qquad \textbf{(4.3)}$$

The resilient modulus, the bulk stress and the octahedral shear stress are normalized in this model by the atmospheric pressure. This will result in non-dimensional model parameters.

Statistical analysis based on multiple linear regression was utilized to determine the resilient modulus model parameters k_1, k_2 and k_3. The statistical analysis software STATISTICA was used to perform the analysis. In order to determine k_1, k_2, and k_3 using the experimental test results, the resilient modulus model Equation 4.1 was transformed to:

$$\log\left(\frac{M_r}{P_a} \right) \quad \log k_1 + k_2 \log\left(\frac{\sigma_b}{P_a} \right) + k_3 \log\left(\frac{\tau_{oct}}{P_a} + 1 \right) \qquad \textbf{(4.4)}$$

The resilient modulus is treated as the dependent variable, while bulk and octahedral shear stresses are used as the independent variables. The analysis was carried out for each soil type to evaluate the model parameters (k_1, k_2 and k_3) from the results of the 15 stress combinations applied during repeated load triaxial test (15 load sequences according to AASHTO T 307). A total of 136 repeated load tests were used in the analysis. Results of this analysis are summarized in Table 4.7.

Table 4.7: Basic statistical data of the resilient modulus model parameters k_i obtained from the test results of the investigated soils

Parameter	Mean	Median	Minimum	Maximum	Std. Dev.	Standard Error
k_1	826.8	832.0	201.2	1318.7	250.4	21.47
k_2	0.517	0.456	0.176	1.083	0.243	0.021
k_3	-2.142	-1.919	-6.013	-0.105	1.373	0.118

The analysis showed that k_1 ranges from 201.2 to 1318.7 with a mean value of 826.8. The magnitude of k_1 was always > 0 since the resilient modulus should always be greater than zero. The parameter k_2 which, is related to the bulk stress, varies between 0.176 and 1.083 with mean value of 0.517. The values of k_2 were also greater than zero since the resilient modulus increases with the increase in the bulk stress (confinement). Since the resilient modulus decreases with the increase in the deviator stress, the parameter k_3 ranges from -6.013 to -0.105 with a mean value of -2.142. The model parameters k_i obtained from the statistical analysis on the repeated load test results are presented in histograms in Figure 4.15.

4.3.2 Correlations of Model Parameters with Soil Properties

The resilient modulus model parameters k_1, k_2 and k_3 were determined for all soil types. These parameters are then correlated to fundamental soil properties using regression analysis. The values of resilient modulus model parameters (k_1, k_2 and k_3) were alternatively used as dependent variables while various fundamental soil properties were treated as independent variables. Various combinations of soil properties (independent variables) were used in the regression analysis. The general multiple linear regression model is expressed as:

$$k_i \quad \beta_0 + \beta_1 x_1 + \beta_2 x_2 + \cdots + \beta_k x_k + \in \qquad \textbf{(4.5)}$$

where:
k_i = the dependent variable for the regression, (model parameters k_1, k_2 or k_3)
β_0 = intercept of the regression plane
β_i = regression coefficient
x_i = the independent or regressor variable, (in this study, soil property or a combination of soil properties)
$\in$ = random error

It should be noted that general nonlinear models that include factorial and polynomial regression were attempted in this study. The resulted correlations were not successful due to the existence of a large intercorrelation between the independent variables. In addition, some of the correlation coefficients conflict with the natural behavior of soils. As an example, the increase in the dry unit weight leads to a decrease in the resilient modulus.

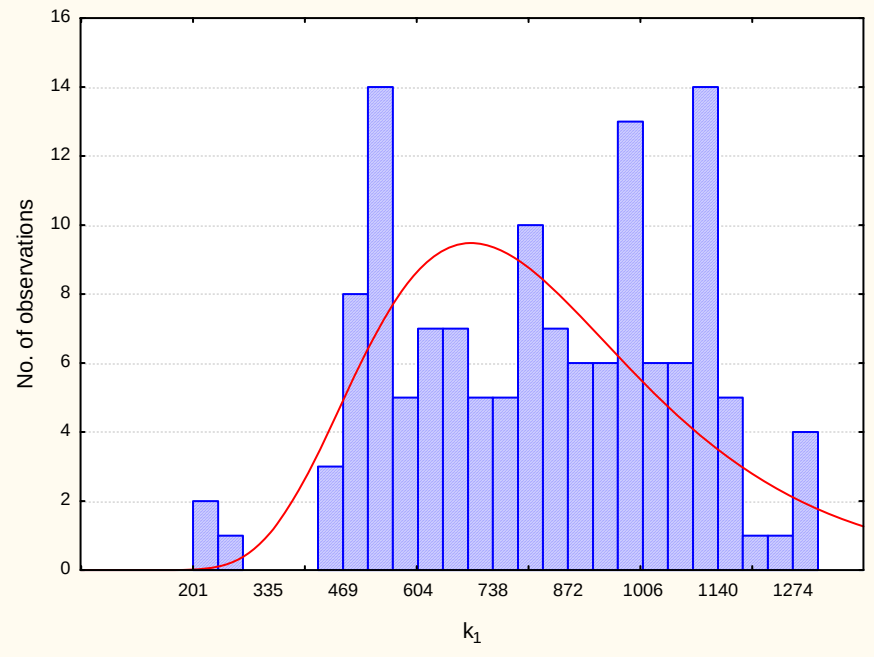

(a) Resilient modulus model parameter k_1

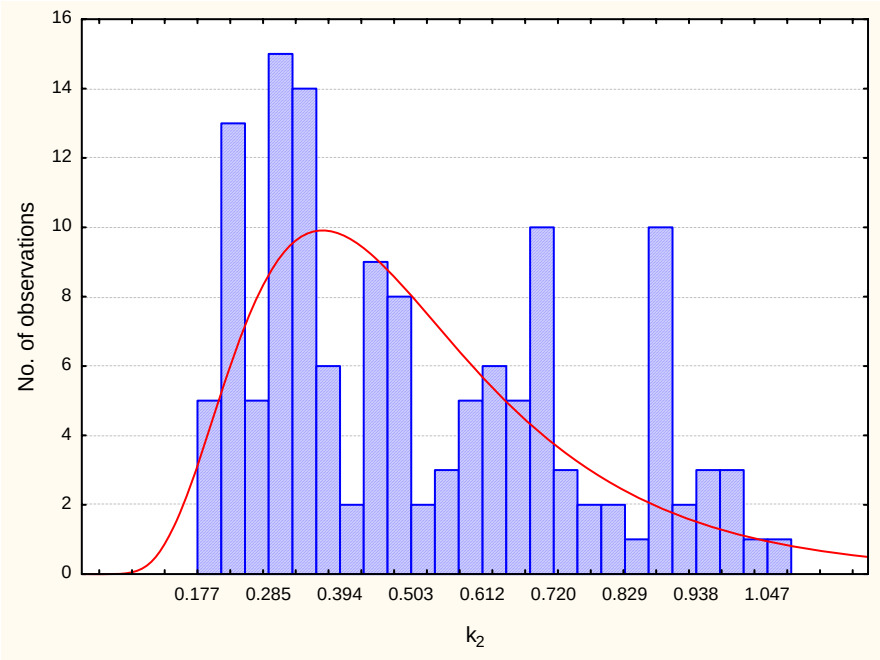

(b) Resilient modulus model parameter k_2

Figure 4.15: Histograms of resilient modulus model parameters k_i obtained from statistical analysis on the results of the investigated Wisconsin soils

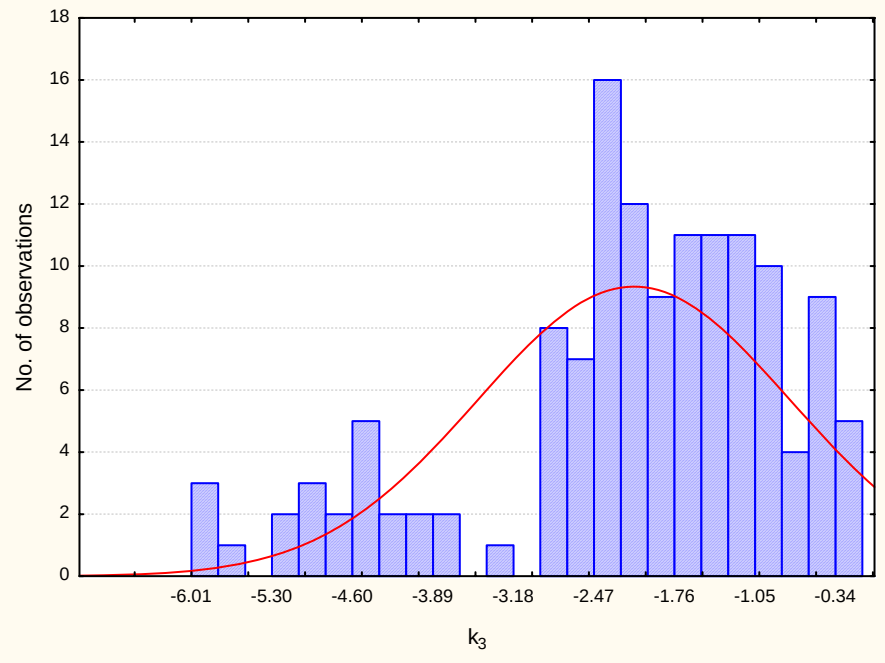

(c) Resilient modulus model parameter k_3

Figure 4.15 (cont.): Histograms of resilient modulus model parameters k_i obtained from statistical analysis on the results of the investigated Wisconsin soils

Selection of Soil Properties

The resilient modulus is used to evaluate the stiffness of bound/unbound materials. Factors that affect resilient modulus are stress state, soil type and the environmental conditions of the soil that influence the soil physical state (unit weight and moisture content). Stress state is expressed in the resilient modulus model by including bulk and octahedral stresses. The soil type and the current soil physical condition should be included in attempted correlations in order to obtain valid estimation/prediction of the resilient modulus.

Sets of independent variables are specified to reflect soil type and current soil physical condition. Independent variables available from basic soil testing that represent soil type and current soil physical condition are: percent passing sieve #4 ($P_{No.4}$), percent passing sieve #40 ($P_{No.40}$), percent passing sieve #200 ($P_{No.200}$), liquid limit (LL), plastic limit (PL), Plasticity Index (PI), Liquidity Index (LI), amount of sand (%Sand), amount of silt (%Silt), amount of clay (%Clay), water content (w) and dry unit weight (γ_d). The optimum water content ($w_{opt.}$) and maximum dry unit weight (γ_{dmax}) and combinations of variables were also included.

The goal of the regression analysis is to identify the best subset of independent variables that results in accurate correlation between resilient modulus model parameters k_i and basic soil properties. Several combinations of regression equations were attempted and evaluated based on the criteria of the coefficient of multiple determination (R^2), the significance of the model and the significance of the individual regression coefficients.

In this study, a correlation matrix was used as a preliminary method for selecting material properties used in the regression analysis models. The magnitude of each element in the correlation matrix indicates how strongly two variables (whether independent or dependent) are correlated. The degree of correlation is expressed by a number that has a maximum value of one for highly correlated variables, and zero if no correlation exists. This was used to evaluate the importance of each independent variable (soil property) among other independent variables to the dependent variable (model parameters k_i).

Measure of Model Adequacy

The coefficient of multiple determination was used as a primary measure to select the best correlation. However, a high R^2 does not necessarily imply that the regression model is a good one. Adding a variable to the model may increase R^2 (at least slightly) whether the variable is statistically significant or not. This may result in poor predictions of new observations. The significance of the model and individual regression coefficients were tested for each proposed model. In addition, the independent variables were checked for multicollinearity to insure the adequacy of the proposed models.

Test for Significance of the Model

The significance of the model is tested using the *F*-test to insure a linear relationship between k_i and the estimated regression coefficients (independent variables).
For testing hypotheses on the model:

H_0: $\beta_1 = \beta_2 = \text{---} = \beta_k = 0$
H_a: $\beta i \neq 0$ for at least one i

where H_0 is the null hypothesis, and H_a is the alternative hypothesis.

The test statistic is:

$$F_0 \quad \frac{SS_R / p}{SS_E / (n - p - 1)} \qquad \textbf{(4.6)}$$

where: SS_R is the sum of squares due to regression, SS_E is the sum of squares due to errors, n is the number of observations and p is the number of independent variables.
H_0 is rejected if $F_0 > F_{\alpha,p,n-p-1}$

where, α is the significance level (used as 0.05 for all purposes in this study).

Test for Significance of Individual Regression Coefficients

The hypotheses for testing the significance of individual regression coefficient β_i is based on the t-test and is given by:

H_0: $\beta_i = 0$
H_a: $\beta_i \neq 0$

The test statistic is:

$$t_0 \quad \frac{\hat{\beta}_i}{\sqrt{\hat{\sigma}^2 C_{ii}}} \qquad \textbf{(4.7)}$$

where C_{ii} is the diagonal element of $(X'X)^{-1}$ corresponding to $\hat{\beta}_i$ (estimator of β_i) and $\hat{\sigma}$ is estimator for the standard deviation of errors, X (n,p) is matrix of all levels of the independent variables, X' is the diagonal X matrix, n is the number of observations, and p is the number of independent variables.

H_0 is rejected if $|t_0| > t_{\alpha/2,n-p-1}$

Multicollinearity Treatment

Multicollinearity is a common problem in multiple regression analysis. It is recognized when a large intercorrelation between the independent variables exists. This can result in an incorrect estimate of regression coefficients. In this study, the inspection of individual elements of correlation matrix was used as a primary check for multicollinearity. A value of 0.8 indicates strong collinearity between two variables and will inflate the standard errors of the regression coefficients.

The variance inflation factor (VIF) was also used to detect multicollinearity for each proposed model. The VIF is the set elements in the diagonal of the inverse of the correlation matrix. A conservative suggestion is to consider the maximum magnitude of an element in the VIF>4 as a multicollinearity problem. Some researchers consider the maximum magnitude of an element in the VIF>8 as a multicollinearity problem (Hines and Montgomery 1980). For this study, all proposed models were checked for multicollinearity.

4.3.3 Statistical Analysis Results

In the first attempt of analysis, all data points were used to develop correlations between the resilient modulus model parameters (k_1, k_2 and k_3) and selected soil properties. This analysis produced poor correlations as R^2 values were too low and models were insignificant for predicting the resilient modulus constitutive model parameters. Another

attempt of analysis was made in which fine-grained and coarse-grained soils were separated and analyzed independently. Table 4.8 presents a summary of the soil constituents based on particle size analysis.

Table 4.8: Constituents of the investigated soils

Soil Type/location	Passing Sieve #200 (%)	Sand (%)	Silt (%)	Clay (%)
Antigo	91	-	76	15
Beecher	48	42	33	15
Goodman	15	53	14	1
Plano	27	66	23	4
Dodgeville	97	-	80	17
Dubuque	72	-	57	15
Chetek	29	69	25	4
Eleva	20	80	15	5
Pence	22	64	21	1
Gogebic	32	63	28	4
Miami	96	-	74	22
Ontonagon - 1	31	60	22	9
Ontonagon - 2	27	63	18	9
Kewaunee-1	30	67	25	5
Kewaunee-2	48	41	32	16
Plainfield	2	98	-	-
Sayner-Rubicon	1	82	-	-
Shiocton	41	58	41	0.1
Withee	35	62	24	11

Fine-Grained Soils

Regression analysis was conducted on the results of the fine-grained soils. Different basic soil properties were included to obtain correlations with the resilient modulus model parameters k_1, k_2, and k_3. Each correlation was examined from both physical and statistical points of view. If the model was not consistent with the observed behavior of soils, it was rejected. Many attempts were made in which basic soil properties were included. Tables 4.9-4.11 present summaries of the regression analysis results in which models to estimate k_1, k_2, and k_3 from basic soil properties were obtained. Figure 4.16 depicts comparisons between k_i values obtained from analysis of the results of the repeated load triaxial test (considered herein as measured values) and k_i values estimated from basic soil properties using the proposed correlations (Tables 4.9-4.11). Examination of Tables 4.9-4.11 shows that these models are consistent with the natural behavior of the soils. These models are statistically validated later in this report. The magnitudes of R^2 for k_1 correlations range between 0.83 and 0.88, which is considered acceptable. Lower R^2 values were obtained for k_2 and k_3 as shown in Tables 4.10 and 4.11. Figure 4.16 also

demonstrates the good estimation capability of these models. It should be emphasized that these models were obtained based on statistical analysis on test data that are limited to fine-grained soils compacted at relatively high unit weight. Extrapolation of these models at soil physical condition levels beyond this is not validated in this study.

Table 4.9: Correlations between the resilient modulus model parameter k_1 and basic soil properties for fine-grained soils

Variable	k_1 correlations			
	Model 1	**Model 2**	**Model 3**	**Model 4**
Intercept	1262.543	1286.35	404.166	1358.33
w **(%)**	-50.592	-	-	-
γ_d **(kN/m^3)**	-	49.84	52.260	-
PI **(%)**	41.128	43.13	42.933	48.30
$P_{No.200}$ **(%)**	-	-	-	-3.4
$\frac{\gamma_d}{\gamma_{d\max}}$	-	-	-	123.28
$\frac{w}{w_{opt.}}$	-	-1478.59	-987.353	-1000.45
$\frac{\gamma_d}{\gamma_{d\max}} \times \frac{w}{w_{opt.}}$	-67.949	-	-	-
$\frac{P_{No.200}}{w}$	-	-67.03	-	-
$\mathbf{R^2}$	0.83	0.88	0.84	0.84

Table 4.10: Correlations between the resilient modulus model parameter k_2 and basic soil properties for fine-grained soils

Variable	k_2 correlations		
	Model 1	**Model 2**	**Model 3**
Intercept	0.25113	1.48741	2.29889
LL **(%)**	-	- 0.029728	
LI	-	-	0.90482
PI **(%)**	-0.02917	-	-0.06352
$\frac{\gamma_d}{\gamma_{d\max}} \times \frac{w}{w_{opt.}}$	0.55733	-	-0.74418
$\frac{\gamma_d}{\gamma_{d\max}} \times \frac{w - w_{opt}}{w_{opt.}}$	-	0.61868	-
$\mathbf{R^2}$	0.65	0.70	0.76

Table 4.11: Correlations between the resilient modulus model parameter k_3 and basic soil properties for fine-grained soils

Variable	k_3 correlations		
	Model 1	**Model 2**	**Model 3**
Intercept	-0.20772	-0.14561	-5.5205
γ_d **(kN/m^3)**	0.00367	-	-
PI **(%)**	0.23088	0.23079	0.22765
$\frac{w}{w_{opt.}}$	-5.42384	-5.4260-	-
$w - w_{opt}$	-	-	0.29906
$\mathbf{R^2}$	0.76	0.76	0.76

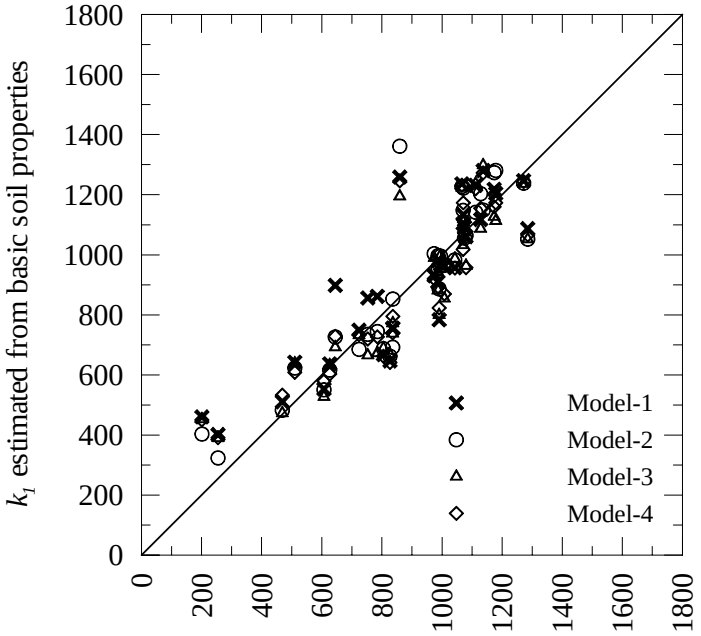

(a) k_1

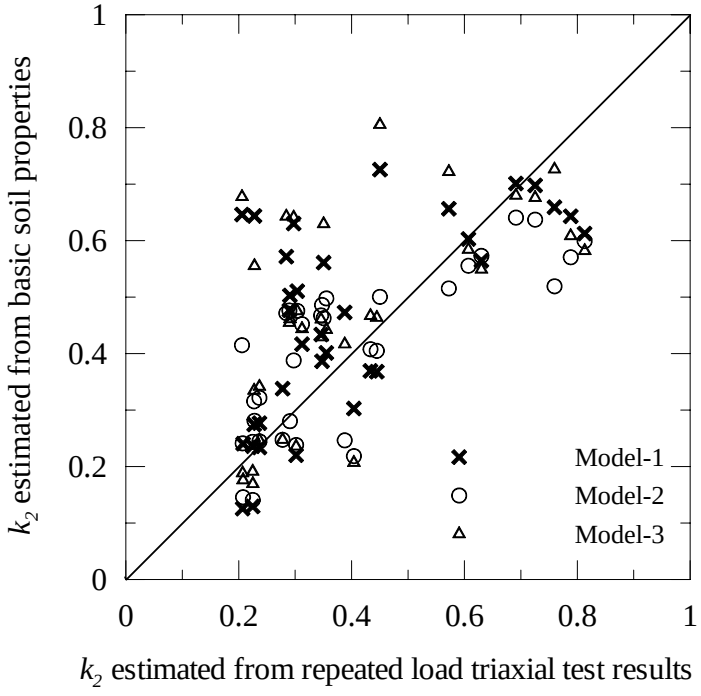

(b) k_2

Figure 4.16: Comparison of resilient modulus model parameters (k_i) estimated from soil properties and k_i determined from results of repeated load triaxial test on investigated fine-grained soils

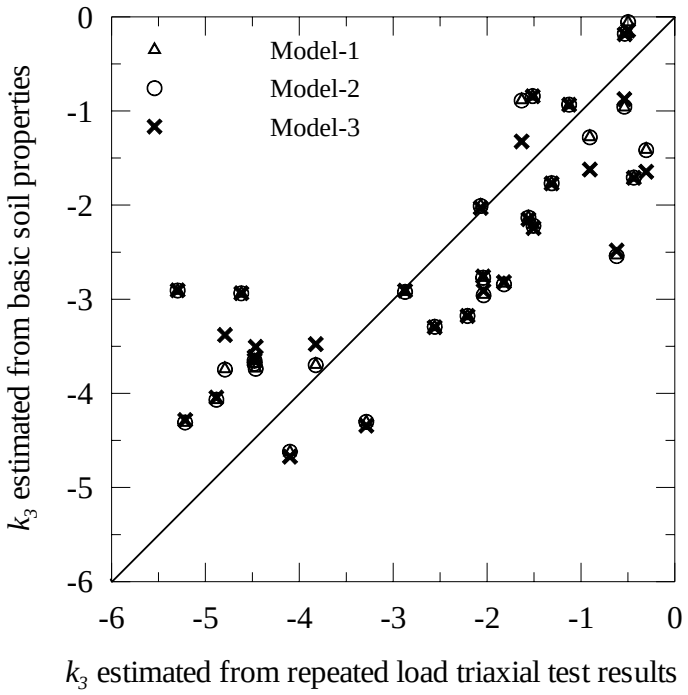

(c) k_3

Figure 4.16 (cont.): Comparison of resilient modulus model parameters (k_i) estimated from soil properties and k_i determined from results of repeated load triaxial test on investigated fine-grained soils

Based on the statistical analysis on the results of the investigated fine-grained soils, the resilient modulus model parameters (k_i) can be estimated from basic soil properties using the following equations:

$$k_1 \quad 404.166 + 42.933PI + 52.260\gamma_d - 987.353\left(\frac{w}{w_{opt}}\right) \qquad \textbf{(4.8)}$$

$$k_2 \quad 0.25113 - 0.0292PI + 0.5573\left(\frac{w}{w_{opt}}\right) \times \left(\frac{\gamma_d}{\gamma_{d\max}}\right) \qquad \textbf{(4.9)}$$

$$k_3 \quad -0.20772 + 0.23088PI + 0.00367\gamma_d - 5.4238\left(\frac{w}{w_{opt}}\right) \qquad \textbf{(4.10)}$$

where PI is the plasticity index, w is the moisture content of the soil, $w_{opt.}$ is the optimum moisture content, γ_d is the dry unit weight, and γ_{dmax} is the maximum dry unit weight.

Table 4.12 presents the correlation matrix of soil properties used in the regression and model parameters for fine-grained soils. A summary of regression coefficients obtained for the fine-grained correlations with *t*-statistics at 95% confidence level is presented in Tables 4.13. The overall significance of k_i correlations was verified based on the *F*-test. This means that k_i and the estimated regression coefficients of independent variables for all correlations constitute a linear relationship. The results of the *t*-statistics showed that, (ignoring the significance of the intercept β_0), the dry unit weight in both k_1 and k_3 models was insignificant in the case of fine-grained soils. The t-statistics were determined as 1.23 and 0.01 for the k_1 and k_3 models, respectively. The *t*-statistics are not significant if the absolute value of t_0 (from table of parameter estimator) is less than $t_{\alpha/2,n-p-1}$ (from statistics tables). The minimum value of t_0 for a parameter to be significant at 95% confidence level is 1.96 if a large population was considered. Although γ_d in k_1 and k_3 models for the fine-grained soils were found to be statistically insignificant, their presence is physically sound based on engineering judgment.

Equations 4.8-4.10 were used in the resilient modulus constitutive Equation (4.1) to estimate the resilient modulus of the investigated fine-grained soils. The results are presented in Figure 4.17, which depicts the predicted versus the measured resilient modulus values. Inspection of Figure 4.17 indicates that the resilient modulus of compacted fine-grained soils can be estimated from Equation 4.1 and the correlations proposed by Equations 4.8-4.10 with reasonable accuracy. It should be emphasized that these correlations are developed based on analysis of test results on soils compacted at high unit weight values (between 95 and 100% of γ_{dmax}) with a moisture content range around the optimum value.

Table 4.12: Correlation matrix of model parameters and soil properties for fine-grained soils

Variable	PI	γ_d	w/w_{opt}	$(w/w_{opt}) \times (\gamma_d/\gamma_{dmax})$	k_1	k_2	k_3
PI	1.00	-0.15	0.16	0.03	0.21	-0.32	0.08
γ_d		1.00	-0.15	0.09	0.19	-0.15	0.06
w/w_{opt}			1.00	0.95	-0.84	0.70	-0.85
$(w/w_{opt})\times(\gamma_d/\gamma_{dmax})$				1.00	-0.83	0.73	-0.86
k_1					1.00	-0.89	0.79
k_2						1.00	-0.82
k_3							1.00

Table 4.13: Summary of t-statistics for regression coefficients used in resilient modulus model parameters for fine-grained soils

Model Parameter	k_1		k_2		k_3	
	Parameter estimator	*t*-statistic (95% CL)	Parameter estimator	*t*-statistic (95% CL)	Parameter estimator	*t*-statistic (95% CL)
β_0	404.166	0.55	0.25113	1.37	-0.2077	-0.04
β_1	52.260	1.23	-0.02917	-2.49	0.0037	0.01
β_2	42.933	3.55	0.55733	5.40	0.23088	2.55
β_3	-987.353	-9.46	-	-	-5.4238	-6.66
R^2	0.84		0.65		0.76	
SEE	128.63		0.126		0.869	

CL: confidence level, SEE: standard error of estimate

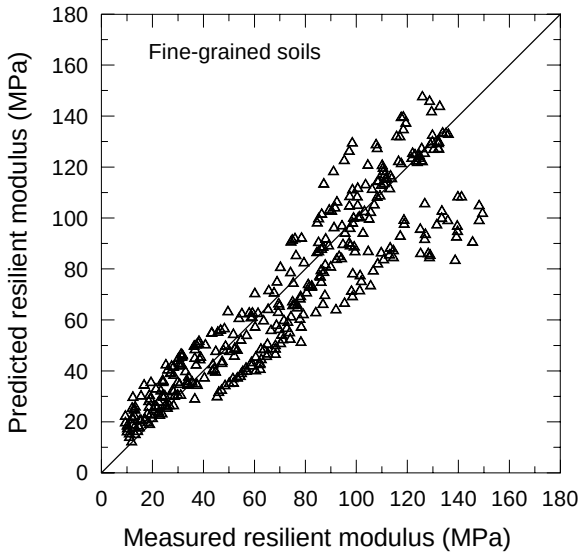

Figure 4.17: Predicted versus measured resilient modulus of compacted fine-grained soils

Coarse-Grained Soils

Regression analysis conducted on the test results of the coarse-grained soils (less than 50% passing sieve #200) resulted in poor correlations between k_i values and basic soil properties. This is due to the fact that some of the investigated coarse-grained soils do not have plasticity characteristics (non-plastic soils). Therefore, coarse-grained soils were separated into two groups for the purpose of statistical analysis: plastic coarse-grained soils and non-plastic coarse-grained soils. This treatment significantly improved the proposed correlations between soil properties and k_i. In addition, parameters related to the grain size characteristics of coarse-grained soils such as coefficient of curvature (C_c), coefficient of uniformity (C_u) and effective size (D_{10}) were included in the analysis (Table 4.14). These parameters did not improve the results of the statistical analysis and therefore were excluded.

Table 4.14: Characteristics of particle size distribution curves of investigated coarse-grained soils

Soil Type	C_u	C_c	D_{10} (mm)	D_{30}(mm)	D_{50}(mm)	D_{60}(mm)
Beecher	102	1.29	9.04E-05	0.001	0.0038	0.0092
Goodman	82.91	1.15	0.0011	0.011	0.0422	0.0938
Plano	27.99	6.09	3.34E-04	0.0044	0.008	0.0094
Chetek	47.54	3.27	2.77E-04	0.0035	0.0106	0.0132
Eleva	29.6	6.2	8.00E-04	0.0109	0.0167	0.0232
Pence	38.35	3.93	5.12E-04	0.0063	0.014	0.0196
Gogebic	48.08	2.75	2.23E-04	0.0026	0.0079	0.0107
Ontonagon-C-1	32.19	4.1	2.39E-04	0.0027	0.0069	0.0077
Ontonagon-C-2	23.74	6.53	3.69E-04	0.0046	0.0076	0.0088
Kewaunee-1	28.8	4.58	2.57E-04	0.003	0.0061	0.0074
Kewaunee-2	110.2	1.2	8.88E-05	0.001	0.0038	0.0098
Plainfield	2.38	0.92	0.0066	0.0098	0.0132	0.0158
Sayner-Rubicon	3.03	0.83	0.0093	0.0143	0.0228	0.0281
Shiocton	30.54	4.32	1.25E-04	0.0014	0.0033	0.0038
Withee	47.6	2.77	1.82E-04	0.0021	0.0061	0.0087

C_c = coefficient of curvature, C_u = coefficient of uniformity, D_{10} = effective size, D_{30} = particle size corresponding to 30% finer, D_{50} = median size, D_{60} = particle size corresponding to 60% finer.

A summary of the regression analysis on non-plastic coarse-grained soils is presented in Tables 4.15-4.17. The resilient modulus model parameters k_i can be estimated from basic soil properties using the models presented in Tables 4.15-4.17. Figure 4.18 depicts comparisons between k_i values obtained from analysis of the results of the repeated load triaxial test and k_i values estimated from basic soil properties using the correlations presented in Tables 4.15-4.17. An examination of Figure 4.18 shows that k_i prediction models are acceptable with R^2 values range from 0.59 to 0.79. These correlations were

obtained based on statistical analysis on test data that are limited to non-plastic coarse-grained soils compacted at relatively high unit weight. Extrapolation of these models at soil physical condition levels beyond this is not validated in this study.

Table 4.15: Correlations between the resilient modulus model parameter k_1 and basic soil properties for non-plastic coarse-grained soils

Variable	k_1 correlations		
	Model 1	**Model 2**	**Model 3**
Intercept	809.547	417.187	698.0361
$P_{No.\ 4}$	10.568	-	-
$P_{No.\ 40}$	-6.112	-	-0.2280
%Sand	-	8.203	-
γ_d	-	-	5.7180
$w\text{-}w_{opt}$	-	-	-55.0174
$\frac{w}{w_{opt.}} \times \frac{\gamma_d}{\gamma_{d\max}}$	-578.337	-591.151	-
$P_{No.\ 200}/\ P_{No.\ 40}$	-	1092.588	-
R^2	0.72	0.71	0.69

Table 4.16: Correlations between the resilient modulus model parameter k_2 and basic soil properties for non-plastic coarse-grained soils

Variable	k_2 correlations		
	Model 1	**Model 2**	**Model 3**
Intercept	0.5661	0.36295	0.2435
$P_{No.\ 40}$	0.00671	-0.00364	0.00372
$P_{No.\ 200}$	-0.02423	-	-0.01567
%Sand	-	0.00828	-
$w\text{-}w_{opt}$	0.05849	0.05641	-
$w_{opt} \times \gamma_{dmax}$	0.001242	-	-
$\frac{w}{w_{opt.}} \times \frac{\gamma_d}{\gamma_{d\max}}$	-	-	0.5671
R^2	0.79	0.74	0.67

Table 4.17: Correlations between the resilient modulus model parameter k_3 and basic soil properties for non-plastic coarse-grained soils

Variable	k_3 correlations		
	Model 1	**Model 2**	**Model 3**
Intercept	-0.50792	2.4747	-1.7529
$P_{No.\ 4}$	-	-	0.8472
$P_{No.\ 40}$	-0.041411	0.02541	0.0403
$P_{No.\ 200}$	0.14820	-	-0.8765
%Sand	-	-0.06859	-0.8849
$w\text{-}w_{opt}$	-0.1726	-0.17352	-0.17176
$w_{opt} \times \gamma_{dmax}$	-0.01214	-0.00873	-
R^2	0.67	0.65	0.59

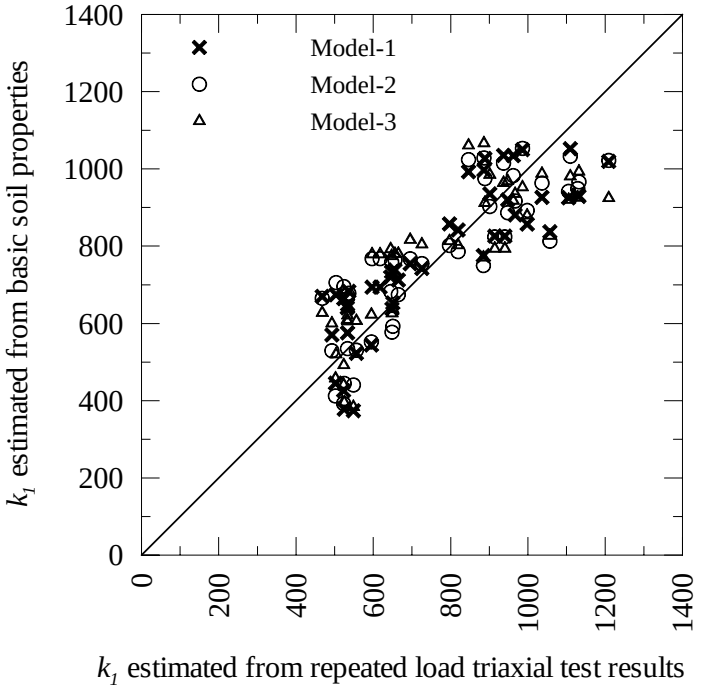

(a) k_1

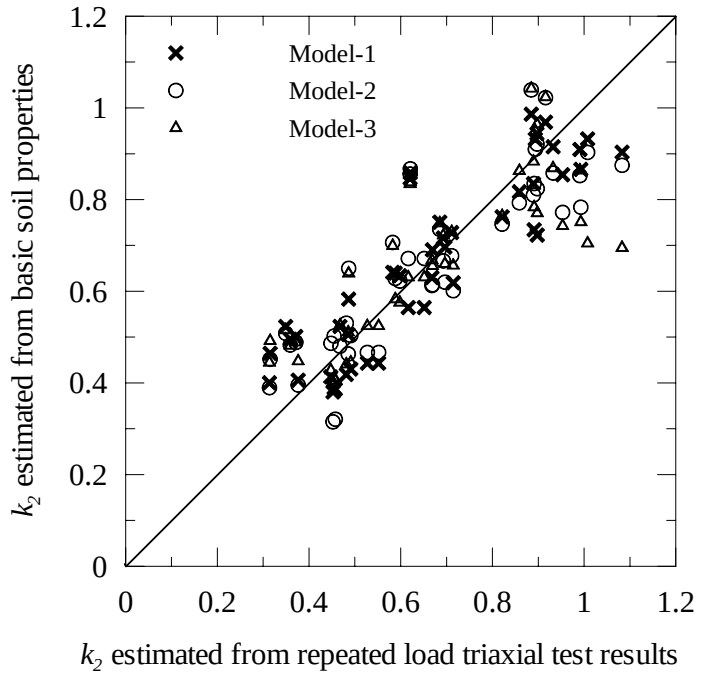

(b) k_2

Figure 4.18: Comparison of resilient modulus model parameters (k_i) estimated from soil properties and k_i determined from results of repeated load triaxial test on investigated non-plastic coarse-grained soils

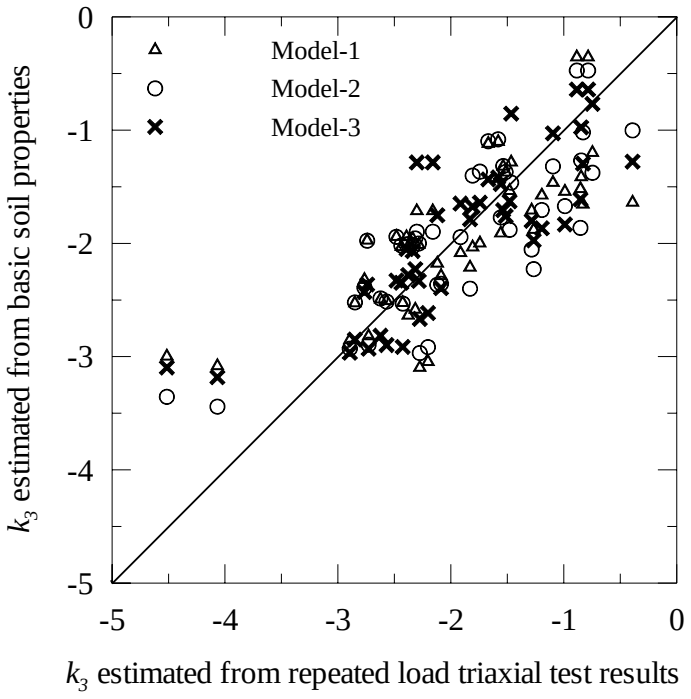

(c) k_3

Figure 4.18 (cont.): Comparison of resilient modulus model parameters (k_i) estimated from soil properties and k_i determined from results of repeated load triaxial test on investigated non-plastic coarse-grained soils

Based on statistical analysis on the investigated non-plastic coarse-grained soils, the resilient modulus model parameters (k_i) can be estimated from basic soil properties using the following equations:

$$k_1 \quad 809.547 + 10.568P_{No.4} - 6.112P_{No.40} - 578.337\left(\frac{w}{w_{opt}}\right)\times\left(\frac{\gamma_d}{\gamma_{d\max}}\right) \qquad \textbf{(4.11)}$$

$$k_2 \quad 0.5661 + 0.006711P_{No.40} - 0.02423P_{No.200} + 0.05849(w - w_{opt}) + 0.001242(w_{opt})\times(\gamma_{d\max}) \qquad \textbf{(4.12)}$$

$$k_3 \quad -0.5079 - 0.041411P_{No.40} + 0.14820P_{No.200} - 0.1726(w - w_{opt}) - 0.01214(w_{opt})\times(\gamma_{d\max}) \qquad \textbf{(4.13)}$$

where $P_{No.4}$ is percent passing sieve #4, $P_{No.40}$ is percent passing sieve #40, $P_{No.200}$ is percent passing sieve #200, w is the moisture content of the soil, $w_{opt.}$ is the optimum moisture content, γ_d is the dry unit weight, and γ_{dmax} is the maximum dry unit weight.

The correlation matrix for basic soil properties and k_i of non-plastic coarse-grained soils is presented in Table 4.18. A summary of regression coefficients obtained for non-plastic coarse-grained soils correlations with *t*-statistics at 95% confidence level is presented in Table 4.19. For non-plastic coarse-grained soils, k_i models were significant based on the *F*-test. With the exception of the intercept in k_3 model, all independent variables used in k_i models were significant based on t_0 (from table of parameters estimates). The absolute value of t_0 for the intercept in k_3 is 1.

Equations 4.11-4.13 were used to estimate the resilient modulus of the investigated non-plastic coarse-grained soils. Figure 4.19 depicts comparison of the predicted versus measured resilient modulus values using these equations. Examination of Figure 4.19 demonstrates that the estimated resilient modulus values of compacted non-plastic coarse-grained soils are consistent with values obtained from repeated load triaxial test results. It should be emphasized that these correlations are developed on analysis of test results on soils compacted at high unit weight values (between 95 and 100% of γ_{dmax}) with moisture content range around the optimum value.

Table 4.18: Correlation matrix of model parameters and soil properties for non-plastic coarse-grained soils

Variable	$P_{No.4}$	$P_{No.40}$	$P_{No.200}$	$w\text{-}w_{opt}$	$w_{opt}\times\gamma_{dmax}$	$\frac{w}{w_{opt}}\times\frac{\gamma_d}{\gamma_{d\max}}$	k_1	k_2	k_3
$P_{No.4}$	1.00	0.88	0.68	0.03	-0.04	0.03	0.05	-0.05	0.07
$P_{No.40}$		1.00	0.84	0.09	-0.00	0.09	-0.10	-0.10	0.19
$P_{No.200}$			1.00	0.11	0.32	0.12	-0.1	-0.19	0.29
$w\text{-}w_{opt}$				1.00	-0.14	0.96	-0.83	0.81	-0.51
$w_{opt}\times\gamma_{dmax}$					1.00	-0.11	0.02	-0.11	-0.18
$\frac{w}{w_{opt}}\times\frac{\gamma_d}{\gamma_{d\max}}$						1.00	-0.82	0.75	-0.45
k_1							1.00	-0.84	0.55
k_2								1.00	-0.81
k_3									1.00

Table 4.19: Summary of t-statistics for regression coefficients used in resilient modulus model parameters for non-plastic coarse-grained soils

Model Parameter	k_1		k_2		k_3	
	Parameter estimator	***t*-statistic (95% CL)**	**Parameter estimator**	***t*-statistic (95% CL)**	**Parameter estimator**	***t*-statistic (95% CL)**
β_0	809.547	3.48	0.5661	5.38	-0.5079	-1.00
β_1	10.568	2.75	-0.02423	-4.76	0.1482	6.03
β_2	-6.112	-2.61	0.00671	3.22	-0.041411	-4.12
β_3	-578.337	-9.65	0.05849	11.98	-0.1726	-7.33
β_4	-	-	0.001242	2.95	-0.01214	-5.98
R^2	0.72		0.79		0.67	
SEE	119.9		0.104		0.503	

CL: confidence level, SEE: standard error of estimate

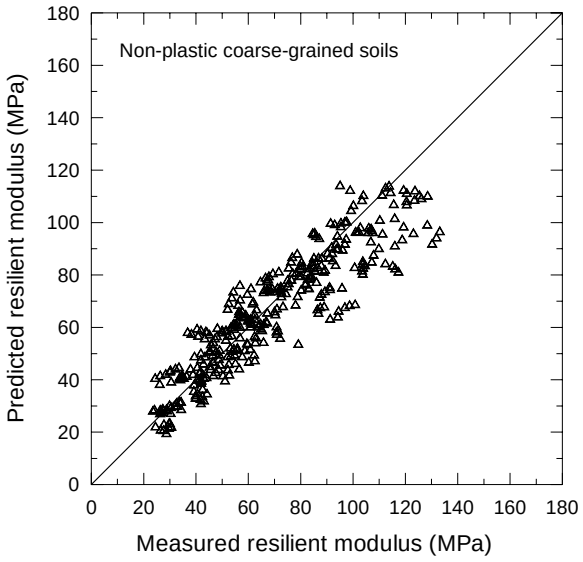

Figure 4.19: Predicted versus measured resilient modulus of compacted non-plastic coarse-grained soils

The results of the regression analysis on plastic coarse-grained soils are summarized in Tables 4.20-4.22. The results are also presented in Figure 4.20 which depicts comparisons between k_i values obtained from analysis of repeated load triaxial test results and k_i values estimated from basic soil properties. Inspection of Figure 4.20 shows that the predicted k_i are consistent with values obtained from test results. The coefficient of multiple determination for the correlations varies between 0.58 and 0.83. These correlations were obtained based on statistical analysis on test data that are limited to plastic coarse-grained soils compacted at relatively high unit weight. Extrapolation of these models at soil physical condition levels beyond this was not validated in this study.

Table 4.20: Correlations between the resilient modulus model parameter k_1 and basic soil properties for plastic coarse-grained soils

Variable	k_1 correlations		
	Model 1	**Model 2**	**Model 3**
Intercept	3596.445	5156.468	8642.873
$P_{No.\ 200}$	-55.975	-63.829	132.643
%Silt	-	-	-428.067
LL	-85.870	-87.526	-
PI	-	-	-254.685
γ_d	-	75.395	197.230
γ_d / γ_{dmax}	2948.246	-	-
w/w_{opt}	-360.099	-	-381.400
$(w-w_{opt})/w_{opt}$	-	-345.612	-
R^2	0.83	0.76	0.83

Table 4.21: Correlations between the resilient modulus model parameter k_2 and basic soil properties for plastic coarse-grained soils

Variable	k_2 correlations
	Model 1
Intercept	2.3250
$P_{No.\ 200}$	-0.00853
LL	0.02579
PI	-0.06224
γ_d / γ_{dmax}	-1.73380
w/w_{opt}	0.20911
R^2	0.58

Table 4.22: Correlations between the resilient modulus model parameter k_3 and basic soil properties for plastic coarse-grained soils

Variable	k_3 correlations		
	Model 1	**Model 2**	**Model 3**
Intercept	-25.9374	-21.3497	-32.5449
$P_{No.\ 200}$	0.7680	-	0.7691
%Silt	-1.1371	-	-1.1370
LL	-	-0.2961	-
PI	-	0.3618	-
γ_d / γ_{dmax}	31.4444	29.9702	31.5542
w/w_{opt}	-6.4483	-6.0909	-
$w-w_{opt}$	-	-	-0.4128
R^2	0.80	0.81	0.82

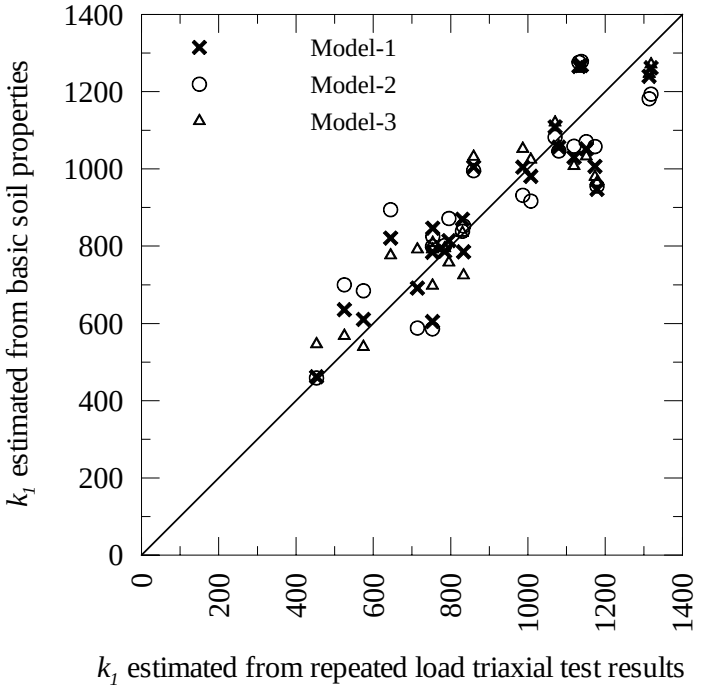

(a) k_1

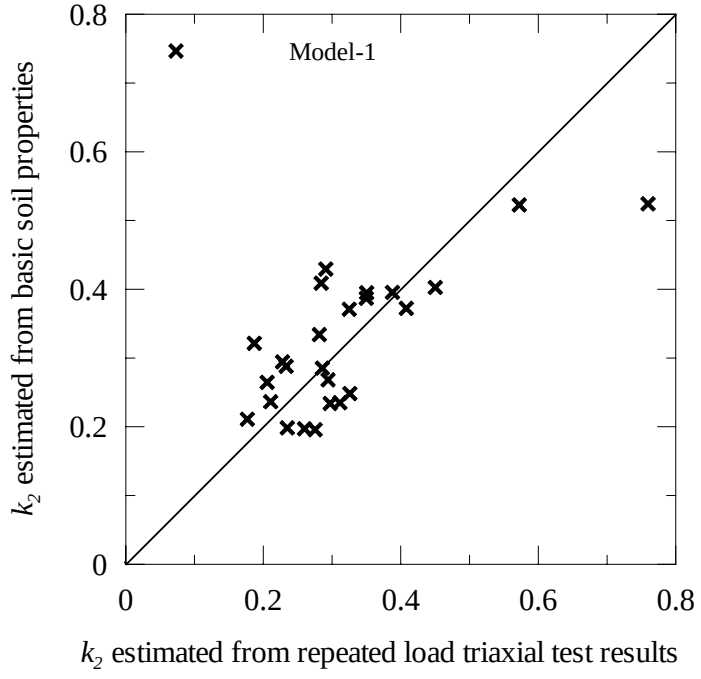

(b) k_2

Figure 4.20: Comparison of resilient modulus model parameters (k_i) estimated from soil properties and k_i determined from results of repeated load triaxial test on investigated plastic coarse-grained soils

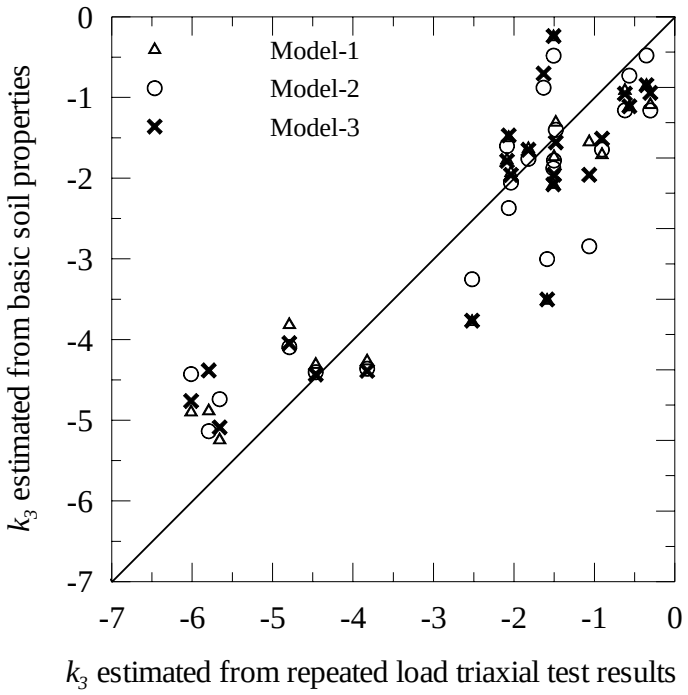

(c) k_3

Figure 4.20 (cont.): Comparison of resilient modulus model parameters (k_i) estimated from soil properties and k_i determined from results of repeated load triaxial test on investigated plastic coarse-grained soils

Based on statistical analysis on the investigated plastic coarse-grained soils, the resilient modulus model parameters (k_i) can be estimated from basic soil properties using the following equations:

$$k_1 \quad 8642.873 + 132.643P_{No.200} - 428.067(\%Silt) - 254.685PI + 197.230\gamma_d - 381.400\left(\frac{w}{w_{opt}}\right) \quad \textbf{(4.14)}$$

$$k_2 \quad 2.3250 - 0.00853P_{No.200} + 0.02579LL - 0.06224PI - 1.73380\left(\frac{\gamma_d}{\gamma_{d\max}}\right) + 0.20911\left(\frac{w}{w_{opt}}\right) \quad \textbf{(4.15)}$$

$$k_3 \quad -32.5449 + 0.7691P_{No.200} - 1.1370(\%Silt) + 31.5542\left(\frac{\gamma_d}{\gamma_{d\max}}\right) - 0.4128\left(w - w_{opt}\right) \quad \textbf{(4.16)}$$

where $P_{No.200}$ is percent passing sieve #200, %Silt is the amount of silt in the soil, *LL* is the liquid limit, *PI* is the plasticity index, *w* is the moisture content of the soil, $w_{opt.}$ is the optimum moisture content, γ_d is the dry unit weight, and γ_{dmax} is the maximum dry unit weight.

The correlation matrix for basic soil properties and k_i of plastic coarse-grained soils is presented in Table 4.23. A summary of regression coefficients obtained for plastic coarse-grained soils correlations with *t*-statistics at 95% confidence level is presented in Tables 4.24. The proposed k_i models obtained for plastic coarse-grained soils were significant based on the *F*-test. For testing the individual variables included in k_i models (ignoring the insignificance of the intercept β_0) the percent passing sieve #200 ($P_{\text{No. 200}}$) in k_2 model was not significant. The absolute value of *t*-statistics for this variable was 0.59. Although the percent of fines ($P_{\text{No. 200}}$) was found statistically insignificant, the presence of this variable in the model is more explanatory than other possible variables and with the overall model still providing closer fit to the measured data.

Equations 4.14-4.16 were used to estimate the resilient modulus of the investigated plastic coarse-grained soils. Figure 4.21 shows a comparison of the predicted versus measured resilient modulus values using these equations. An inspection of Figure 4.21 demonstrates that the estimated resilient modulus values of compacted plastic coarse-grained soils are consistent with values obtained from repeated load triaxial test results. It should be emphasized that these correlations are developed on the analysis of test results on soils compacted at high unit weight values (between 95 and 100% of γ_{dmax}) with moisture content range around the optimum value.

Table 4.23: Correlation matrix of model parameters and soil properties for plastic coarse-grained soils

Variable	$P_{No.200}$	%Silt	LL	PI	γ_d	$\frac{\gamma_d}{\gamma_{d\max}}$	w/w_{opt}	$w-w_{opt}$	k_1	k_2	k_3
$P_{No.200}$	1.00	0.99	-0.96	-0.99	0.79	0.01	0.06	0.07	0.34	0.37	0.11
%Silt		1.00	0.96	-0.99	0.78	-0.00	0.06	0.06	0.31	0.40	0.09
LL			1.00	0.97	-0.79	-0.05	-0.02	-0.03	-0.52	-0.27	-0.22
PI				1.00	-0.75	-0.01	-0.04	-0.04	-0.38	-0.39	-0.13
γ_d					1.00	0.50	0.07	0.07	0.46	0.06	0.29
$\frac{\gamma_d}{\gamma_{d\max}}$						1.00	0.05	0.05	0.41	0.39	0.44
w/w_{opt}							1.00	0.99	-0.37	0.35	-0.70
$w-w_{opt}$								1.00	-0.36	0.33	-0.71
k_1									1.00	-0.48	0.81
k_2										1.00	-0.61
k_3											1.00

Table 4.24: Summary of t-statistics for regression coefficients used in resilient modulus model parameters for plastic coarse-grained soils

Model Parameter	k_1		k_2		k_3	
	Parameter estimator	*t*-statistic (95% CL)	Parameter estimator	*t*-statistic (95% CL)	Parameter estimator	*t*-statistic (95% CL)
β_0	8642.873	5.66	2.32504	1.77	-32.5449	-4.93
β_1	197.230	4.92	-0.00853	-0.59	0.7691	2.76
β_2	132.634	3.55	0.02579	2.23	-1.1370	-2.65
β_3	-254.685	-6.48	-0.06224	-2.25	31.5542	4.74
β_4	-428.067	-6.19	-1.73380	-2.36	-0.4128	-8.08
β_5	-381.400	-3.48	0.20911	2.30	-	-
R^2	0.83		0.58		0.82	
SEE	112.71		0.093		0.849	

CL: confidence level, SEE: standard error of estimate

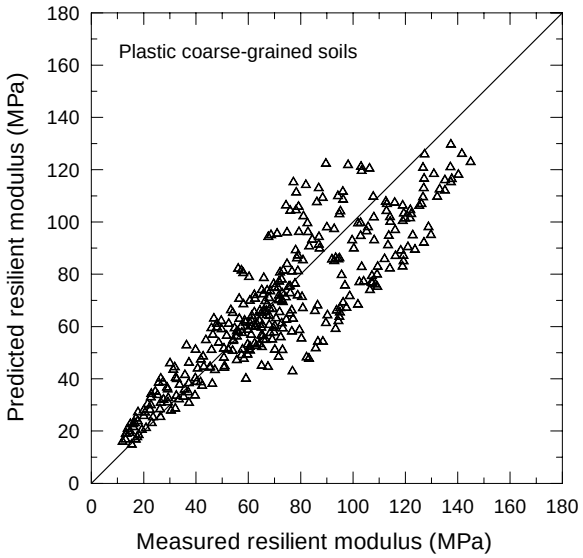

Figure 4.21: Predicted versus measured resilient modulus of compacted plastic coarse-grained soils

4.4 Predictions Using LTPP Models

In order to inspect the performance of the models developed in this study, comparison with the models developed by Yau and Von Quintus (2004) based on the Long Term Pavement Performance database was made. It should be noted that the data used to develop LTPP models and the database of this study are not similar. One difference is that the AASHTO T 307 was used herein to perform the repeated load triaxial test. Other sources that may affect the outcome include sample preparation and nature of soils samples (undisturbed versus compacted).

LTPP models (Yau and Von Quintus, 2004) are used to predict the resilient modulus of Wisconsin subgrade soils from the test results of this study. The resilient modulus values of Wisconsin subgrade soils predicted by LTPP models are then compared to the values obtained from test results and to the values predicted by the models developed herein.

The LTPP prediction models (Yau and Von Quintus, 2004) used are presented in the following equations:

LTPP equations for clay soils

$$k_1 \quad 1.3577 + 0.0106(\%Clay) - 0.0437w \tag{4.17}$$

$$k_2 \quad 0.5193 - 0.0073P_{No.4} + 0.0095P_{No.40} - 0.0027P_{No.200} + 0.0030LL - 0.0049w_{opt} \tag{4.18}$$

$$k_3 \quad 1.4258 - 0.0288P_{No.4} + 0.0303P_{No.40} - 0.0521P_{No.200} + 0.0251(\%Silt) + 0.0535LL - 0.0672w_{opt} - 0.0026\gamma_{d\max} + 0.0025\gamma_d - 0.6055\left(\frac{w}{w_{opt}}\right) \tag{4.19}$$

LTPP equations for silt soils

$$k_1 \quad 1.0480 + 0.0177(\%Clay) + 0.0279PI - 0.0370w \tag{4.20}$$

$$k_2 \quad 0.5097 - 0.0286PI \tag{4.21}$$

$$k_3 \quad -0.2218 + 0.0047(\%Silt) + 0.0849PI - 0.1399w \tag{4.22}$$

LTPP equations for sand soils

$$k_1 \quad 3.2868 - 0.0412P_{3/8} + 0.0267P_{No.4} + 0.0137(\%Clay) + 0.0083LL + 0.0379w_{opt} + 0.0004\gamma_d \tag{4.23}$$

$$k_2 \quad 0.5670 + 0.0045P_{3/8} - 2.98\times10^{-5}P_{No.4} - 0.0043(\%Silt) - 0.0102(\%Clay) - 0.0041LL + 0.0014w_{opt} - 3.41\times10^{-5}\gamma_d - 0.4582\left(\frac{\gamma_d}{\gamma_{d\max}}\right) + 0.1779\left(\frac{w}{w_{opt}}\right) \tag{4.24}$$

$$k_3 \quad -3.5677 + 0.1142P_{3/8} - 0.0839P_{No.4} - 0.1249P_{200} + 0.1030(\%Silt) + 0.1191(\%Clay) - 0.0069LL - 0.0103w_{opt} + 0.0017\gamma_d + 4.3177\left(\frac{\gamma_d}{\gamma_{d\max}}\right) - 1.1095\left(\frac{w}{w_{opt}}\right) \tag{4.25}$$

LTPP equations for all soils:

$$k_1 \quad 0.9848 - 0.0050P_{3/8} + 0.0011P_{No.40} + 0.0085(\%Clay) + 0.0089LL - 0.0094PI - 0.0235w + 0.3290\left(\frac{w}{w_{opt}}\right) \tag{4.26}$$

$$k_2 \quad 0.4808 - 0.0037P_{3/8} + 0.0062P_{No.4} - 0.0016P_{No.40} - 0.0008P_{No.200} - 0.0018(\%Clay) - 0.0078LL + 0.0019PI + 0.0111w - 0.1232\left(\frac{\gamma_d}{\gamma_{d\max}}\right) - 0.0009\left(\frac{w}{w_{opt}}\right) \tag{4.27}$$

$$k_3 \quad 9.6691 - 0.0302P_{3/8} + 0.0065P_{No.4} + 0.0192P_{No.40} - 0.0115P_{200} + 0.0040(\%Clay) + 0.0075LL + 0.0401PI + 0.0020w_{opt} - 0.0039\gamma_{d\max} - 0.2750w - 0.7177\left(\frac{\gamma_d}{\gamma_{d\max}}\right) + 1.0262\left(\frac{w}{w_{opt}}\right) + 5.28x10^{-6}\left(\frac{(\gamma_{d\max})^2}{P_{No.40}}\right) \tag{4.28}$$

Figures 4.22-4.24 present comparisons of predicted and measured resilient modulus of fine-grained, non-plastic coarse-grained, and plastic coarse-grained Wisconsin soils using the LTPP models (Yau and Von Quintus, 2004). Inspection of Figures 4.22- 4.24 demonstrates that the models developed herein were able to estimate the resilient modulus of Wisconsin compacted soils better than the models of the LTPP study. The difference in the test procedures and other conditions involved with development of both LTPP and the models of this study contributed to this outcome.

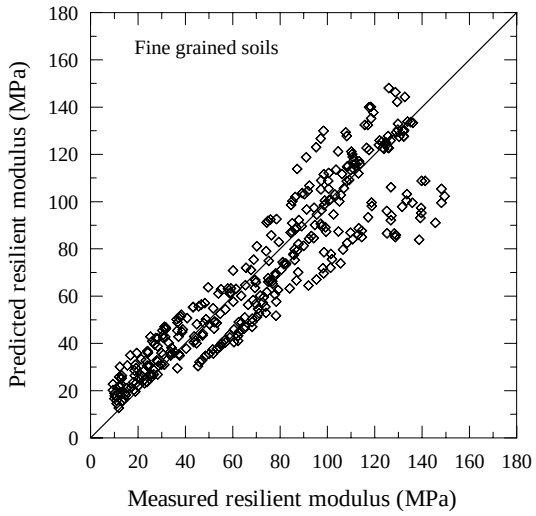

(a) Using proposed model

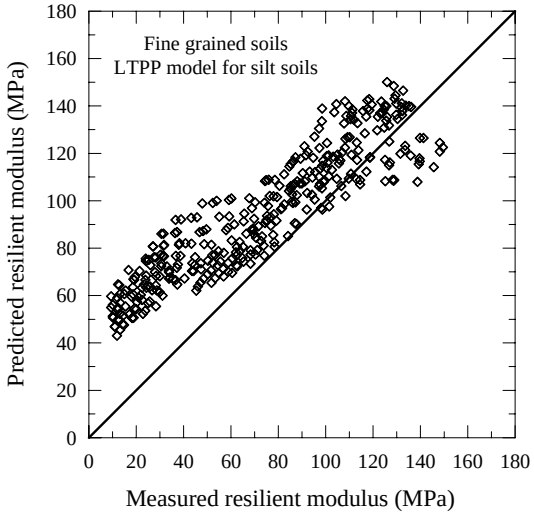

(b) Using LTPP silt model

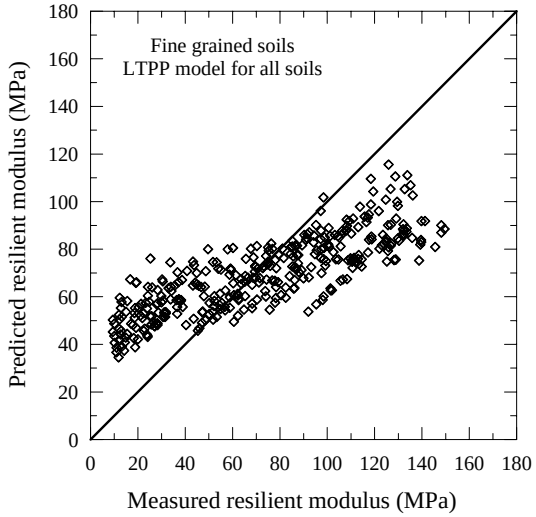

(c) Using LTPP model for combined (all) subgrade soils

Figure 22: Predicted versus measured resilient modulus of Wisconsin fine-grained soils using the mode developed in this study and the LTPP database developed models

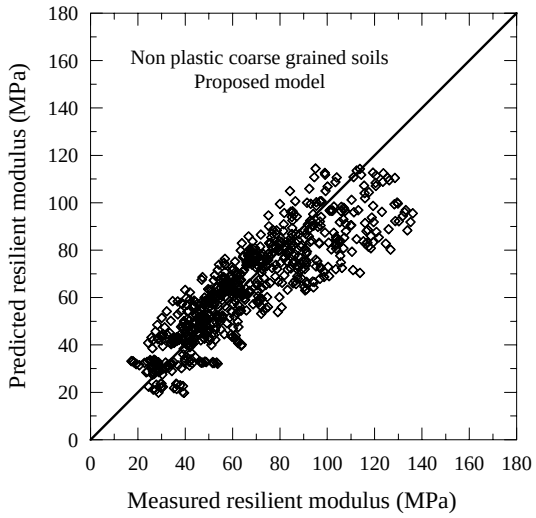

(a) Using proposed model

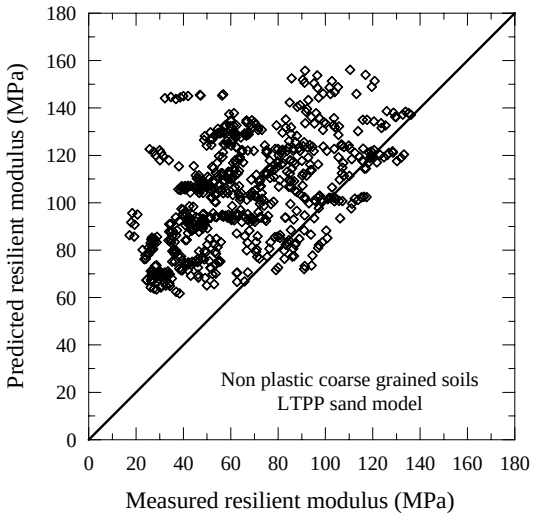

(b) Using LTPP sand model

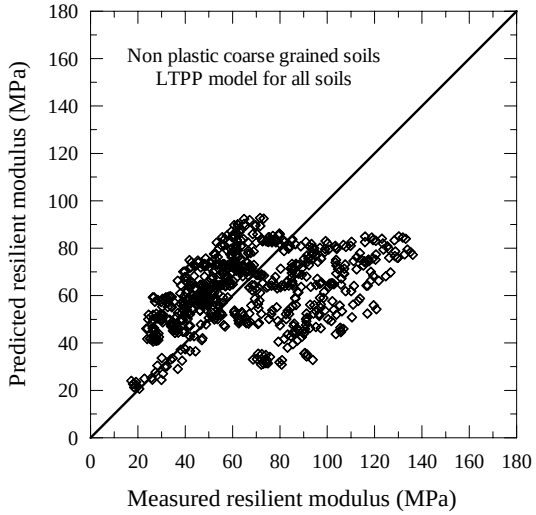

(c) Using LTPP model for combined (all) subgrade soils

Figure 23: Predicted versus measured resilient modulus of Wisconsin non-plastic coarse-grained soils using the mode developed in this study and the LTPP database developed models

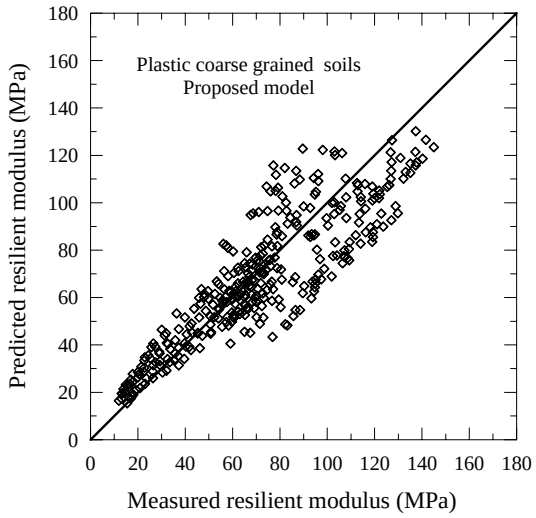

(a) Using proposed model

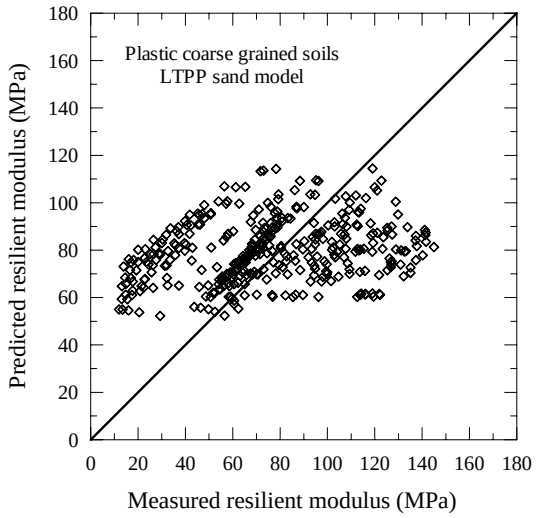

(b) Using LTPP sand model

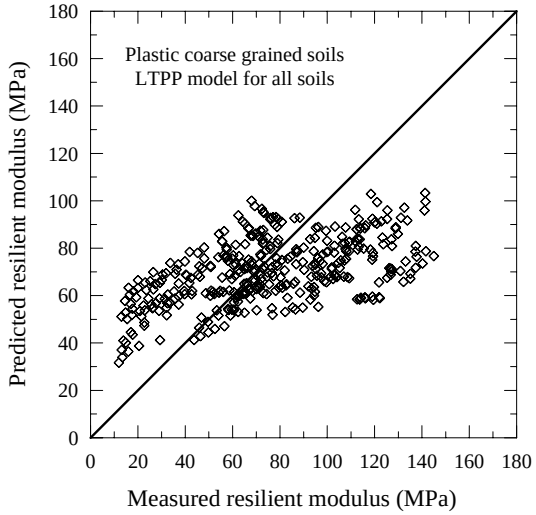

(c) Using LTPP model for combined (all) subgrade soils

Figure 24: Predicted versus measured resilient modulus of Wisconsin plastic coarse-grained soils using the mode developed in this study and the LTPP database developed models

Chapter 5

Conclusions and Recommendations

This research report presented the results of a comprehensive study conducted to evaluate the resilient modulus of common Wisconsin subgrade soils. The primary objective of this research project was to develop a methodology for estimating the resilient modulus of various Wisconsin subgrade soils from basic soil properties. This was achieved by carrying out laboratory-testing program on common Wisconsin subgrade soils. The program included tests to evaluate basic soil properties and repeated load triaxial tests to determine the resilient modulus. High quality test results were obtained in this study by insuring the repeatability of results and also by performing two tests on each soil replicate specimens at the specified physical condition.

The resilient modulus model given by Equation 4.1 is the constitutive equation developed by NCHRP project 1-28A and adopted by the NCHRP project 1-37A for the "Guide for Mechanistic-Empirical Design of New and Rehabilitated Pavement Structures." This study focused on developing correlations between basic soil properties and the parameters k_1, k_2, and k_3 (Equation 4.1).

The laboratory-testing program provided the research team with high quality database that was utilized to develop and validate correlations between resilient modulus model parameters and basic soil properties. Comprehensive statistical analysis including multiple linear and nonlinear regression was performed to develop these correlations. Statistical analysis conducted on all test results combined did not produce good correlations between model parameters and basic soil properties. When test results for coarse-grained and fine-grained soils were treated separately, good correlations were obtained. Comparisons of predicted and measured resilient modulus values indicated that the correlations proposed by this study are of acceptable accuracy.

The LTPP resilient modulus models (Yau and Von Quintus, 2004) were used to predict the resilient modulus of Wisconsin subgrade soils from the test results of this study. Comparisons of predicted and measured resilient modulus showed that the LTPP models did not yield good results compared to the models proposed herein.

Based on the results of this research, the following conclusions are reached:

1. The repeated load triaxial test (which is specified by AASHTO to determine the resilient modulus of subgrade soils for pavement design) is complicated, time consuming, expensive, and requires advanced machine and skilled operators.
2. The results of the repeated load triaxial test on the investigated Wisconsin subgrade soils provide resilient modulus database that can be utilized to estimate values for mechanistic-empirical pavement design in the absence of basic soils testing (level 3 input parameters)

3. The equations that correlate resilient modulus model parameters (k_1, k_2, and k_3) to basic soil properties for fine-grained and coarse-grained soils can be utilized to estimate level 2 resilient modulus input for the mechanistic-empirical pavement design. These equations are presented in Chapter 4.
4. The equations (models) developed in this research were based on statistical analysis of laboratory test results that were limited to the soil physical conditions specified. Estimation of resilient modulus of subgrade soils beyond these conditions was not validated.

Based on the results of this research, the research team recommends the following:

1. The use of the resilient modulus test database in the absence of any basic soil testing when designing low volume roads as indicated by AASHTO.
2. The use of the equations provided in Chapter 4 to estimate the resilient modulus of subgrade soils from basic soil properties. There are on average three different models to estimate each k_i for each soil type (fine-grained, non-plastic coarse-grained, and plastic coarse-grained). These equations can be used based on available basic soil test results.
3. Further research is needed to explore newly developed field devices such as light drop weight. This can provide Wisconsin DOT and contractors with field tools to assure quality of compacted subgrade soils in terms of stiffness.
4. Further research is needed to explore the effect of freeze-thaw cycles on the resilient modulus of Wisconsin subgrade soils. This is essential since the resilient modulus is highly influenced by the seasonal variations in moisture and extreme temperatures.

References

AASHTO 2002 Guide for Mechanistic-Empirical Design of New and Rehabilitated Pavement Structures. NCHRP Project 1-37A Final Report by ERES Consultants, March 2004.

Allen, A. J. (1996). Development of A Correlation Between Physical and Fundamental Properties of Louisiana Soils. Master's Thesis, Dept. of Civil Eng., Louisiana State University, Baton Rouge.

Barksdale, R. D. (1972). "A Laboratory Evaluation of Rutting in Base Course Materials," *Proceedings of the 3rd International Conference on the Structural Design of Asphalt Pavements*, University of Michigan, pp. 161-174.

Barksdale, R. D., Rix, G.J., Itani, S., Khosla, P.N., Kim, R., Lambe, C., and Rahman, M.S., (1990). "Laboratory Determination of Resilient Modulus for Flexible Pavement Design," NCHRP, Transportation Research Board, Interim Report No. 1-28, Georgia Institute of Technology, Georgia.

Butalia, T. S., Huang, J., Kim, D. G., and Croft, F., (2003). "Effect of Moisture Content and Pore Water Pressure Build on Resilient Modulus of Cohesive Soils," *Resilient Modulus Testing for Pavement Components, ASTM STP 1437.*

Chamberlain, E.J., Cole, D. M., and Durell, G. F., (1989). "Resilient Modulus Determination for Frost Conditions, State of the Art Pavement Response Monitoring Systems for Roads and Air Field," Special Report 89-23, U.S. Army Cold Region Research and Engineering Laboratory (CRREL), Hanover, H, 1989, pp. 230-333.

Chou, Y. T., (1976) "Evaluation of Nonlinear Resilient Modulus of Unbound Granular Materials from Accelerated Traffic Test Data," U.S. Army Engineer Waterways Experiment Station, Vicksburg, MS, Final Technical Report.

Drumm, E. C., Boateng-Poku, Y., and Pierce, T. J. (1990). "Estimation of Subgrade Resilient Modulus from Standard Tests," *Journal of Geotechnical Engineering, Vol. 116, No. 5*, pp. 774-789.

Drumm E. C., Reeves, J. S., Madgett, M. R., and Trolinger, W. D. (1997). "Subgrade Resilient Modulus Correction for Saturation Effects," *Journal of Geotechnical and Geoenvironmental Engineering, Vol.* 123, *No. 7.*

Fredlund, D.G., Bergan, A. T. and Wong, P. K. (1977). "Relation Between Resilient Modulus and Stress Research Conditions for Cohesive Subgrade Soils" *Transportation Research Record No. 642,* Transportation Research Board, pp.73-81.

Groeger, J. L., Rada, G. R., and Lopez, A. (2003). "AASHTO T 307-Background and Discussion," *Resilient Modulus Testing for Pavement Components, ASTM STP 1437.*

Heydinger, A. G., (2003). "Evaluation of Seasonal Effects on Subgrade Soils," *Transportation Research Record No. 1821*, Transportation Research Board, pp.47-55.

Hines, William W. and Montgomery, Douglas C (1980). Probability and Statistics in Engineering and Management Science. 2nd Edition, John Willey & Sons Inc., New York.

Hole, F. D. (1980) "Soil Guide For Wisconsin Land Lookers." *Bul. 88, Soil Series No. 63*, Geological and Natural History Survey University of Wisconsin-Extension and University of Wisconsin-Madison.

Hole, F. D. (1974). "Soil Regions of Wisconsin," Geological and Natural History Survey University of Wisconsin-Extension, (Map).

Huang, J. 2001. Degradation of Resilient Modulus of Saturated Clay Due to Pore Water Pressure Buildup under Cyclic Loading, Master Thesis, Department of Civil Engineering and Environmental Engineering, The Ohio State University.

Janoo, V.C., and Bayer II J.J. (2001). "The effect of Aggregate Angularity on Base Course Performance," *U.S. Army Corps of Engineers, ERDC/CRREL TR-01-14*.

Lekarp, F., Isacsson, U. and Dawson, A. (2000). "State of the Art. I: Resilient Response of Unbound Aggregates," *Journal of Transportation Engineering, Vol. 126, No. 1.*

Li, D., and Selig, E. T. (1994). "Resilient Modulus for Fine Grained Subgrade Soils," *Journal of Geotechnical Engineering, Vol. 120, No. 6.*

Maher, A., Bennert T., Gucunski, N., and Papp, W. J., (2000) "Resilient Modulus of New Jersey Subgrade Soils," FHWA Report No. 2000-01, Washington D.C.

May, R. W., and Witczak, M. W. (1981). "Effective Granular Modulus to Model Pavement Responses," *Transportation Research Record No. 810*, Transportation Research Board, pp. 1-9.

Madison, F. W., and Gundlach, H. F. (1993). "Soil Regions of Wisconsin," Wisconsin Geological and Natural History Survey and U.S. Department of Agriculture, (Map).

Nazarian, S., and Feliberti, M. (1993). "Methodology for Resilient Modulus Testing of Cohesionless Subgrades," *Transportation Research Record No. 1406,* Transportation Research Board, pp.108-115.

NCHRP Project 1-37A Summary of the 2000, 2001, and 2002 AASHTO Guide for The Design of New and Rehabilitated Pavement Structures, NCHRP, Washington D.C.

Ooi, Philip S. K., Archilla A. R, and Sandefur K. G. (2004). "Resilient Modulus Models for Compacted Cohesive Soils," *Transportation Research Record No. 1874*,

Transportation Research Board, National Research Council, Washington, D. C., 2004, pp. 115-124.

Pezo, R. and Hudson, W. R. (1994). "Prediction Models of Resilient Modulus for Nongranular Materials," *Geotechnical Testing Journal*, GTJODJ, *Vol. 17 No. 3*, pp. 349-355.

Pezo, R., Claros, G., Hudson, W.R., and Stoke, K.H., (1992). "Development of a Reliable Resilient Modulus Test for Subgrade and Non-Granular Subbase Materials For Use in A Routine Pavement Design," Research Report 1177-4F., University of Texas-Austin.

Rada, G., and Witczak, M. W. (1981). "Comprehensive Evaluation of Laboratory Resilient Moduli Results for Granular Material," *Transportation Research Record No. 810*, Transportation Research Board, pp. 23-33.

Scrivner, F.H., R., Peohl, W.M. Moore and M.B. Phillips (1969). "Detecting Seasonal Changes in Load-Carrying Capabilities of Flexible Pavements," NCHRP Report 7, Highway Research Board, National Research Council, Washington, D.C.

Seed, H., Chan, C., and Lee, C. (1962). "Resilient Modulus of Subgrade Soils and Their Relation to Fatigue Failures in Asphalt Pavements," Proceedings, International Conference on the Structural Design of Asphalt Pavements, University of Michigan, Ann Arbor, Michigan, 611-636.

Smith, W. S., and Nair, K. (1973). "Development of Procedure for Characterization of Untreated Granular Base Course and Asphalt Treated Course Materials," FHWA, Final Report, FHWA-A-RD-74-61, Washington D.C.

Thompson, M. R. and Q.L. Robnett (1979). "Resilient Properties of Subgrade Soils" Transportation Engineering Journal, ASCE, 105(TE1), pp. 71-89.

Thomson, M. R., and Robnett, Q. L., (1976). "Resilient Properties of Subgrade Soils," Final Report, Illinois Cooperative Highway and Transportation Serial No. 160, University of Illinois Urbana Champaign.

Titi, H. H., Elias, M. B., and Helwany, S. (2005). "Effect of Sample Size on Resilient Modulus of Cohesive Soils," Proceedings of the 16th International Conference on Soil Mechanics and Geotechnical Engineering (ICSMG), Osaka, Japan, September 12-16, 2005, Vol. 2, pp. 499-502.

Titi, H. H., Mohammad, L. N., and Herath, A. (2003). "Characterization of Resilient Modulus of Coarse-Grained Materials Using the Intrusion Technology," Special Technical Publication 1437: Resilient Modulus Testing for Pavement Components, American Society for Testing and Materials pp. 252-270.

Uzan, J. (1985) “Characterization of Granular Material,” *Transportation Research Record No. 1022*, pp. 52-59.

Yau, A., and Von Quintus (2004). “Predicting Elastic Response Characteristics of Unbound Materials and Soils,” *Transportation Research Record No. 1874*, Transportation Research Board, National Research Council, Washington, D. C., pp. 47-56.

Zaman, M., Chen, D., and Larguros, J. (1994). “Resilient Modulus of Granular Materials,” *Journal of Transportation Engineering. Vol. 120, No. 6*, pp. 967-988.

Appendix A

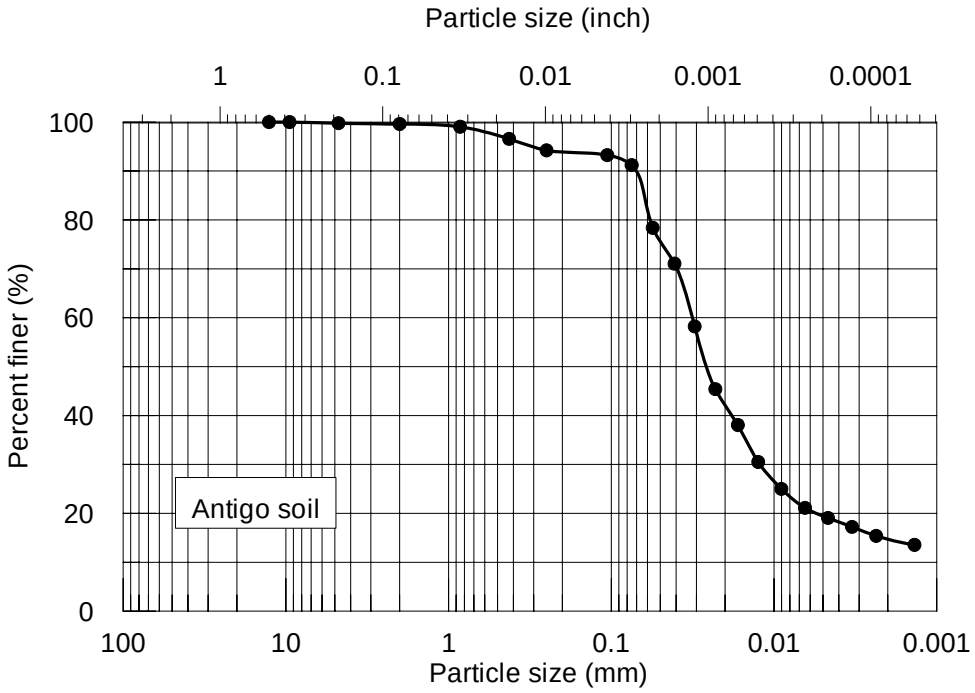

Figure A.1: Particle size distribution curve for Antigo soil

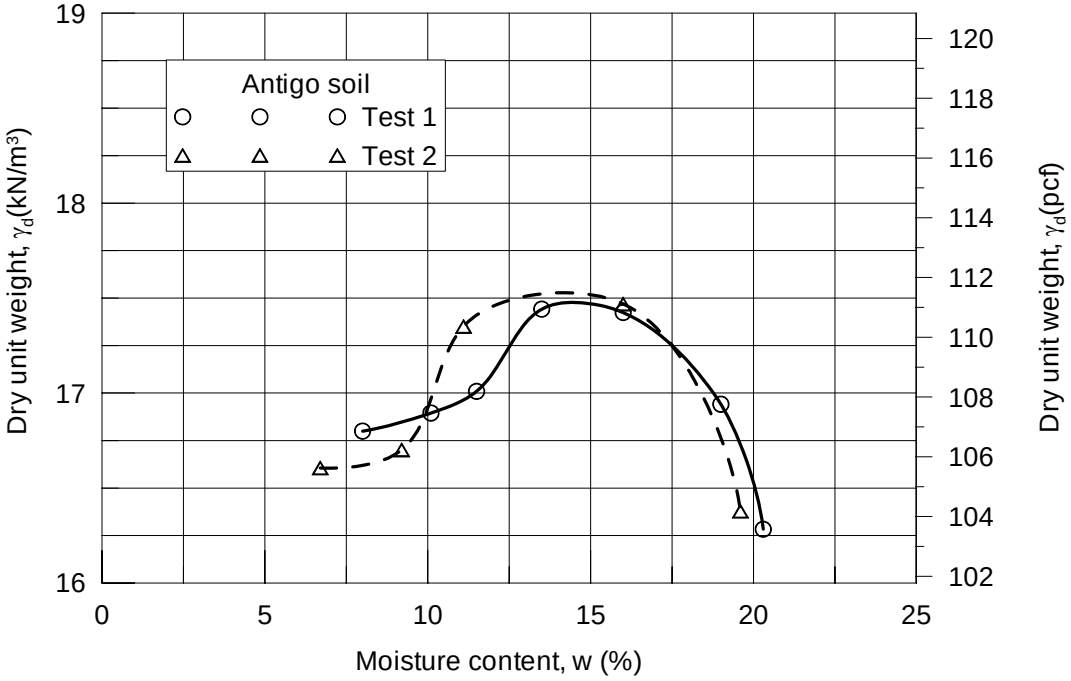

Figure A.2: Results of Standard Proctor test for Antigo soil

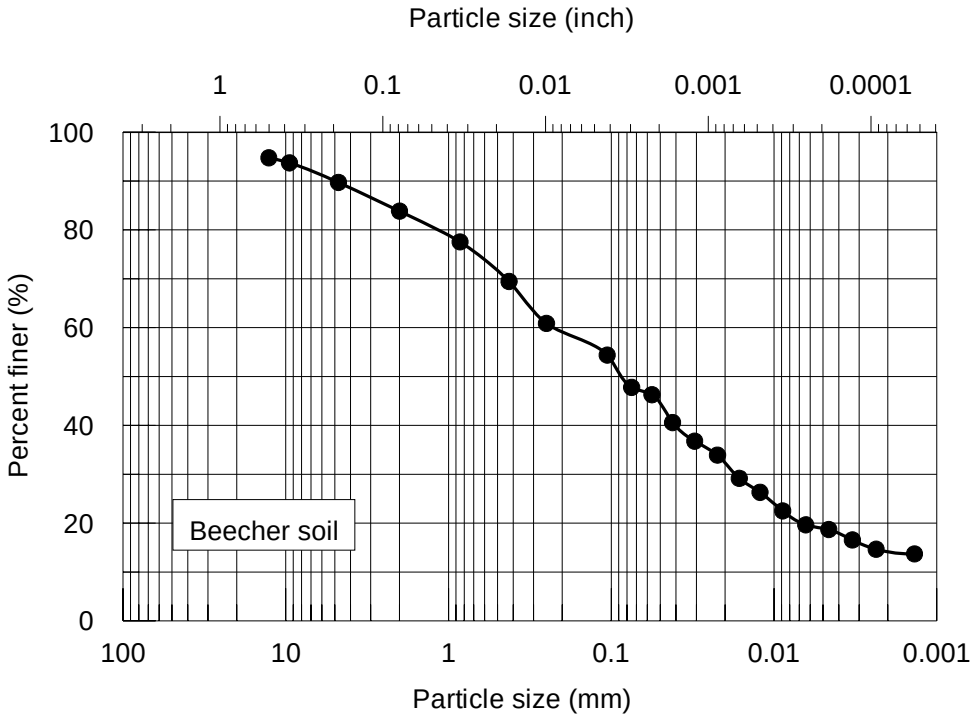

Figure A.3: Particle size distribution curve for Beecher soil

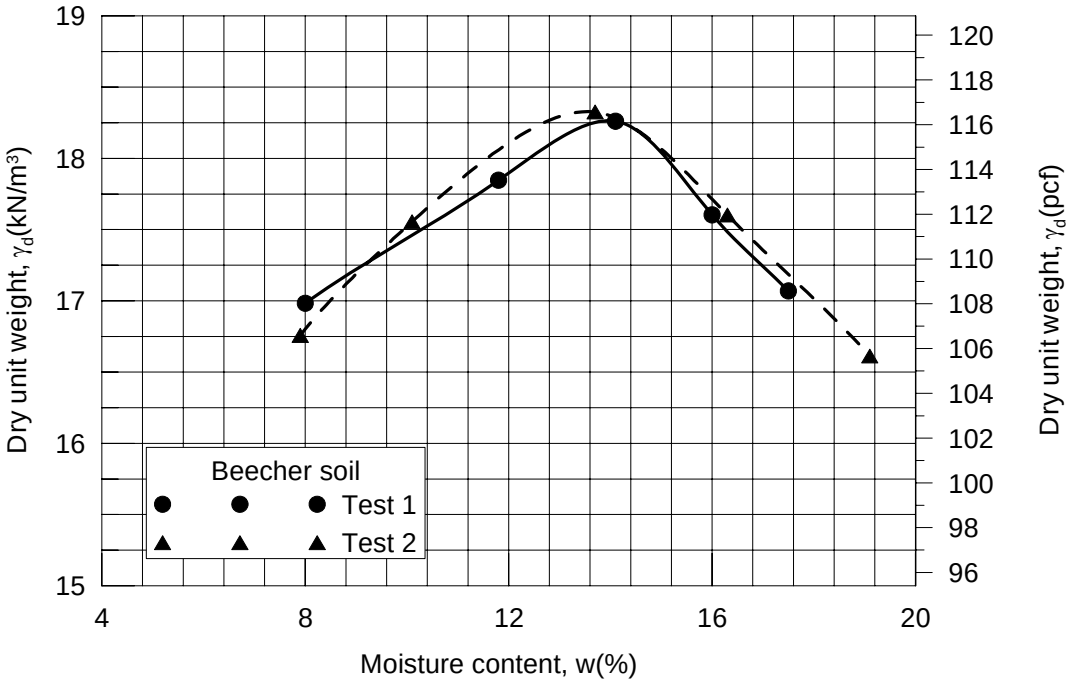

Figure A.4: Results of Standard Proctor test for Beecher soil

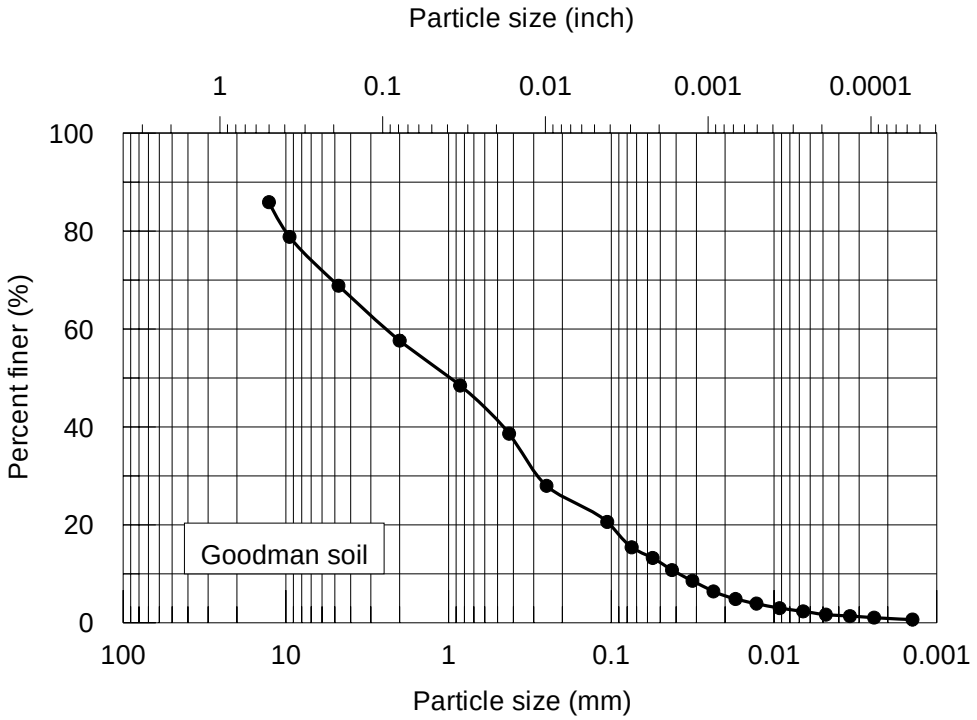

Figure A.5: Particle size distribution curve for Goodman soil

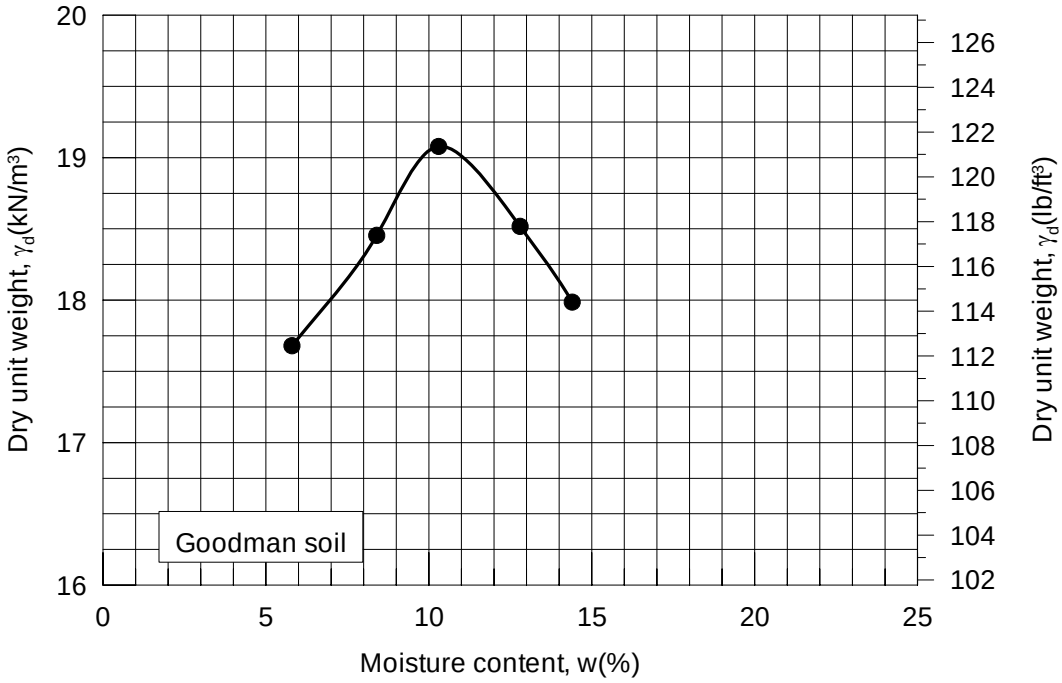

Figure A.6: Results of Standard Proctor test for Goodman soil

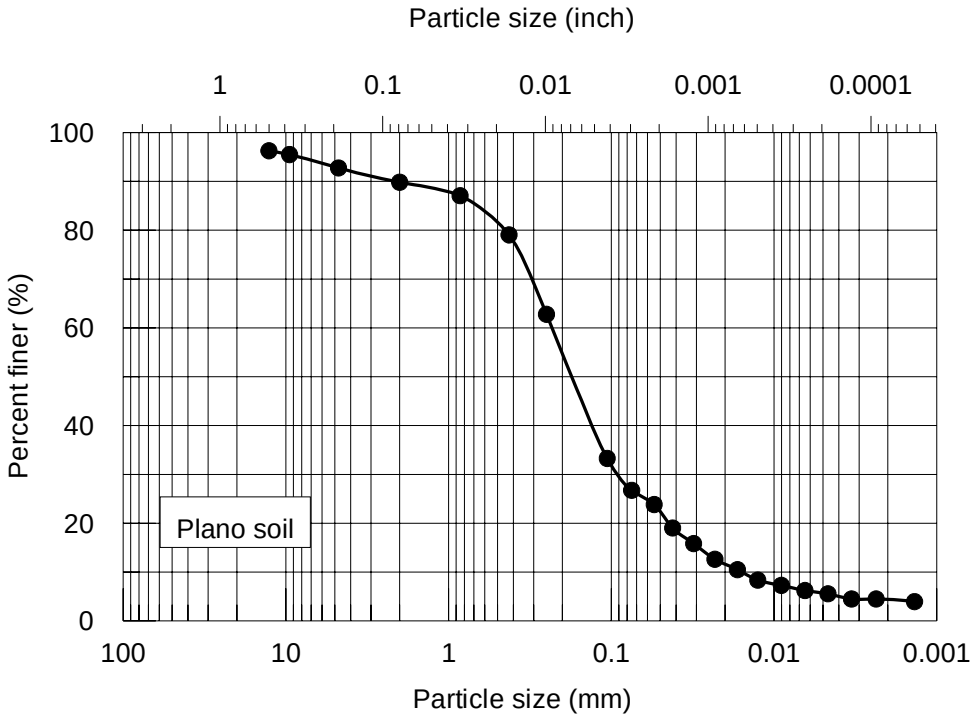

Figure A.7: Particle size distribution curve for Plano soil

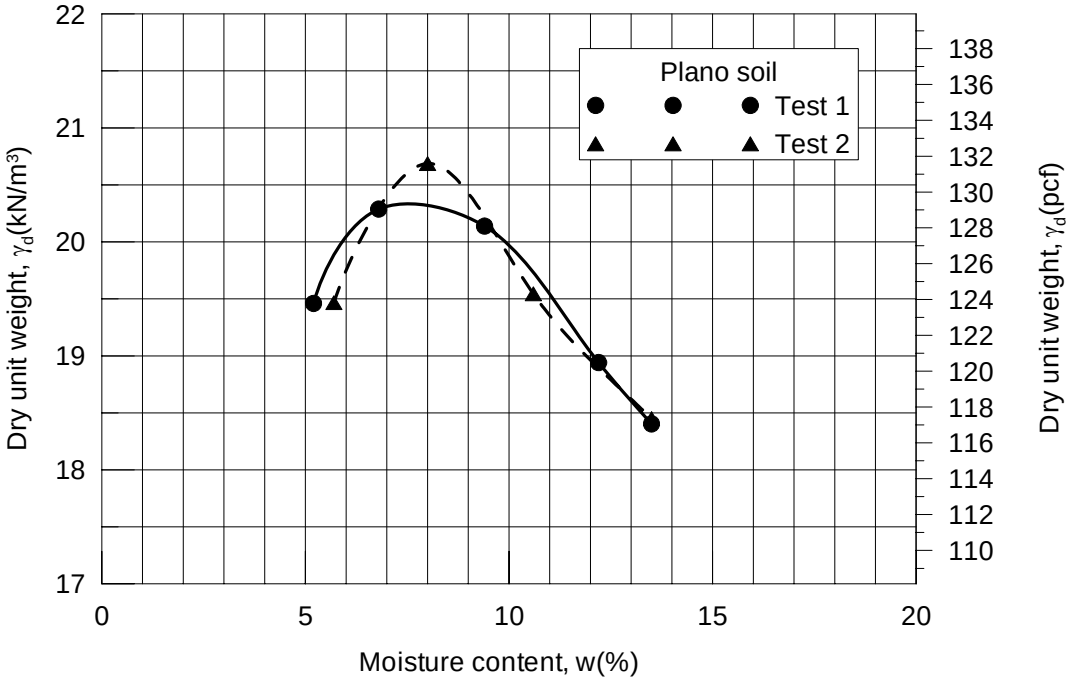

Figure A.8: Results of Standard Proctor test for Plano soil

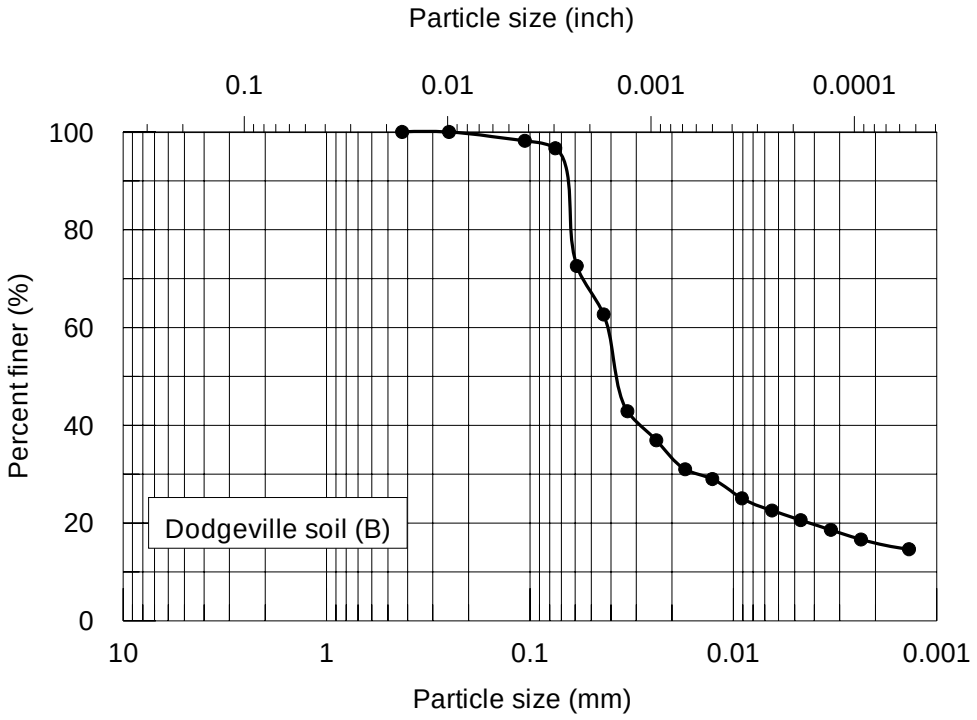

Figure A.9: Particle size distribution curve for Dodgeville soil

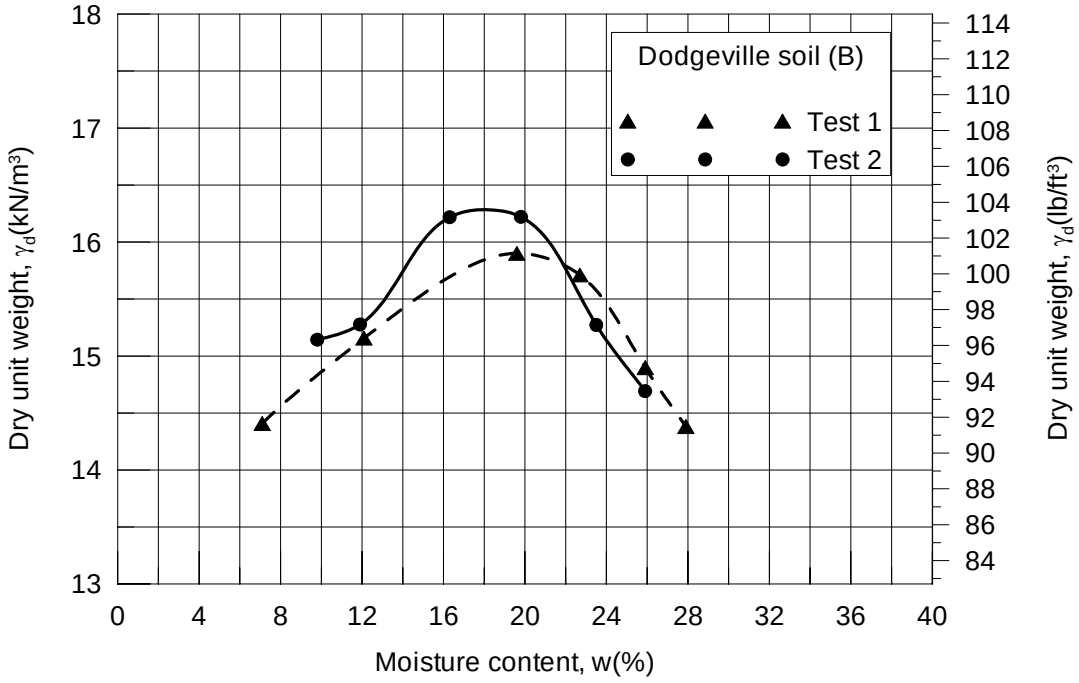

Figure A.10: Results of Standard Proctor test for Dodgeville soil

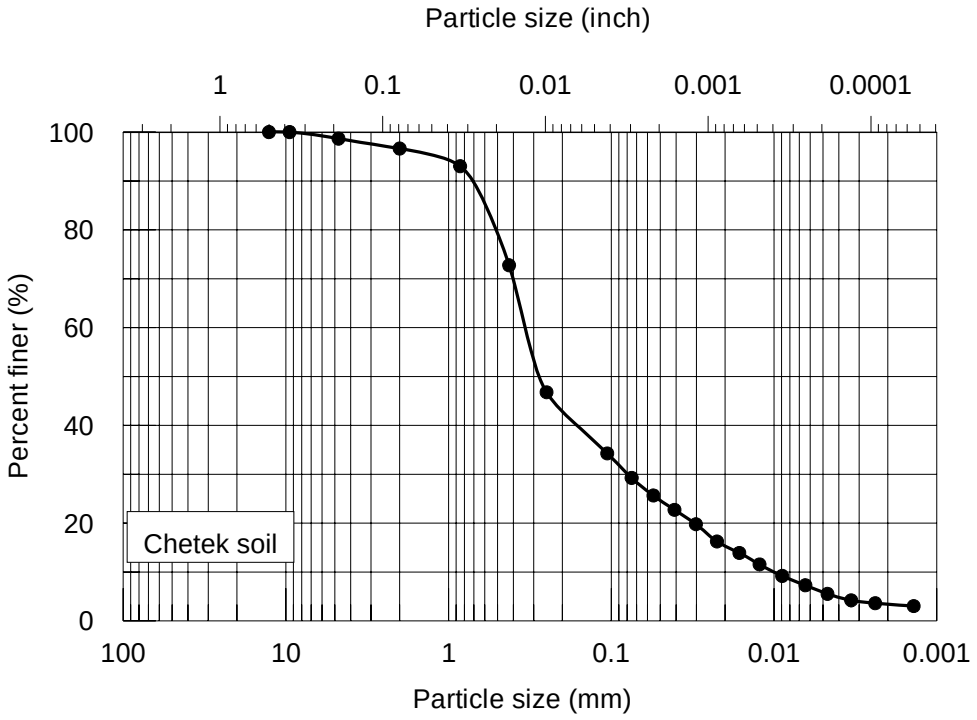

Figure A.11: Particle size distribution curve for Chetek soil

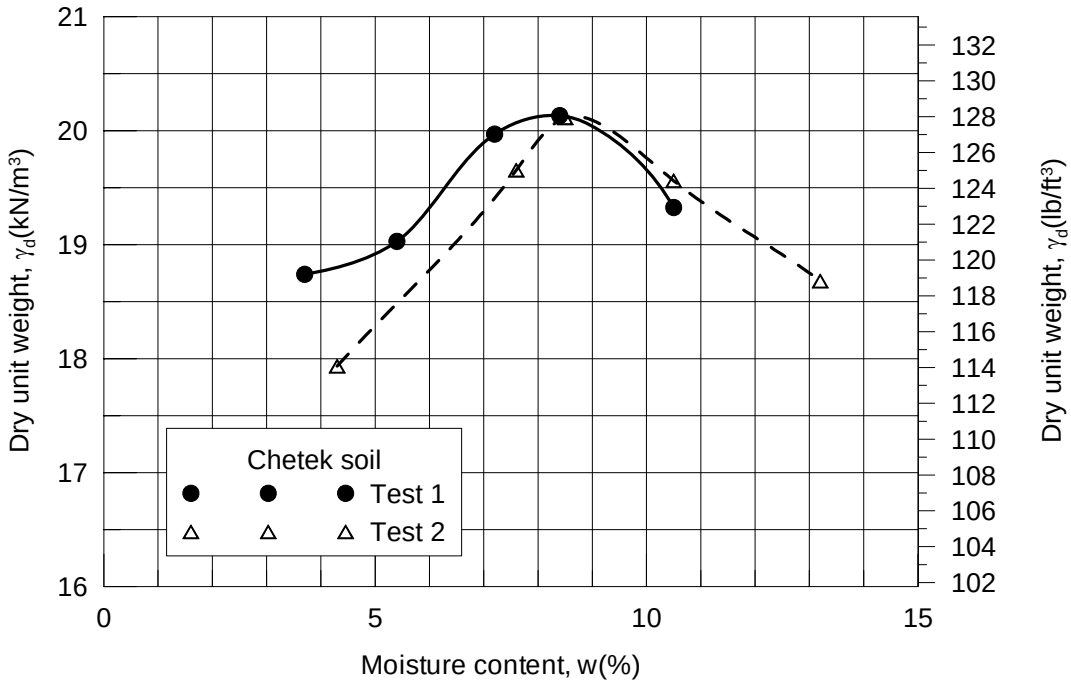

Figure A.12: Results of Standard Proctor test for Chetek soil

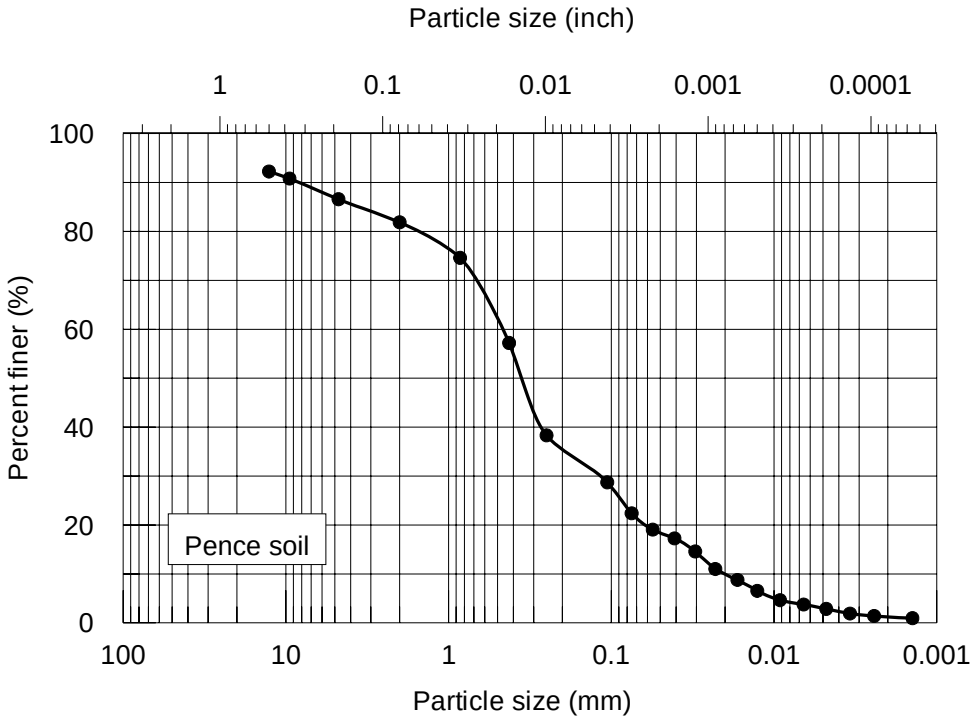

Figure A.13: Particle size distribution curve for Pence soil

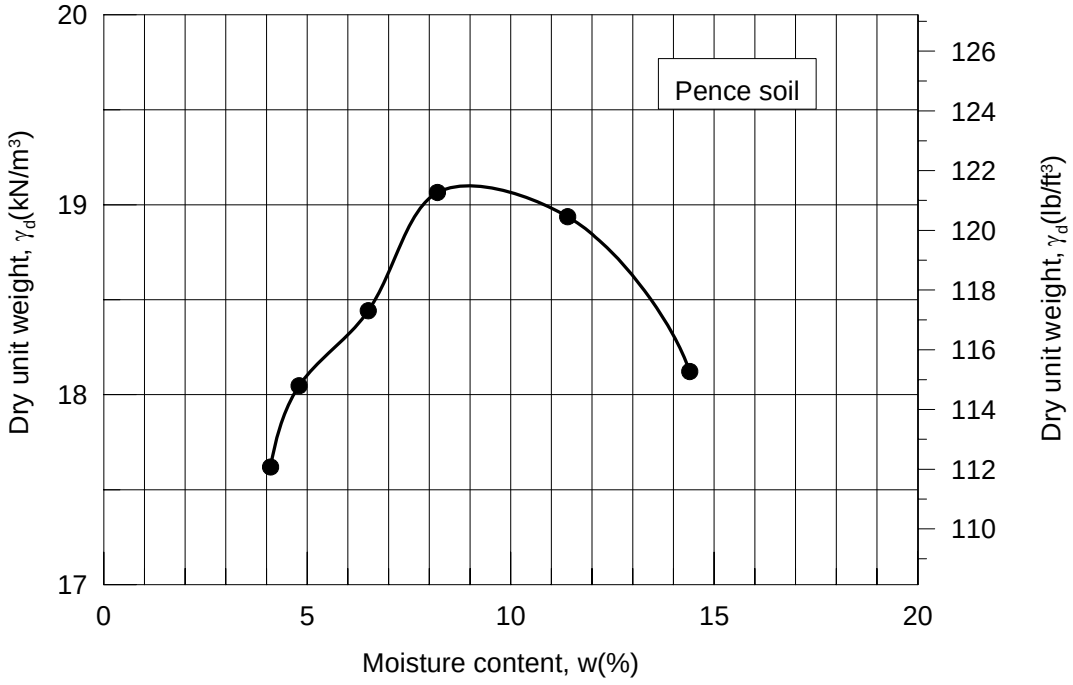

Figure A.14: Results of Standard Proctor test for Pence soil

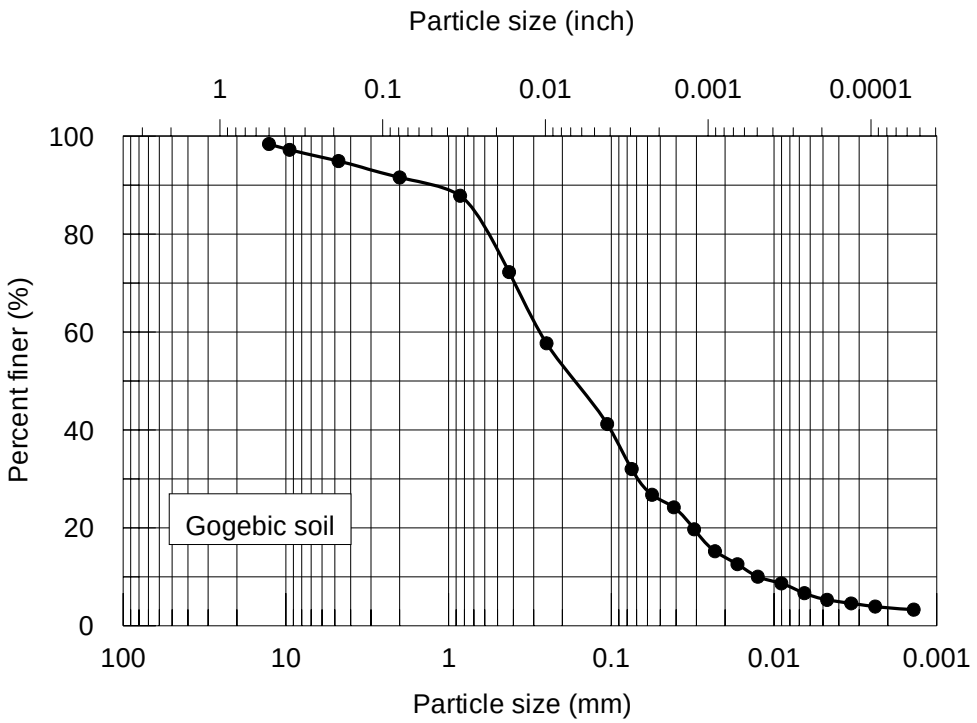

Figure A.15: Particle size distribution curve for Gogebic soil

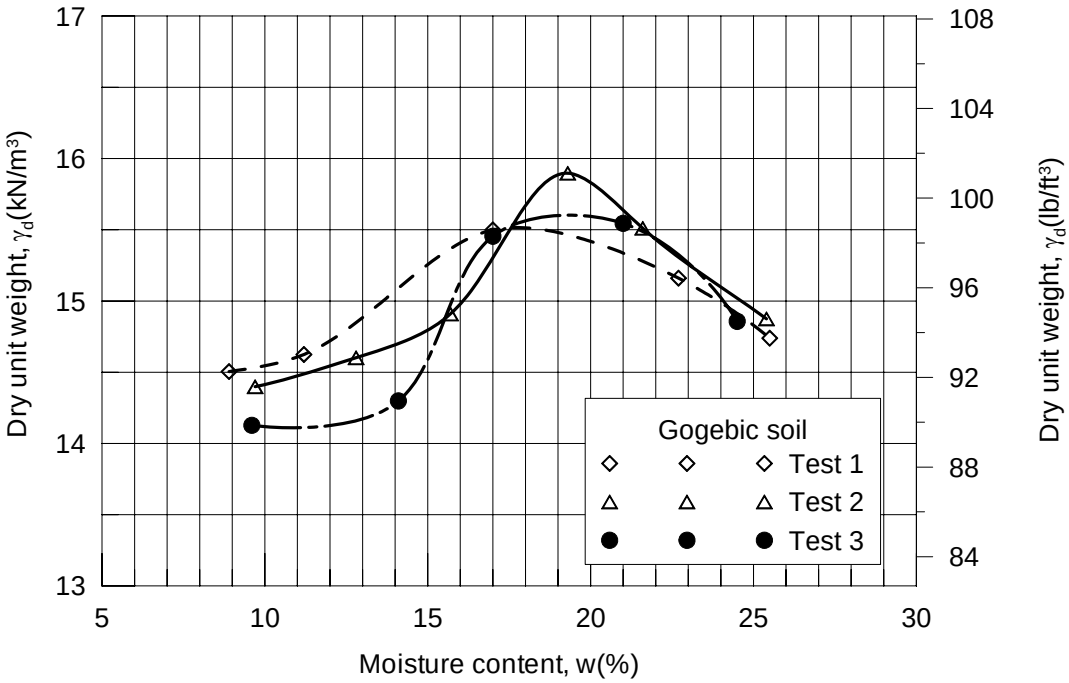

Figure A.16: Results of Standard Proctor test for Gogebic soil

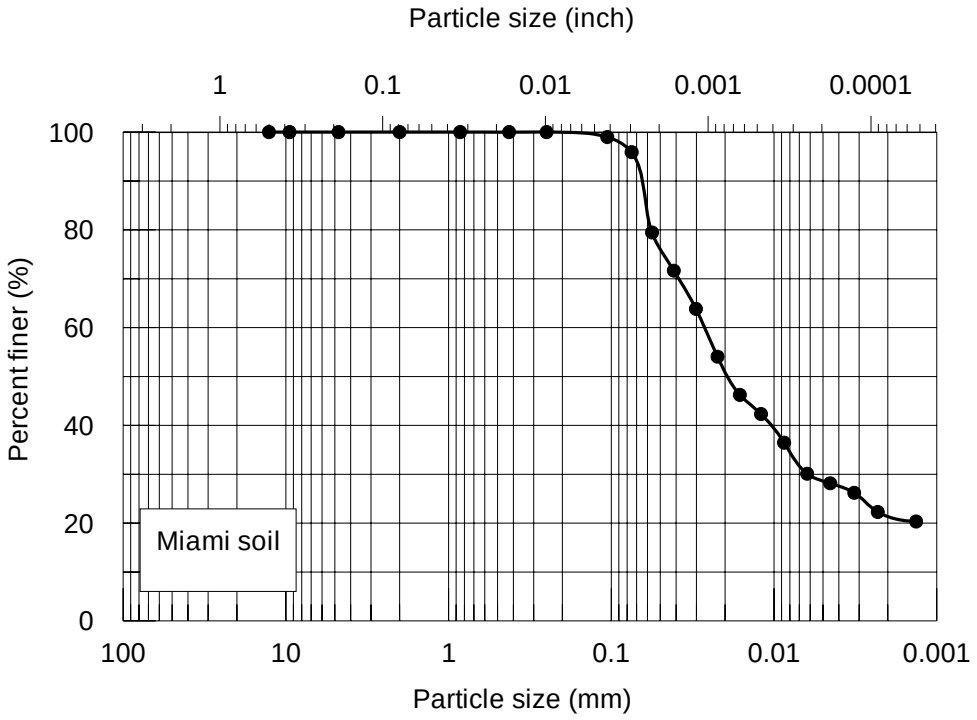

Figure A.17: Particle size distribution curve for Miami soil

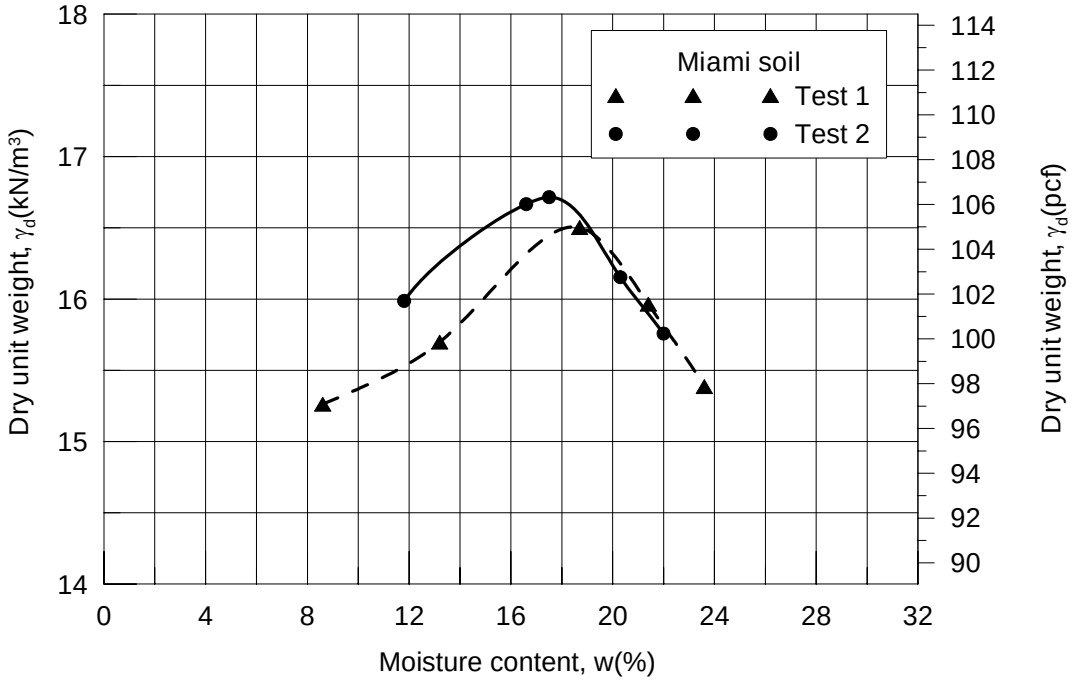

Figure A.18: Results of Standard Proctor test for Miami soil

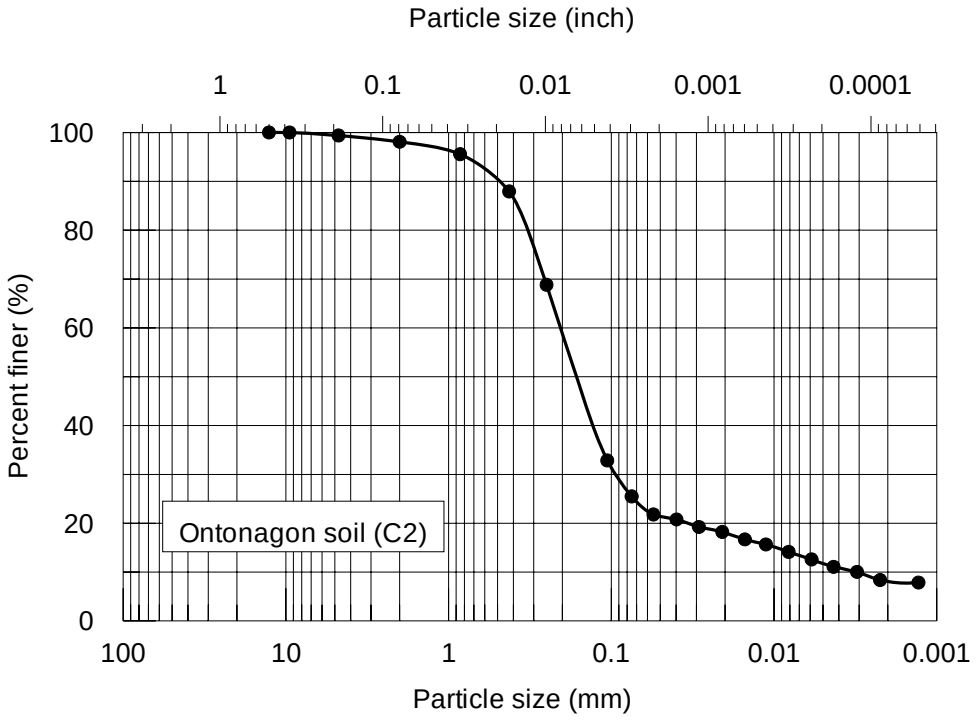

Figure A.19: Particle size distribution curve for Ontonagon soil - 2

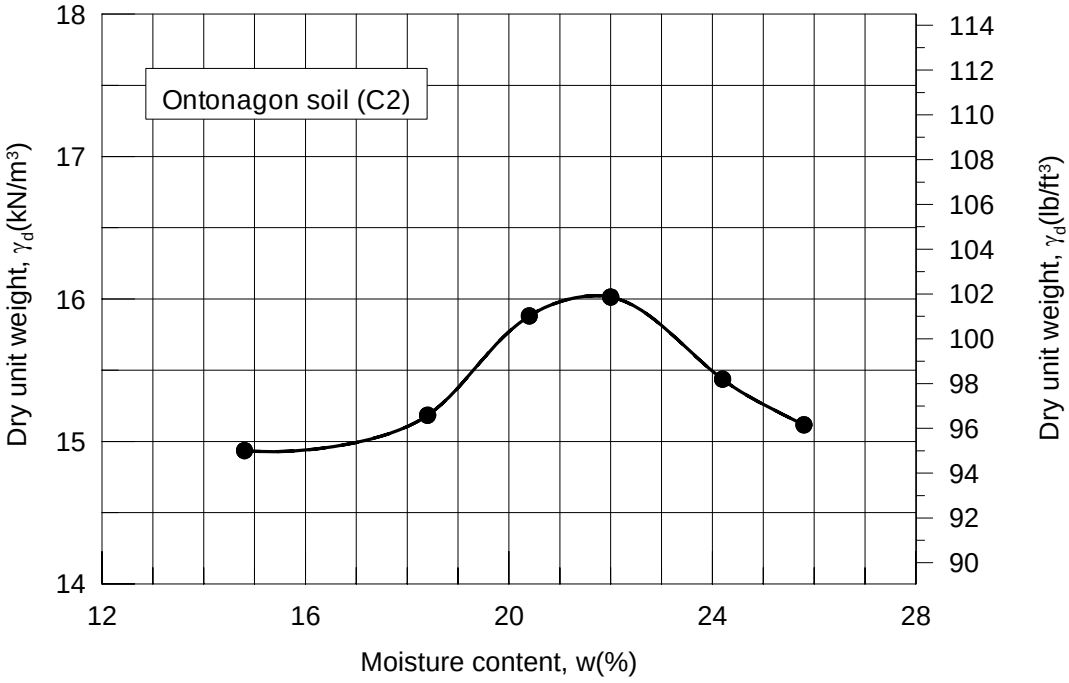

Figure A.20: Results of Standard Proctor test for Ontonagon soil - 2

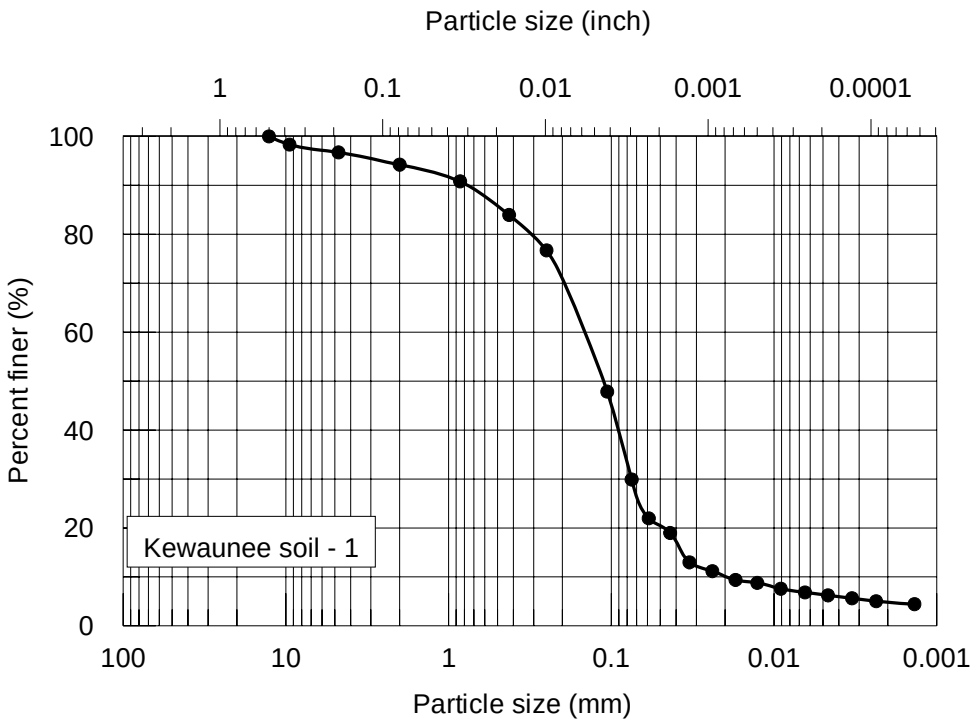

Figure A.21: Particle size distribution curve of Kewaunee soil - 1

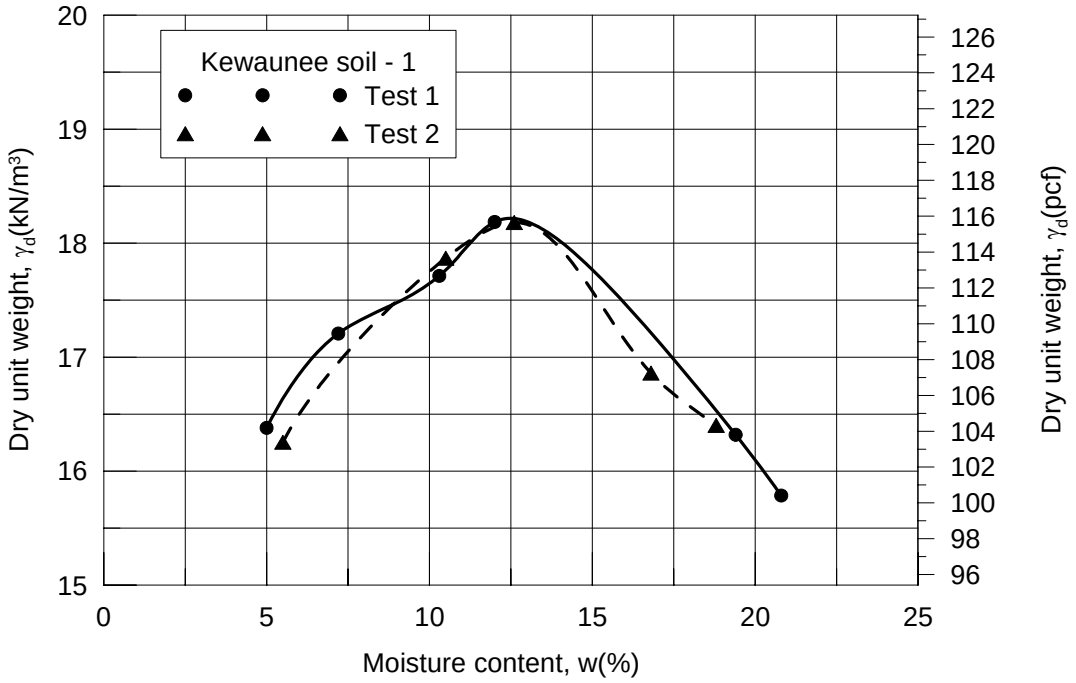

Figure A.22: Results of Standard Proctor test for Kewaunee soil - 1

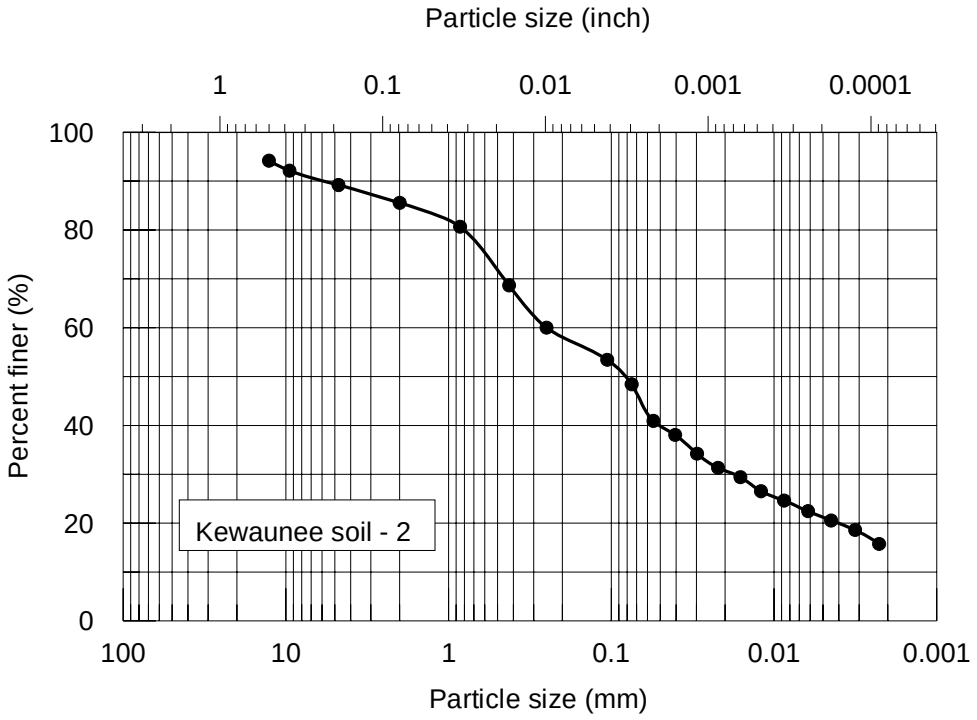

Figure A.23: Particle size distribution curve for Kewaunee soil - 2

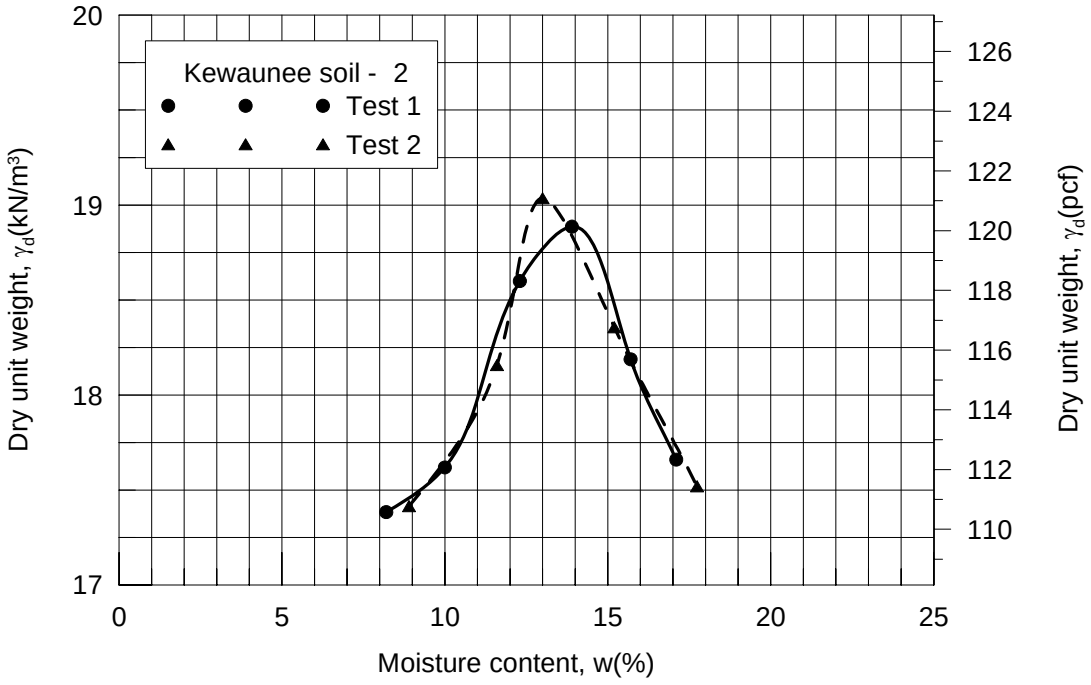

Figure A.24: Results of Standard Proctor test for Kewaunee soil - 2

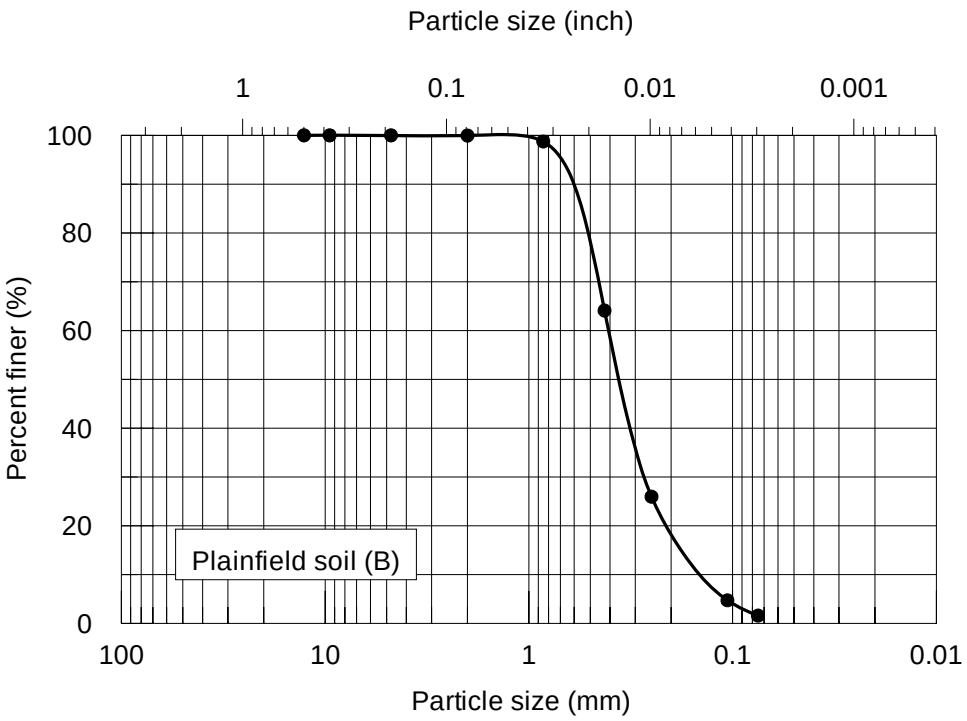

Figure A.25: Particle size distribution curve for Plainfield soil

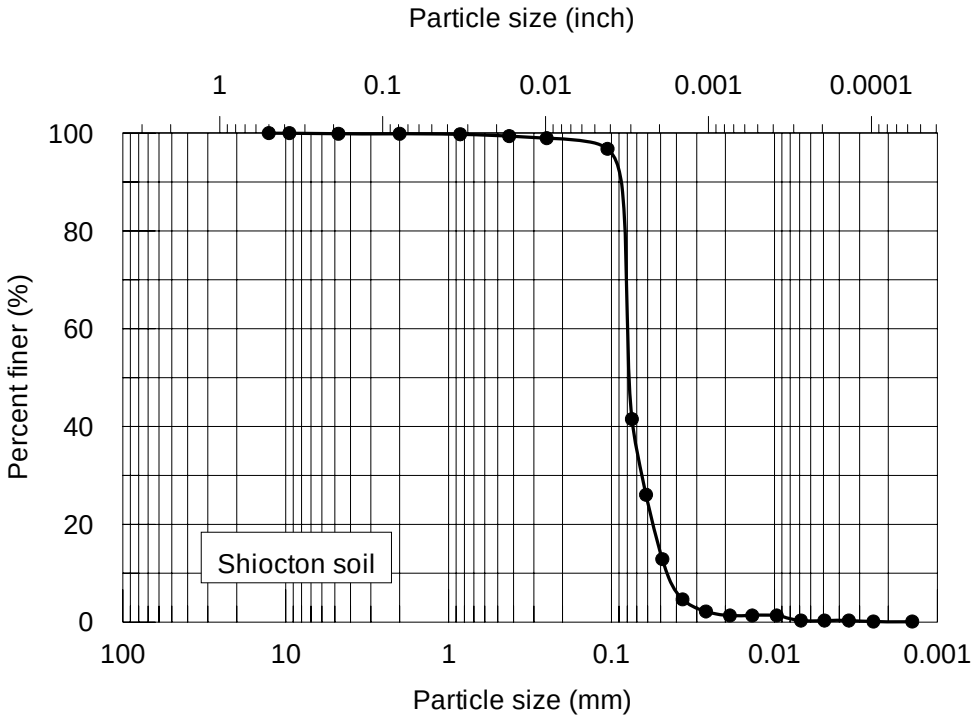

Figure A.26: Particle size distribution curve for Shiocton soil

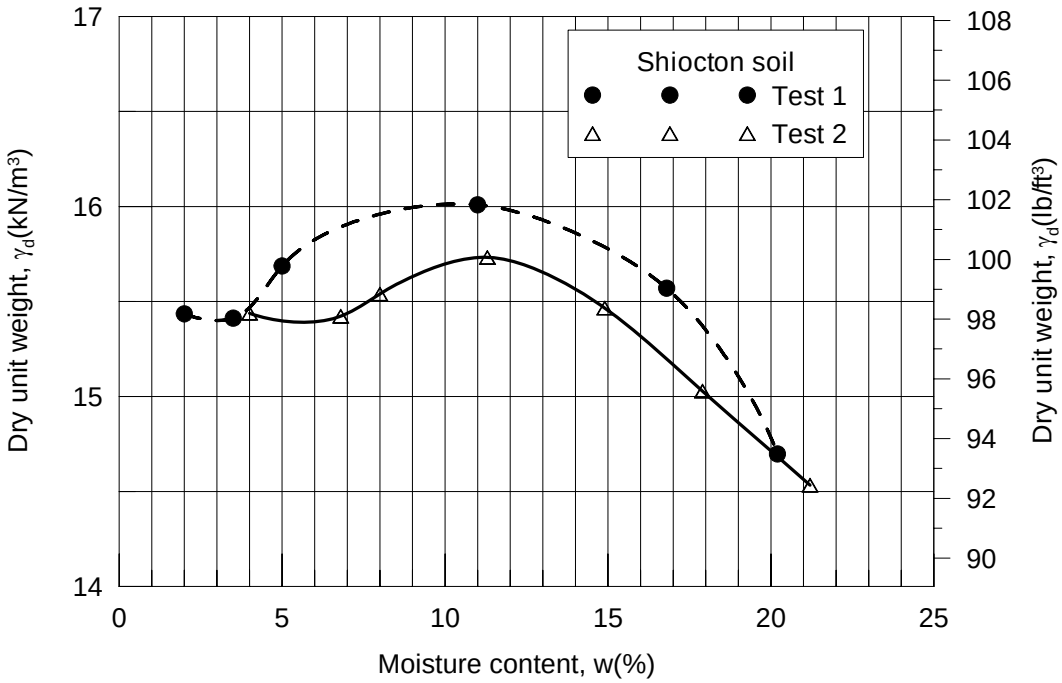

Figure A.27: Results of Standard Proctor test for Shiocton soil

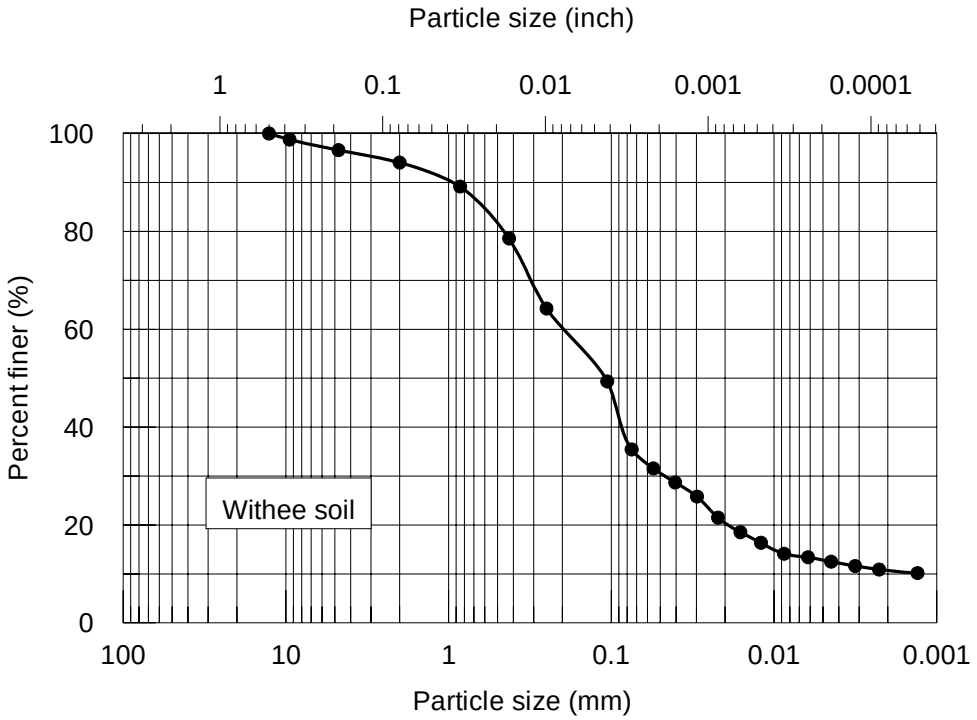

Figure A.28: Particle size distribution curve for Withee soil

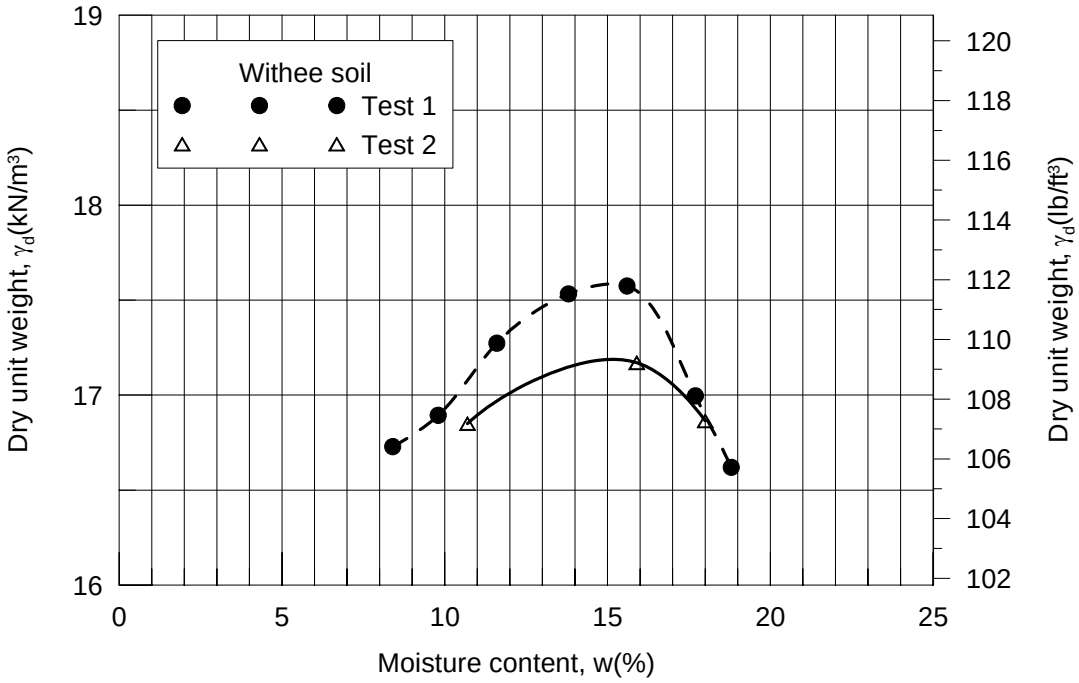

Figure A.29 Results of Standard Proctor test for Withee soil

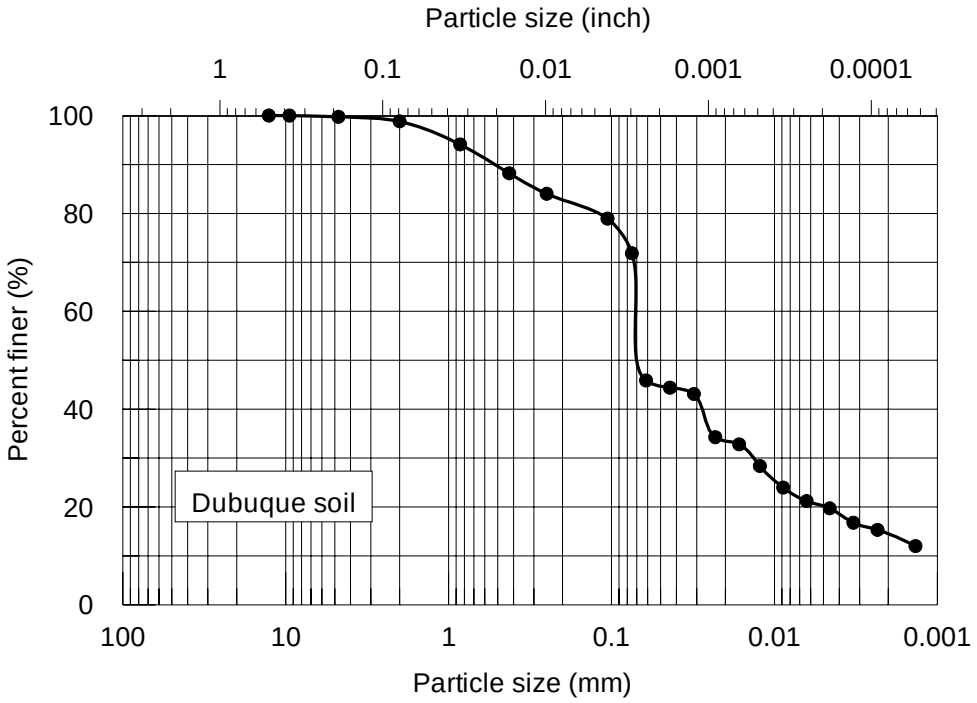

Figure A.30: Particle size distribution curve for Dubuque soil

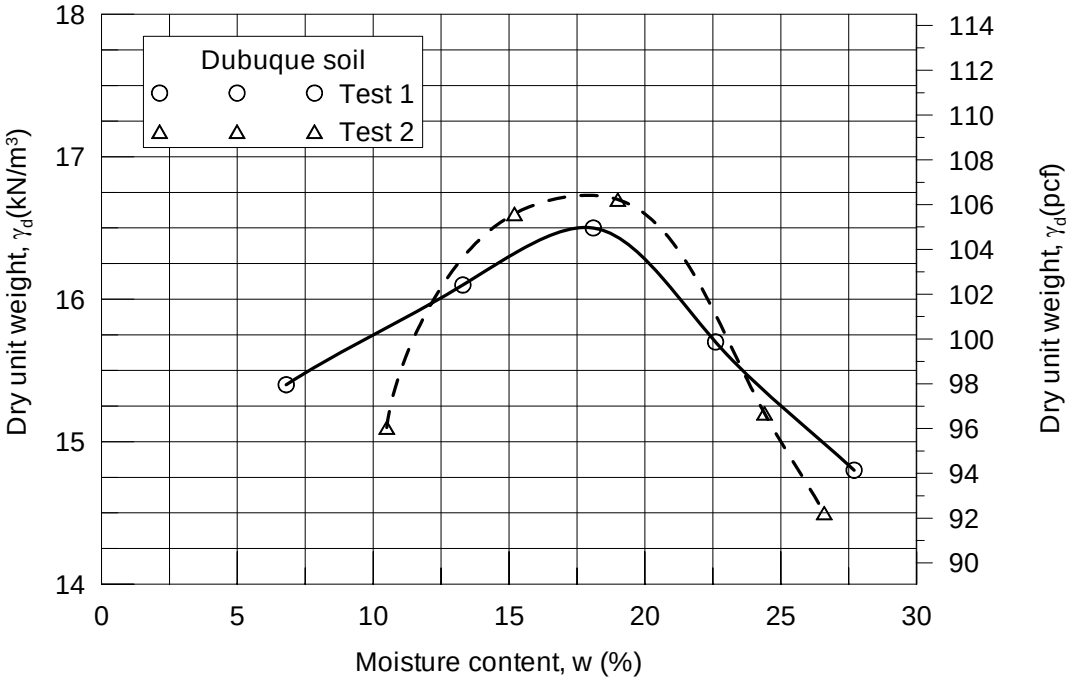

Figure A.31 Results of Standard Proctor test for Dubuque soil

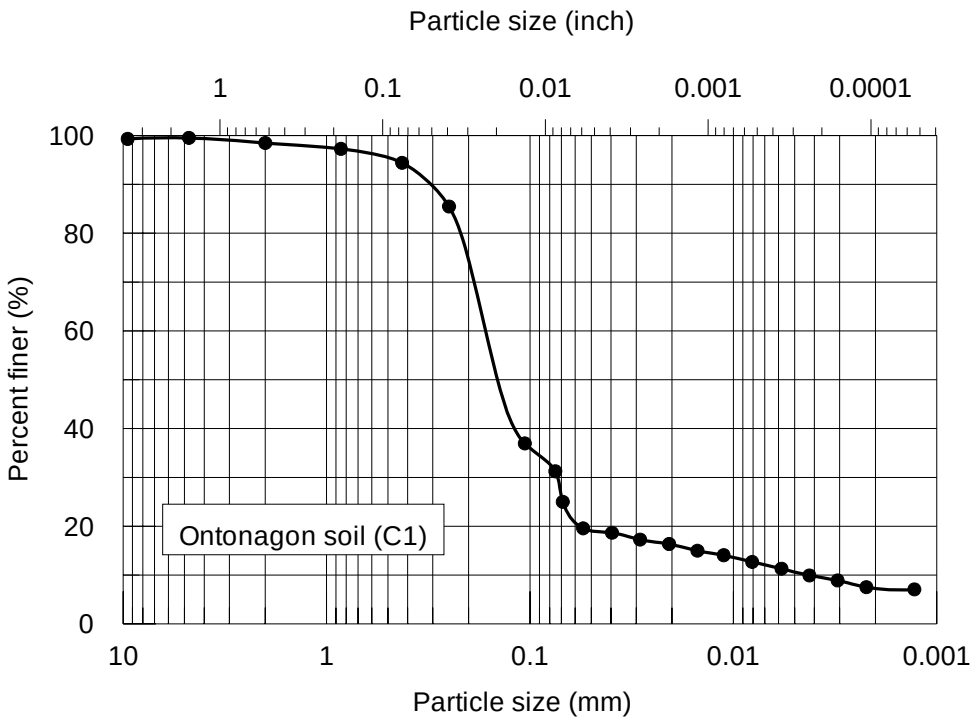

Figure A.32: Particle size distribution curve for Ontonagon soil -1

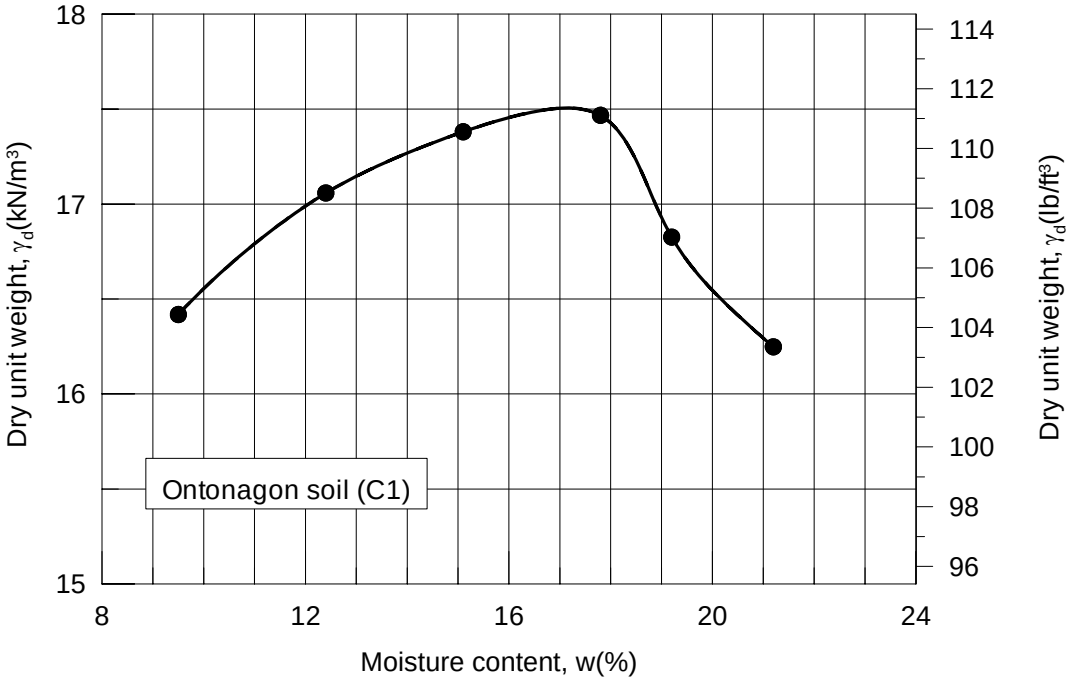

Figure A.33: Results of Standard Proctor test for Ontonagon soil - 1

Appendix B

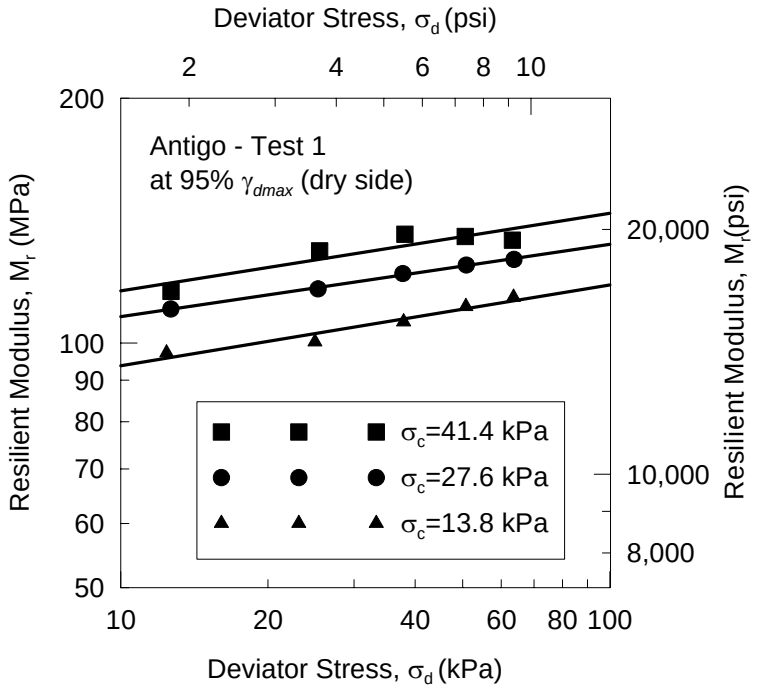

(a) Test on soil specimen #1

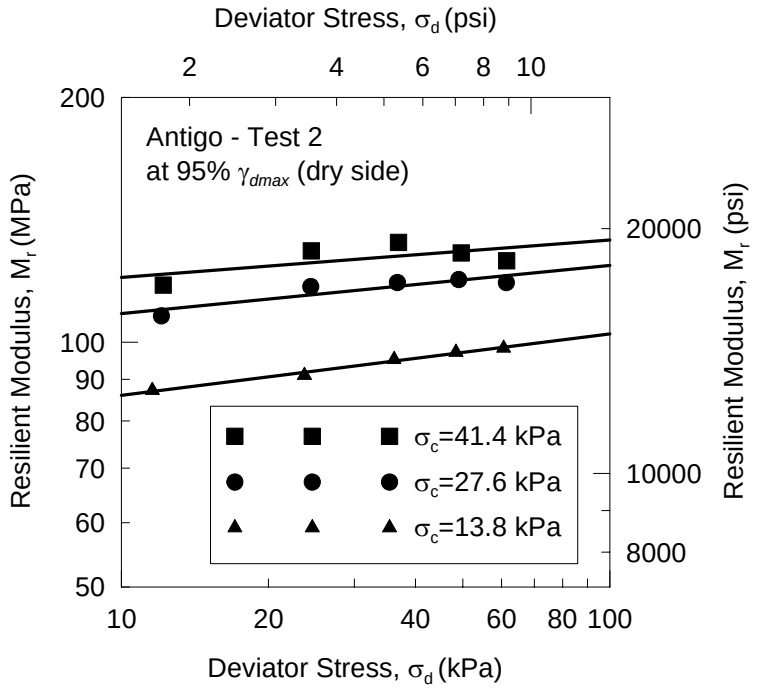

(b) Test on soil specimen #2

Figure B-1: Results of repeated load triaxial test on Antigo soil compacted at 95% of maximum dry unit weight (γ_{dmax}) and moisture content less than $w_{opt.}$ (dry side)

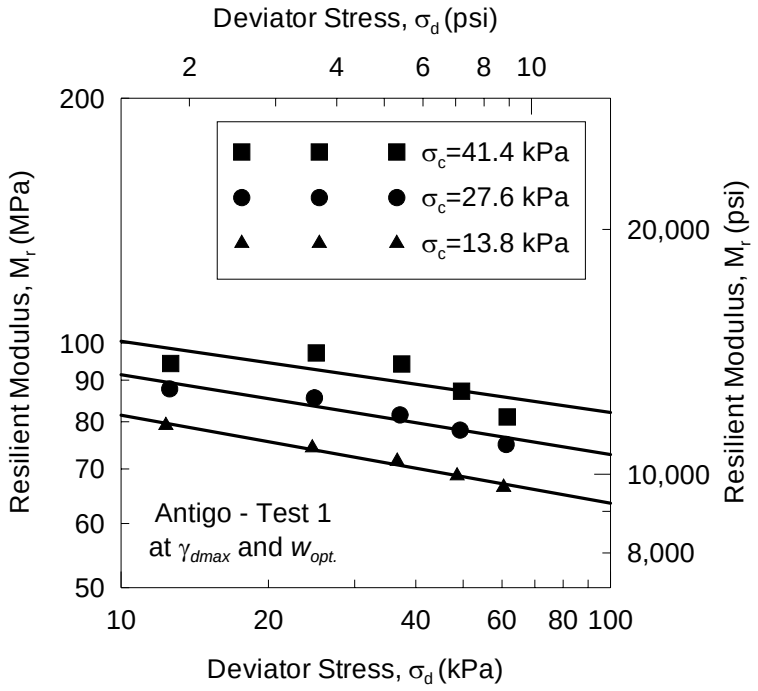

(a) Test on soil specimen #1

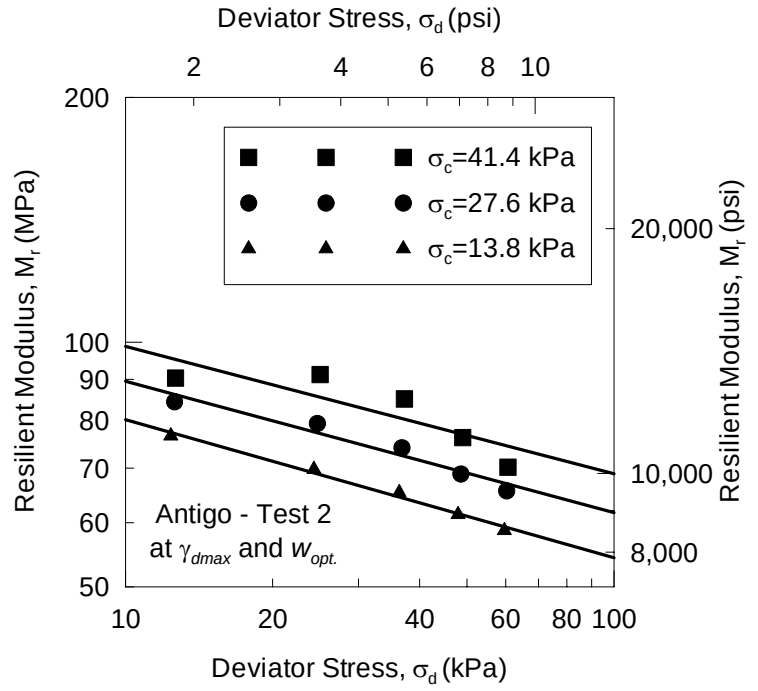

(b) Test on soil specimen #2

Figure B-2: Results of repeated load triaxial test on Antigo soil compacted at maximum dry unit weight (γ_{dmax}) and optimum moisture content ($w_{opt.}$)

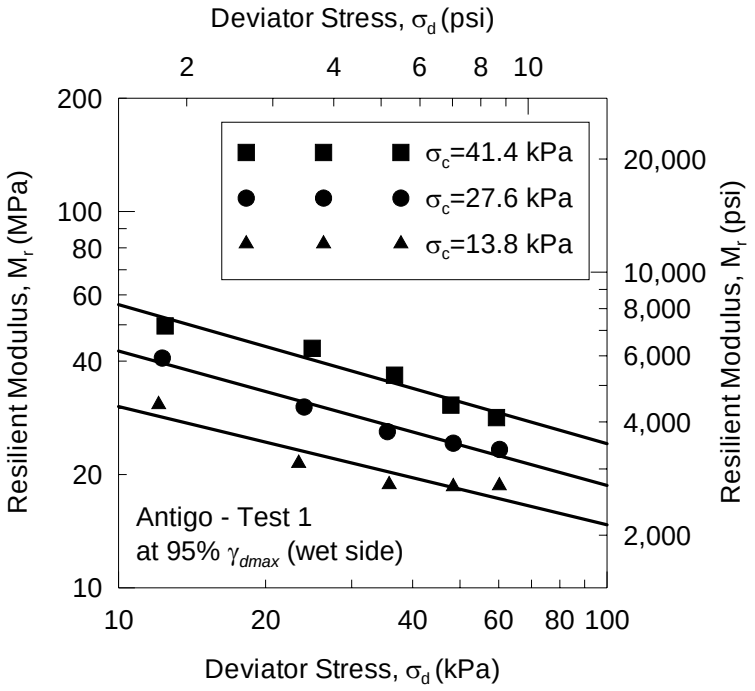

(a) Test on soil specimen #1

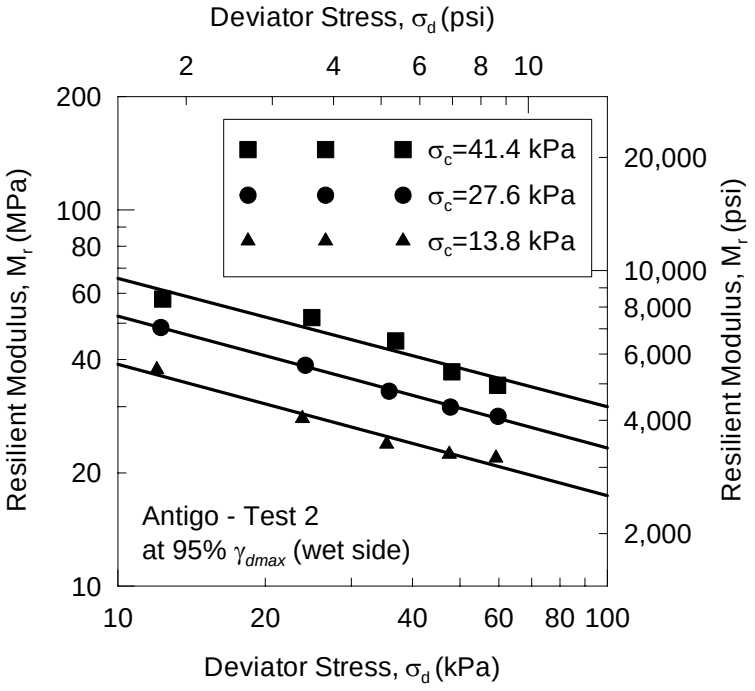

(b) Test on soil specimen #2

Figure B-3: Results of repeated load triaxial test on Antigo soil compacted at 95% of maximum dry unit weight (γ_{dmax}) and moisture content more than $w_{opt.}$ (wet side)

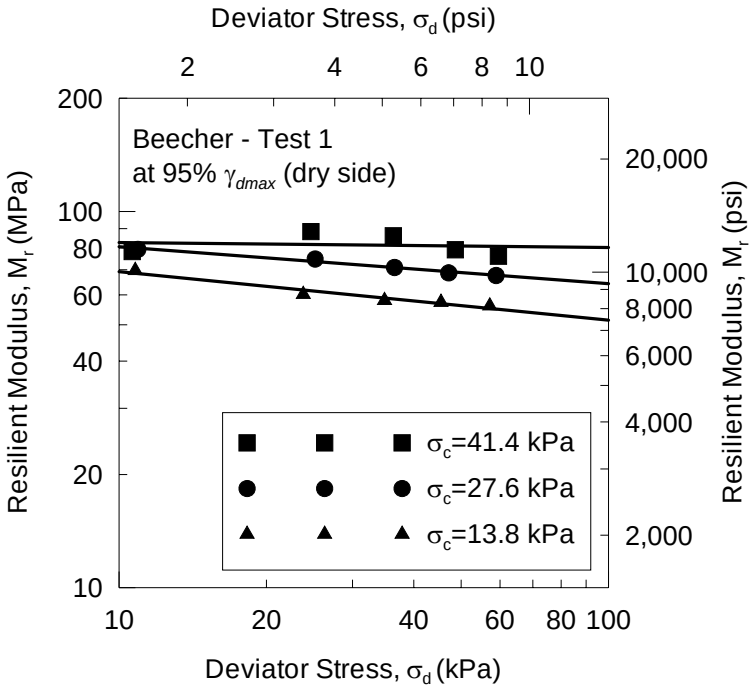

(a) Test on soil specimen #1

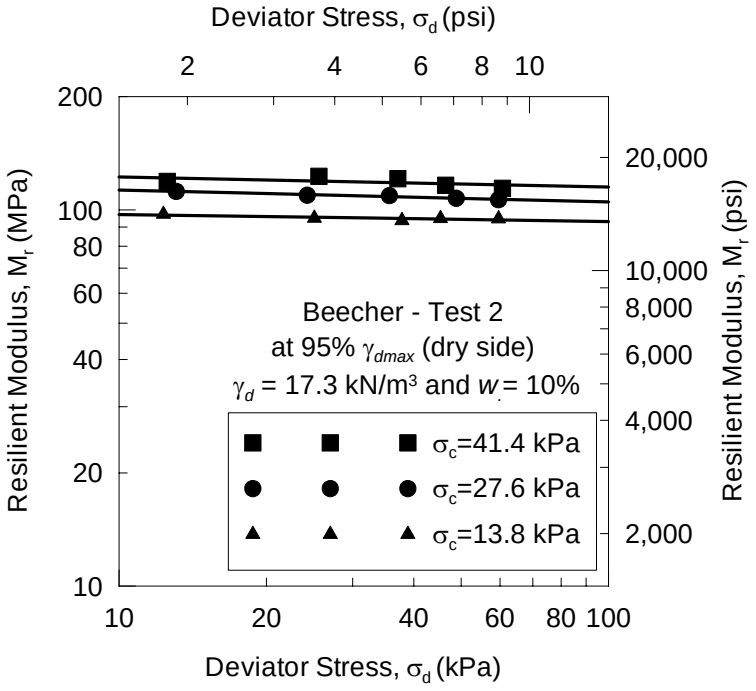

(b) Test on soil specimen #2

Figure B-4: Results of repeated load triaxial test on Beecher soil compacted at 95% of maximum dry unit weight (γ_{dmax}) and moisture content less than $w_{opt.}$ (dry side)

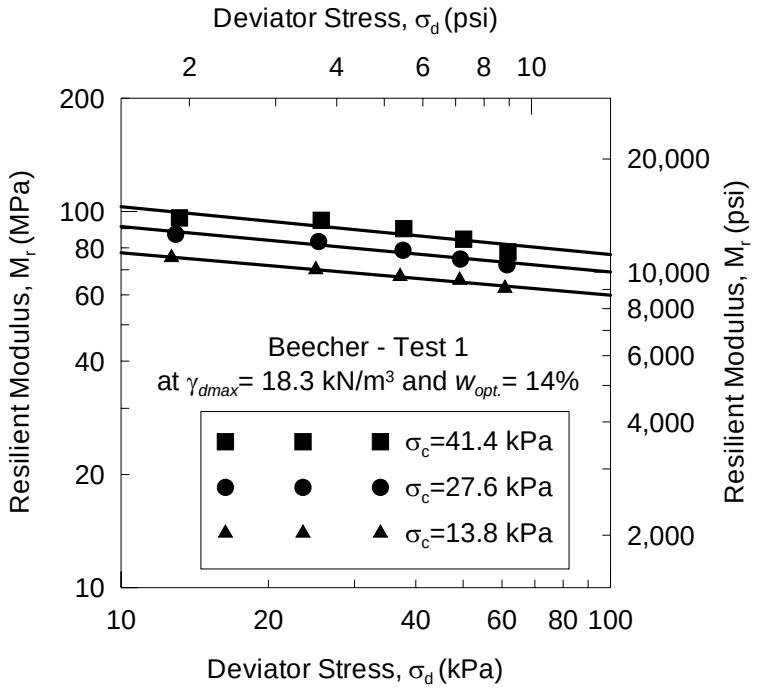

(a) Test on soil specimen #1

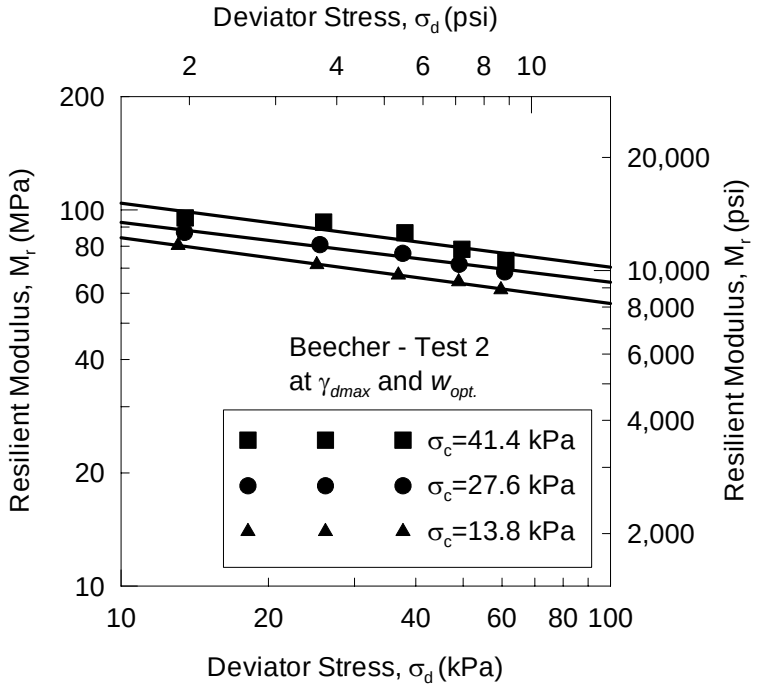

(b) Test on soil specimen #2

Figure B-5: Results of repeated load triaxial test on Beecher soil compacted at maximum dry unit weight (γ_{dmax}) and optimum moisture content ($w_{opt.}$)

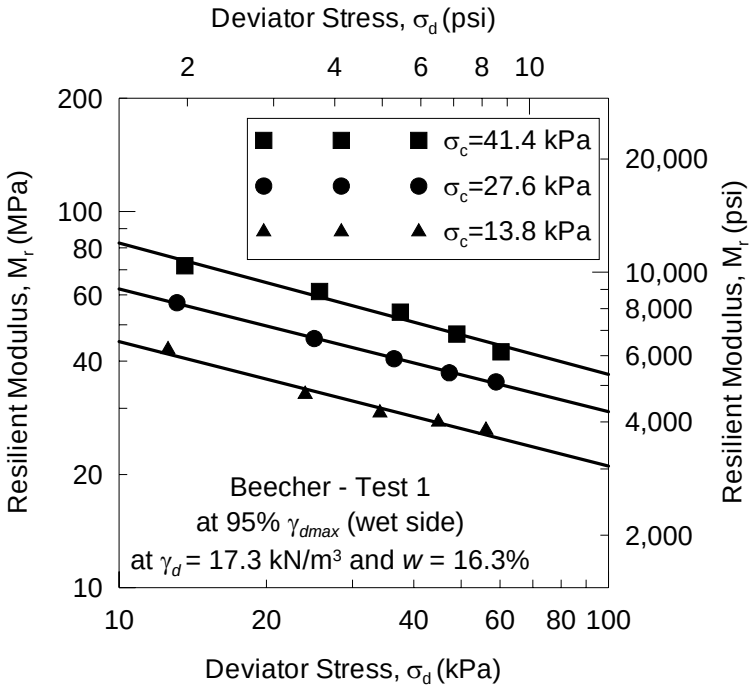

(a) Test on soil specimen #1

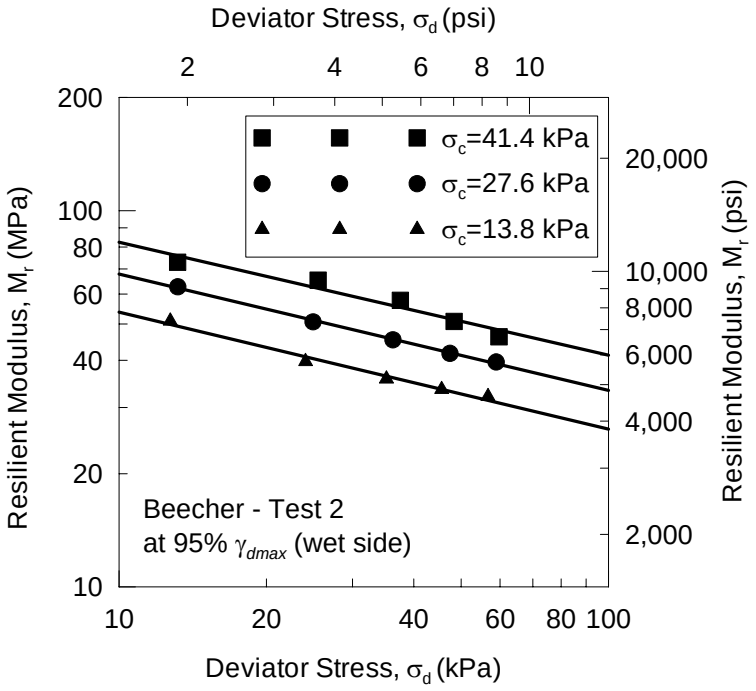

(b) Test on soil specimen #2

Figure B-6: Results of repeated load triaxial test on Beecher soil compacted at 95% of maximum dry unit weight (γ_{dmax}) and moisture content more than $w_{opt.}$ (wet side)

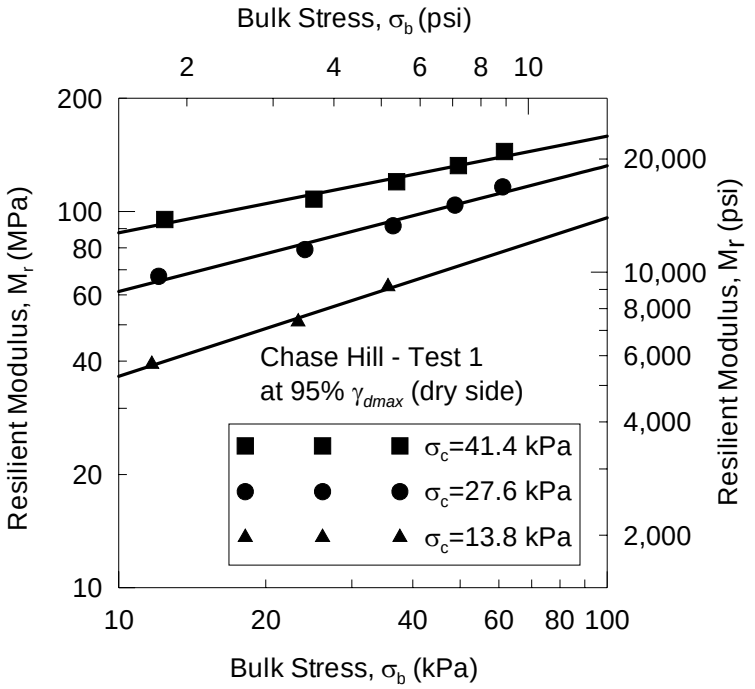

(a) Test on soil specimen #1

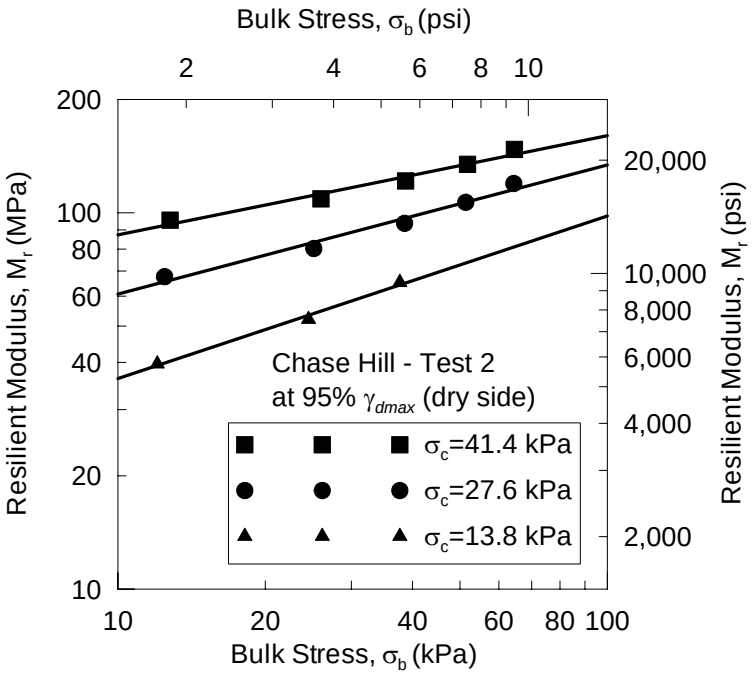

(b) Test on soil specimen #2

Figure B-7: Results of repeated load triaxial test on Goodman soil compacted at 95% of maximum dry unit weight (γ_{dmax}) and moisture content less than $w_{opt.}$ (dry side)

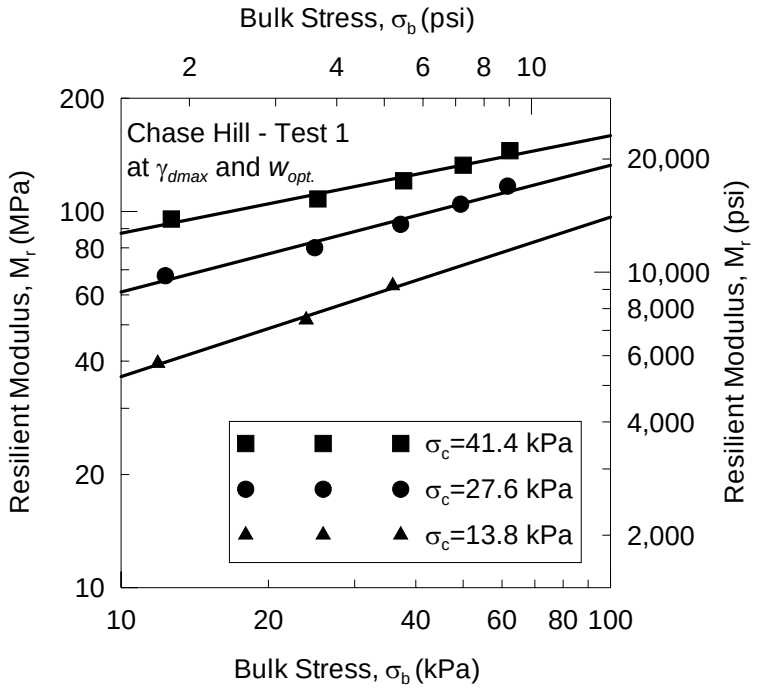

(a) Test on soil specimen #1

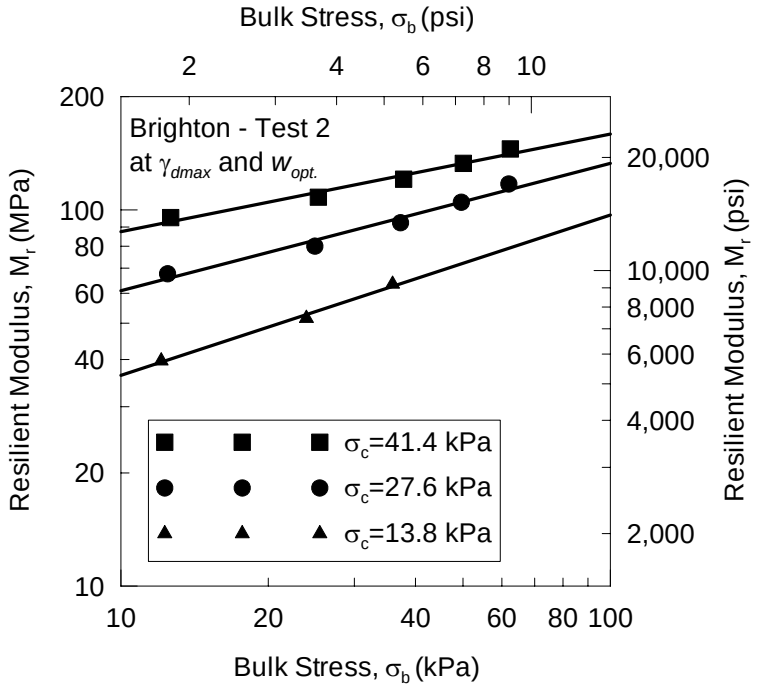

(b) Test on soil specimen #2

Figure B-8: Results of repeated load triaxial test on Goodman soil compacted at maximum dry unit weight (γ_{dmax}) and optimum moisture content ($w_{opt.}$)

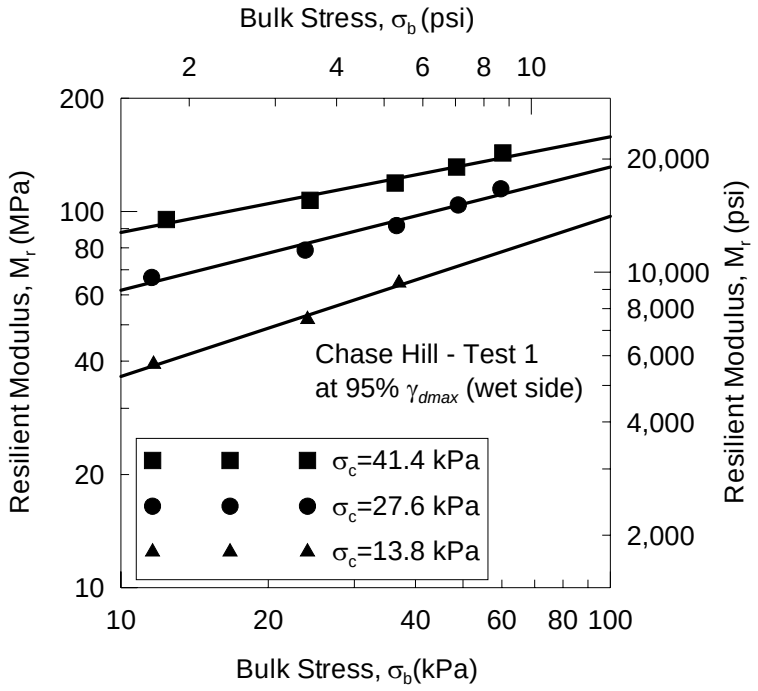

(a) Test on soil specimen #1

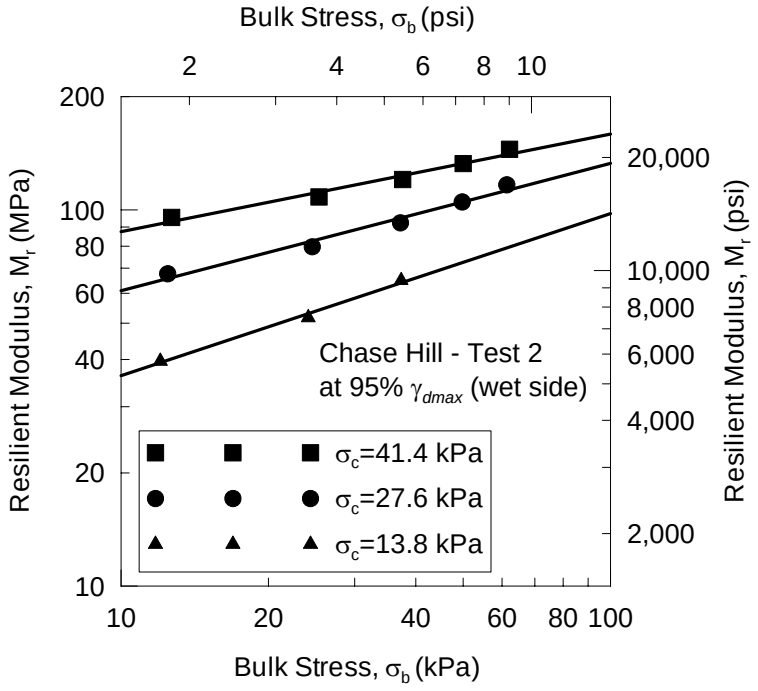

(b) Test on soil specimen #2

Figure B-9: Results of repeated load triaxial test on Goodman soil compacted at 95% of maximum dry unit weight (γ_{dmax}) and moisture content more than $w_{opt.}$ (wet side)

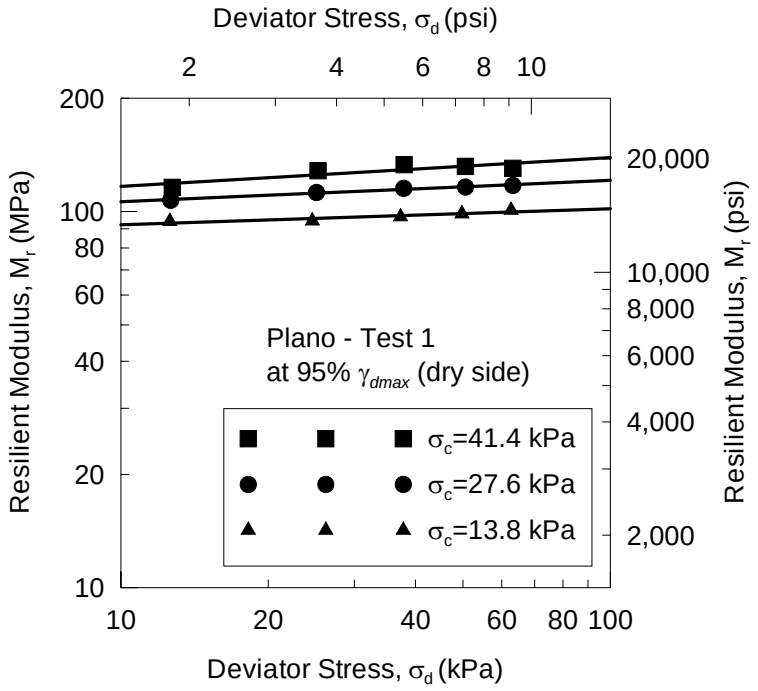

(a) Test on soil specimen #1

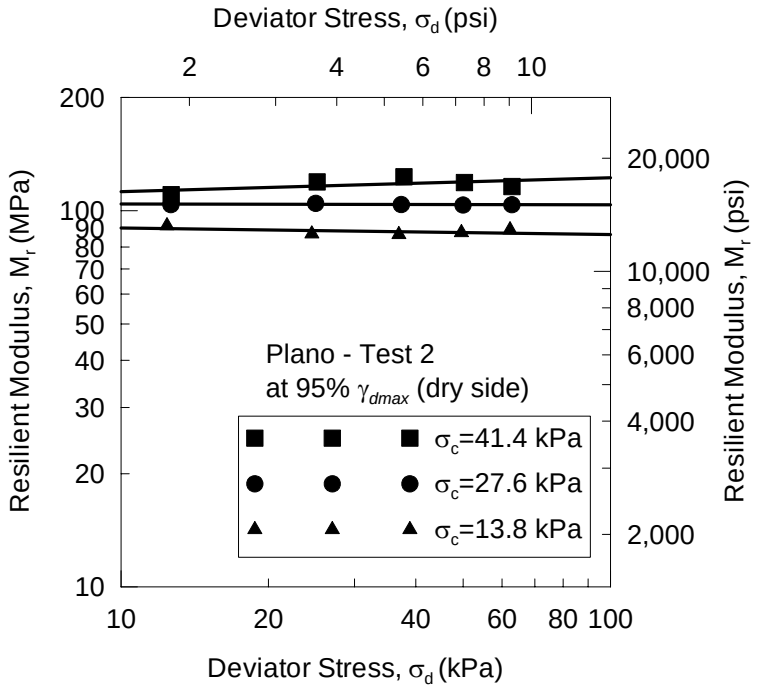

(b) Test on soil specimen #2

Figure B-10: Results of repeated load triaxial test on Plano soil compacted at 95% of maximum dry unit weight (γ_{dmax}) and moisture content less than $w_{opt.}$ (dry side)

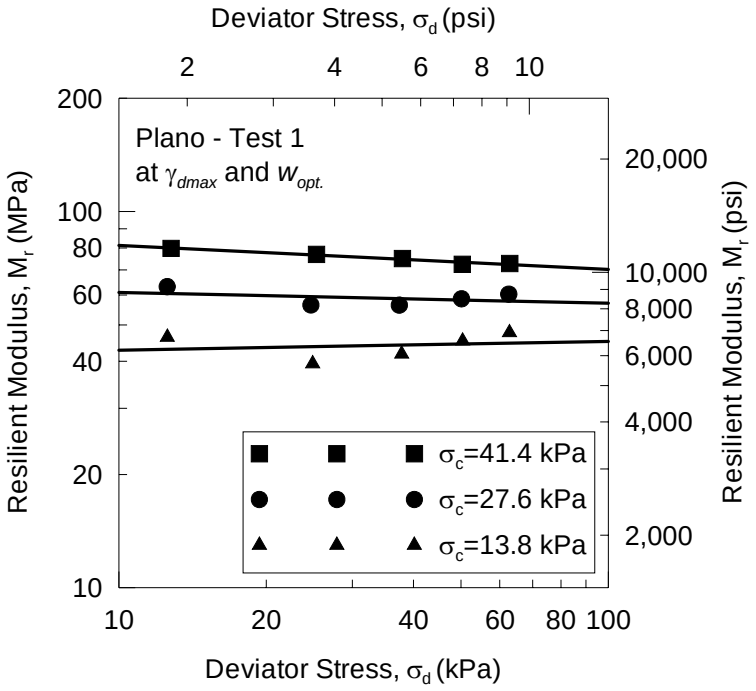

(a) Test on soil specimen #1

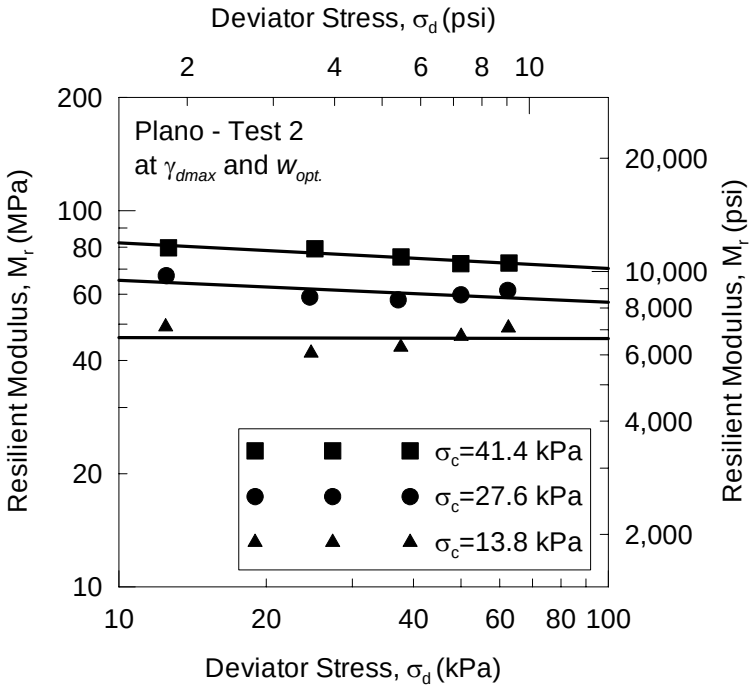

(b) Test on soil specimen #2

Figure B-11: Results of repeated load triaxial test on Plano soil compacted at maximum dry unit weight (γ_{dmax}) and optimum moisture content ($w_{opt.}$)

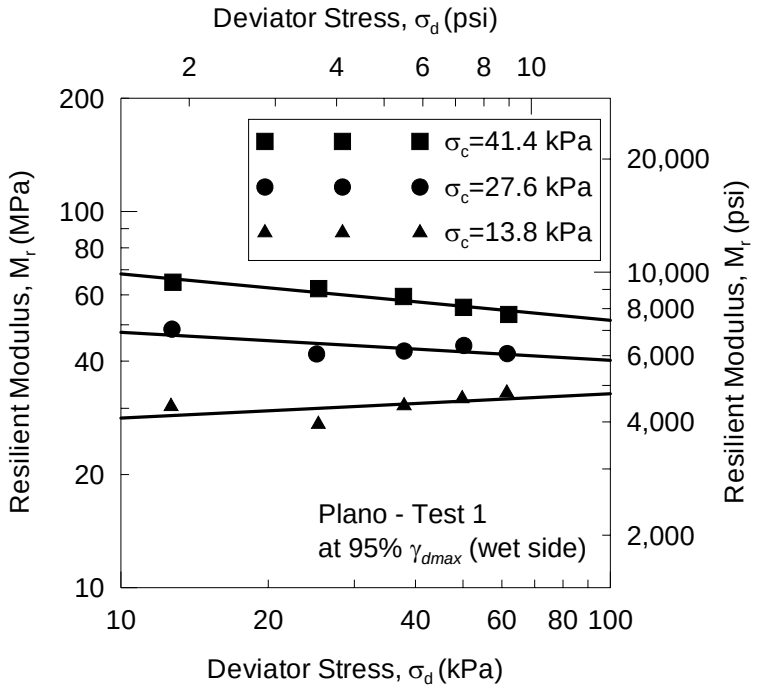

(a) Test on soil specimen #1

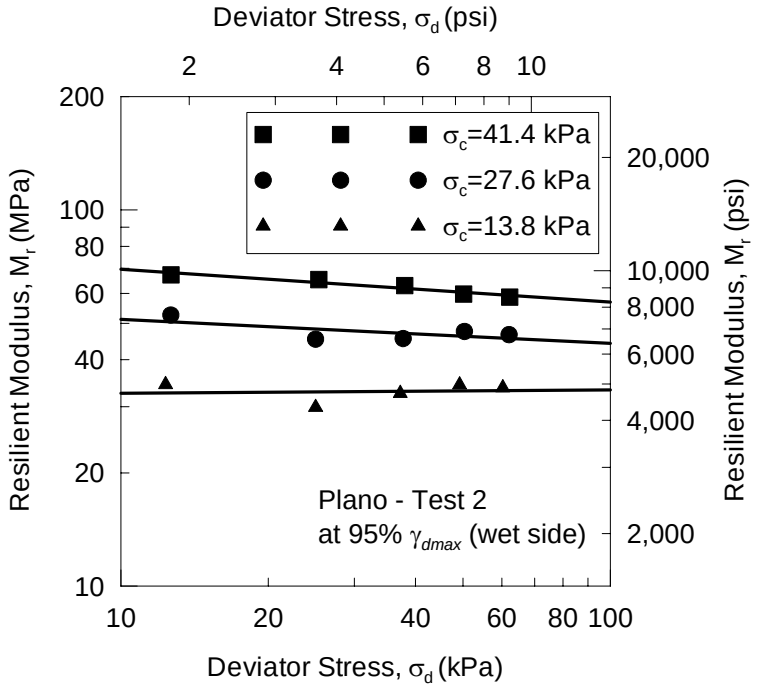

(b) Test on soil specimen #2

Figure B-12: Results of repeated load triaxial test on Plano soil compacted at 95% of maximum dry unit weight (γ_{dmax}) and moisture content more than $w_{opt.}$ (wet side)

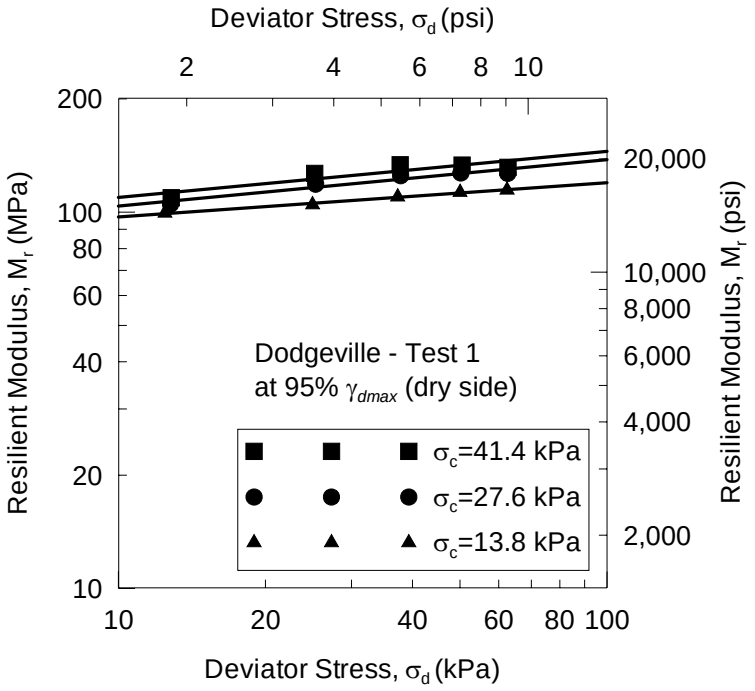

(a) Test on soil specimen #1

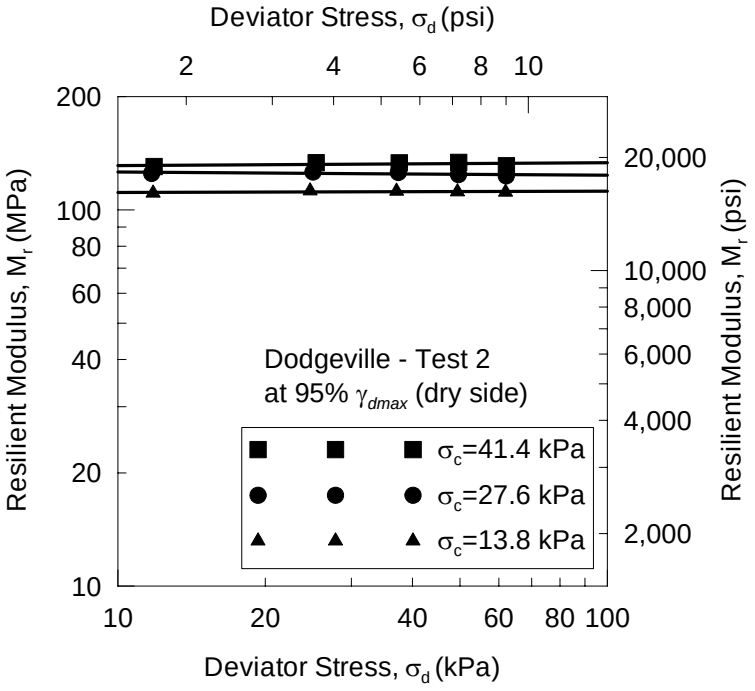

(b) Test on soil specimen #2

Figure B-13: Results of repeated load triaxial test on Dodgeville soil compacted at 95% of maximum dry unit weight (γ_{dmax}) and moisture content less than $w_{opt.}$ (dry side)

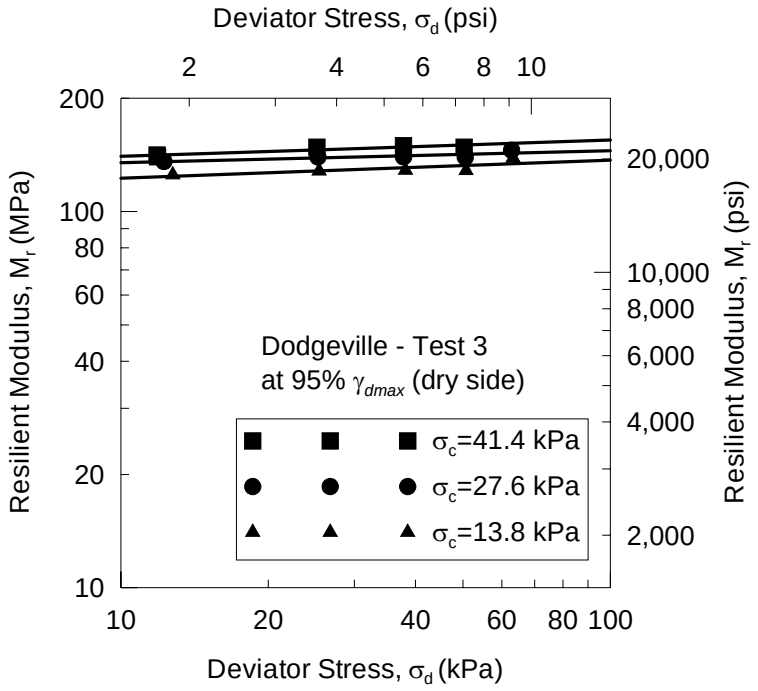

(c) Test on soil specimen #3

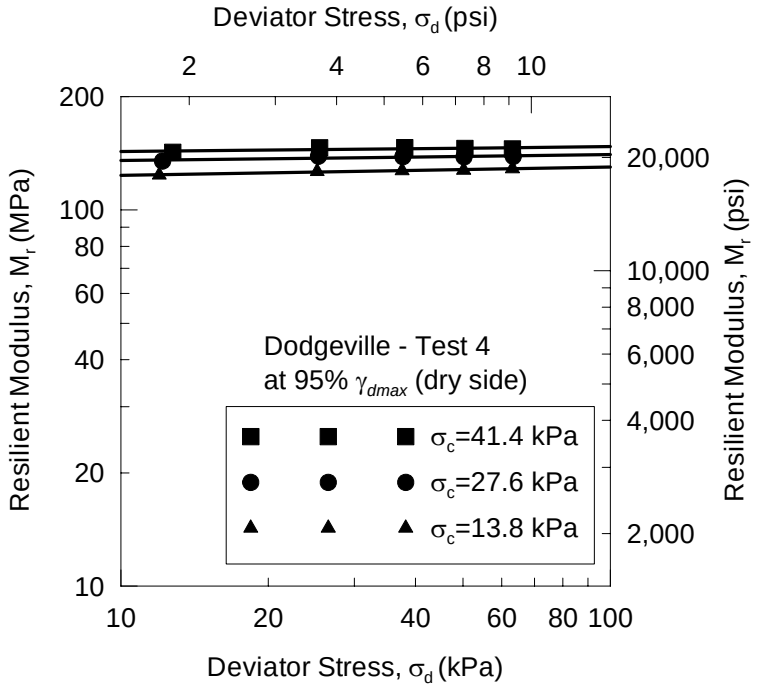

(d) Test on soil specimen #4

Figure B-13 (cont.): Results of repeated load triaxial test on Dodgeville soil compacted at 95% of maximum dry unit weight (γ_{dmax}) and moisture content less than $w_{opt.}$ (dry side)

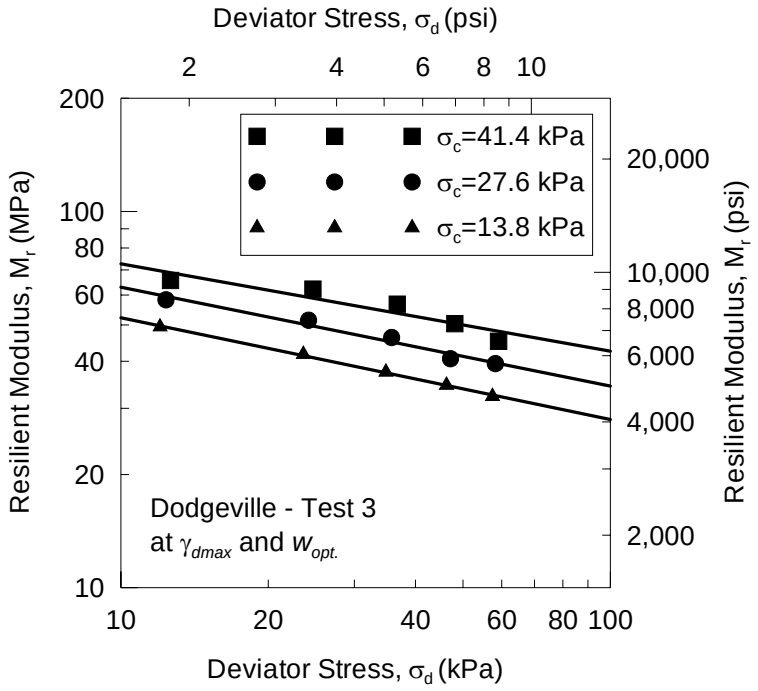

(a) Test on soil specimen #1

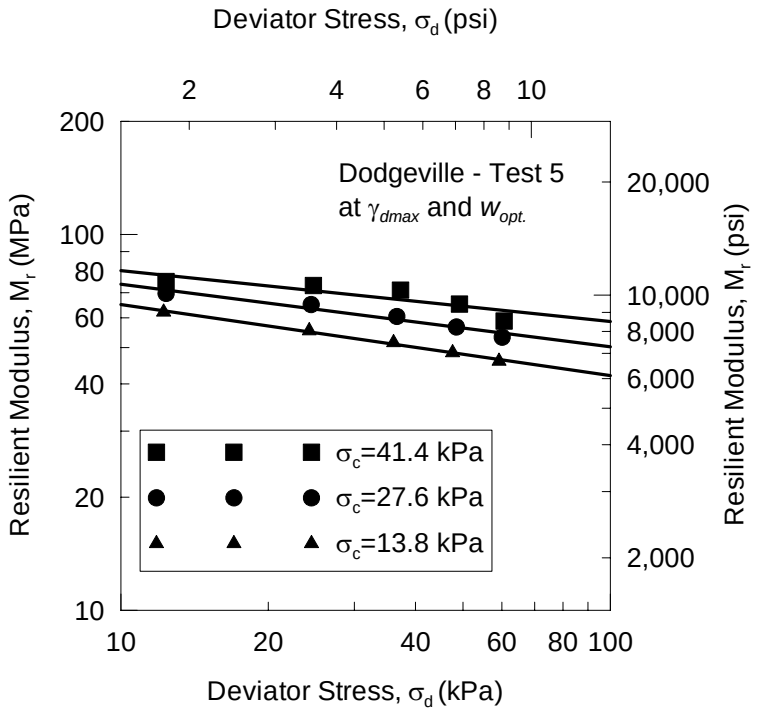

(b) Test on soil specimen #2

Figure B-14: Results of repeated load triaxial test on Dodgeville soil compacted at maximum dry unit weight (γ_{dmax}) and optimum moisture content ($w_{opt.}$)

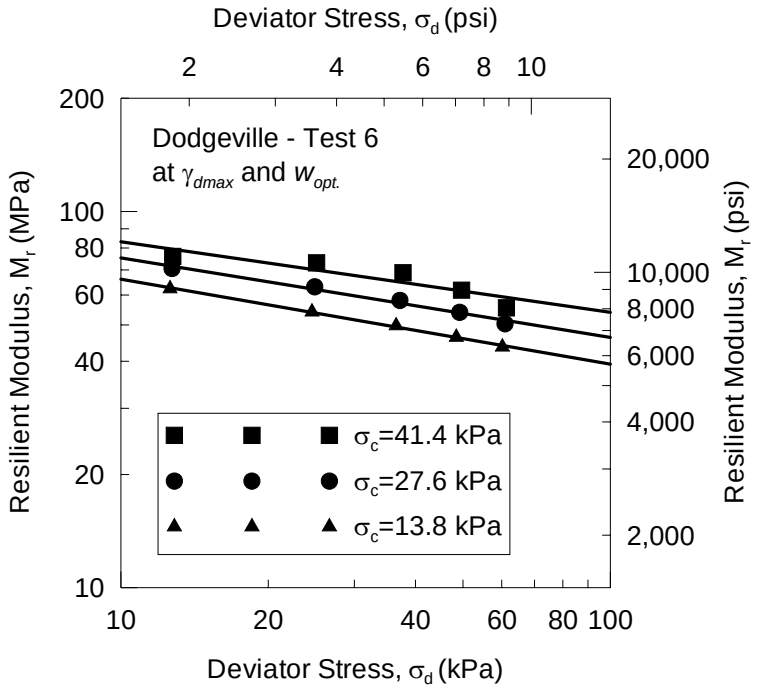

(c) Test on soil specimen #3

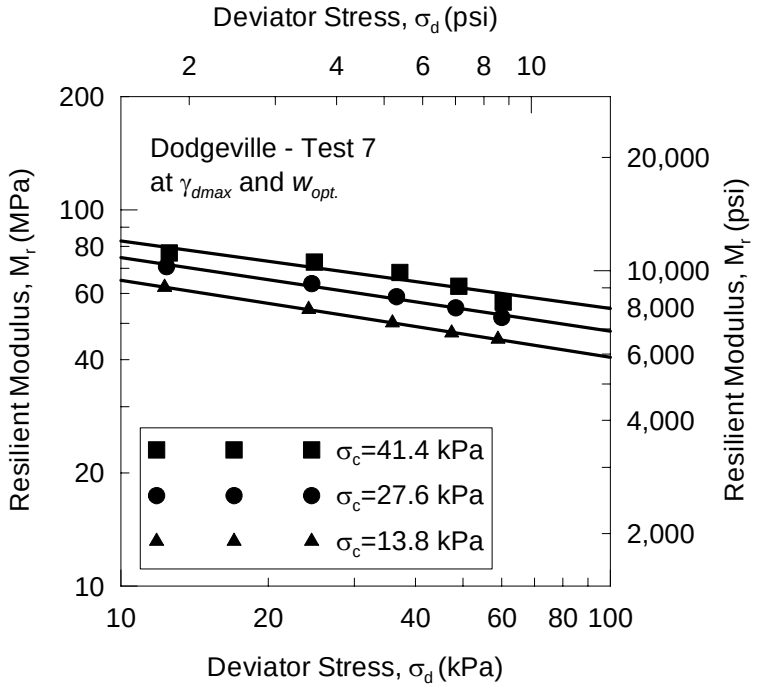

(d) Test on soil specimen #4

Figure B-14 (cont.): Results of repeated load triaxial test on Dodgeville soil compacted at maximum dry unit weight (γ_{dmax}) and optimum moisture content ($w_{opt.}$)

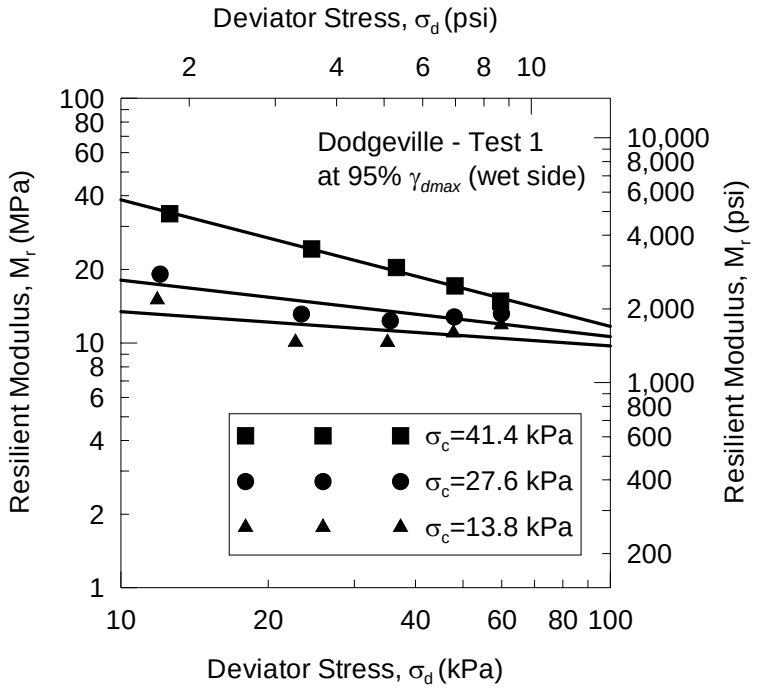

(a) Test on soil specimen #1

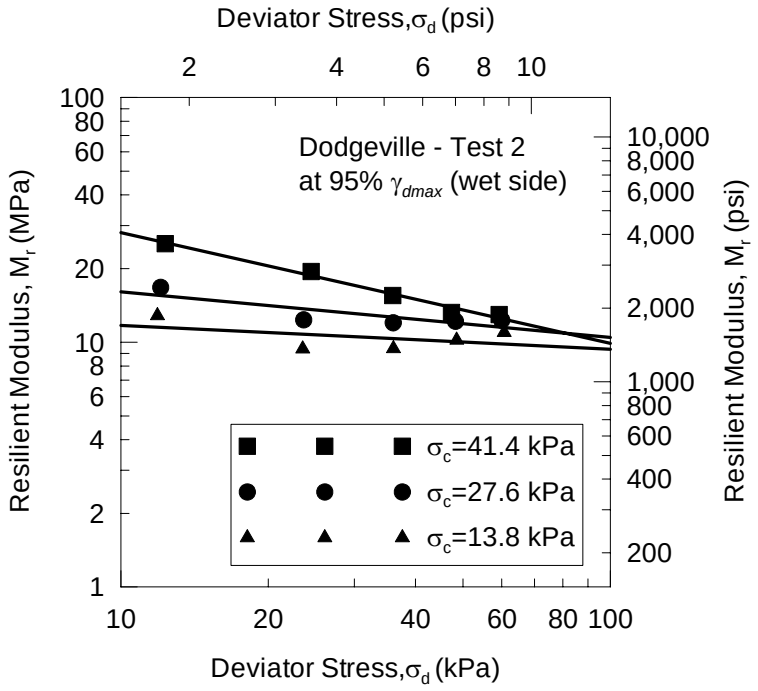

(b) Test on soil specimen #2

Figure B-15: Results of repeated load triaxial test on Dodgeville soil compacted at 95% of maximum dry unit weight (γ_{dmax}) and moisture content more than $w_{opt.}$ (wet side)

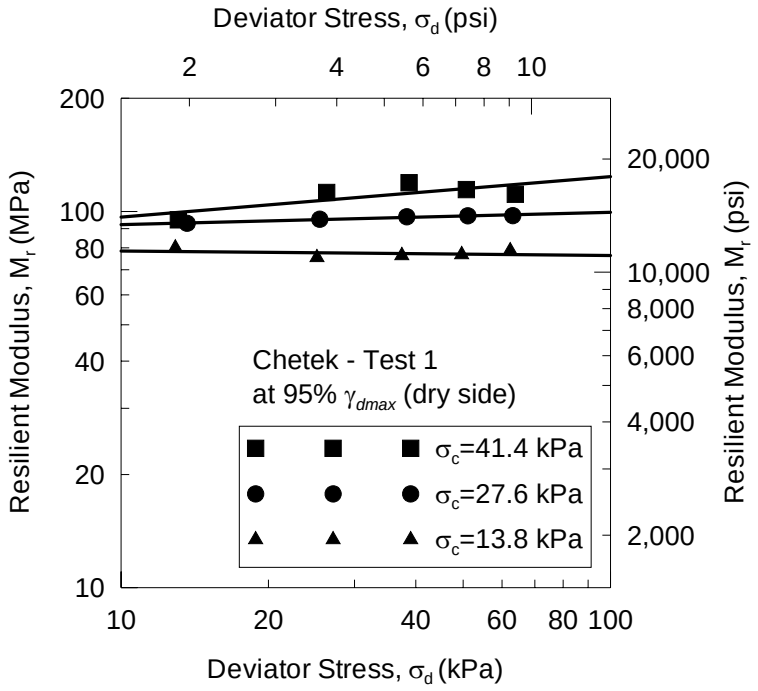

(a) Test on soil specimen #1

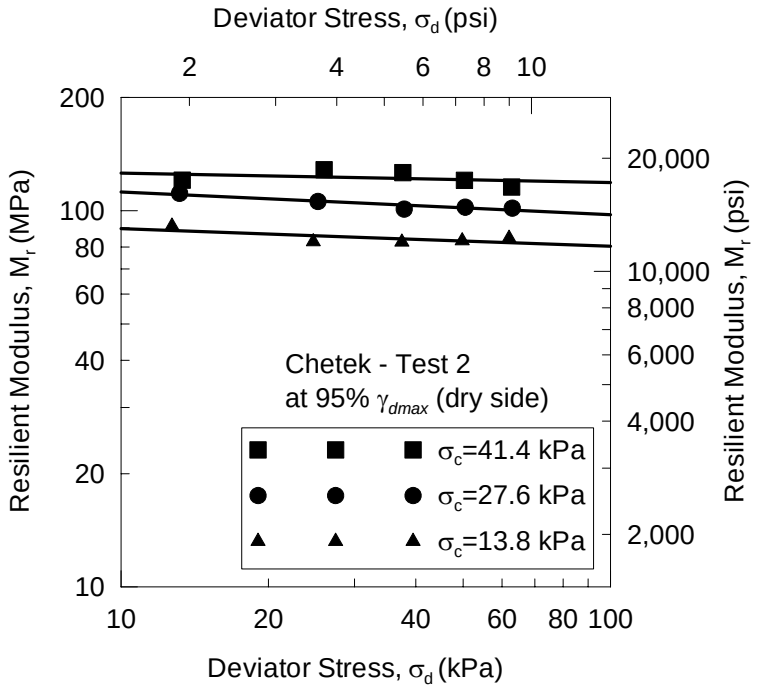

(b) Test on soil specimen #2

Figure B-16: Results of repeated load triaxial test on Chetek soil compacted at 95% of maximum dry unit weight (γ_{dmax}) and moisture content less than $w_{opt.}$ (dry side)

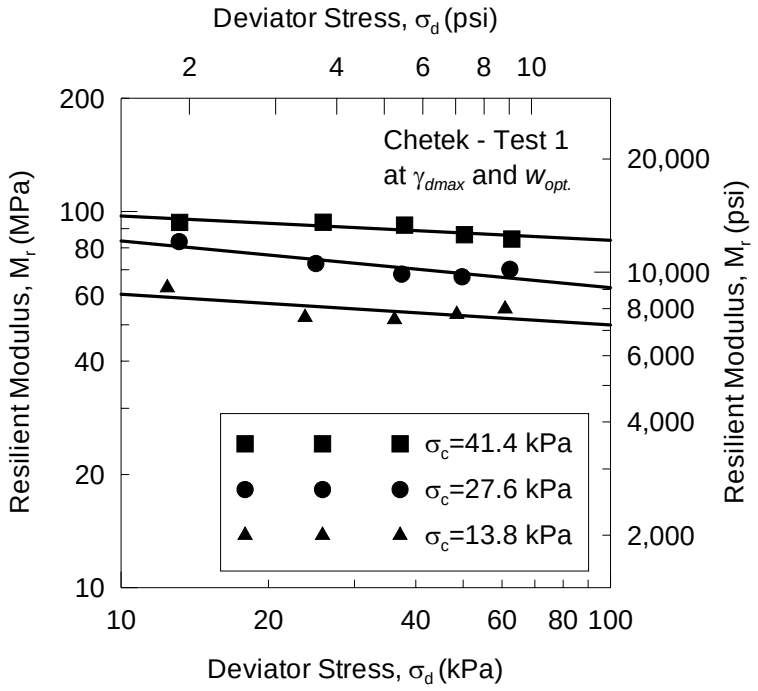

(a) Test on soil specimen #1

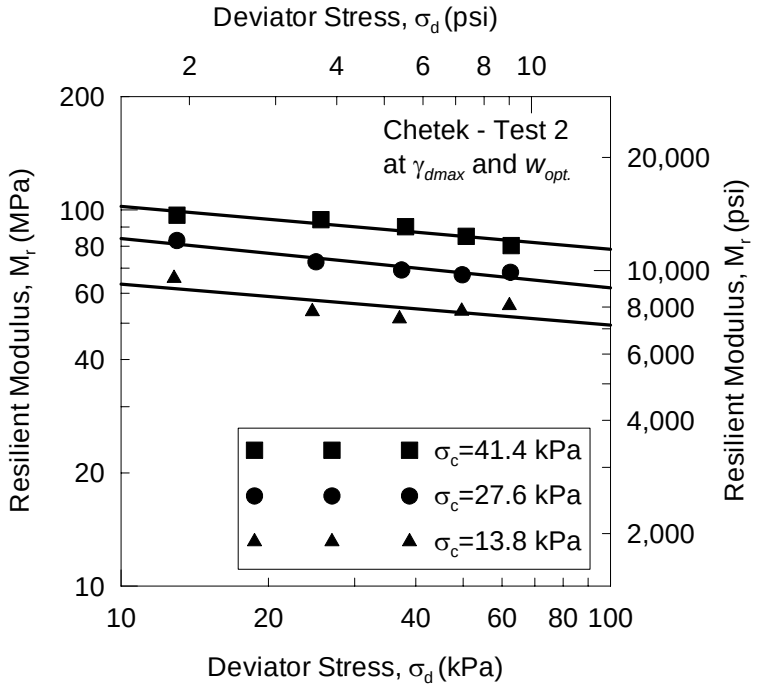

(b) Test on soil specimen #2

Figure B-17: Results of repeated load triaxial test on Chetek soil compacted at maximum dry unit weight (γ_{dmax}) and optimum moisture content ($w_{opt.}$)

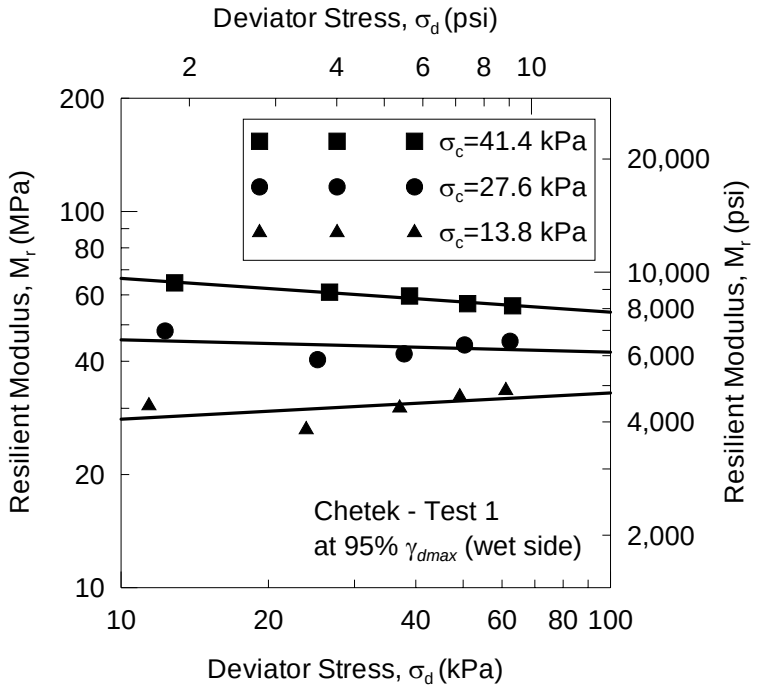

(a) Test on soil specimen #1

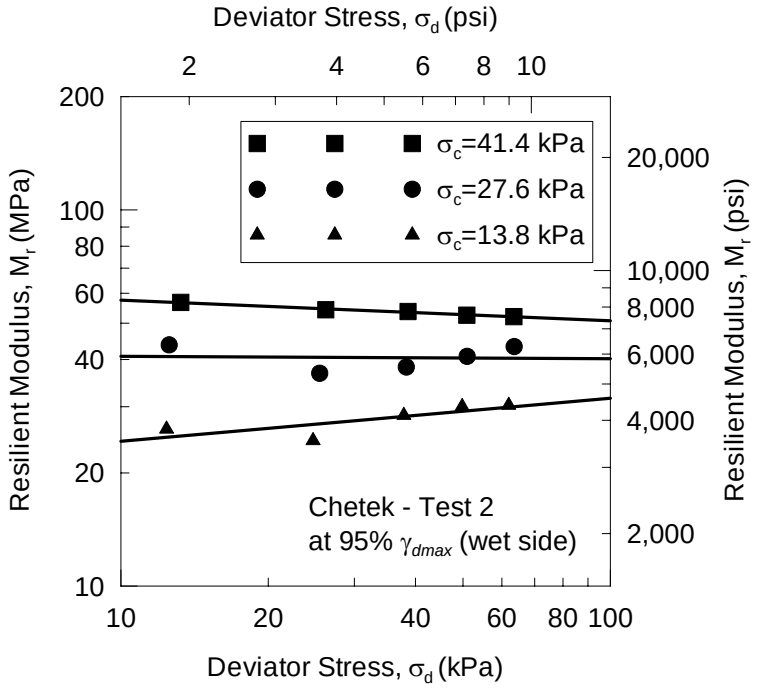

(b) Test on soil specimen #2

Figure B-18: Results of repeated load triaxial test on Chetek soil compacted at 95% of maximum dry unit weight (γ_{dmax}) and moisture content more than $w_{opt.}$ (wet side)

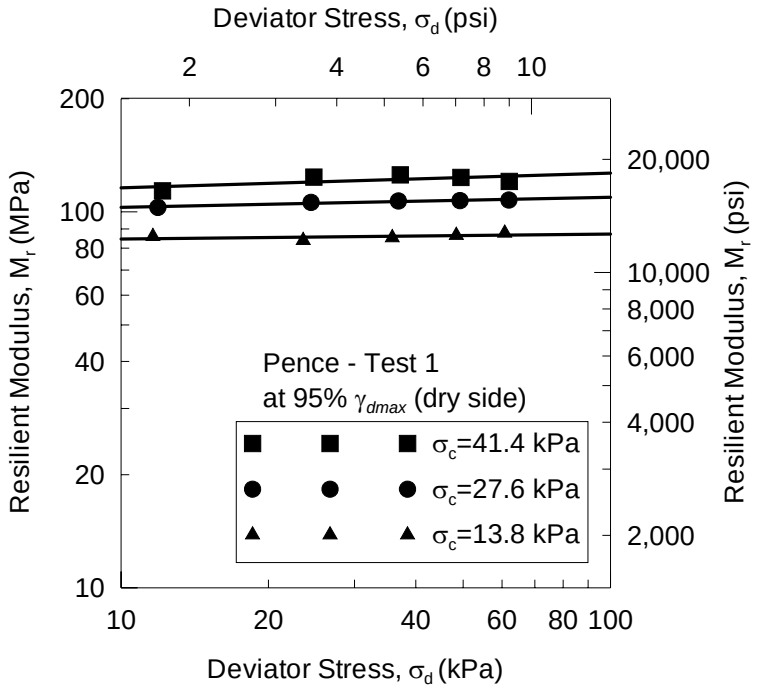

(a) Test on soil specimen #1

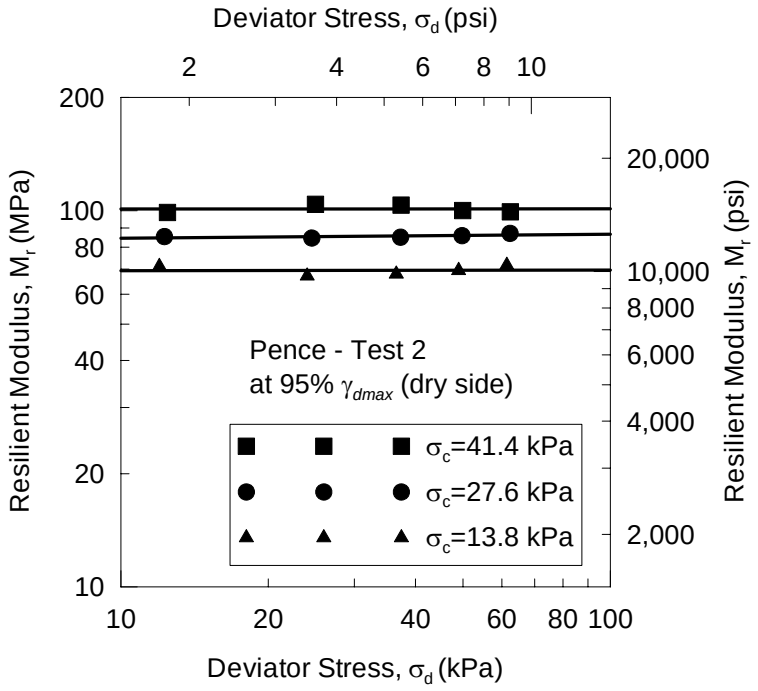

(b) Test on soil specimen #2

Figure B-19: Results of repeated load triaxial test on Pence soil compacted at 95% of maximum dry unit weight (γ_{dmax}) and moisture content less than $w_{opt.}$ (dry side)

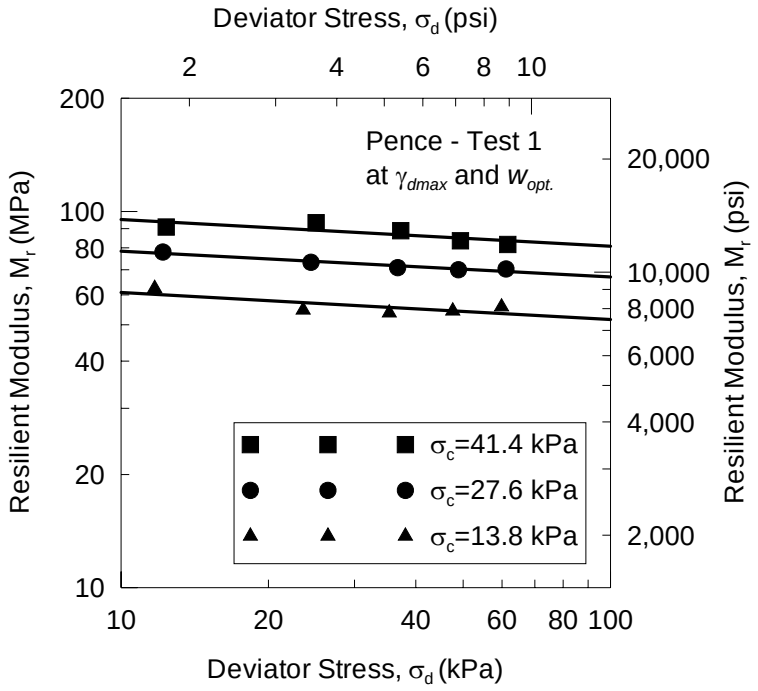

(a) Test on soil specimen #1

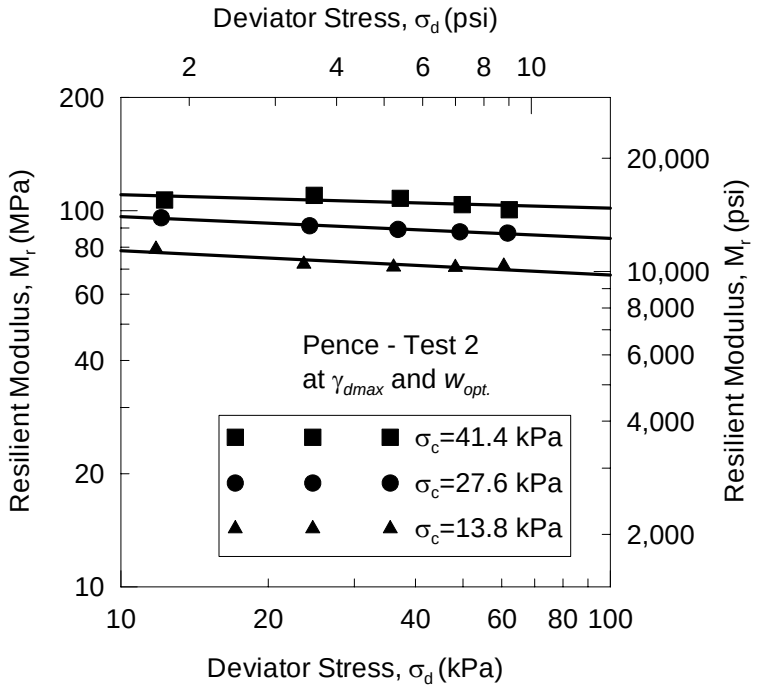

(b) Test on soil specimen #2

Figure B-20: Results of repeated load triaxial test on Pence soil compacted at maximum dry unit weight (γ_{dmax}) and optimum moisture content ($w_{opt.}$)

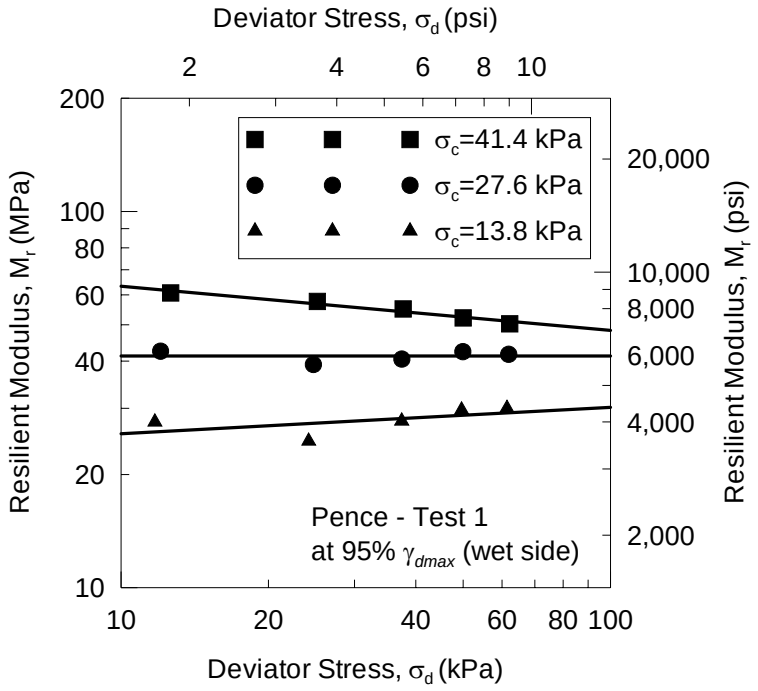

(a) Test on soil specimen #1

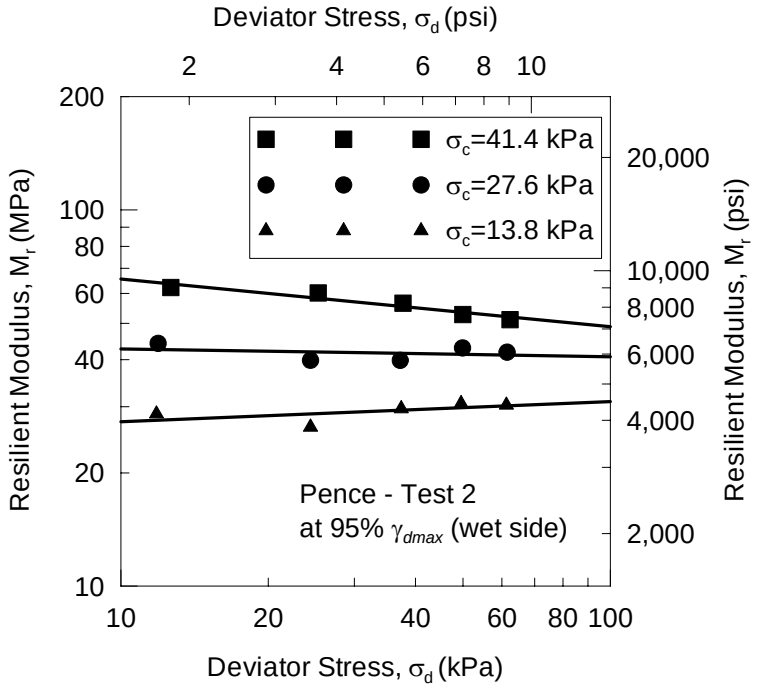

(b) Test on soil specimen #2

Figure B-21: Results of repeated load triaxial test on Pence soil compacted at 95% of maximum dry unit weight (γ_{dmax}) and moisture content more than $w_{opt.}$ (wet side)

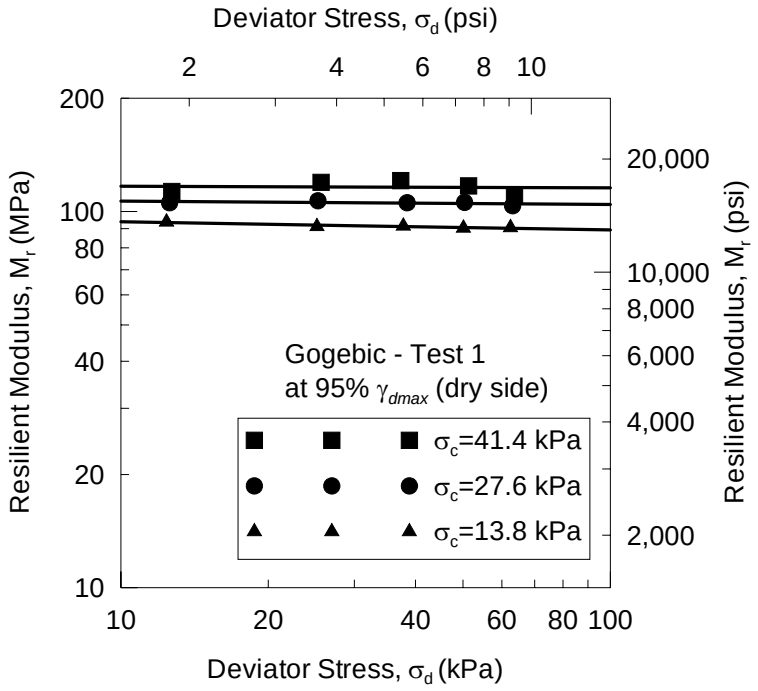

(a) Test on soil specimen #1

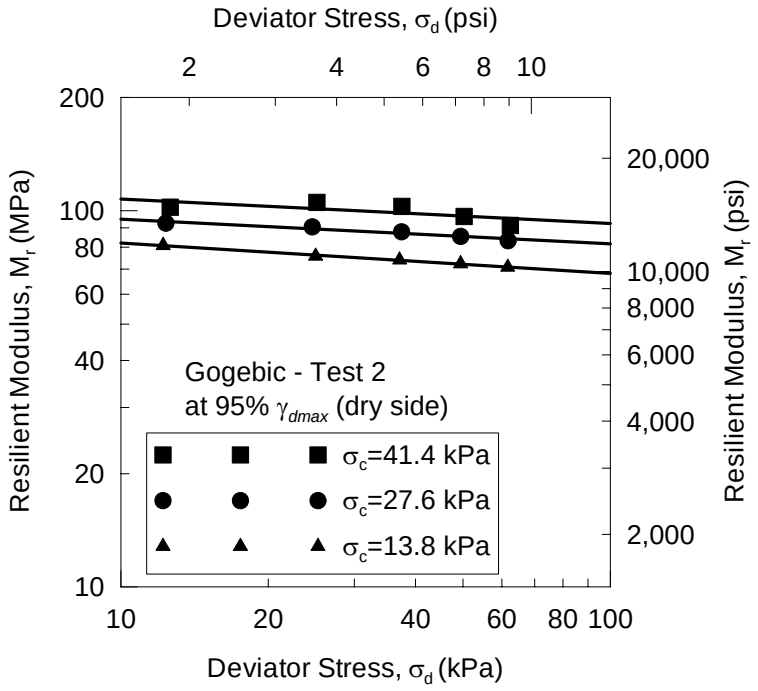

(b) Test on soil specimen #2

Figure B-22: Results of repeated load triaxial test on Gogebic soil compacted at 95% of maximum dry unit weight (γ_{dmax}) and moisture content less than $w_{opt.}$ (dry side)

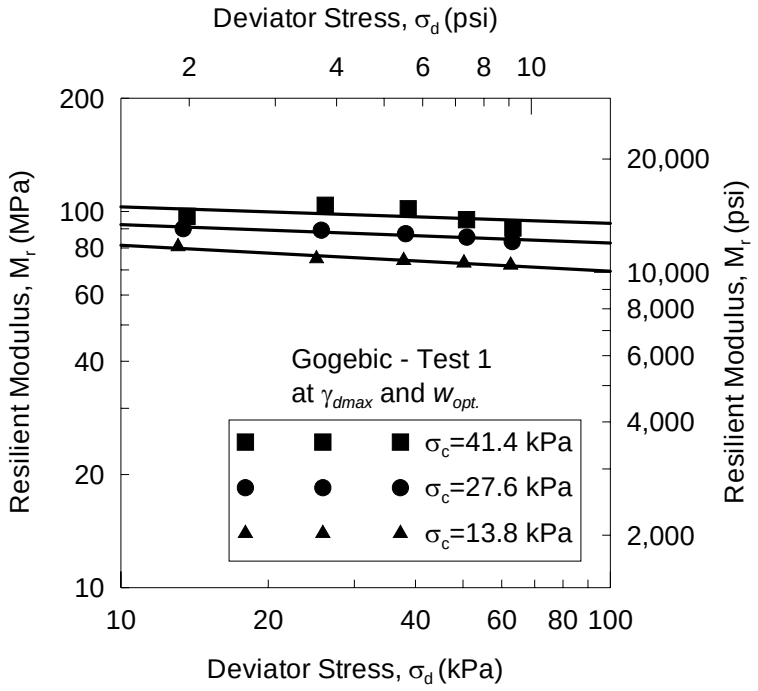

(a) Test on soil specimen #1

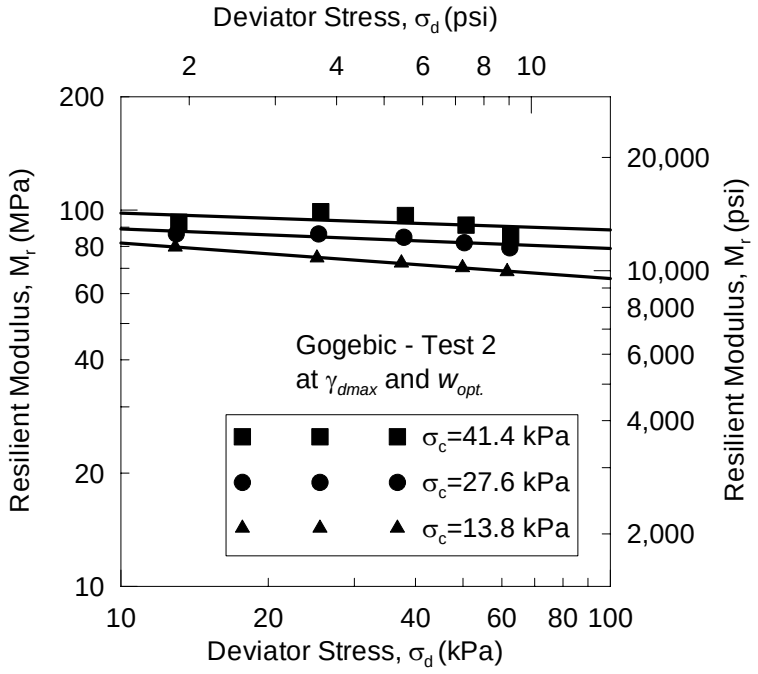

(b) Test on soil specimen #2

Figure B-23: Results of repeated load triaxial test on Gogebic soil compacted at maximum dry unit weight (γ_{dmax}) and optimum moisture content ($w_{opt.}$)

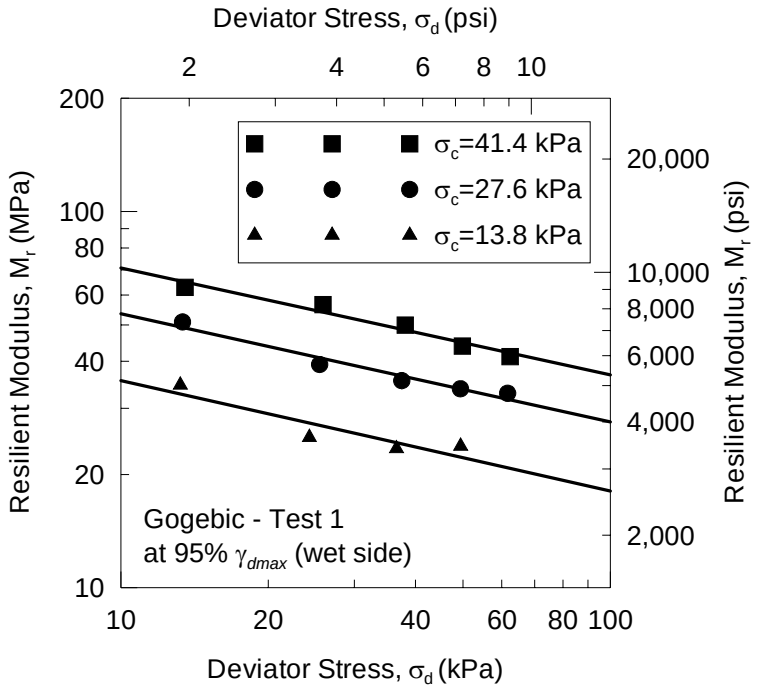

(a) Test on soil specimen #1

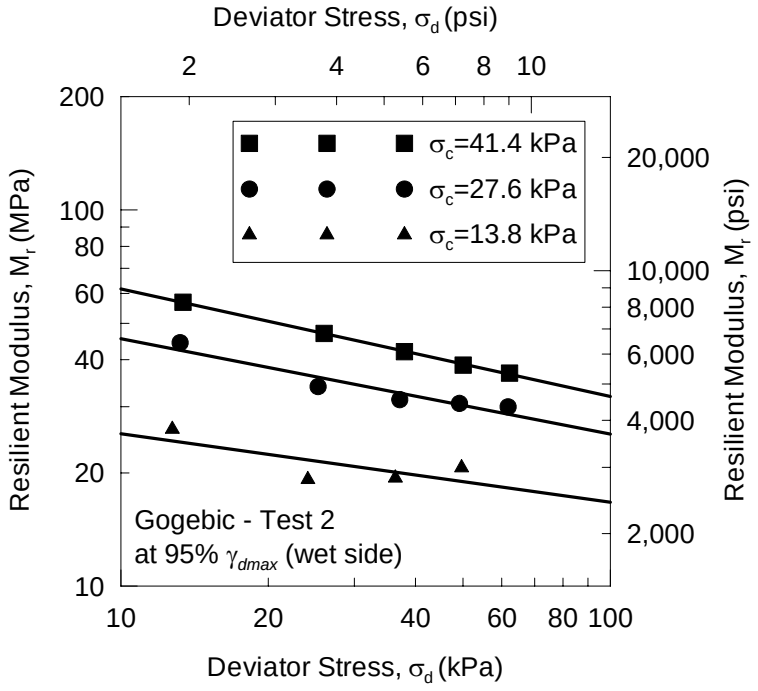

(b) Test on soil specimen #2

Figure B-24: Results of repeated load triaxial test on Gogebic soil compacted at 95% of maximum dry unit weight (γ_{dmax}) and moisture content more than $w_{opt.}$ (wet side)

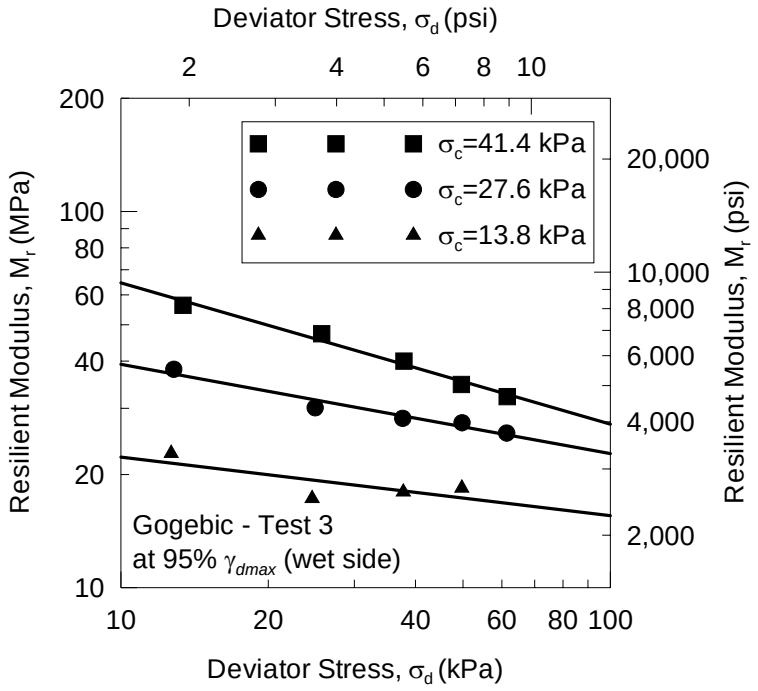

(c) Test on soil specimen #3

Figure B-24 (cont.): Results of repeated load triaxial test on Gogebic soil compacted at 95% of maximum dry unit weight (γ_{dmax}) and moisture content more than $w_{opt.}$ (wet side)

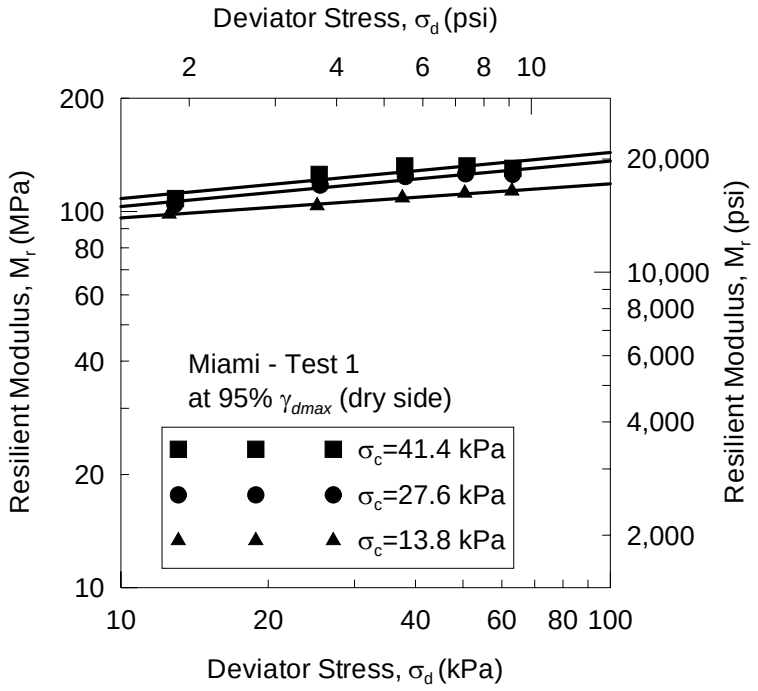

(a) Test on soil specimen #1

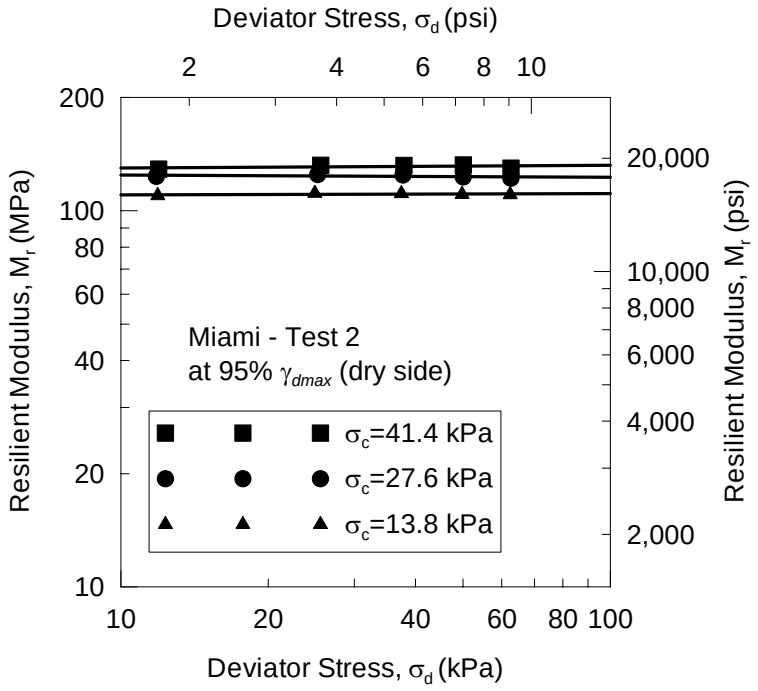

(b) Test on soil specimen #2

Figure B-25: Results of repeated load triaxial test on Miami soil compacted at 95% of maximum dry unit weight (γ_{dmax}) and moisture content less than $w_{opt.}$ (dry side)

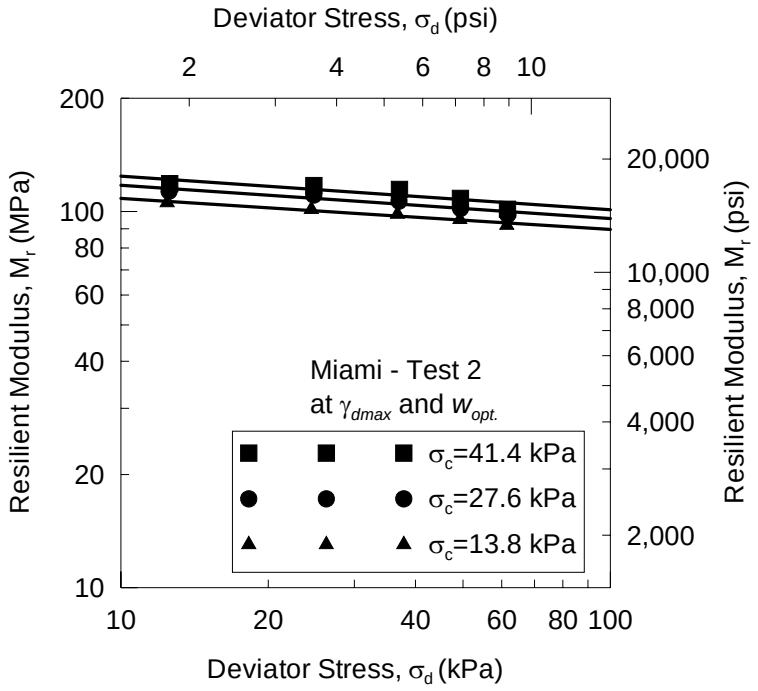

(a) Test on soil specimen #2

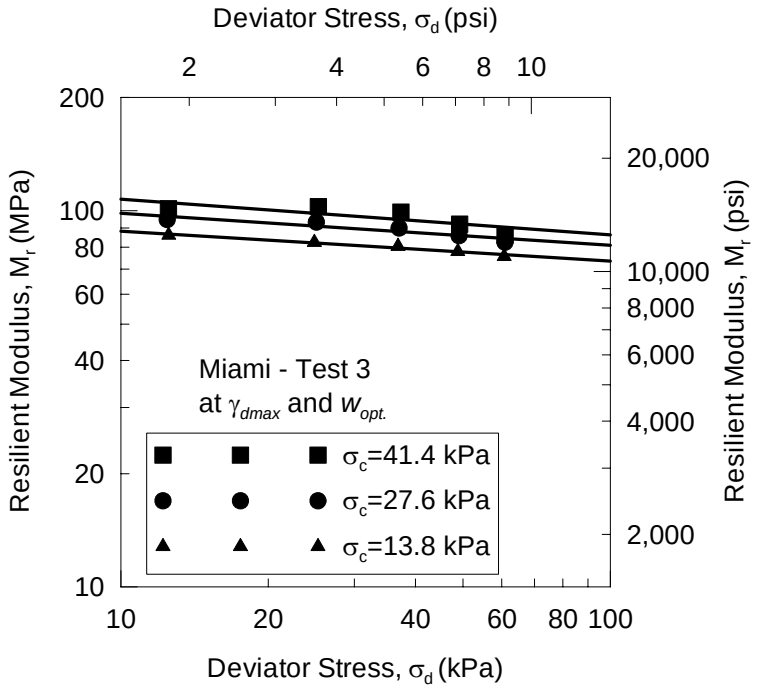

(b) Test on soil specimen #3

Figure B-26: Results of repeated load triaxial test on Miami soil compacted at maximum dry unit weight (γ_{dmax}) and optimum moisture content ($w_{opt.}$)

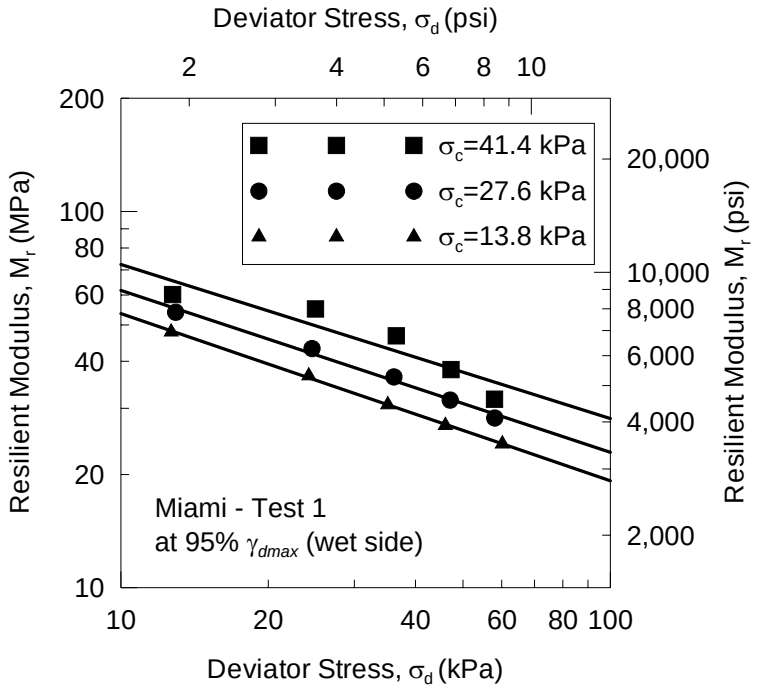

(a) Test on soil specimen #1

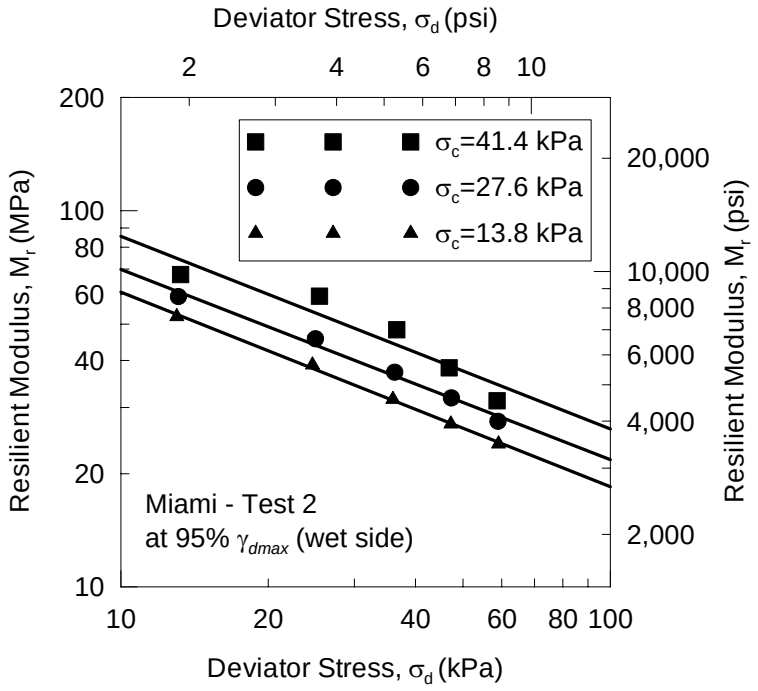

(b) Test on soil specimen #2

Figure B-27: Results of repeated load triaxial test on Miami soil compacted at 95% of maximum dry unit weight (γ_{dmax}) and moisture content more than $w_{opt.}$ (wet side)

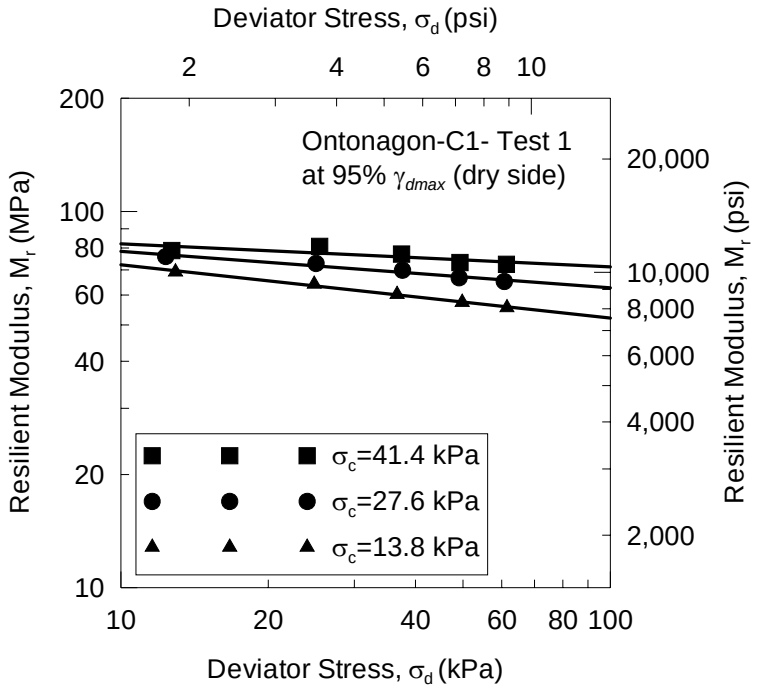

(a) Test on soil specimen #1

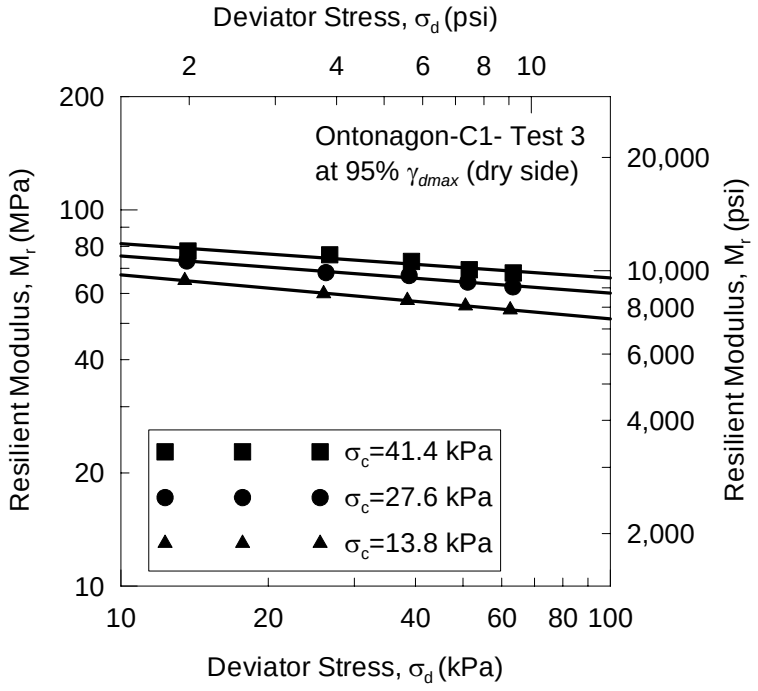

(b) Test on soil specimen #3

Figure B-28: Results of repeated load triaxial test on Ontonagon soil - 1 compacted at 95% of maximum dry unit weight (γ_{dmax}) and moisture content less than $w_{opt.}$ (dry side)

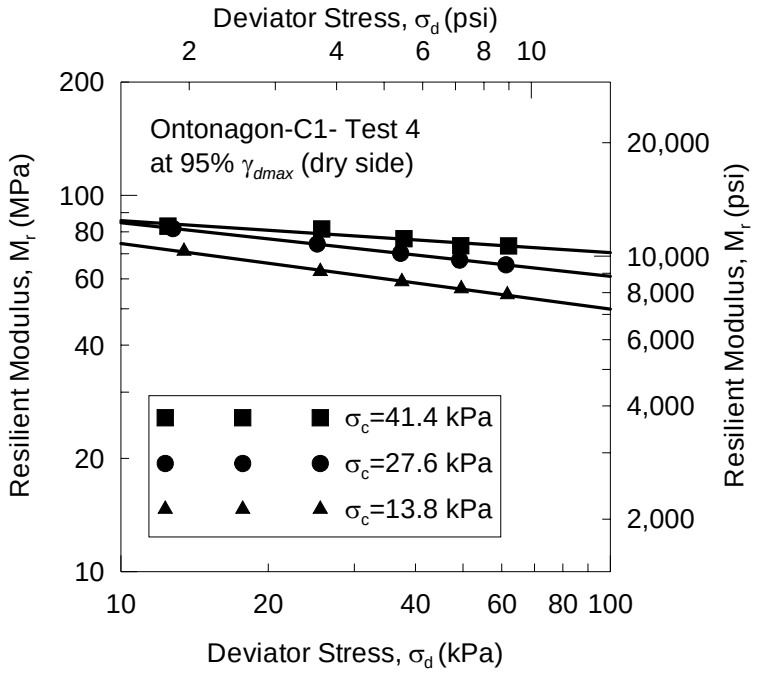

(c) Test on soil specimen #4

Figure B-28 (cont.): Results of repeated load triaxial test on Ontonagon soil - 1 compacted at 95% of maximum dry unit weight (γ_{dmax}) and moisture content less than $w_{opt.}$ (dry side)

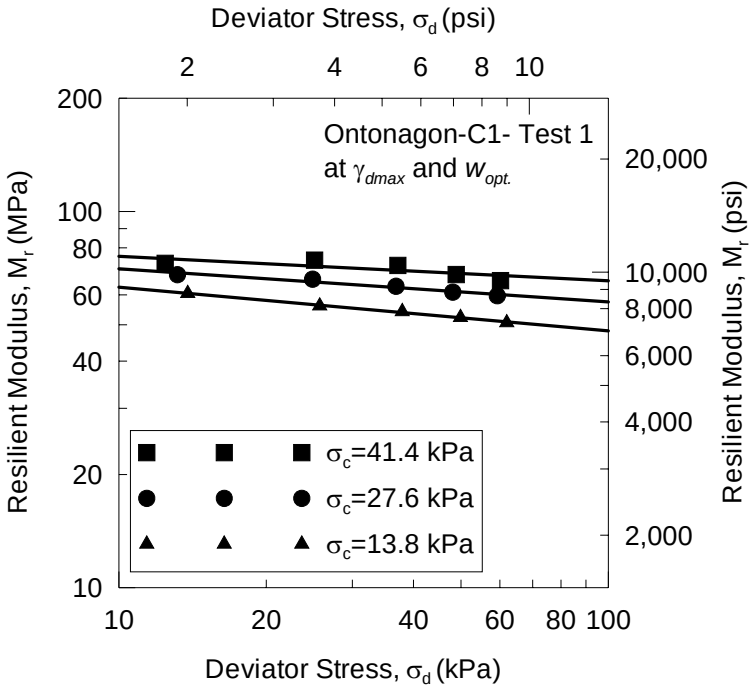

(a) Test on soil specimen #1

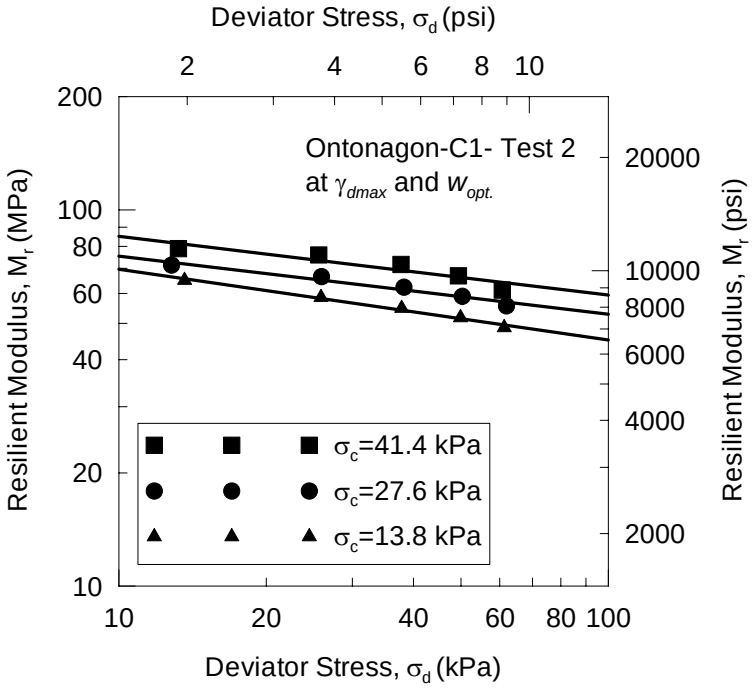

(b) Test on soil specimen #2

Figure B-29: Results of repeated load triaxial test on Ontonagon soil - 1 compacted at maximum dry unit weight (γ_{dmax}) and optimum moisture content ($w_{opt.}$)

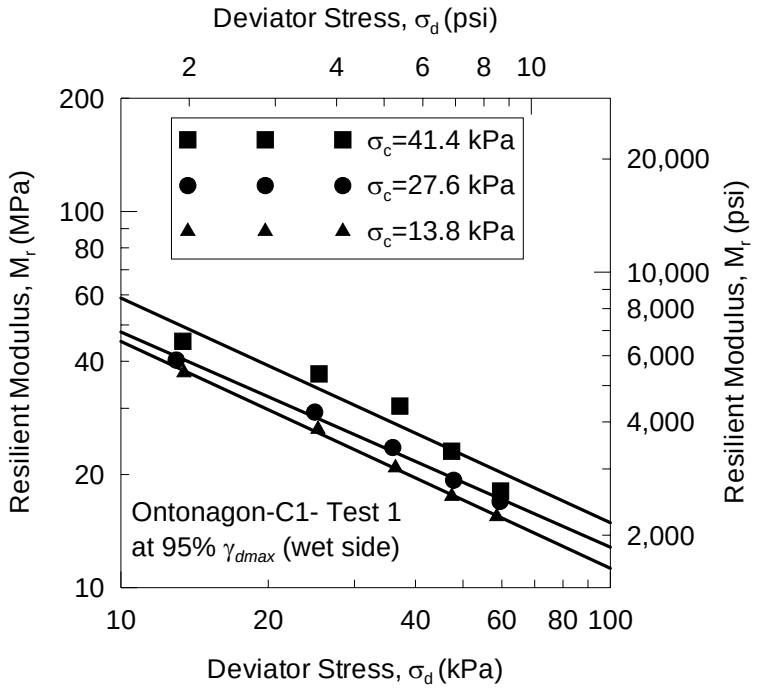

(a) Test on soil specimen #1

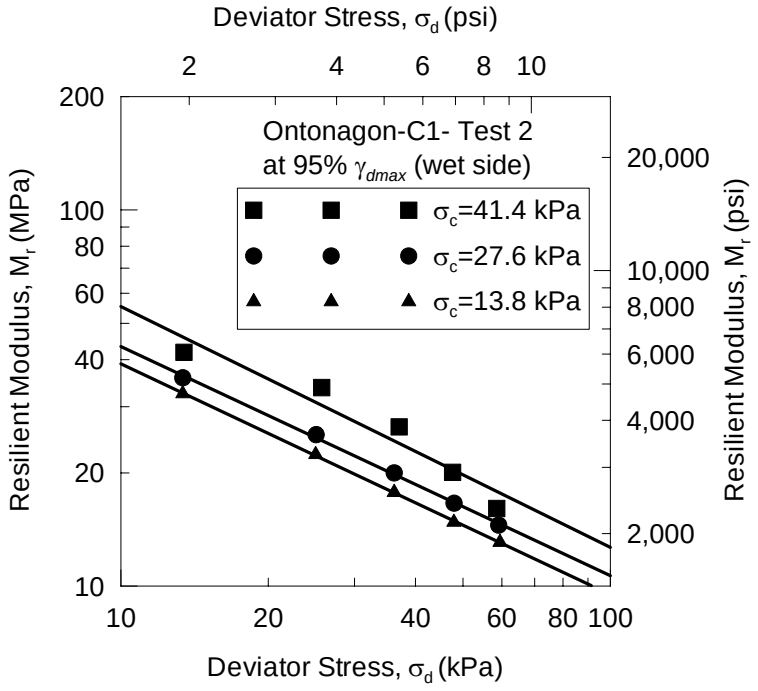

(b) Test on soil specimen #2

Figure B-30: Results of repeated load triaxial test on Ontonagon soil - 1 compacted at 95% of maximum dry unit weight (γ_{dmax}) and moisture content more than $w_{opt.}$ (wet side)

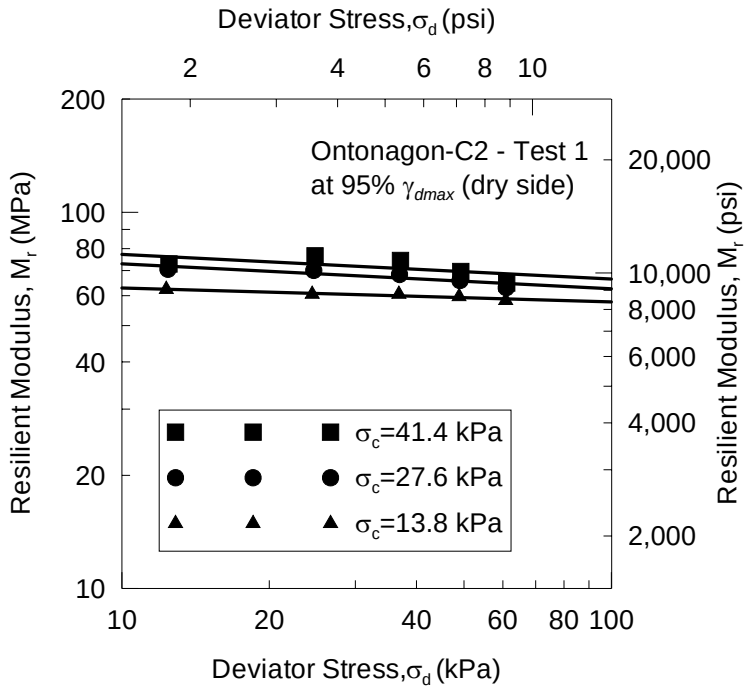

(a) Test on soil specimen #1

Figure B-31: Results of repeated load triaxial test on Ontonagon soil - 2 compacted at 95% of maximum dry unit weight (γ_{dmax}) and moisture content less than $w_{opt.}$ (dry side)

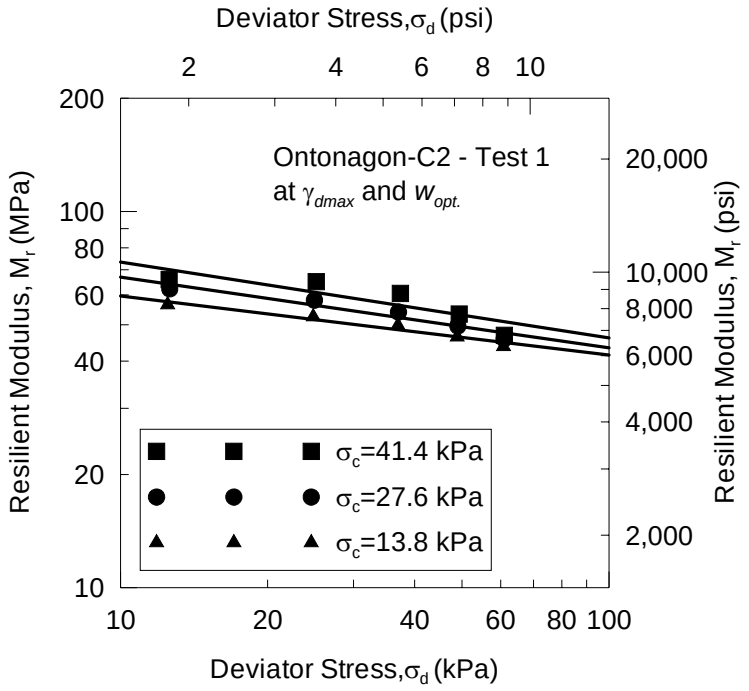

(a) Test on soil specimen #1

Figure B-32: Results of repeated load triaxial test on Ontonagon soil - 2 compacted at maximum dry unit weight (γ_{dmax}) and optimum moisture content ($w_{opt.}$)

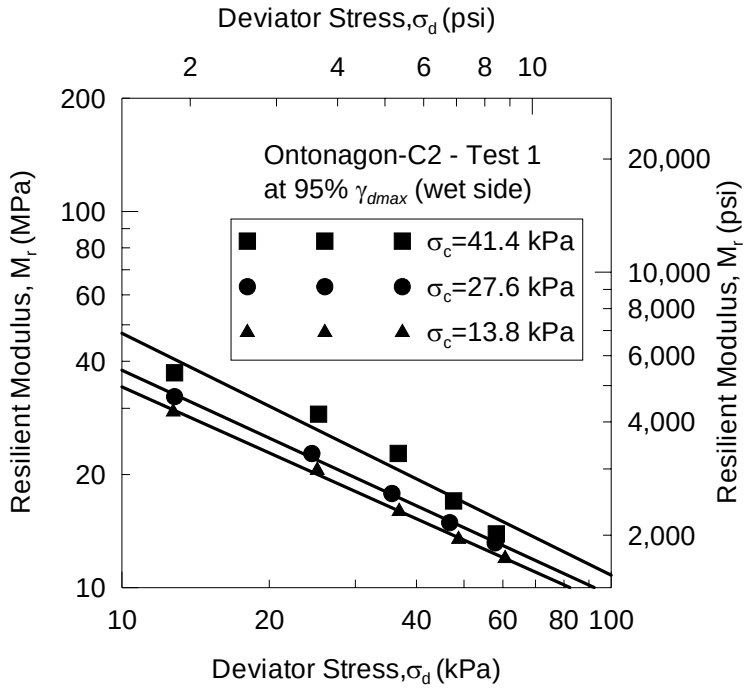

(a) Test on soil specimen #1

Figure B-33: Results of repeated load triaxial test on Ontonagon soil - 2 compacted at 95% of maximum dry unit weight (γ_{dmax}) and moisture content more than $w_{opt.}$ (wet side)

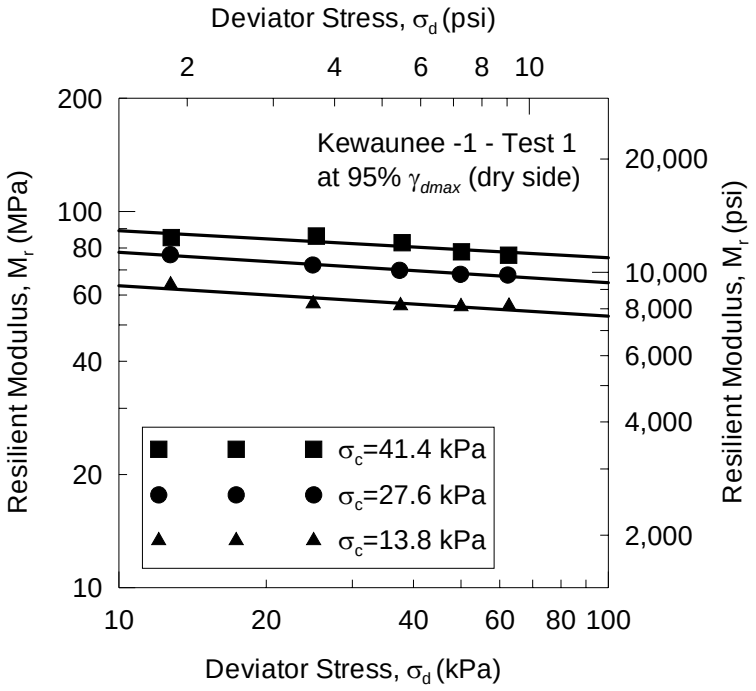

(a) Test on soil specimen #1

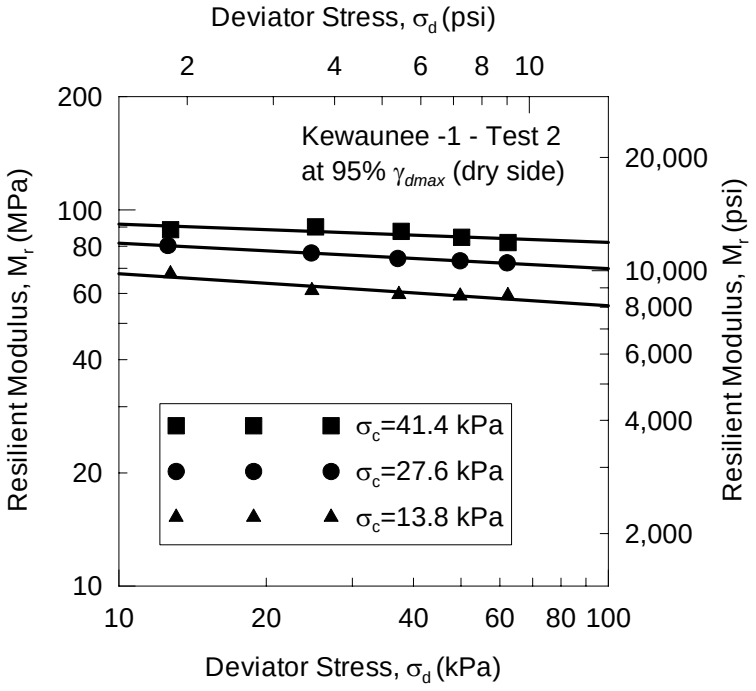

(b) Test on soil specimen #2

Figure B-34: Results of repeated load triaxial test on Kewaunee soil - 1 compacted at 95% of maximum dry unit weight (γ_{dmax}) and moisture content less than $w_{opt.}$ (dry side)

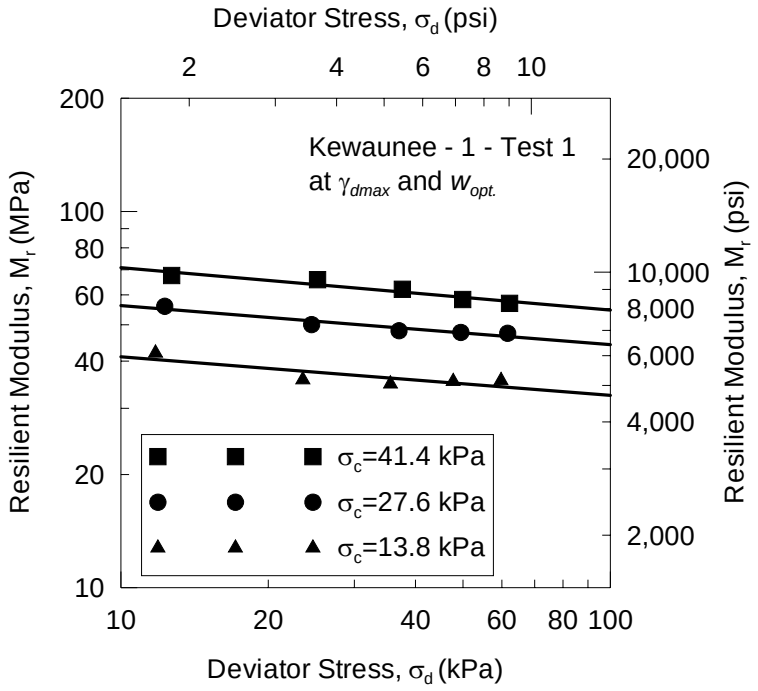

(a) Test on soil specimen #1

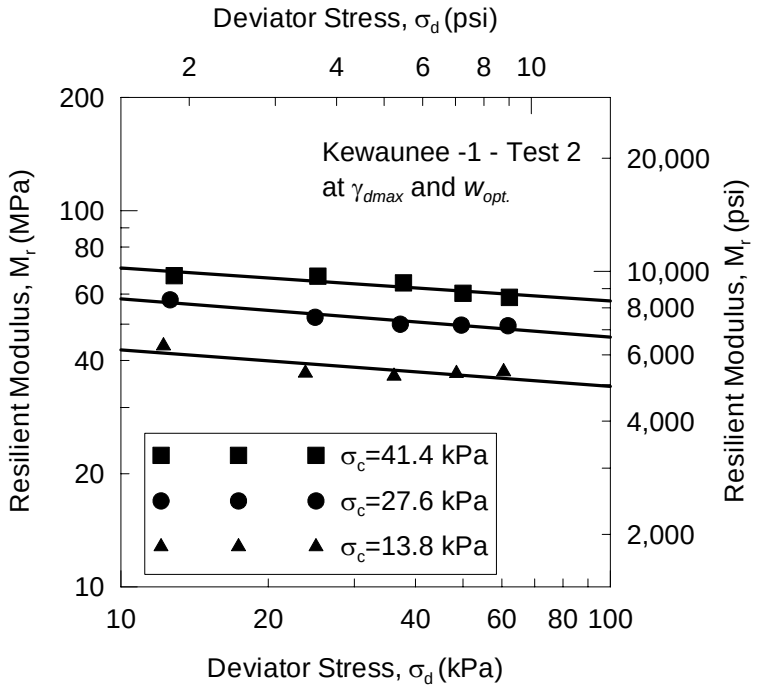

(b) Test on soil specimen #2

Figure B-35: Results of repeated load triaxial test on Kewaunee soil - 1 compacted at maximum dry unit weight (γ_{dmax}) and optimum moisture content ($w_{opt.}$)

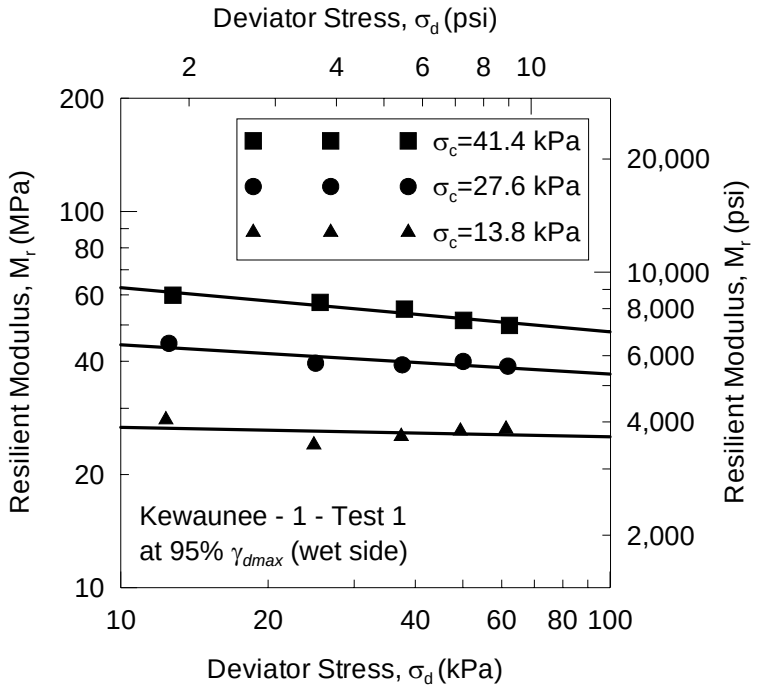

(a) Test on soil specimen #1

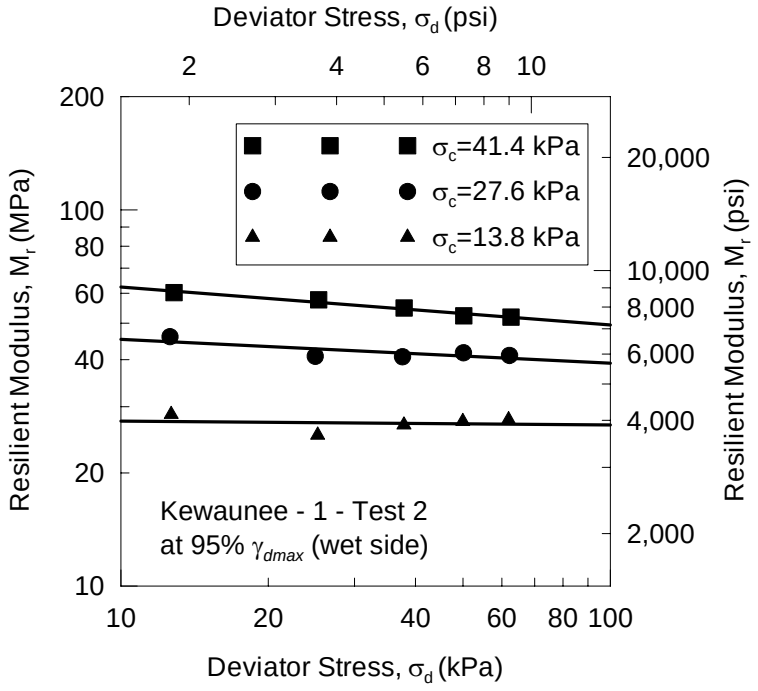

(b) Test on soil specimen #2

Figure B-36: Results of repeated load triaxial test on Kewaunee soil -1 compacted at 95% of maximum dry unit weight (γ_{dmax}) and moisture content more than $w_{opt.}$ (wet side)

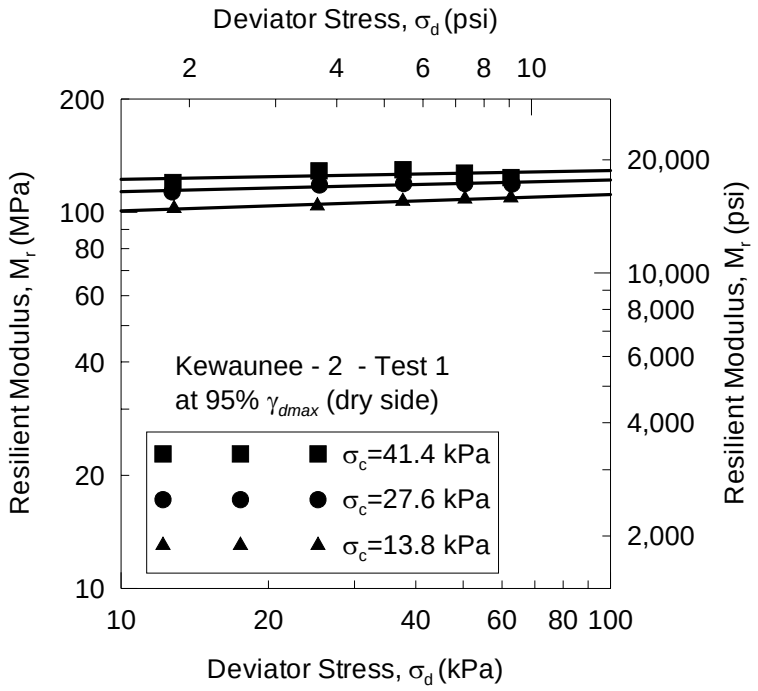

(a) Test on soil specimen #1

Figure B-37: Results of repeated load triaxial test Kewaunee soil - 2 compacted at 95% of maximum dry unit weight (γ_{dmax}) and moisture content less than $w_{opt.}$ (dry side)

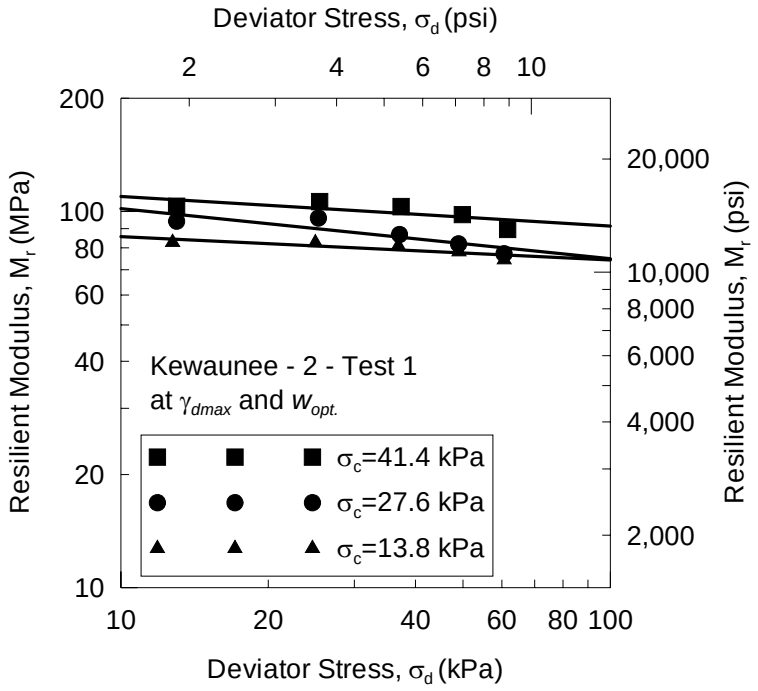

(a) Test on soil specimen #1

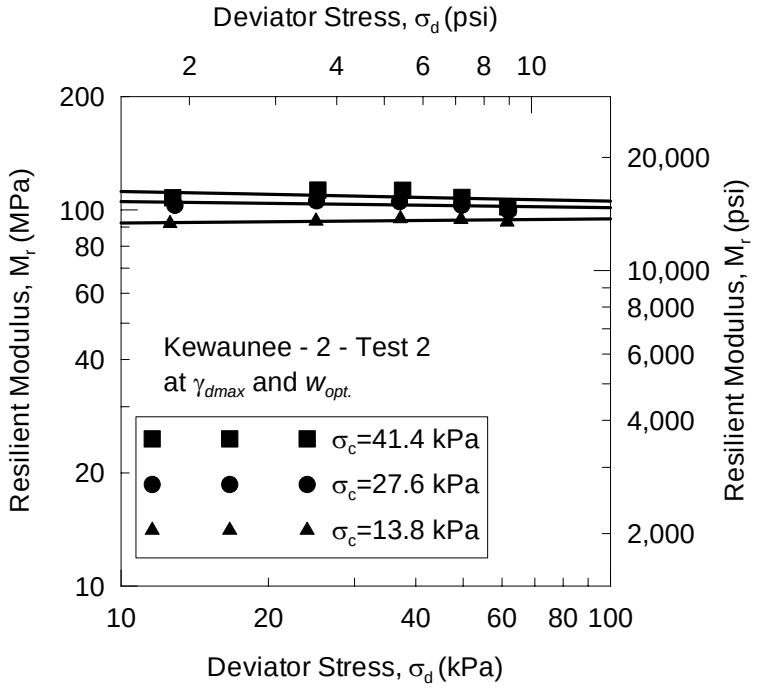

(b) Test on soil specimen #2

Figure B-38: Results of repeated load triaxial test on Kewaunee soil - 2 compacted at maximum dry unit weight (γ_{dmax}) and optimum moisture content ($w_{opt.}$)

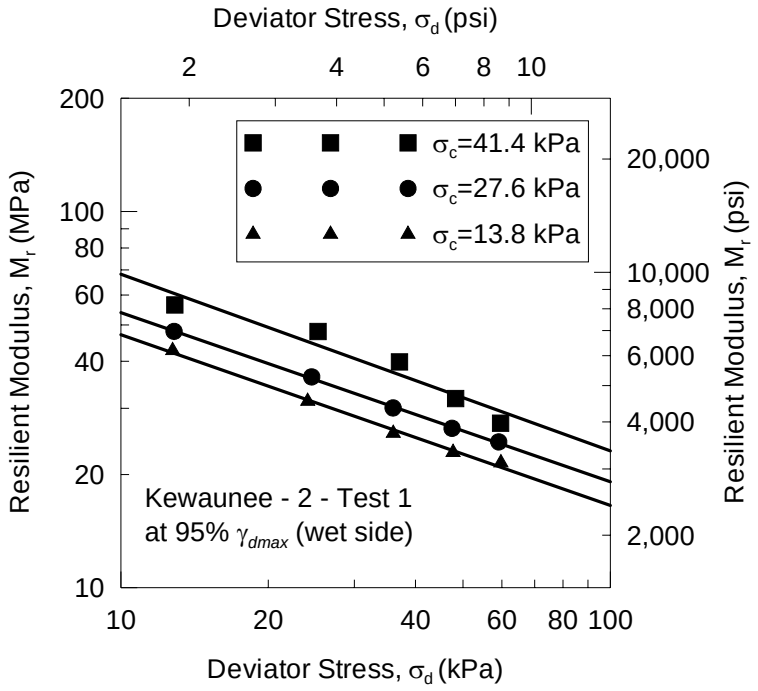

(a) Test on soil specimen #1

Figure B-39: Results of repeated load triaxial test on Kewaunee soil - 2 compacted at 95% of maximum dry unit weight (γ_{dmax}) and moisture content more than $w_{opt.}$ (wet side)

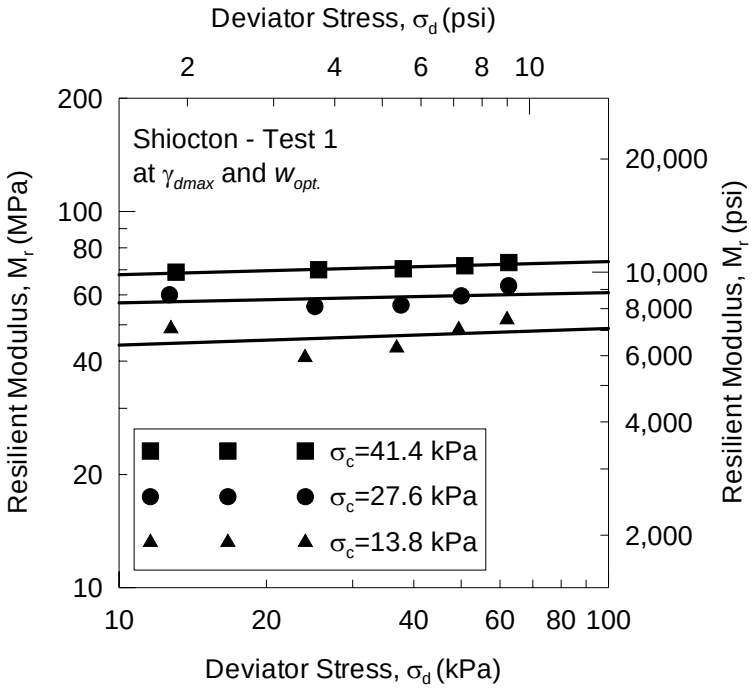

(a) Test on soil specimen #1

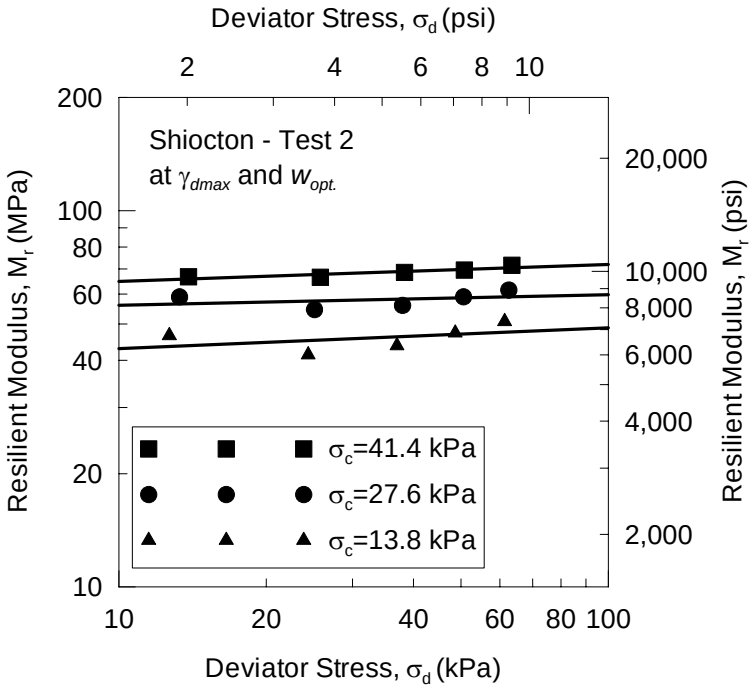

(b) Test on soil specimen #2

Figure B-40: Results of repeated load triaxial test on Shiocton soil compacted at maximum dry unit weight (γ_{dmax}) and optimum moisture content ($w_{opt.}$)

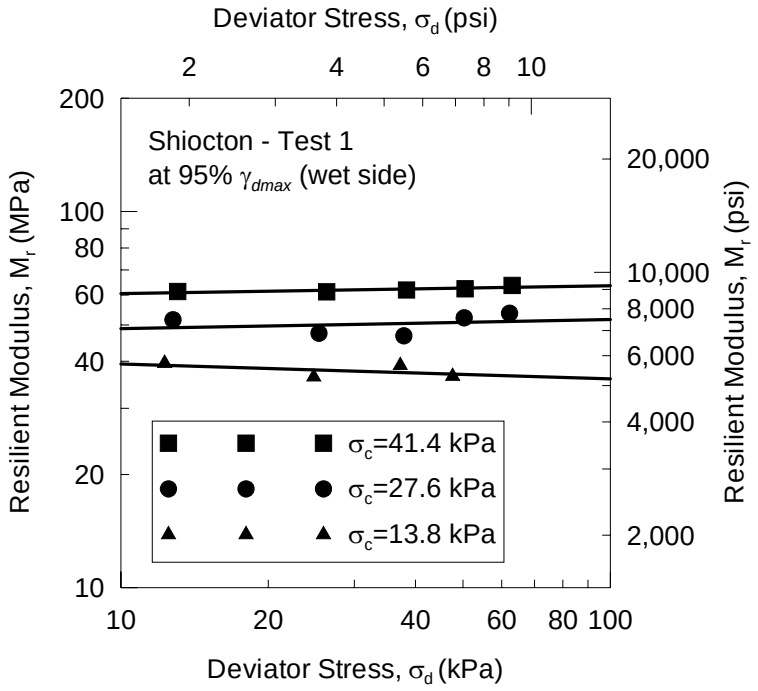

(a) Test on soil specimen #1

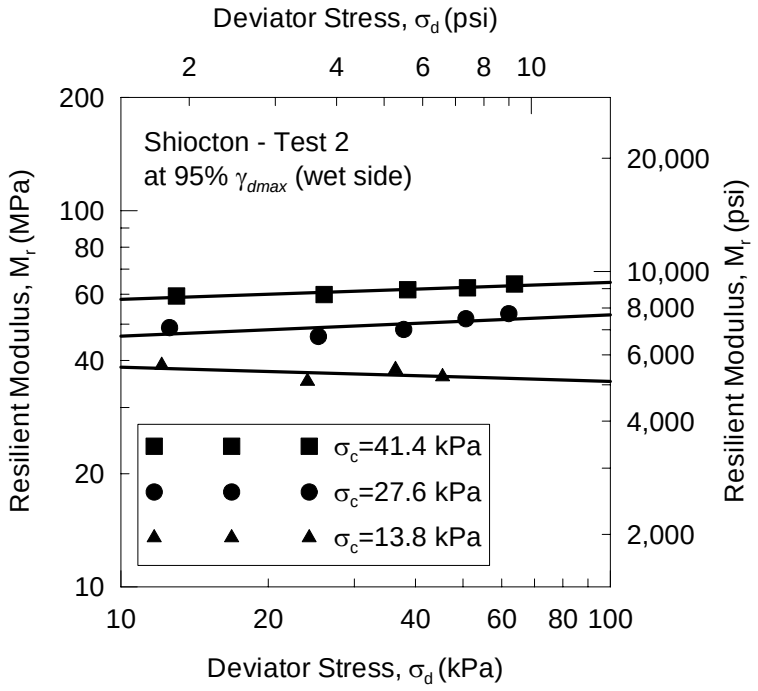

(b) Test on soil specimen #2

Figure B-41: Results of repeated load triaxial test on Shiocton soil compacted at 95% of maximum dry unit weight (γ_{dmax}) and moisture content more than $w_{opt.}$ (wet side)

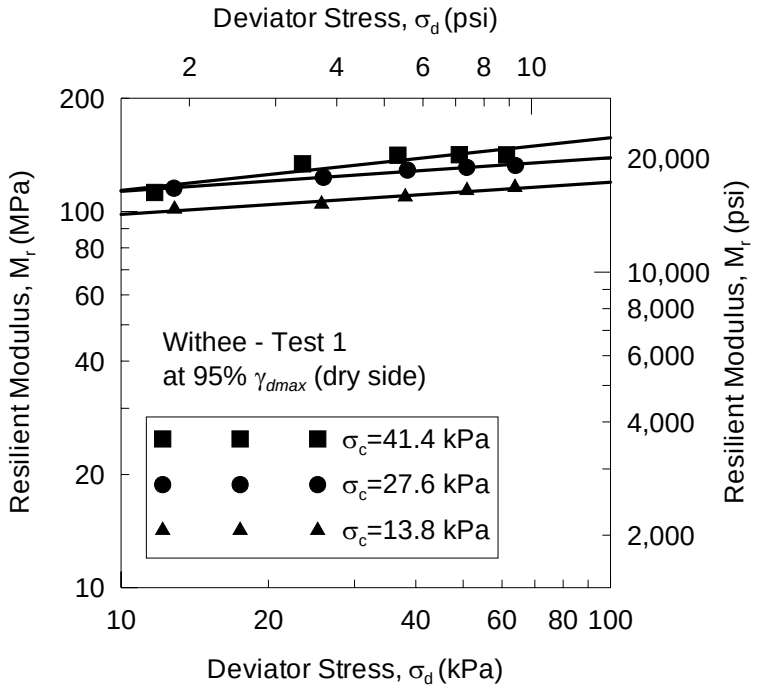

(a) Test on soil specimen #1

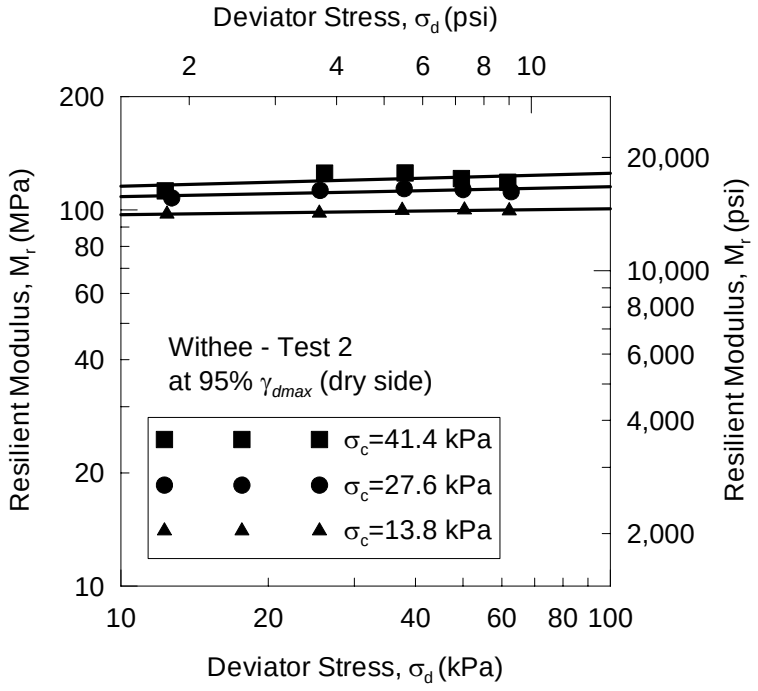

(b) Test on soil specimen #2

Figure B-42: Results of repeated load triaxial test on Withee soil compacted at 95% of maximum dry unit weight (γ_{dmax}) and moisture content less than $w_{opt.}$ (dry side)

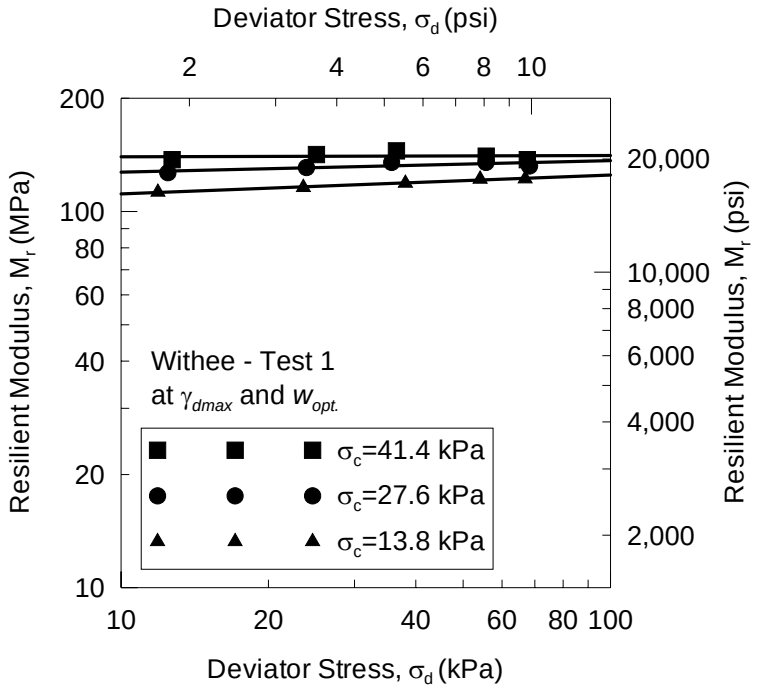

(a) Test on soil specimen #1

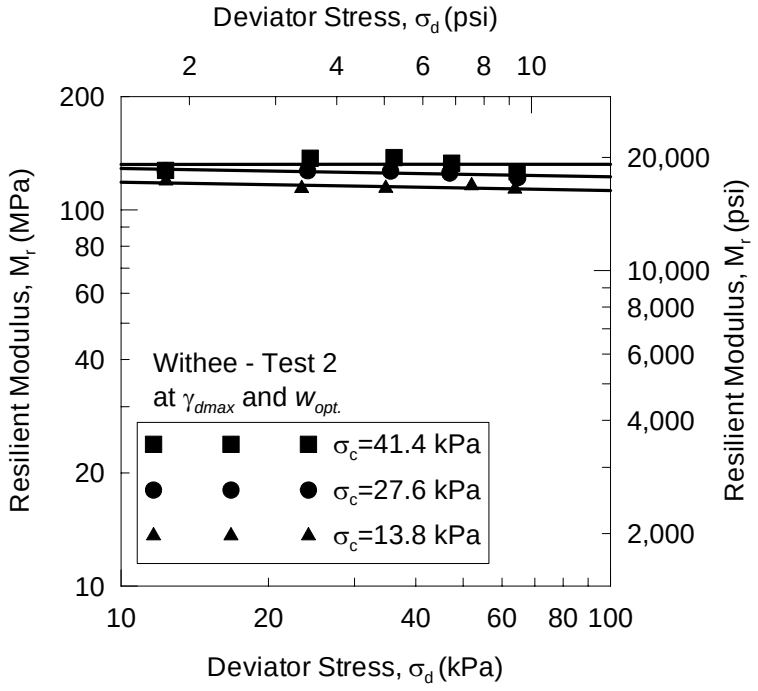

(b) Test on soil specimen #2

Figure B-43: Results of repeated load triaxial test on Withee soil compacted at maximum dry unit weight (γ_{dmax}) and optimum moisture content ($w_{opt.}$)

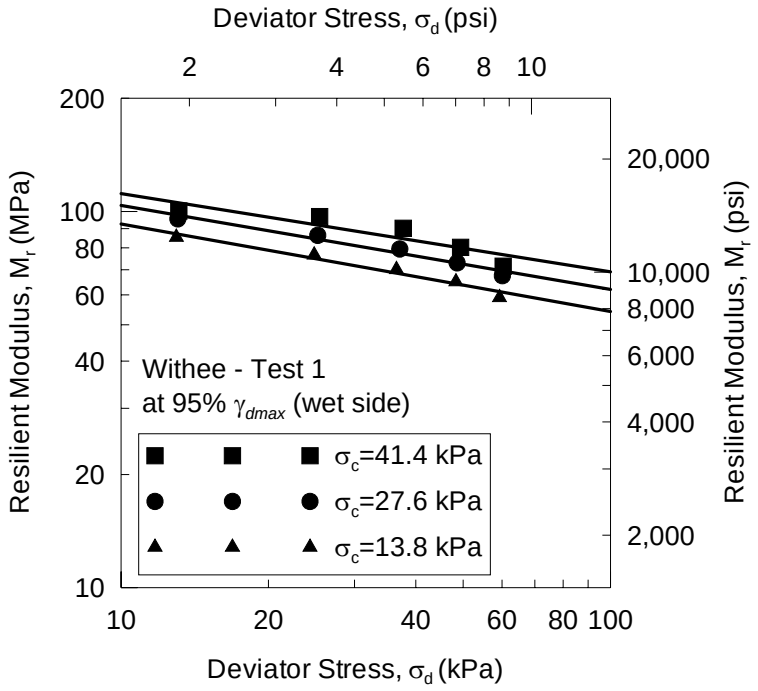

(a) Test on soil specimen #1

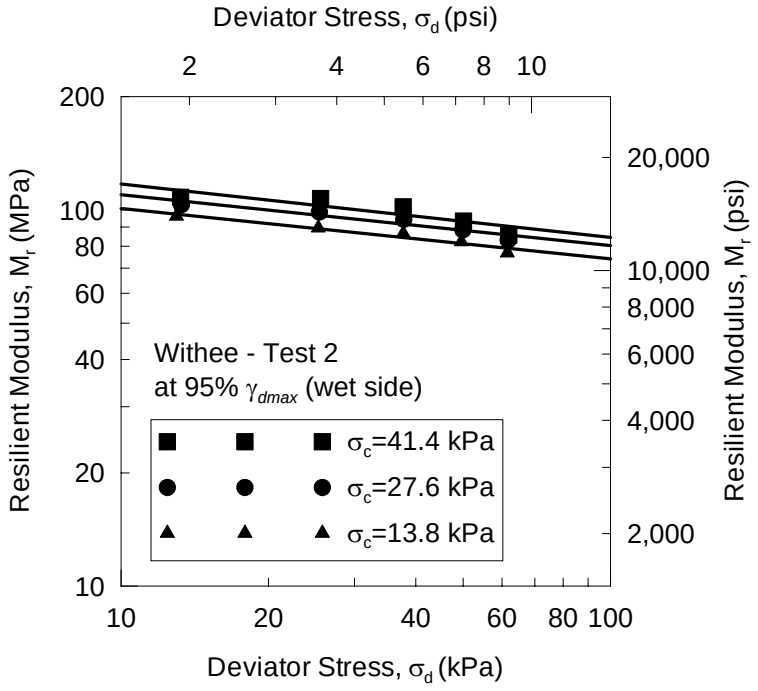

(b) Test on soil specimen #2

Figure B-44: Results of repeated load triaxial test on Withee soil compacted at 95% of maximum dry unit weight (γ_{dmax}) and moisture content more than $w_{opt.}$ (wet side)

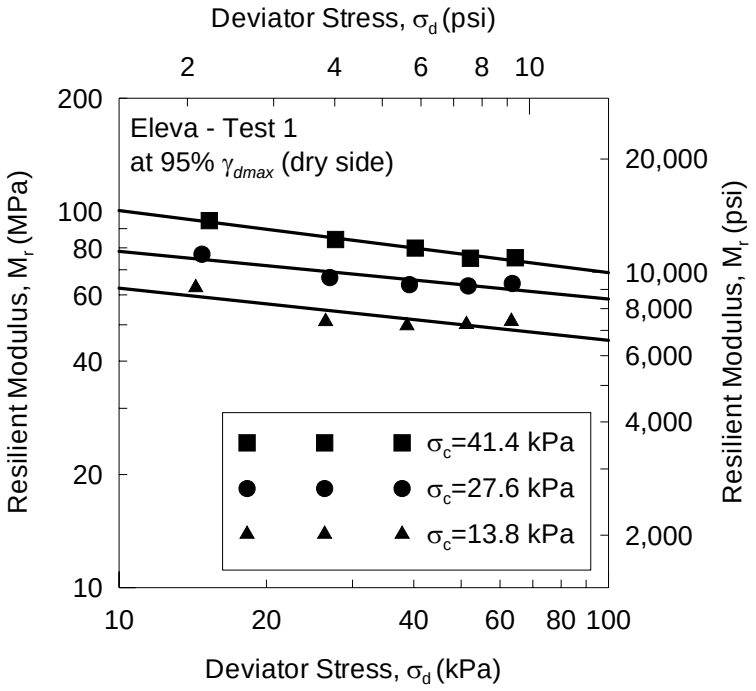

(a) Test on soil specimen #1

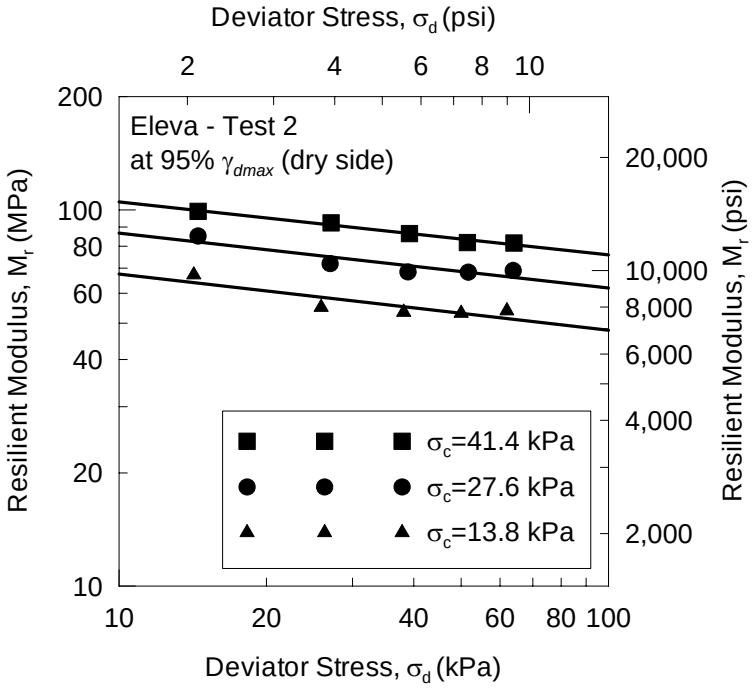

(b) Test on soil specimen #2

Figure B-45: Results of repeated load triaxial test on Eleva soil compacted at 95% of maximum dry unit weight (γ_{dmax}) and moisture content less than $w_{opt.}$ (dry side)

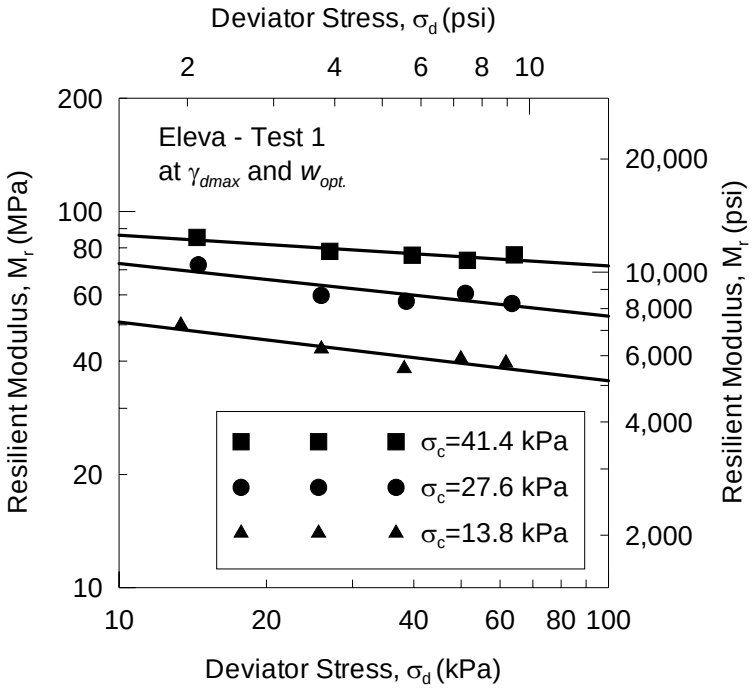

(a) Test on soil specimen #1

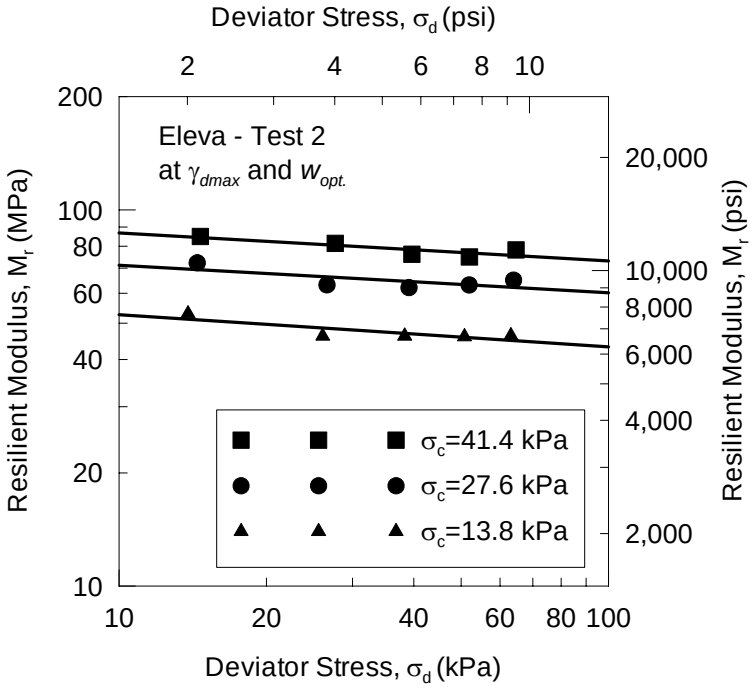

(b) Test on soil specimen #2

Figure B-46: Results of repeated load triaxial test on Eleva soil compacted at maximum dry unit weight (γ_{dmax}) and optimum moisture content ($w_{opt.}$)

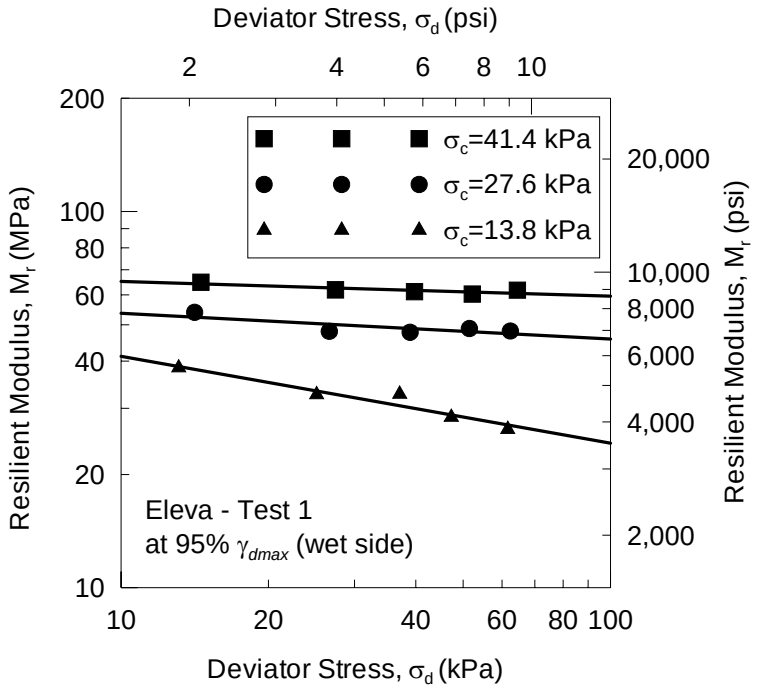

(a) Test on soil specimen #1

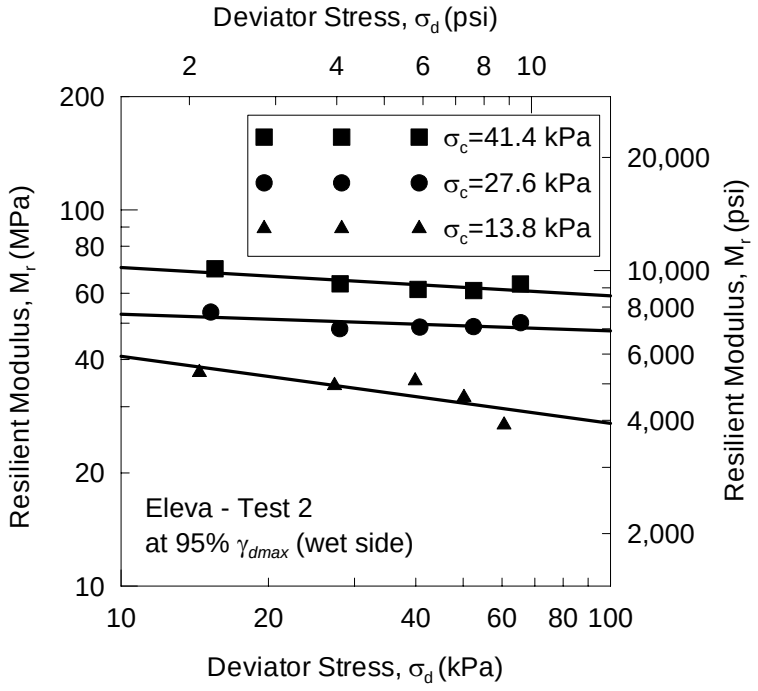

(b) Test on soil specimen #2

Figure B-47: Results of repeated load triaxial test on Eleva soil compacted at 95% of maximum dry unit weight (γ_{dmax}) and moisture content more than $w_{opt.}$ (wet side)